MODELLING OF SMALL CAPACITY ABSORPTION CHILLERS DRIVEN BY SOLAR THERMAL ENERGY OR WASTE HEAT

Jerko Labus

Dipòsit Legal: T.1716-2011

Jerko Labus

Modelling of small capacity absorption chillers driven by solar thermal energy or waste heat

A thesis submitted in partial fulfillment of the requirements of Rovira i Virgily University for the degree of Doctor of Philosophy

Supervised by: Dr. Alberto Coronas Salcedo
Dr. Joan Carles Bruno Arguilaget

UNIVERSITAT ROVIRA I VIRGILI

Tarragona

2011

UNIVERSITAT
ROVIRA I VIRGILI
DEPARTAMENT D'ENGINYERIA MECÀNICA
Escola Tècnica Superior d'Enginyeria Química (ETSEQ).
Av. Països Catalans 26. 43007 Tarragona (Spain)

Los abajo firmantes, Dr. Alberto Coronas, Catedrático de Universidad del Área de Máquinas y Motores Térmicos y Dr. Joan Carles Bruno, Profesor Agregado, del Departament d'Enginyeria Mecánica de la Universitat Rovira i Virgili de Tarragona

HACEN CONSTAR:

Que el trabajo titulado: "Modelling of Small Capacity Absorption Chillers Driven by Solar Thermal Energy or Waste Heat" presentado por el Sr. Jerko Labus para optar al grado de Doctor de la Universitat Rovira i Virgili, ha sido realizado bajo su dirección inmediata en el CREVER – Grup de recerca d'Enginyeria Tèrmica Aplicada del Departament d'Enginyeria Mecànica de la Universitat Rovira i Virgili, que todos los resultados han sido obtenidos en las experiencias realizadas por dicho doctorando y que cumple los requisitos para poder optar a la Mención Europea.

Y para que así conste a los efectos oportunos, firmamos este documento.

Tarragona, 09 de Septiembre de 2011.

Abstract

The current energy systems, mainly based on fossil fuels, are largely responsible, among others, for the present environmental and economic crisis. The electrical air-conditioning units are significant contributors to the primary energy consumption. The continued rise in living as well as working comfort conditions, coupled together with reduced prices of air-conditioning units and lower electricity prices, have caused a great expansion of these systems. The consequence is the negative impact on electricity demand and environment. Since absorption machines have a small requirement for electrical power, electric utilities have promoted them as a measure of reducing utility demand peaks. Another advantage of absorption units is that working fluids are not harmful to the environment, unlike the CFC's and HCFC's refrigerants used in compression units. Recently, there is a rising tendency in demand for small capacity absorption machines, particularly for residential and small office applications. However, high investment cost, requirement of additional equipment and only a few manufacturers are main causes why these machines are not economically competitive with conventional compression machines. Also, there is a lack of adequate standards, best practice guides and test procedures for their evaluation. In order to overcome these shortcomings, it is necessary to intensify the work in all important fields: starting from design and experimental work, over modelling and control to their implementation in complex air-conditioning systems.

This research deals with the development of the simple, yet accurate steady-state models of small capacity absorption machines which are based on highly reliable data obtained in the state-of-the-art test bench. These models can further be used in simulation tools or to develop supervisory control strategies for air-conditioning systems with absorption machines. Therefore, the main aim of this research is to develop and to describe a comprehensive methodology which will enclose entire process which consists of testing, modelling and control strategy development of small capacity absorption machines.

To achieve this aim, the first task is to obtain highly reliable data. This task required development of a simple test procedure based on existing knowledge and

experience. The final result is the procedure which contains several important steps: test planning, data modelling, how to develop detector for steady-state conditions, the uncertainty estimation and the analysis of the results.

The second part of the research is focused on the development of small capacity absorption chiller models based on the obtained datasets. The study includes five different modelling methods using both mechanistic and empirical approaches: thermodynamic, adapted Gordon-Ng, adapted characteristic equation, multivariate polynomial regression and artificial neural networks modelling. The results clearly indicate that it is possible to develop highly accurate empirical models by using only the variables of external water circuits as input parameters. The excellent statistical indicators such as coefficient of determination (>0.99) and coefficient of variation (<5%) confirm that. The study also describes statistical tests which might assist in selection of the most appropriate model.

The last part of the research deals with supervisory control of small capacity absorption chillers. Two optimal control strategies are developed to demonstrate how advanced modelling and optimization methods such as Artificial Neural Networks (ANN) and Genetic Algorithms (GA) can be implemented in on-line control of air-conditioning systems with absorption chillers.

Resumen

Los sistemas energéticos basados en combustibles fósiles se encuentran entre los principales responsables de la situación ambiental y crisis económica que afectan al mundo en estos momentos, siendo los equipos tradicionales de aire acondicionado uno de los mayores consumidores de energía primaria. Estos sistemas han logrado ocupar un nicho muy importante en la vida cotidiana debido al incremento en la demanda de confort, en el reducido coste de estos equipos y a las bajas tarifas eléctricas; pero también han llevado a que se produzcan impactos negativos tanto en la demanda eléctrica como a nivel medioambiental. Una solución a estos sistemas es el uso de máquinas de absorción debido a que su bajo consumo eléctrico permitiría reducir los picos de demanda de las generadoras eléctricas. Otra ventaja de las máquinas de absorción es el uso de mezclas de trabajo no perjudiciales para el medio ambiente como sí lo son los refrigerantes utilizados en las máquinas de compresión (CFCs y HCFCs). En los últimos años se ha dado un incremento en el uso de máquinas de absorción de pequeña potencia especialmente en el sector residencial y en pequeñas oficinas; sin embargo, sus elevados costes junto a la necesidad de equipo adicional y al reducido número de fabricantes han propiciado que estas máquinas no sean económicamente competitivas con las máquinas convencionales de compresión. Además a esto hay que sumar la falta de estándares adecuados, guías de mejores prácticas y procedimientos de ensayos para su evaluación. Para superar estas deficiencias es necesario intensificar el trabajo en todas las áreas importantes, comenzando desde el diseño y trabajo experimental, pasando por el modelado y control hasta llegar a su implementación en sistemas de aire acondicionado complejos.

Esta investigación se centra en el desarrollo de modelos en régimen estacionario de máquinas de absorción de pequeña potencia basados en datos sumamente fiables obtenidos en un banco de ensayos de última tecnología. Estos modelos pueden ser utilizados más adelante en herramientas de simulación o para desarrollar estrategias de control de supervisión en sistemas de aire acondicionado con máquinas de absorción. El objetivo principal de esta investigación es por lo tanto desarrollar y describir una metodología comprensiva que abarque los ensayos, el modelado y el desarrollo de estrategias de control para máquinas de absorción de pequeña potencia.

Para lograr este objetivo, la primera tarea es obtener datos sumamente fiables por lo que se requiere desarrollar un procedimiento simple de pruebas basado en conocimiento y experiencia del banco de ensayos. El resultado final es un procedimiento que contiene algunos pasos importantes como son: el planeamiento de los ensayos o pruebas, el modelado de los datos, el saber detectar las condiciones de estado estacionario, la evaluación de la incertidumbre y el análisis de los resultados.

La segunda parte de esta investigación se centra en el desarrollo de un modelo de enfriadoras de absorción de pequeña potencia basado en resultados obtenidos experimentalmente. Este estudio incluye cinco métodos de modelación con enfoques tanto mecanicista como empírico: método termodinámico, método adaptado de Gordon-Ng, método de la ecuación característica adaptada, método de regresión polinomial multivariable y modelo de redes neuronales artificiales. Los resultados obtenidos demuestran que es posible desarrollar modelos empíricos, altamente precisos, con tan solo el uso de las variables de los circuitos de agua externos como parámetros de entrada. Esta última aseveración se confirma con la obtención de indicadores estadísticos tales como el coeficiente de determinación (>0.99) y el coeficiente de variación (<5%). Además se describen pruebas estadísticas que podrían ser utilizadas al momento de seleccionar el modelo más apropiado.

La última parte de esta investigación trata sobre el control de supervisión para enfriadoras de absorción de pequeña potencia. Se han desarrollado dos estrategias de control óptimas: la primera se encuentra basada en la modelación avanzada con Redes Neuronales Artificiales (RNA), mientras que la segunda utiliza métodos de optimización con Algoritmos Genéticos (AG). Se demuestra que estas dos estrategias pueden ser implementadas para el control online de sistemas de aire acondicionado con enfriadoras de absorción.

Acknowledgements

I would like to acknowledge financial support of this research which formed part of the CITYNET project funded via the Marie Curie Research Training Network. Also, special thanks go to all participants from the CITYNET project led by coordinator Dr. Ursula Eicker, without whom this work would not have been possible.

I also happily acknowledge the contributions of many IESD Colleagues who provided me with moral support and useful advices during my stage in the UK. I will never forget the time spent in Leicester, long discussions on Friday and especially the opportunity to work with Dr. Yi Zhang. I am honoured to have a person like you as a friend. I also acknowledge the contribution of Dr. Alfredo Hernandez from UEAM, Mexico who first introduced me to ANN modelling and worked with me on developing the ANNi control methodology. I will never forget Dr. Mahmoud Bourouis, who was suffering almost three years stacked in the same office with myself. Thank you for understanding me.

I also happily acknowledge the contributions of all the Colleagues from URV CREVER Group who sheared the good and the bad with me during this long four years. Thank you all for support and help I received from you. Thanks also go to the whole Department of the Mechanical engineering at URV for their assistance, especially to the Secretary office.

Most of all I would like to acknowledge the contribution of my Colleagues, but first friends, Ivan Korolija and Andres Montero. I would not get this thesis to the end without you. Thank you for being friends and my moral support during this period. I also use the opportunity to ask forgiveness from Miss Nuria Quince for all the teasing she has suffered the last four years. You now that you are my friend.

Of course, many thanks go to my supervisors Dr. Alberto Coronas Salcedo and Dr. Joan Carles Bruno. It may be said that I am not the easiest student to supervise, but

it seems that you have found the way to handle it. During the hard process of writing up my thesis my requests for guidance were received with patience and generosity.

Finally, I use this opportunity to express my gratitude to my parents for all the support and education they gave me. I am sorry that you are not here to share this moment with me. Also, I want to acknowledge the support of my brother Peter, you have always been my inspiration. So this is it. The PhD is finally finished. Now I can get on with something else, finding new challenges and trying to make up the time to my girlfriend and brother.

"We will either find a way, or make one"

Hannibal

Dedicated to my parents and brother

Table of Contents

List of Figures

List of Tables

Chapter 1

Introduction

"The great thing in the world is not so much where we stand,
as in what direction we are moving."
Oliver Wendell Holmes

1.1. Energy context

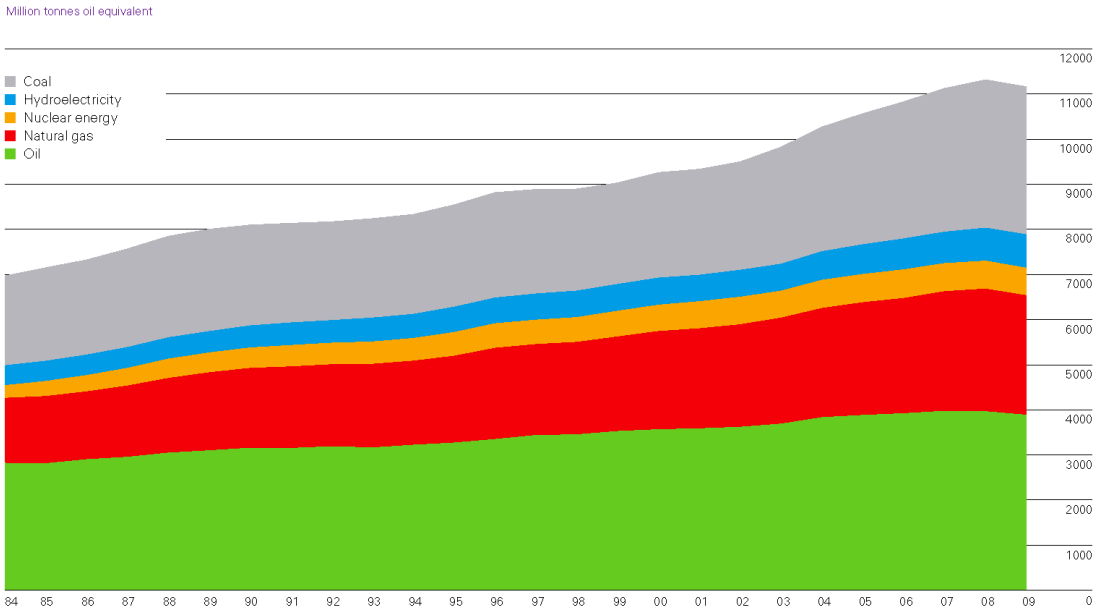

Figure 1.1 World primary energy consumption [1]

Fractional changes in solar radiation, volcanic eruptions and natural fluctuations in the climate system itself are some of the natural reasons responsible for the global warming. However, natural causes can explain only a small part of this warming. According to majority of scientists, the main cause for climate change is raising concentration of heat-trapping greenhouse gases in the atmosphere caused by human activities. Over the past 100 years the average surface air temperature has increased by 0.74ºC, and the Intergovernmental Panel on Climate Change (IPCC) projects that by 2100 the global average temperature is most likely to increase by a further 1.8ºC to 4ºC

unless the world takes action to limit greenhouse gasses emissions [2]. The enhanced effects of the global warming caused by intensive use of fossil fuels have already started to affect our everyday lives and have severe consequences on Earth's ecosystem. Melting polar ice caps, higher seismic activity, hurricanes, retreating glaciers, rising sea level, higher concentration of ozone in the lower atmosphere, extreme weather and nature under risk are some of the consequences of the global warming. The economic consequences are also visible such as the recent growth of the oil price in 2008 when the oil prices overreached the level during the oil crisis in the seventies. Naturally expected lack of the fossil fuel sources supported by actual economic crisis and by numerous climate-related incidents will most likely increase the cost for energy even further. World primary energy consumption decreased by 1.1% in 2009, which is the first decline since 1982. Figure 1.1 illustrates primary energy consumption showing that oil is still the world leading fuel while coal remains the fastest-growing fuel [1].

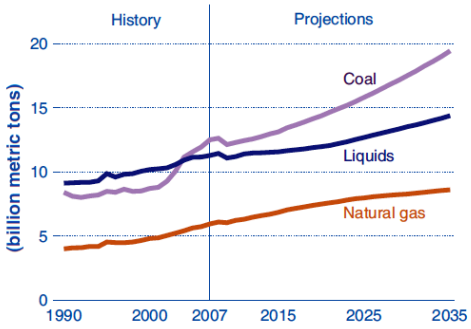

Figure 1.2 World energy-related carbon dioxide emissions by fuel type [3]

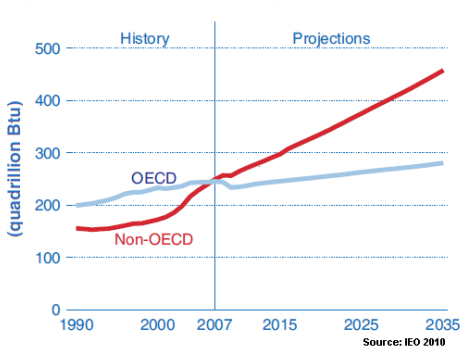

Figure 1.3 World energy consumption in developed and developing countries [3]

In response to rising concerns about climate change, world governments gathered in Japanese town Kyoto adopted the protocol which identifies fiscal and regulatory measures at local, national and international levels in order to begin the battle to tackle climate change. The Kyoto protocol set the legally binding targets on greenhouse gas emissions from industrialised countries. This protocol was only the first step in the fight against climate change. Much more efforts and long-term commitments have to be made by international community to avoid potentially disastrous impacts. Rising carbon dioxide emission and prediction which is not promising (Figure 1.2) have forced all major countries to intensify their efforts in this battle since the emissions reduction commitment under the Kyoto protocol would not be enough. A crucial

element is that both developed and developing countries need to take the action. In order to fight against climate change, EU adopted the climate and energy package in 2009 [4] which focuses on greenhouse gases cuts, increasing use of renewables and improved energy efficiency. The package includes the amount of money which needs to be invested in low-carbon development, innovative sources of international funding, an international carbon market by 2015, and steps to help countries to adapt to climate change.

The current energy systems, which are based on fossil fuels, are largely responsible among others for the present environmental and economic crisis. A significant contributor to the primary energy consumption of both developed and developing countries are electrical air-conditioning units. The continued rise in living and working comfort conditions with reduced prices of air-conditioning units and lower electricity prices have caused a great expansion of these systems. Worldwide sales of room air-conditioners are rapidly growing [5]. The consequence is the negative impact on electricity demand and environment. Projected cooling and heating energy demands shows a rising trend in next decades (Figure 1.3). The direct emissions from buildings together with the indirect emissions coming from the electricity use are responsible for 30% of global CO_2 emissions according to the International Energy Agency [6].

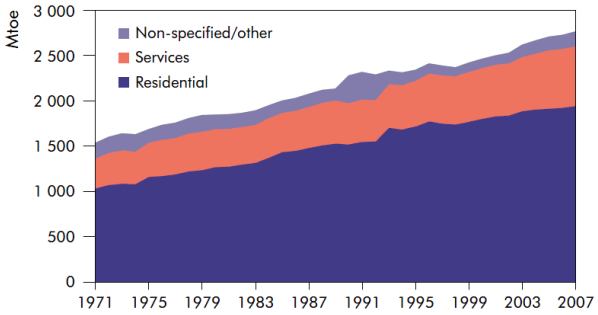

Figure 1.4 Energy consumption of buildings by sector on global level [6]

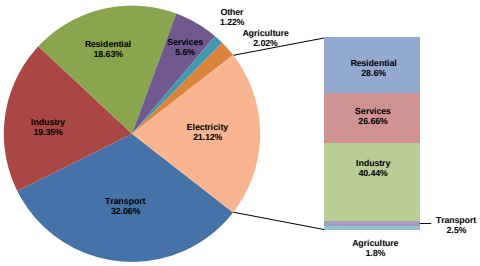

Figure 1.5 EU-27 Breakdown of final energy consumption between sectors and final electricity consumption in 2007

In general, buildings are responsible for nearly 40% of the world's total final energy consumption [6]. Between 1971 and 2007, total energy consumption in the building sector grew by 1.6% a year (Figure 1.4). An important part of that energy refers to electricity used for space and water heating and air-conditioning. Electricity

generation in the EU-27 grew, on average, by 1,7% annually between 1997 and 2007 [7]. During the 2007, the tertiary (services) and residential sectors were responsible for 55% of total electricity consumption in the EU (Figure 1.5). One third of total electricity consumed in buildings was used for space and water heating and air-conditioning [8]. The same trend is visible in other leading industrial countries. The building sector in the United States recorded annual growth of 3.1% from 1995 to 2007. In addition, the share of electricity in total energy consumption increased from 41% in 1990 to 49% in 2007. In 2006, residential and commercial sector consumed 72% of total electricity production according to DOE report [9] while around 27% of that amount was used for space and water heating and air-conditioning. On the other side, energy consumption in China has increased rapidly in the last decade as a result of tremendous economic growth. Total final energy consumption nearly doubled from 2000 to 2007. Over the same period, electricity consumption in buildings increased almost three times. Similar situation is in India, where electricity used in buildings multiplied by factor of 3 in a period between 1990 and 2007. Brazil, Russia, India, China and the Middle East as the fastest emerging world construction markets have a strong potential for further growth in demand for comfortable indoor conditions.

These world energy demand trends and rising concern about climate change have promoted renewable energy technologies as highly promising solution. These technologies use the sun's energy and its direct and indirect effects on the earth (solar radiation, wind, falling water, and various plants: i.e. biomass) as the resources from which the energy is generated. Nowadays, significant progress is made by improving the collection and conversion efficiencies, lowering both initial and maintenance costs, and increasing the reliability and applicability of renewable energy systems. The use of solar energy for cooling has the advantage of synchronization between solar irradiation and cooling demand and can result in an interesting alternative for conventional systems. Another potential alternative is the use of the waste heat form Combined Heat and Power (CHP) plants to produce cooling. Solar assisted air-conditioning and CHP plants are an emerging market with huge growth potential. Summer peak loads associated with high availability of solar radiation and use of waste heat offer an excellent opportunity to exploit energy with heat-driven cooling machines. Many different technologies are available for solar cooling and CHP. However, absorption

systems are by far the dominating technology which has been applied in numerous applications.

1.2. Background and motivation

Absorption machines[1] provide opportunities for energy saving because they can use heat to produce cooling (or heating, if necessary), instead of electricity used by conventional compression machines. They are based on sorption process where a liquid or solid sorbent absorbs refrigerant molecules into its inside and changes physically and chemically in the process. Physical or chemical attraction between a pair of substances is used to produce cooling effect. Thermal energy is directly transformed into cooling power, and therefore, shaft power is not required. In this way, where power is expensive or unavailable or where is solar, waste, gas, geothermal or heat available, absorption machine provide reliable and noise-free cooling. Another advantage of absorption machines is that they use environmentally friendly working fluid pairs which do not deplete the ozone layer of the atmosphere, contrary to most working fluids in conventional compression machines. Absorption machines have been present at the market for a long time. Commercially available absorption chillers range in capacity from medium (50-300kW) to high (300kW and up). They have been successfully implemented in a great number of large-scale solar cooling systems and CHP applications for large commercial building and industrial applications. However, the interest in small capacity absorption machines (less than 50kW, especially less than 20kW) has started growing in the last two decades with concern about the environment and increasing cooling demand in residential and small size office applications. The initiative which began with the International Energy Agency (IEA) Task 25 [10] and continued with IEA Task 38 [11] has given the results and today we have few small capacity absorption units released to the market. The market potential for small-scale cooling systems with absorption chillers is very large, but the full potential of these systems is far from being realised. Despite the economic advantage of solar cooling and CHP systems, which results from much lower operation costs (power, water and maintenance) and reduced CO_2 emission, there are many flaming issues to be solved in order to be profitable and competitive to the conventional compression systems. The

[1] Term “absorption machines” refers to both absorption chilers and absorption heat pumps

results obtained during the monitoring of around 150 small-scale solar cooling systems based on absorption within IEA Task 38 and the study of Henning [12] gave some experience and hints for improvements. Field data and experience gained from installations under real operating conditions have shown that there are frequent shortcomings in the system's hydraulic design as well as with the control. The design phase for these systems requires a greater effort than a conventional system for the same application. That often requires computer simulations of different system configurations in order to identify the one with the best energy-cost performance. Also, special care has to be given to the electrical consumption of the auxiliary equipment. A control strategy of the absorption machine is maybe the most delicate issue. It often requires sophisticated control to increase overall performance. Thus, improvements in the performance of these thermally driven machines play a key role in order to approach economic feasibility.

Bearing in mind that small-scale commercial absorption machines are still the technology in its infancy, there is a lack of adequate standards, best practice guidelines and test procedures for their evaluation which exist in the case of conventional compression machines. The manufacturer catalogues often provide very poor information about the absorption machine's performance. Performing a comprehensive performance analysis based on real operating data is still the best method for their evaluation. This is the main reason why experimental work with this equipment in appropriately equipped and monitored test facilities is essential for their further improvement. Sometimes, the machine assembly does not permit access to internal parameters, and performance should be analysed by measured parameters of external circuits. On the other hand, almost all experimental works are based on analogy with large-scale absorption systems, compression systems or on researcher's experience. Besides, trends toward improved system energy efficiency have changed, depending on the actual conditions for specific applications. Therefore, there is a need for methodology which would comprehend all the knowledge collected in this field. This methodology should cover all important steps necessary for efficient experimental work and data analysis in order to obtain a complete performance map of small capacity absorption machine. The experimental data are the first important step for obtaining precise and reliable mathematical models which are crucial for further development.

The importance of modelling was emphasized by several authors [13, 14]. The modelling allows engineers to assess different operating strategies of absorption machines in order to find the most economic operating conditions and to develop optimal ways of control in air-conditioning systems. Despite the fact that various authors have reported the work on absorption chiller modelling [15-18], there is no a reported study which would compare different modelling approaches as, for instance, in paper reported on vapour compression chiller modelling [19]. A comprehensive study which considers the both physical and empirical modelling approaches, compares the differences and provides a guideline for further use of the models.

With respect to all the facts stated above, this thesis contributes important knowledge and methods for performance evaluation and modelling of small capacity commercial absorption equipment when only external measurements are accessible. This is an important issue for integrating this kind of equipment in systems which reduce energy consumption and provide environmental benefits in residential and light commercial buildings. Different modelling approaches developed in this thesis will help software developers to find suitable method to simulate the interaction of the absorption machine with other parts of a system: energy supply side, heat rejection side and chilled water distribution side with different indoor air conditions and various load profiles. The thesis aims to give assistance to overcome shortcomings such as insufficient system design and control strategy selection of this innovative and promising technology.

1.3. Aims and objectives

The aim of this thesis is to produce a comprehensive methodology of testing, modelling and control strategy development for small capacity absorption machines. Reliable and accurate test dataset allows development of several mathematical models, which describe small capacity absorption machine behaviour under various operating conditions. These models can be further used for testing and validating different control strategies as well as to provide the basis for optimizing the operation of absorption machine in air-conditioning systems. The methods demonstrated in this thesis can be widely used both in experimental work and in building energy system design.

In order to achieve this aim, the following objectives were defined:

- Comprehensive literature review on absorption technology and standards with special care to small capacity absorption machines and their integration in solar-assisted air-conditioning systems and micro-CHP systems

- Literature review on different modelling approaches applicable to absorption machines and possible control strategies

- To develop simple procedure for testing small-scale commercial absorption equipment which can provide complete performance evaluation of the same based only on the external measurements

- To choose and install small-capacity commercial absorption unit in a state-of-the-art test bench. The experimental results of the absorption unit will also serve to validate this novel test bench

- To establish a simple analytical procedure to assess the performance of the absorption machines based on the collected data, by using previous research works and experience in this field

- To develop a data-filter which detects when absorption machine operates in steady-state regime based on statistical approach and relevant standards

- Estimation of uncertainty in measurements

- To develop various steady-state models based on experimental results using both physical and empirical approaches: from thermodynamic modelling to grey and black box models

- To develop optimal control strategies based on these models which can be implemented in on-line control systems

1.4. Research approach

To achieve research objectives, this thesis focuses on equipment installation and test in an state-of-the-art test facility, data analysis, model development and

development of optimal control strategies using novel approaches such as Artificial Neural Networks (ANN) and Genetic Algorithms (GA). Experimental data and computational models are two basic components of this work. The experience gained during the PhD period has been transformed in a form of specific guideline for other researchers in this area, as a step by step procedure from test planning through experimental work, data analysis to model and control strategy developments where the final product can be useful for simulation software developers or control engineers.

1.5. Structure of the thesis

This thesis is divided into seven Chapters and three Appendixes where each Chapter is written in a way that it also can be observed as a separate entity depending on interest of future readers.

Chapter 1 describes the current energy situation and points out the main culprits for the excessive consumption of primary energy and the negative impact on the environment. The need for research in the field of small capacity absorption machines is highlighted as a possible solution for conventional compression systems. The research objectives have been selected and justified as well as the research approach which was used to achieve these objectives.

Chapter 2 is an overview on absorption systems. The aim of this Chapter is to help the reader to fully understand the absorption machines, their fundamental principles and applications. A state of the art of small capacity absorption machines is presented in the framework of the two most promising technologies: solar thermal and Combined Cooling Heating and Power (CCHP). Based on comprehensive literature review, Chapter 2 covers techno-economic aspects as well as the opportunities and obstacles to further development of small capacity absorption machines.

Chapter 3 introduces a state of the art test bench as useful and necessary tool for experimental work with small absorption machines. Based on existing standards for absorption equipment and necessary instrumentation, this multifunctional test bench provides a wide range of opportunities for testing in various applications under different conditions. Different operating modes and required equipment are explained in detail.

Chapter 4 deals with the testing procedures for small capacity absorption machines, in particular with commercial units and prototypes. This is an attempt of creating standard procedure based on previous achievements and experience in this field in order to create the complete performance map of the absorption machine by having only external measurements and to generate database for absorption machine modelling. Illustrated with examples of two commercial absorption units, this procedure is a step by step guide that covers data analysis, development of a steady-state regime detector and estimation of uncertainties.

Chapter 5 deals with modelling of small capacity absorption units based on experimental database. Five different models have been developed using both physical and empirical methods. Models are discussed in detail and evaluated through the prism of statistical parameters. Special attention is given to ANN modelling.

Chapter 6 is addressed to the control issues of small capacity absorption machines. This Chapter shows how developed models can be used for development of different control strategies which can be implemented in on-line operations. Optimal control was demonstrated by implementing optimization methods such as Nelder-Mead simplex algorithm and genetic algorithms.

Chapter 7 summarizes all the results and work done in this thesis providing the perspective for future research at the same time.

Appendix A lists the additional indicators which can be used to evaluate the performance of absorption machines.

Appendix B presents the detailed explanation of uncertainty analysis procedure.

Appendix C contains the tables with detailed test results.

Chapter 2

An overview on absorption technology

"Without continual growth and progress, such words as improvement, achievement, and success have no meaning."

Benjamin Franklin

2.1. Historical development

The roots of absorption technology can be traced to the mid of 17th century and the works of Dr. William Cullen and Nairne, as indicated in the comprehensive study of Burgett et al. [20]. In the year 1823, Michael Faraday demonstrated that absorption of ammonia gas can be used for cold production. Faraday used U tube where the cooling effect was produced on one side by evaporating the ammonia and absorbed by silver nitrate on the other side. Twenty-two years after, Edmund Carre designed and sold a water-sulphuric acid machine which was used for cooling a drinking water. Shortly after, in the year 1851, his brother Ferdinand released to the market the first successful ammonia-water absorption refrigeration system. Some years later, in 1862, Mignon and Rouard built the first ammonia-water machine of continuum cycle. Subsequent years brought numerous improvements but nothing so crucial until 1913 when Edmund Altenkirch established the thermodynamics of binary mixtures in absorption. The work of Altenkirch contributed to the rising interest and development of absorption refrigeration systems in following years. The period between two World wars was marked mostly by disclosures of two companies in the field of refrigeration: Electrolux in Sweden and Servel in the USA. The period after the Second World War is known as the Golden Age of Absorption, especially in the USA where the HVAC industry was booming with respect to absorption machines. The use of LiBr-H_2O as working pair, new disclosures and fast development of large capacity single-effect absorption machines, first by Carrier (1945) and then by other leading HVAC companies (Trane, York, Worthington) contributed to the penetration of absorption technology on the US market. The sale of absorption chillers reached their peak in 1969, with one quarter of the US market (1000 sold units). Primarily the oil crisis in 1973 as well as the

development of higher efficient vapour compression equipment caused the sharp fall of interest for the absorption technology, leaving the share of annual sales in the USA on the sidelines. On the other side of the globe, Japan started its post-war recovery. Faced with shortage of its own natural energy resources and very expensive electricity produced from Middle East oil, Japanese Government promoted natural gas as favoured fuel. Japanese companies Kawasaki, Mitsubishi, Ebara, Sanyo, Hitachi and Yazaki became aware of the possibility to improve efficiency of the absorption equipment by using high temperature energy sources. The era of double-effect, indirect fired absorption units have started in 1964, when Kawasaki released their unit to the market. Further improvements of double-effect absorption machines and gas oriented policies caused that large absorption equipment surpassed the electric chillers in 1975 for the first time and a decade later, absorption chillers had more than 80% share of Japanese large capacity market. The role of Japan as world leader in this field had a positive impact on other countries in the Far East. Nowadays, India, China and Korea have a very important role in the distribution of world market for absorption equipment. For example, 6917 absorption chillers of around 12000 released to the market in 2005 were manufactured in China [21]. Still, the share of absorption equipment in air-conditioning and refrigeration is far from the share of conventional vapour compression equipment.

In the last three decades, after Montreal and especially after Kyoto protocol, the interest in absorption equipment has become topical as a possible solution to the rising concern of protecting the ozone layer. Environmental friendly fluids, as well as possibility to use solar energy and waste heat make this equipment very interesting for further research and development. The technological progress, particularly the progress of solar collectors, has opened new horizons for absorption equipment. However, lots of research efforts have to be done in order to make absorption equipment fully competitive with conventional compression equipment in terms of both efficiency and profitability.

2.2. The basic principles of absorption cycle

The common approach to explain the absorption refrigeration cycle is by comparing it with the more familiar vapour compression cycle. The working principle of the absorption cycle is similar to that of the vapour compression cycle with two main differences. The first difference is that absorption cycle is heat-driven thermal cycle, where only thermal energy is exchanged with surroundings. No appreciable mechanical energy is exchanged (or conversion of heat to work) as in the case of mechanical compression cycle [22]. The second difference with respect to vapour compression cycle is existence of secondary fluid in addition to the refrigerant, known as liquid sorption medium or absorbent. Accordingly, the basic idea of absorption cycle is to avoid compression work by using the suitable working pair: a refrigerant and a solution which can absorb the refrigerant.

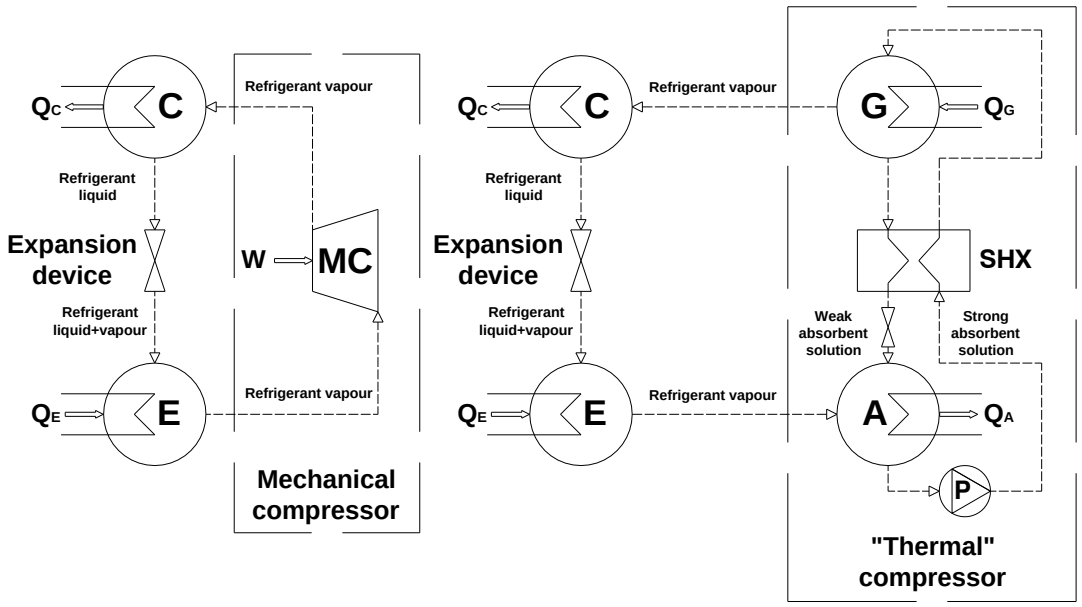

Figure 2.1 Compression and absorption refrigeration cycles

In the absorption cycle (Figure 2.1), the role of the mechanical compressor in compression cycle is replaced by "thermal compressor" which consists of generator, absorber, solution heat exchanger, solution pump and throttling valve. Just like the vapour compression cycle, the absorption cycle operates under two pressure levels. High pressure level (refrigerant separation side) corresponds to the condenser-generator

while low pressure level of absorption process in vacuum corresponds to evaporator-absorber. The high pressure level is approximately ten times higher than low pressure level in order to allow the heat rejection of the refrigerant at commonly available temperatures. The working principle is based on different boiling temperatures of the refrigerant and the absorbent. External heat input in the generator causes that refrigerant is boiled out of a solution and compressed to the refrigeration vapour at higher pressure while the concentrated absorbent stays liquid. The hot refrigerant vapour flows to the condenser where heat is removed by external heat sink, condensing the refrigerant vapour to liquid. The high-pressure liquid then passes through an expansion device reducing its pressure to the evaporator pressure level. External heat input causes a refrigerant to evaporate. The low pressure refrigerant vapour is then passed into the absorber where it condenses diluting the concentrated absorbent coming from the generator. The diluted solution (rich in refrigerant) is then pumped back to the generator where it evaporates again, closing the cycle. In other words, the "thermal" compressor of the absorption cycle uses a heat-driven concentration difference to move refrigerant vapour from the evaporator to the condenser.

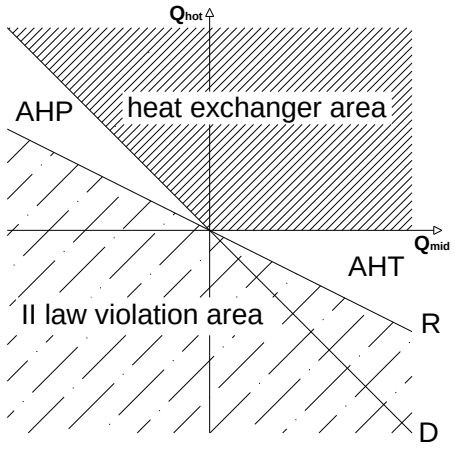

Figure 2.2 I and II law analysis of thermal cycles

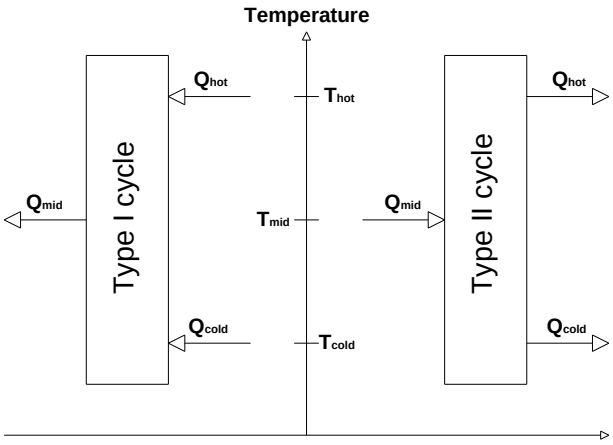

Figure 2.3 Thermal cycles

The simplest device based on any absorption cycle (stands also for any heat driven cycle) transfers the heat at three temperature levels with their surroundings. Herold et al. [23] and ASHRAE Fundamentals [22] discuss this topic in more detail. By applying the First and the Second Law of Thermodynamics:

$$Q_{hot} + Q_{cold} = -Q_{mid} \tag{2.1}$$

$$\frac{Q_{hot}}{T_{hot}} + \frac{Q_{cold}}{T_{cold}} + \frac{Q_{mid}}{T_{mid}} \geq 0 \tag{2.2}$$

and combining these equations (2.1 and 2.2) we can obtain the relation between Q_{hot} and Q_{mid} (equality stands for ideal case-reversible cycle):

$$Q_{hot} \leq -Q_{mid} \cdot \frac{T_{mid} - T_{cold}}{T_{mid}} \cdot \frac{T_{hot}}{T_{hot} - T_{cold}} \tag{2.3}$$

Using two additional lines, one for the ditherm-machine D ($Q_{hot}=Q_{mid}$) and another for the reversibility of entropy balance R, it is possible to plot the diagram which shows where energy exchange between the thermal machine and surroundings is possible and where are the limitations on cycle performance. Figure 2.2 shows that bellow the reversibility line we have the second law violation and in shaded area above we have only heat transfer from high to low level. The interesting zones for energy upgrading are the ones depicted as AHP and AHT. Therefore, there are two possible variations of this thermal (absorption and any heat driven) cycle. In the first variation the driving heat is the input at highest temperature level and the output is either cooling at the lowest temperature level or heating at the intermediate level as illustrated on the left side of Figure 2.3. This type of absorption cycle is called Type I cycle (also known as heat amplifier, heat pump, conventional cycle or forward cycle). The temperature indicated on the vertical axis represent the thermal boundary conditions with which machine have to interact. The heat flows into or out of the cycle at different temperature levels determine the cycle performance. Combining the equations (2.1) and (2.2) in another way the performance of the cycle can be represented as ratio of the produced cold divided by supplied heat, known as the coefficient of the performance (COP):

$$COP_{cooling} = \frac{Q_{cold}}{Q_{hot}} = \frac{T_{hot} - T_{mid}}{T_{hot}} \cdot \frac{T_{hot}}{T_{hot} - T_{mid}} \tag{2.4}$$

Equation (2.4) stands for absorption device made for cooling purpose, i.e. chiller. Since the distinction between a chiller and a heat pump is only function of the

application, the coefficient of performance for the absorption device with heating purpose would be (2.5):

$$\mathrm{COP}_{\mathrm{heating}} = \mathrm{COP}_{\mathrm{cooling}} + 1 \tag{2.5}$$

The second variation of the absorption thermal cycle is so-called Type II cycle (also known as heat transformer, temperature amplifier, temperature booster or reverse cycle), which is illustrated on the right side of Figure 2.3. The purpose of this cycle is to use heat from intermediate temperature level to convert it to high temperature heat. At the same time, as a consequence of the second law of thermodynamics, part of input heat has to be rejected at lower temperature level. However, while Type I cycle have found wide use in numerous HVAC and refrigeration application, with long existing market for these equipment, Type II cycle have been demonstrated at laboratory level and in pilot installations. Industrial applications with the absorption heat transformers are very rare, and most of them can be found in Japanese industry [24].

2.3. Classification

The absorption machines can be classified based on several criteria: main function, firing method, number of effects and stages, condensing method, working fluids, application and capacity.

With respect to the main function, the absorption machines can be classified as:

- Absorption chiller: to produce chilled water
- Absorption chiller/heater: to produce chilled and hot water
- Absorption heat pump: to produce hot water or steam by heat pump action
- Absorption heat transformer: to produce heat on higher temperature level using the mid-temperature level as explained in Section 2.2

With respect to the firing method absorption machine can be:

- Indirect fired: driving heat is recovered from another process or heat cycle machine. The driving heat to generator is normally delivered through an intermediate element (heat exchanger). This heat in the form of steam, hot liquid or hot exhausted gases is typically supplied by solar collectors, district heating network, boiler, gas turbine or by some other heat recovery device.

- Direct fired: driving heat comes from combustion of fossil fuels. As a result, these systems normally contain a liquid fuel or natural gas burner.

Within this classification, various subclasses can be made. Thus, depending on the type of heat source exist: steam-driven, fuel-driven, exhaust gas-driven and hot water-driven machine, etc. Also, a division on low, medium and high-grade heat equipment can be made with respect to the activation temperature level in the generator.

In order to increase the efficiency, the basic absorption cycle which consists of four basic components (generator, absorber, evaporator and condenser) can be extended with one or more components at different pressures or concentrations. With respect to the number and type of additional components, absorption machines can be categorized by the number of effects or by the number of stages. According to terminology adopted from Dorgan et al. [25], the term effect refers to the number of times the driving heat is used by the absorption equipment, or simplified, the number of generators determines the number of effects. In this way, we can distinguish between single-effect, double-effect or triple-effect systems. Similarly, multistage absorption systems (single-stage, double-stage or triple-stage) differ by the number of basic cycles (single-effect) that are combined. Simplified, the number of evaporator/absorber pairs at different temperatures in absorption machines determines the number of stages.

With respect to the employed condensation method (which fluid is used for heat dissipation in the absorber and condenser), absorption machines can be classified to:

- Air-cooled: the heat fluid is air and heat dissipation is normally realized through an air-condenser. These equipment can also be indirect (heat transfer from the absorber and condenser firstly to a closed water loop

and then to the ambient air) or direct (heat rejection directly to the surroundings).

- Water-cooled: the heat fluid is water and heat dissipation is normally realized through a cooling tower.

Another classification is by the type of working pair used in the absorption machine. The most common working pairs are water-lithium bromide (H_2O-LiBr) and ammonia-water (NH_3-H_2O) but there are also others which will be more discussed in the following section.

Absorption machines can also be classified by working mode. The phases inside the absorption cycle can be processed continuously or shifted periodically; and therefore, we can distinguish between:

- Continuous mode
- Semi-continuous mode and
- Discontinuous (batch) mode equipment.

With respect to the application purpose and based on cooling temperature demand, absorption machines can be divided into three categories:

- Space air-conditioning (7-18ºC)
- Food and pharmaceutical storage refrigeration (0-7ºC)
- Freezing (<0ºC) for ice-making or congelation.

Finally, absorption equipment (particularly absorption chillers) can be ranged according to the produced cooling capacity:

- Large-scale absorption chillers: cooling capacity higher than 300kW
- Mid-scale absorption chillers: cooling capacity between 50 and 300kW
- Small-scale absorption chillers: cooling capacity up to 50kW

The last classification might look somewhat arbitrary since some authors move the boundary for small-scale absorption chillers to 20kW and others to 30kW. Anyway, the logical explanation would be that the classification is market dependant, i.e. depends on the capacity of the units which can be found at the market.

2.4. Working fluids

The performance and efficiency of absorption systems is directly correlated with the chemical, thermo physical and thermodynamic properties of the working fluid. A margin of miscibility in liquid phase within the operating temperature range of the absorption cycle is one of the fundamental requirements for suitable absorbent/refrigerant combination. The suitability of the absorbent/refrigerant pairs is determined by several necessary or desirable properties, which have been subject of various studies in the past. A summary of these properties is given in following paragraphs. It is preferable that the latent heat of the refrigerant is high in order to minimize the circulation rate of the refrigerant and absorbent. Operating pressure of the refrigerant should be moderate while for the absorbent operating pressure is recommendable to be low. The refrigerant should have low freezing temperature and should be much more volatile than the absorbent in order to separate them easily. The refrigerant and absorbent should be chosen in a way to avoid solid phase over the expected range of composition and temperature, otherwise, inappropriate choice can cause operation shut down. Also, the chosen absorbent should have a strong affinity for the refrigerant. High chemical stability is required to avoid unwanted formation of gases, solids, or corrosive substances. Physical properties such as viscosity, surface tension, density, thermal conductivity, specific heat capacity, heat of mixing and mass diffusivity should be favourable for suitable selection of the working pair. Thus, low viscosity increases heat and mass transfer and reduces pumping power. The low toxicity of the working pair is another important parameter in order to avoid negative impact on the environment. The care has to be taken with respect to corrosion and flammability, too. However, the desirable properties are sometimes mutually exclusive and it is very difficult (if not impossible) to find a working pair which fulfils all the requirements. More precisely, it is a matter of compromise.

Many working fluids have been considered for absorption systems. One of the most exhaustive studies which can be found in the literature is the review of absorption fluids provided by Macriss et al. [26] which discloses 40 refrigerant compounds and 200 absorption compounds available. Another exhaustive study is the report of IEA Heat Pump Centre with survey [27] which updates previous report with some additional mixtures. Nevertheless, the most common working fluids with practical application in absorption systems are H_2O-NH_3 and LiBr-H_2O. Recently, with new trends in absorption machines presented by Gluesenkamp et al. [28], the promising results have been found in experiments with ternary (LiBr, $LiNO_3$ and LiCl) and quaternary (LiBr, LiI, $LiNO_3$ and LiCl) salt mixtures. These mixtures were subject of investigation of several authors [29, 30]. A summary of the possible working pairs for absorption systems is shown in Table 2.1.

Table 2.1 Summary of working pairs for absorption systems

Refrigerant	**Absorbent(s)**
H_2O	Salts
	Alkali halides
	LiBr
	$LiClO_3$
	LiBr based multi-component salt mixtures (LiBr + single salt, LiBr + binary salt systems, LiBr + ternary salt system)
	$CaCl_2$
	$ZnCl_2$
	ZnBr
	Alkali nitrates
	Alkali thiocyanates
	Bases
	Alkali hydroxides
	Acids
	H_2SO_4
	H_3PO_4
NH_3	H_2O
	$LiNO_3$
	$LiNO_3 + H_2O$
	Alkali thiocyanates
TFE (Organic)	NMP
	E181
	DMF
	Pyrrolidone
SO_2	Organic solvents

However, the great majority of commercial absorption equipment uses traditional working pairs such as H_2O-NH_3 or LiBr-H_2O [28]. The only "intruders" are H_2O-LiCl and NH_3-$LiNO_3$ mixture. The following sections discuss more closely the advantages and disadvantages of four working pairs.

2.4.1. Water-Lithium Bromide (H_2O-LiBr)

One of the two most common working pairs is water-lithium bromide, which has been used in absorption equipment since 1950s. Lithium bromide is a salt and drying agent. The lithium ion (Li+) in the lithium bromide solution has a strong affinity to the water molecules, which is essential to produce absorption cooling effect. The advantages of this working pair include high safety, volatility ratio, affinity, stability and latent heat. Water is the refrigerant, which evaporates at very low pressures producing the cooling effect. Since water freezes at bellow 0°C, the minimum chilled water temperature in the absorption system with H_2O-LiBr is around 5°C. This is the reason why these systems are used for air-conditioning applications and cannot be used for low temperature refrigeration. These systems operate under high vacuum pressures. For the large-scale H_2O-LiBr systems, the vacuum pumps are necessary to maintain the vacuum inside the equipment and to eliminate unwanted gases. H_2O-LiBr mixture is miscible if the LiBr mass fraction is lower than 70%, approximately. Consequently, this determines the maximum limit for the absorption temperature. The LiBr crystallization occurs at moderate concentrations, which normally limits the pair where the absorber is water-cooled and the concentrations are lower. On the other hand, some recent systems can use air for heat dissipation. The phase boundaries are usually included on the working fluid diagrams to remind on the proximity of the crystallization risk as shown on Duhring plot in Figure 2.4. Normally, an internal control system is installed inside the absorption equipment to assure operation under predetermined range, and therefore, to avoid crystallization.

The lithium bromide solution is corrosive to some metals used for construction of absorption equipment (i.e. steel or copper). Corrosion inhibitors may be used to overcome this problem. These additives protect the metal parts and can improve heat and mass transfer performance.

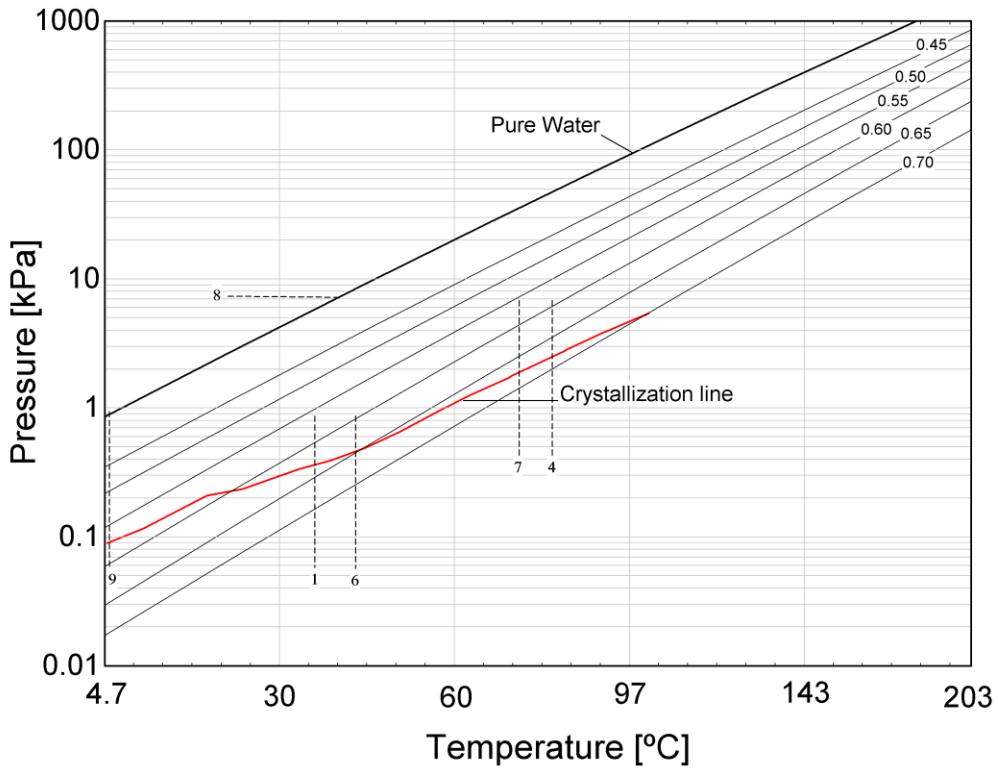

Figure 2.4 Pressure-temperature diagram for H_2O-LiBr (Duhring plot)

2.4.2. Ammonia-Water (NH_3-H_2O)

Ammonia-water working pair is one of the oldest working pairs, which has been in use since the 18th century. Ammonia as the refrigerant offers the opportunity to operate with evaporating temperatures below 0ºC. Generally, ammonia-water is used for refrigeration applications in the range from 5ºC down to -60ºC. It can also be used for air-conditioning, but sometimes there are restrictions for use in building applications because of risks associated with the use of ammonia. The preferred heat source temperature for ammonia-water equipment is from 95ºC to 180ºC. The absorption systems with this working pair operate at moderate pressure and no vacuum is required till -30ºC. The advantage of this working pair is that ammonia is completely soluble in water (at all concentrations), and therefore, there is no risk of crystallization. Another benefit is that dry coolers can be easily applied in this case since the pressure in any part of the ammonia-water absorption system is higher than atmospheric pressure. The minimum pressure of the ammonia-water cycle is higher than 3 bars, and the pressure drop is not as critical as in the case of other conventional fluids. This also allows the use

of plate heat exchanges with extended surfaces and high heat transfer coefficients. This further assures compact design with reduced ammonia charge, and consequently, increased safety of the absorption system. On the other hand, operation at high pressures (in particular the pressure of high temperature generator) is the main reason why there are no double-effect absorption systems with ammonia-water. Also, ammonia is both toxic and flammable. Another disadvantage of ammonia is incompatibility with materials such as copper or brass. For that reason, steel is normally used as the construction material for ammonia-water absorption equipment. Finally, small temperature difference between the boiling points of the refrigerant and the absorbent requires an additional device to obtain a high purity vapour of the refrigerant. This device called rectifier cools the vapour produced in the generator, demanding more supply heat. The consequence is lower COP.

2.4.3. Ammonia-Lithium Nitrate (NH_3-$LiNO_3$)

Ammonia-lithium nitrate as the alternative working fluid for absorption cycles have been studied in the past by several authors. Infante Fereira [31] collected and correlated the thermodynamic properties reported by various authors. Oronel et al. [32] reported the study in which ammonia/lithium nitrate has been proposed as a working pair for absorption refrigeration systems driven by low temperature heat sources. The authors pointed out the main advantages and disadvantages of the NH_3-$LiNO_3$ mixture compared with conventional working fluids. When compared with water-lithium bromide mixture, the advantages of ammonia-lithium nitrate are:

- The absorption cycle does not operate under vacuum conditions (this permits less volume and not so heavy raw materials for absorption equipment)
- No risk of crystallization at the operation conditions of interest
- No required cooling tower (higher dissipation temperature than H_2O-LiBr)

The refrigeration cycle with ammonia-lithium nitrate can be operated at lower generator temperatures than with ammonia-water and does not require rectification of

the refrigerant vapour leaving the generator. On the other side, the main disadvantage of this mixture is high viscosity, which penalizes heat and mass transfer processes, especially in the absorber.

Until recently, this working pair was only studied at the laboratory level. However, cycle simplicity and a good potential for solar cooling applications have led to the construction of the first absorption chiller prototype with ammonia-lithium nitrate. Thus, the first operating results of one air-cooled ammonia-lithium nitrate absorption chiller can be found in the study of Zamora et al. [33].

2.4.4. Water-Lithium Chloride (H_2O-LiCl)

The last working pair which can be found with practical application in absorption equipment is water-lithium chloride. Although water-lithium chloride is more common in desiccant technology, this working pair is used for a specific absorption cooling technology called triple-phase absorption technology. Term triple-phase indicates that this technology employs three states of matter during the process: liquid, gas (vapour) and solid state. It is important to mention that triple-phase absorption is chemically driven instead of thermally driven absorption we are used to. Crystallization, which might happen in liquid phase and can cause the problems during the operation of the absorption equipment, occurs at lower concentrations than in the case of LiBr. However, in the case of LiCl, crystallization can be beneficial. In the absorption equipment with this technology, charging is achieved by means of a chemical process where energy is stored by the drying of the lithium chloride. By using the LiCl, the absorption machine differs from other absorption chillers that use LiBr, a chemical that is less sensitive to the low temperatures. Same as H_2O-LiBr, H_2O-LiCl working pair operates under vacuum conditions and the activation temperature are lower than in the case of NH_3-H_2O. Also, one of the drawbacks of this working fluid is a relatively high cost.

2.5. Configurations

This section discusses some of the possible configurations of the absorption cycle which can be found in absorption equipment already present at the market or, at least, in form of tested prototype.

2.5.1. Single-effect absorption chiller

The simplest absorption cycle configuration, single-effect (or single-stage) absorption chiller shown in Figure 2.5, consists of a generator, a condenser, an evaporator, an absorber, solution heat exchanger, solution pump and two expansion devices (throttling valves). In the generator, absorbent/refrigerant solution receives heat from a high-temperature energy source (steam or hot water). The "weak absorbent" solution starts to boil, separating refrigerant vapour from the concentrated absorbent solution.

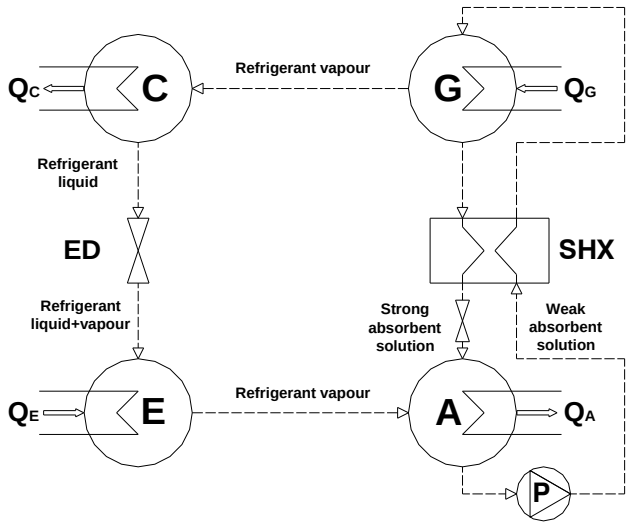

Figure 2.5 Single-effect absorption chiller

The hot refrigerant vapour continues to the condenser, while the concentrated solution ("strong absorbent solution") returns to the absorber. In case when ammonia-water is used as working fluid, an additional device called rectifier is needed to provide the purity of the refrigerant. The vapour generated in the generator contains a certain amount of water as a consequence of close pressure levels of ammonia and water vapour. Inside the condenser, refrigerant vapour condenses transferring the heat through

the external heat carrier (usually water) circuit. The external heat carrier circuit is typically connected to a cooling tower or a dry cooler enabling the heat rejection to the surrounding. The condensed liquid refrigerant flows through an expansion device into the evaporator. The purpose of the expansion device is to reduce the refrigerant pressure and temperature to the desired evaporator conditions. Inside the evaporator, the refrigerant receives the heat from another external heat carrier circuit and evaporates, producing the cooling effect on the circulating water. The low pressure refrigerant vapour then proceeds to the absorber where it is absorbed by the strong absorbent solution. The absorbed refrigerant vapour condenses to a liquid, releasing the heat received in the evaporator to the external heat carrier circuit. In absorption equipment, this circuit is usually designed to be common for absorber and condenser (cooling water circuit). The weak absorbent solution is then pumped through the solution heat exchanger to the generator where heat is used to separate the refrigerant again. The main function of the solution heat exchanger is to preheat the weak absorbent solution which goes to the generator with the heat released by strong absorbent solution returning from the generator. The single-effect configurations are predominating of all absorption configurations with all the previously mentioned working fluids applied in commercial units. The COP is around 0.7.

2.5.2. Double-effect absorption chiller

In a double-effect configuration (Figure 2.6), the refrigerant is separated from the absorbent by two stage generation. This means that besides the basic components, which are the same as for the single-effect chiller, it includes an additional generator, solution heat exchanger and pump. In principle, this chiller operates between three pressure levels. The energy source for double-effect chiller has to be at much higher temperature level than for the single-effect chiller. This heat is supplied to the high generator where refrigerant starts to boil and leaves the absorbent solution. The hot refrigerant vapour of the high pressure generator enters to the high condenser where the heat released during the process of condensation is used to drive the low generator at intermediate pressure. In practice, high condenser and low generator are incorporated in one heat transfer device where one side of the heat exchanger is the high condenser and the other side is low generator. The refrigerant vapour then enters to the low condenser

together with the liquid refrigerant condensed inside the tubes of the low generator. The refrigerant is then throttled before entering into the evaporator where the cooling effect is produced in the same way as in the case of single-effect chiller. All double-effect chillers consist of same components. However, there are three variations regarding the way in which the solution is circulated: parallel, series and reverse-series flow cycle. In the parallel flow shown in Figure 2.6a, the weak absorbent solution is divided between the low and the high generator. Within each of the generators, the weak absorbent solution is concentrated before returning to absorber section. Figure 2.6b shows the serial flow where the weak absorbent solution is pumped directly to the high generator and concentrated to an intermediate solution concentration. The resulting intermediate solution then flows to the low generator where is further concentrated before returning to absorber. Finally, in the reverse-series flow (Figure 2.6c), the weak absorbent solution is partially concentrated in low generator and then completely in the high generator. The concentrated solution returns directly to absorber, avoiding the low generator. These differences between the variations are mainly due to the preferences of absorption equipment manufacturers. The main benefit of the double-effect absorption chiller is higher efficiency obtained by using the input heat a second time. The COP is around 1.2 and only H_2O-LiBr commercial units are available (ammonia-water requires much higher pressures).

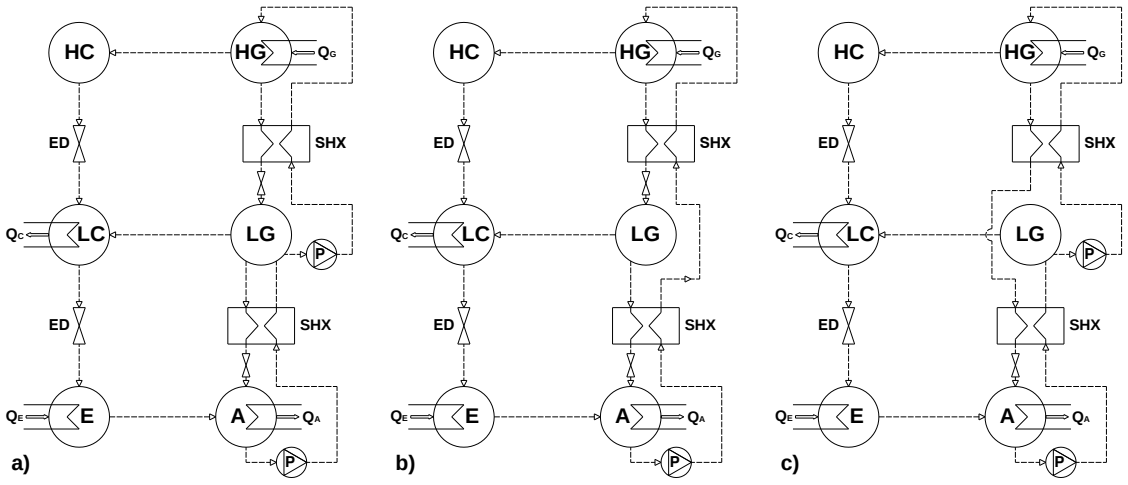

Figure 2.6 Double-effect absorption chiller

2.5.3. Triple-effect chiller

The easiest way to explain triple-effect chiller is as an extension of a double-effect absorption cycle which operates between four pressure levels (Figure 2.7). The triple-effect chiller has three generators and includes two internal heat processes (high condenser/mid generator and mid condenser/low generator). The refrigerant vapour from the high and mid generators is condensed and the heat is used to provide heat to the next lower generator. The refrigerant from all three condensers flows to the evaporator where the cooling effect occurs. The first H_2O-LiBr commercial unit has been developed and released to the market in 2005 with the COP of around 1.7 [34].

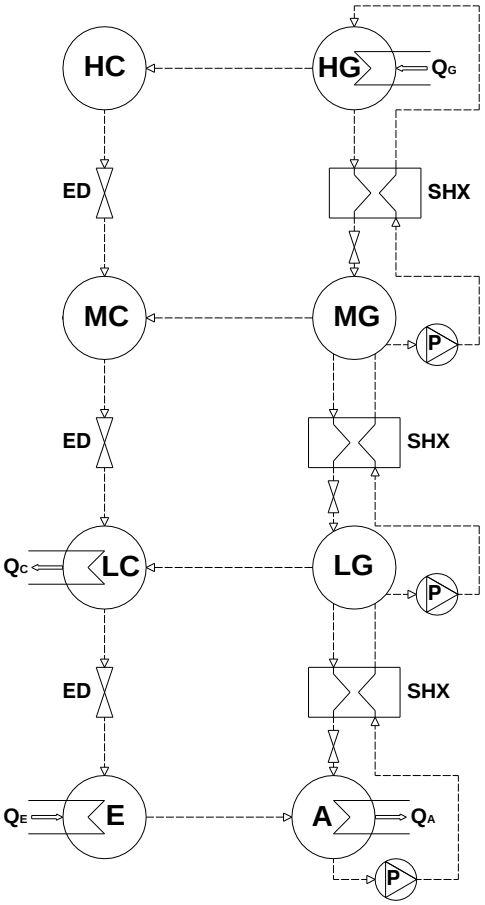

Figure 2.7 Triple-effect absorption chiller

2.5.4. Half-effect chiller

The half-effect chiller is considered for use when working with lower activation temperatures, lower than the minimum necessary to activate single-effect chiller. It

works between three pressure levels. The difference with respect to the single-effect chiller is intermediate pressure level with two additional components: absorber and generator (Figure 2.8). At this level, the refrigerant vapour from low generator enters to the high absorber. The refrigerant is then transported to the high generator through upper solution circuit where it evaporates a second time and proceeds to the condenser. The penalization for operation at lower temperatures is lower COP; approximately twice lower than of the single-effect cycle. That is the main reason why the cycle has been named half-effect, no matter it contains two generators and two absorbers.

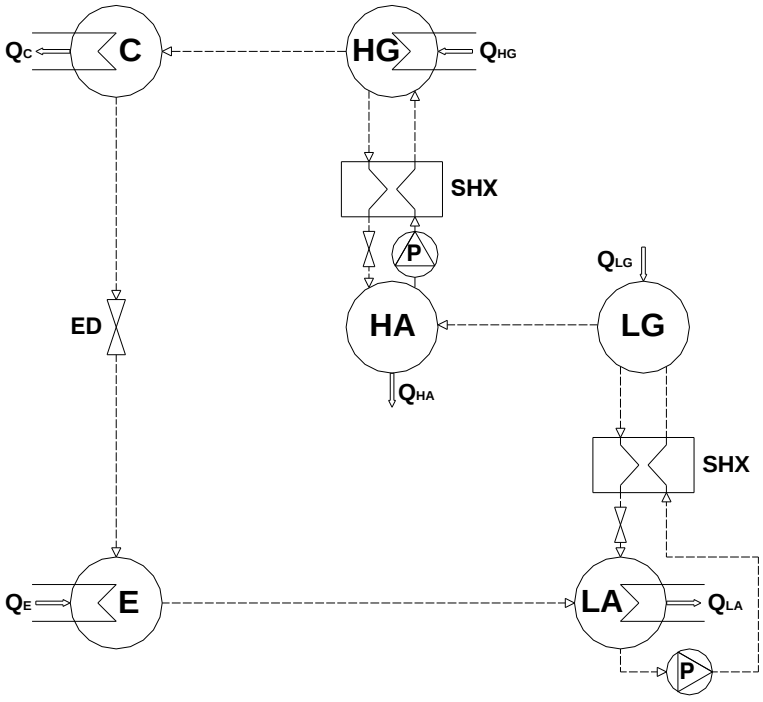

Figure 2.8 Half-effect absorption chiller

2.5.5. GAX (Generator Absorber heat eXchanger)

In the GAX cycle (Figure 2.9), the basic components are similar to the single-effect absorption cycle. The concentration in the absorber and generator are maintained in such a way that there is the possibility of temperature overlap between them. This gives the possibility for a heat recovery process by means of the internal transfer of the "overlapped" heat from the absorber to the generator. In this way, the external heat input required by the generator is reduced which has as a consequence efficiency enhancement visible in a higher COP. The GAX cycle can also be used for heating

providing the significant energy savings on an annual basis. The $COP_{cooling}$ for GAX chiller is around 0.9, while the $COP_{heating}$ for GAX heat pump is around 1.8. GAX chillers and heat pumps are potentially an ideal complement to the micro turbines and fuel cells due to the high operating temperatures of cycle.

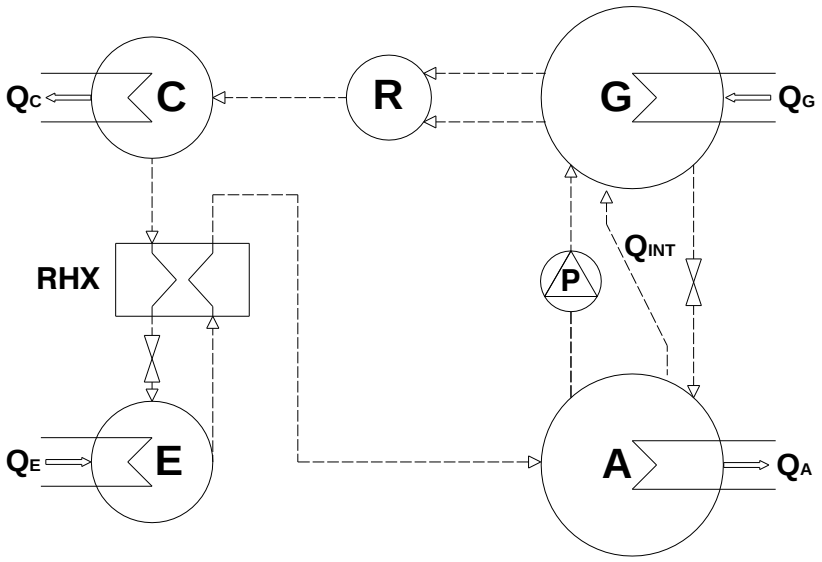

Figure 2.9 GAX

A summary of main parameters concerning different absorption cooling configurations existing at the market has been summarised in Table 2.2.

Table 2.2 Summary of absorption cooling technology

Parameter/Fluid	**LiBr-H_2O**				**H_2O-NH_3**		**H_2O-LiCl**	**NH_3-$LiNO_3$**
Effect	SE	DE	TE	HE[2]	SE	GAX	SE	SE
Nominal cooling capacity [kW]	4.5->7000	17->20000	530-1400	10	12-1000	10-250	10-20	10
Thermal COP	0.6-0.75	1.1-1.3	1.4-1.7	0.3-0.35	0.5-0.7	0.7-0.9	0.6-0.7	0.6-0.7
Heat source temperature range [ºC]	70-120	120-170	200-250	50-70 (60-110)	70-140	150-220	65-110	80-110

[2] Prototype, information found in [35]

2.5.6. Heat pump

As explained at the beginning of this Chapter, the distinction between a chiller and a heat pump is only a function of the application, i.e. which temperature level will be used. In the case of the absorption heat pump, this means that the driving heat at the highest temperature level is used to produce heating at intermediate temperature level. Since heat distribution units (fan-coils, radiators, etc) require higher temperature for building heating and DHW applications, the operating temperatures of the cooling water from absorber and condenser have to be at higher level (40-60ºC) than in case when it operates as chiller. Also, this further affects the evaporator to operate at higher temperatures as a direct consequence of the dependence between the three temperature levels within the absorption cycle [35].

2.5.7. Chiller/heater

Chiller/heaters are in principle direct fired chillers which can be used to provide both cooling and heating. This can be done in two ways. First way is to add an auxiliary heating bundle allowing the chiller to produce both hot and chilled water. The auxiliary heating bundle withdraws a portion of refrigerant vapour from the high generator to heat the water to a temperature suitable for domestic hot water or heating. Second way is to use evaporator as a condenser in the heating mode. This can be achieved by switching the changeover valve for cooling/heating. The advantage of the first design is that it can be used to operate in cooling only, heating only or simultaneous cooling and heating modes while the second design permits only cooling or heating mode (no simultaneous operation is possible). The chiller/heaters, therefore, can be installed in systems to supplement, or even replace, primary heating or domestic hot water equipment.

2.6. Applications and trends

Synergy of absorption technology with other technologies can be performed by using various applications. However, synergy with absorption does not guarantee that these applications will be efficient and able to compete with other technologies, in particular with conventional compression technology. The absorption becomes attractive in specific applications when there are possibilities to use waste heat or

thermal energy coming from renewable energy sources. Some of specific applications when absorption technology can be beneficial are: when there is a large amount of thermal energy generated through solar collectors or waste energy usually discarded from industrial processes; in facilities that have simultaneous need for heat and power; in cases when electricity is unreliable, costly or when absorption can help to decrease peak loads; and in cases when governmental policies support the use of clean energy. The absorption technology is the most abundant in two types of applications:

1) Solar assisted systems for air-conditioning and refrigeration and

2) Polygeneration systems

The use of solar energy is maybe one of the most prominent ways of harnessing natural resources to conserve the energy. The increasing cooling demand in both residential and tertiary sectors all over the world is visible at every step. The solar assisted systems for air-conditioning and refrigeration offer opportunities to meet this increasing cooling demand in a very efficient way. The heat from the solar radiation is used to drive a thermally-driven machine such as absorption chiller. The solar radiation is converted to the heat through the solar collectors. The continuous interest in the field of solar collectors together with recent advances have led that today there is a wide range of products for possible use in applications with absorption technology. Table 2.3 provides an insight into what type of solar collectors is suitable for chosen absorption technology [36, 37].

Table 2.3 Absorption chiller-solar collector matching

Chiller type	Heat Source Temperature [ºC]	Solar Collector Type
Single-effect	90 (60-140)	Flat-plate Evacuated tube
Double-effect	130 (120-180)	Evacuated tube Parabolic trough Linear Fresnel Compound parabolic Cylindrical trough
Triple-effect	220 (200-250)	Parabolic trough Linear Fresnel Cylindrical trough

Polygeneration systems, and particularly combined cooling, heating and power systems are another alternative for solving energy-related problems and also another attractive application where absorption technology can be implemented to enhance the efficiency and productivity. Polygeneration usually refers to simultaneous production and delivery of more than one form of energy to the final user, from one or more primary energy sources such as several fossil fuels and renewable primary energy sources. Thus, term polygeneration stands for the combined production of electricity, heat, cold and products (fuels and chemicals), district heating and cooling systems or other advanced energy services and CO_2 capture [38]. Combined cooling, heating and power systems (known as tri-generation) are in fact derived from combined heat and power systems (also called co-generation) where exists simultaneous production of electrical and useful thermal energy from the same energy source. In tri-generation, the useful thermal energy is further used to provide cooling by coupling it with suitable thermally activated technology such as absorption chiller. The energy flow of typical tri-generation system with a theoretical calculation of prime energy calculation is shown in Figure 2.10. A review of Wu and Wang [39] explains in detail all the basic elements of tri-generation systems: the prime mover, electricity generator, heat recovery system, thermally driven equipment and control system. Prime movers can be chosen between various options: steam turbines, combustion engines, combustion turbines, micro-turbines, reciprocating internal combustion engines, biomass power plants, fuel cells and Stirling engines. Among the thermally driven technologies which include absorption, adsorption and desiccant dehumidifiers, the absorption is by far the most exploited technology.

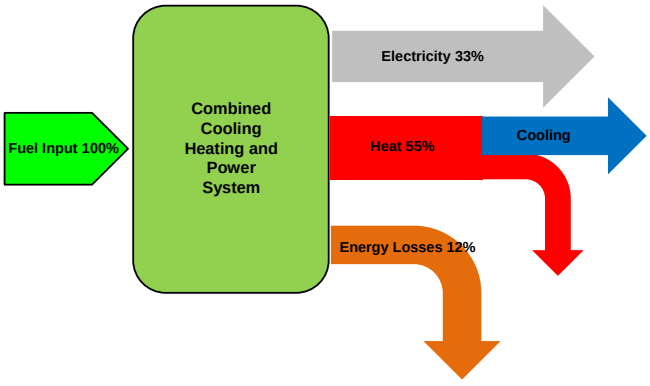

Figure 2.10 Energy flow of typical tri-generation system

Within the polygeneration systems, solar assisted and cogeneration technologies are in many cases complementary technologies combined with absorption machines. Industrial processes with waste heat are another application where absorption machines can be implemented efficiently both for cooling and heating. Absorption equipment has also found its place in district cooling and heating networks where it can be implemented in various ways. To avoid confusion, district cooling and heating networks can be considered as a part of poly-generation since they normally serve for energy distribution, but also can be observed as an individual concept which can be coupled with absorption technology. Very interesting conceptual solutions with absorption machines such as plant processing heating and boiler water heating, district heating by utilizing waste heat recovered from industrial processes or by utilizing hot underground water, utilizing well water for greenhouse floriculture or for fish farm are suggested in [40]. Absorption technology can also be used for desalination as reported in one of the studies of Alarcón-Padilla et al. [41] on solar thermal desalination system in Almeria, Spain. The existing desalination system based on multi-effect desalination was connected to a double-effect absorption heat pump. The results of the study showed that 50% reduction of the required solar field area can be achieved in this way compared to solar multi-effect desalination. Hybrid systems with coupled compression-absorption refrigeration cycles are also among the actual applications. Hwang [42] presented the integrated refrigeration system with micro turbine and absorption chiller. The absorption chiller was used to subcool the refrigerant in a vapour compression system, enhancing the efficiency of the cycle and consequently reducing the required size of the micro turbine. Another example are hybrid refrigeration systems for mobile applications as one presented in the paper of Monsberger et al. [43] where the solid oxide fuel cell was used to power compression-absorption cycle for transport refrigeration. As it can be seen from the examples described above, the absorption technology is not only attractive for refrigeration, air-conditioning and freezing, but also can meet the demand for energy conservation and protection. There are many other applications, which are not described above, because they are still in development or not mature yet. Actually, a great number of the absorption applications are in the stage of demonstration and prototyping. With respect to the trends in absorption machines, research and development of new working fluids is inexhaustible subject of interest. The advantages

of promising binary, ternary and quaternary salt mixtures are depicted and discussed thoroughly in Section 2.4 on working fluids. Lower efficiency and cost of absorption machine are still the flaming issue. That is the reason why a lot of research work is focused on enhancing the heat and mass transfer in order to improve the performance. As indicated in [28] the improved efficiency depends on inexpensive, compact components (compact heat exchangers primarily). Jeong and Garimela [44] used three-flow-regime model to evaluate the influence of the tube diameters in falling-film absorbers. The results showed that cooling capacity can increase significantly as the tube diameter decrease. On the other hand, tube surface wettability decreases which can be a limiting factor to miniaturization. The advanced micro heat exchangers are also the trend of development as shown in the study of the feasibility to apply the micro absorption heat pump in protective clothing [45]. A various micro electromechanical components are reviewed in this study. The effect of nanoparticles was investigated in the study of Lee et al. [46], where it was confirmed that nanoparticles can enhance heat transfer and help in design of highly effective compact absorber for NH_3-H_2O absorption system. Ali [47] demonstrated that the use of membranes can be advantageous when designing compact plates-and-frames absorber due to higher specific mass transfer area to the absorber volume. The developments in solar energy collecting and transferring technology have produced the positive impact on absorption technology. Thus, the use of parabolic trough collectors and linear Fresnel collectors which can produce water at medium temperatures have opened the interest in the fields of power and cooling cycles [48] and multi-effect absorption equipment [49, 50]. In order to achieve higher efficiency, the hybrid and GAX cycles become very interesting, especially in the USA. The focus is more on system integration. How to integrate absorption machines in complex, polygeneration systems in the most efficient way. This further implies the interest in optimization and control strategies of the absorption machine and whole system. The paper of Ziegler [51] points out the importance of appropriate control strategies for whole absorption system with external pumps and fans in order to reduce their parasitic power consumption and increase overall efficiency of the system. Thermal storage for the (ab)sorption machine is another important issue since lots of objects in residential and tertiary sector needs cooling during the night. Phase Change Materials (PCM) and ice-storage are some of the interesting solutions

[52]. Historical trend in absorption research, presented in [28], shows increased number of papers from 1996 till 2010 in all areas, with especially rising interest for absorption heat transformers. Finally, a lot of effort has been made lately in commercialization of a small scale absorption equipment and their integration with solar and micro-cogeneration systems for residential (single-family and multi-family) and light-commercial applications [12, 53, 54]. In the development of small scale absorption equipment a special attention has been given to the development of air-cooled chillers. Having in mind that the main objective of this thesis is the methodology for small scale absorption chillers, the following paragraphs will try to highlight all the relevant achievements together with the current situation in the field of small scale absorption chillers.

2.7. Small capacity absorption machines - state of the art

The development of small capacity absorption machines has been mostly connected to the research in the field of solar powered systems for air-conditioning. The milestone was the moment when the International Energy Agency (IEA) started Task 25 "Solar Assisted Air Conditioning of Buildings". Under this task, thermally driven chillers (mainly absorption chillers) have been identified as a very promising technology for solar assisted air conditioning in order to meet the increased demand for cooling in the residential sector. As one of the main objectives, the IEA has set the intensive R&D in the field of small scale thermally driven chillers and preparation for market entry of these chillers. IEA Task 38 "Solar Air-Conditioning and Refrigeration" and Annex 34 "Thermally Driven Heat Pumps for Heating and Cooling" has continued the same trend. Several European projects such as SOLHEATCOOL, ASODECO, SACE, NEGST, ROCOCO, SAHC, CAMELIA, SolarCombi+, etc have promoted and supported the development of the small scale absorption chillers as a part of the IEA SHC initiative. Another important factor which has contributed to the development of small scale absorption machines are micro CHP systems which has been identified as one of the possible solutions to reduce energy consumption and CO_2 emission by 20% until 2020. These small systems can help the operation of the local electricity distribution grid as well as to provide heating and hot water for small commercial buildings, apartments and individual houses. The heat from micro CHP systems can be

used to drive small capacity thermally driven chillers opens new opportunities and market potential for small scale absorption machines as has been identified in one of the deliverables of the POLYSMART project [55]. All these factors have contributed the rapid development of the small scale absorption machines and as a consequence several units released to the market and remarkable number of research studies and prototypes has been reported.

2.7.1. Commercial units

Table 2.4 Absorption machines available in the market

Manufacturer	Country	Type	Working pair	Nominal capacity [kW]	COP	Heat Source [ºC]	Application	Coolant
AGO	Germany	Single effect	NH_3-H_2O	50	0.61	HW [3] (95)	R	Water
Broad	China	Double effect	H_20-LiBr	16/23	1.2	GF PHW (160)	AC	Water
Cooltec5	USA	GAX	NH_3-H_2O	17.6/35	0.68	GF	AC	Air
Climatewell	Sweden	Single effect With storage	H_20-LiCl	10	0.68	HW (110)	AC	Water
EAW Wergcall	Germany	Single effect	H_20-LiBr	15/30	0.75	HW (90)	AC	Water
Pink (SolarNext)	Austria (Germany)	Single effect	NH_3-H_2O	10/12	0.63	HW (85)	AC/R	Water
Rinnai Osaka gas	Japan	Double effect	H_20-LiBr	6.7	1.2	GF	AC	Water
Robur	Italy	Single effect	NH_3-H_2O	17.7 12.8	0.7 0.53	GF PHW	AC/R	Air
Rotartica	Spain	Single effect	H_20-LiBr	4.5	0.67	HW (90)	AC	Water Air
Solarice	Germany	Single effect	NH_3-H_2O	25/40	0.6	HW (80)	R	Water
Sonnenklima (Phonix)	Germany	Single effect	H_20-LiBr	10	0.78	HW (75)	AC	Water
Termax	India	Single effect	H_20-LiBr	17.5/35	0.7	HW (90)	AC	Water
Yazaki	Japan	Single effect	H_20-LiBr	17.6/35	0.7	HW (88)	AC	Water
Yazaki	Japan	Double effect	H_20-LiBr/ LiCl/LiI	28	0.85	GF	AC	Air

Table 2.4 summarises the information on small capacity absorption machines released to the market which has been compiled from various papers [28, 56, 57], reports [58, 59] and manufacturer's websites.

[3] HW-hot water; GF-gas fired; PHW-pressurized hot water; R-refrigeration; AC-air-conditioning

2.7.2. Research and development, prototypes

Despite the increased interest in the last two decades and a number of commercialized units, the development of small capacity absorption machines has started much earlier. This fact is supported by a large number of scientific papers, research efforts and numerous prototypes developed worldwide. An overview of the scientific achievements is given to complete the image of the possibilities which small absorption machines can offer, but also to point out the deficiencies of the technology. With emphasis on use of renewable energy sources, this review covers all the relevant applications, disclosures and prototypes connected to the small absorption machines.

In a period from 1975-1984, the Carrier Corporation made lots of efforts on research and development of solar powered absorption chillers which can dissipate directly to air [58, 60]. As a result of this research, a prototype of air-cooled, single-effect absorption chiller with cooling capacity of around 35kW was developed. Sun powered with H_2O-LiBr working pair, the prototype could achieve a COP of 0.71. Unfortunately, this prototype has never entered into serial production. The double-effect air-cooled absorption machine with a compact body and suitably small installation area is described in the patent of Kurosawa et al. [61]. The disclosure was based on the 15kW prototype which used H_2O-LiBr working pair. The COP of this double-effect absorption chiller was 0.93. Gas Research Institute from Chicago was also involved in research with small capacity air-cooled machines. The result of the research was direct-fired double-effect absorption machine [62]. A 10kW prototype used H_2O-LiBr working pair and could operate both as chiller and as a heat pump. This air-cooled absorption machine had a COP around 0.95 in cooling mode and was intended for small residential applications. One of the interesting issues connected to this prototype was the automatic decrystallization technique. The second interesting issue was modular type of plate heat exchangers for the evaporator and absorber [63]. This disclosure enables direct heat exchange with the cold air (evaporator) and cooling air (absorber). The Yazaki Company was also working on development of small air-cooled absorption chiller/heater [64]. The reported COP of the 4.5kW double-effect absorption chiller prototype was 0.8 and it was working with their newly developed LiBr-LiCl-LiI solution [65]. This solution, also called Carroll mixture offers a safer operation of the

absorption chiller due to sufficiently low crystallization temperature. Another absorption product from Yazaki can be found in the experimental study of Li and Sumathy [66] on solar air-conditioning system with storage tank. The absorption chiller used in system is Yazaki WFC-400S with nominal capacity of 4.7kW. The chiller has a generator inlet temperature range of 75-100ºC and a cooling water temperature range of 24-31ºC. It is based on single-effect cycle which uses H_2O-LiBr working pair, but with one difference. This chiller belongs to the group of the self-circulate absorption refrigeration systems or, more precisely, to the systems which use hot-air-bubble pump principle. The difference of these systems with respect to the classical absorption system is that they do not require any electricity to drive a circulation pump. With water as a refrigerant, the difference between pressure levels of the condenser and the evaporator becomes very low and can be maintained by using the principle of hydrostatic-head. The bubble pump circulates the solution strong in refrigerant from the absorber to the generator while the gravitation force enables the return of the solution weak in refrigerant back to the absorber. Also, it is worth to mention that Yazaki is one of the first who started the mass production of small capacity absorption chillers for air-conditioning applications. In 1970, Yazaki launched first "Aroace" absorption chiller/heater series with CH-1000 (12.25kW capacity) and CH-1500 (17.5kW) models. In 1978, the company started with production of models WFC-400 and WFC-600 (7 kW), water fired chillers which use bubble pump principle [67]. These models are not any more available at the market. At the Gazi University in Turkey, Sozen et al. [68] developed a prototype of an NH_3-H_2O absorption heat pump. This absorption system was designed to operate with a parabolic solar collector, having an optimum performance at generator inlet temperature of 90ºC. Typical COP values for cooling mode were in the range of 0.58-0.8 and in the range of 1.5-1.8 for heating mode. Due to the minimum evaporator temperature of 3ºC, the authors recommended the use of the system both for food preservation and for air-conditioning. Also, authors recommended the modification of the evaporator and absorber in order to decrease high exergy loss of the heat pump. Ben Ezzine et al. [69] considered the possibility of solar cooling with double-effect ammonia-water absorption cycle. A thermodynamic analysis based on the Second Law indicate that absorber, solution heat exchanger and condenser have the greatest potential to improve the chiller's efficiency which can be more viable for

residential and small commercial applications. The main obstacle for development and commercialization of double-effect ammonia-water chillers are the safety problems which may be caused by higher operating pressures of ammonia. An experimental prototype of 10kW single-effect H_2O-LiBr absorption heat pump was developed and evaluated by Argiriou et al. [70]. A 10kW prototype, suitable for residential and small building applications, was connected to a cooling tower and driven by solar heat at low driving temperatures through solar collectors. The maximum obtained COP was 0.74. The comparison with a conventional cooling installation using a compression type heat pump showed that this type of system could achieve 20-27% of energy savings. The University of Applied Sciences in Stuttgart, Germany developed several prototypes of solar heat driven ammonia-water diffusion absorption cooling machine for air-conditioning applications [71]. A diffusion absorption cooling machine also belongs to self-circulate absorption systems. Since now ammonia is the refrigerant, a bubble-pump is not sufficient to overcome differential pressure between the condenser and the evaporator. The solution is to charge an auxiliary gas to the evaporator and absorber in order to keep the partial pressure of ammonia low enough to correspond with the required temperatures inside the evaporator. In this way, the pressure difference of the system is decreased which further enables the utilization of the bubble-pump. The designed cooling capacity of the diffusion absorption cooling machine was 2.5kW and Helium was used to keep the pressure equilibrium. The best results were obtained with the third prototype when the initially chosen plate heat exchangers were replaced by coaxial solution heat exchangers. In the operating range of the generator inlet temperature from 100 to 150ºC, the experimental results of the prototype showed cooling capacities from 0.7kW up to 3.0kW with maximum reached COP of 0.38. Another ammonia-water absorption chiller prototype was also developed in Germany, at the ITW Stuttgart [72]. The designed cooling capacity of this single-effect absorption chiller is 10kW and it is powered directly with the hot water from the solar collectors, without any thermal storage tank in between. The solution circulation to the required high pressure level in this case is achieved by a membrane pump. According to the experiments reported by Zetzsche et al. the cooling capacity was in the range of 5.4-10.7kW and the COP in the range 0.58-0.74. Around the same time, the Technical University Graz in Austria built another prototype of a ammonia-water absorption heat

pump with 5kW cooling capacity [73]. The prototype was indirectly driven through a heat medium circuit which can use any type of renewable energy. Although mainly designed for solar air-conditioning, the operating temperature range of cold water (-10-20ºC) makes it suitable for refrigeration as well. The reported COP for cooling mode was in the range of 0.4-0.75. At the University Politecnica de Cataluña, Castro et al. [74] developed and tested the prototype of an air-cooled absorption chiller of about 2 kW cooling capacity using H_2O-LiBr working fluid. The prototype has a mechanical solution pump, horizontal-tube falling film generator, an evaporator and the air-cooled absorber and condenser consisted of vertical finned tube batteries. The maximum obtained COP of the chiller was 0.65 with the electrical consumption of the fan of approximately 250W. In a period from 2001 to 2002, the German Aerospace Centre (DLR) developed the prototype of a double-effect H_2O-LiBr absorption chiller driven by parabolic solar collectors. For the generator inlet temperature range of 150-180ºC the COP was in the range of 1.2-1.4. An air-cooled GAX prototype powered by natural gas and solar energy was developed in Mexico, at the University Autonoma de Baja California. The prototype with a cooling capacity of 10.6kW could achieve COP of 0.86 [75]. Kim and Infante Ferreira [76] were investigating the development of half-effect parallel-flow absorption chiller for solar air-conditioning in hot weathers. Based on the theoretical design, a prototype of an air-cooled H_2O-LiBr absorption chiller with the purpose to be combined with low-cost flat solar collectors was constructed at Delft University of Technology, the Netherlands. After performing the experiments, during which the heat rejection temperature was varied in the range of 30-50ºC and the generator inlet temperature in the range of 67-108 ºC, the maximum reached COP was 0.35 [35]. Another market ready prototype of ammonia-water chiller was developed by Austrian company SolarFrost [77]. Actually, it is diffusion absorption cooling machine with cooling capacity of 2kW, and COP in the range of 0.6-0.7. A steam driven solution pump was developed for that purpose. It is based on the principle that hot ammonia solution has a high steam pressure while cold ammonia solution absorbs ammonia gas. The company developed two versions, one with plate heat exchangers and the second with tube heat exchangers. In Portugal, under the framework of the EU project Polysmart, the institute INETI together with the company AoSol developed another prototype of an air-cooled ammonia-water absorption chiller. This single-effect

absorption chiller had a cooling capacity between 5-6 kW and could achieve COP of approximately 0.65. One of the most recent disclosures was the newly developed ammonia-lithium nitrate mixture patented by Bourouis et al. [78]. Using the patented solution, several single-effect prototypes were recently developed at Rovira i Virgili University in Spain [33]. First developed prototype was water-cooled, with designed cooling capacity of 10kW. Experimental results showed that for generator inlet temperature and chilled water temperature of 90ºC and 15ºC, respectively, chiller can produce 11.5kW of cooling. The maximum obtained COP was 0.69. The second developed prototype was air-cooled, which could obtain slightly lower capacity of 9.1kW and COP of around 0.64.

The use of absorption technology in the low temperature applications like food and medicament storage or ice-making is also possible. Small capacity absorption machine with refrigeration purpose were subject of interest for many researchers. The absorption technologies become very attractive for refrigeration purpose in remote or rural areas where the electricity is unavailable. This fact is supported by numerous research studies and developed prototypes.

In 1986, Uppal et al. [79] built a low cost, solar driven NH_3-H_2O absorption refrigerator. The purpose of this small capacity (56 litres) refrigerator was vaccine storage in the remote locations of Third World countries. Bansal et al. [80] designed and constructed a prototype of a solar cooling unit based on solid-vapour intermittent absorption system. The unit of 1.5 kWh/day cooling capacity used ammonia as a refrigerant and IMPEX material (80% SrCl, and 20% Graphite) as absorbent. However, the unit had a very poor performance with an overall COP less than 0.1 and also had the problem with the corrosion. Erickson [81] used half-effect absorption cycle to develop icemaker for isolated fishing villages in Alaska. This absorption refrigeration prototype was powered by waste heat from Diesel engine at 75ºC with the obtained COP of 0.3. An intermittent absorption refrigerator powered by solar pond and using NH_3-H_2O solution was built by Sierra et al. [82]. The refrigerator had the COP in the range of 0.24-0.28 and the minimum operating evaporation temperature was -2ºC. Another absorption refrigerator prototype with cooling capacity of 4.65kW was designed and tested in Turkey by Dincer et al. [83]. The experimental COP at generator inlet

temperature of 90ºC was around 0.45. One more example of absorption refrigeration for vaccine storage was reported by Hammad and Habali [84]. They used solar-powered absorption refrigeration cycle with NH_3–H_2O working pair to design a prototype which would cool a vaccine cabinet in remote desert areas. The simulated COP was in the range of 0.5-0.65. At the Politecnical University of Madrid, a group of researchers [85] developed and tested a prototype of 2kW absorption refrigerator to operate with a concentrating solar power system. The main purpose of this small NH_3–H_2O absorption system was to meet refrigeration requirements in small rural operations. However, the test results showed very poor performance of the prototype with the COP lower than 0.05. Pilatowsky et al. [86] investigated the use of absorption refrigeration systems coupled with evacuated tube collectors for milk cooling in the rural regions of Mexico. The results showed that the monomethylamine-water pair is satisfactory to obtain evaporator temperature range of -5 to 10ºC at generation temperature range of 60-80ºC. This further permits the use of high efficiency evacuated tube collectors to provide required cooling energy for typical daily milk production in the rural regions of Mexico. The obtained COP values varied from 0.15 to 0.7. In addition, the example of small capacity absorption machine which operates as absorption heat transformer can be found in the paper of Abrahamsson et al. [87]. The authors designed and tested a 10kW absorption heat transformer unit based on self-circulation principle and using NaOH-water working pair. Viewed from the perspective of the absorption components, very interesting research studies were conducted by Bourouis et al. [88] and Lorton et al. [89]. Bourouis et al. investigated the possibility of using multi component salt solutions in the air-cooled absorbers. The conclusion was that these solutions have the advantage over the conventional H_2O-LiBr working pair due to the higher solubility at higher salt concentrations and, in accordance with that fact, these solutions are very suitable for the air-cooled absorbers. Lorton et al. presented the prototype of the double-effect absorption machine based on rotational technology which intensifies heat and mass transfer inside the components. For more information about recent developments in absorption cooling and more exhaustive R&D analysis, the author recommends several review papers [90-92].

2.7.3. Installations

The progress in the field of small-scale absorption machines is also visible by the number of installed units in the solar cooling systems around the world. One of the surveys under the IEA Task 38 [93] showed that the number of the solar cooling systems has been multiplied by factor 6 in a period from 2004 to 2009, according to documented installations (Figure 2.11). The estimate is that this factor is higher and close to 9. The growth was more than evident during the 2009 when the number of installed systems increased by 100.

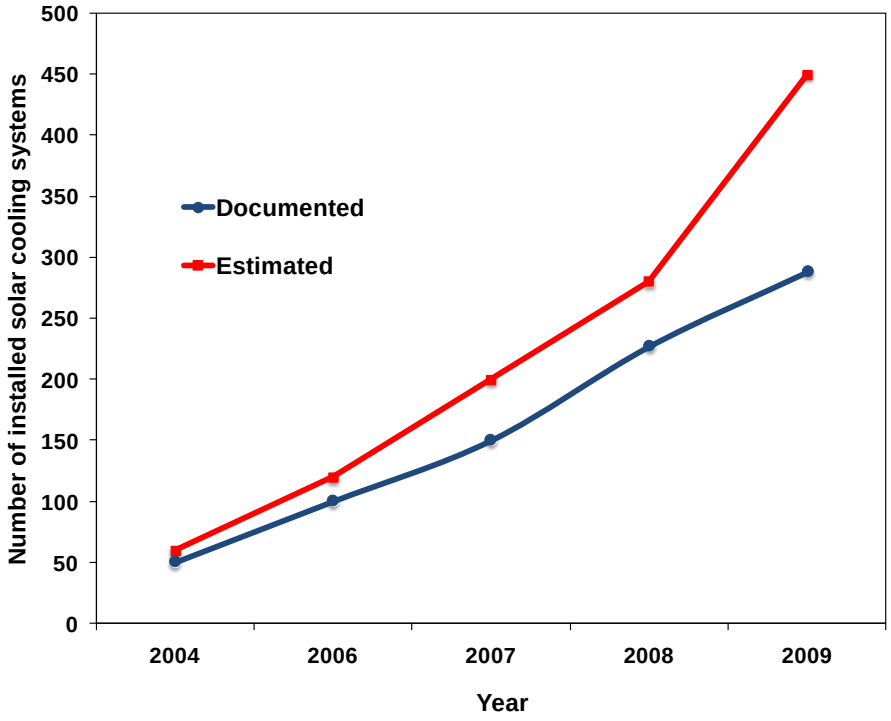

Figure 2.11 Number of installed solar cooling systems in a period 2004-2009

This trend is based on the list of existing solar heating and cooling installations made by Sparber et al. [94]. Among the 288 collected systems, 223 systems belong to the small-scale systems with cooling capacity less than 50kW. Within the small-scale systems, the number of installed absorption unit is 198 and the rest are adsorption and desiccant units. Figure 2.12 represents percentage contribution for each of three technologies.

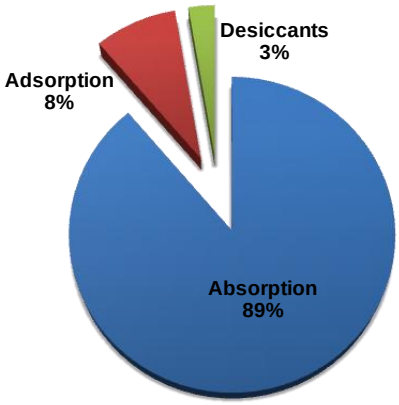

Figure 2.12 Percentage of use of different thermally driven technologies.

As mentioned before, this list has to be taken with a certain doze of reserve since the estimated number of these systems is significantly higher, but there is no information. Market analysis illustrated in Figure 2.13 shows that the among the installed absorption units the largest share has Climatewell with 34%, followed by Rotartica with 23%, Yazaki with 12%, Sonnenklima with 2%, etc.

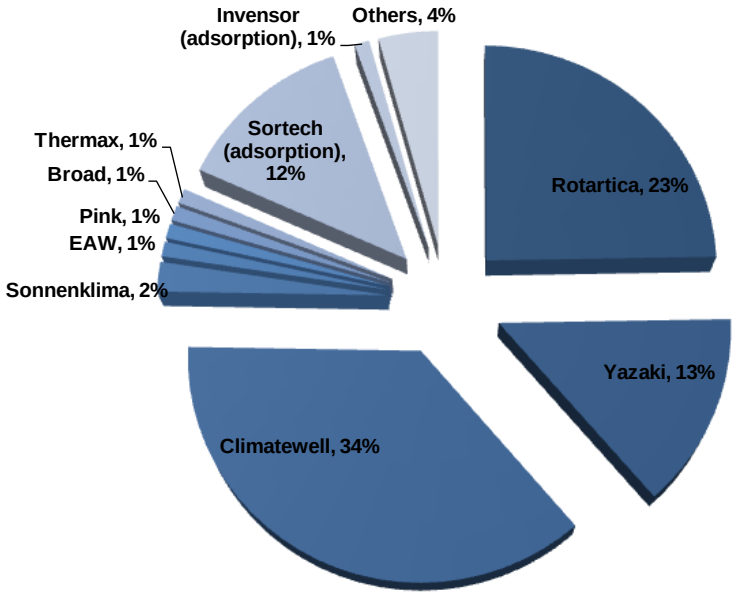

Figure 2.13 The share of installed small capacity absorption chillers

With a market size of 50 million potential installations, micro-cogeneration technology gives another opportunity for development of small-scale absorption machines. Despite this large potential, micro tri-generation systems are still under development. The number of micro tri-generation systems with absorption units is very

small and mostly limited on experimental set ups. Thus, several demonstration systems were built to investigate the tri-generation potential under the framework of PolySMART project. One of these demo systems was located in a recreation centre in Madrid. Mini-CHP unit DACHS which provides 5.5kW of electricity and 12.5kW of heat is coupled with Climatewell absorption chiller to produce 10kW of cooling. The same system was installed in the Technological Park Boecillo, Valladolid with only difference that absorption chiller was working with 7kW cooling capacity. In Vitoria-Gasteiz, 5.5kW$_e$ Senertec DACHS and 4.5kW Rotartica were used to supply laboratory hall with heating, cooling and electricity. Joaneum Research from Austria used 3kW$_e$ Stirling engine and Pink absorption chiller for winery process application. In Portugal, two AoSol prototypes of 8kW cooling capacity were used in micro-trigeneration systems in office buildings in Lisboa and in Samora Correira. The first prototype was driven by heat from biodiesel engine while the second was driven by mini-CHP unit. For the purpose of air-conditioning a laboratory hall in Milan, 17.8kW Robur unit and desiccant system were powered by 52kW$_e$ Avesco CHP unit. In Germany, one Sonnenklima chiller with 10kW capacity was installed in Diessen as a part of show room while the second chiller was installed in a computer centre in Berlin. The first chiller was connected to mini-CHP unit and the second to district heating network [95]. Small capacity tri-generation application has been installed in Central Forum building of Districlima Association in Barcelona as a part of EU project Hegel. The exhaust gasses of 28kW$_e$ micro gas turbine (MGT) were used to drive an air-cooled absorption chiller (Robur). Southern California Gas has built another micro tri-generation system with 30kW$_e$ gas micro turbine and 35kW absorption chiller in Downey, USA. More powerful, 115kW$_e$ MGT was installed in tri-generation system to drive 35kW absorption chiller (Yazaki WFC 10) in Graz-Thondorf, Austria [96]. In order to evaluate the performance of tri-generation system for supermarket applications, an experimental set up was built at Brunel University, UK [54]. The system designed to satisfy concurrent need for electricity, heating and cooling consisted of 80kW$_e$ recuperated micro turbine generation package and ammonia-water absorption chiller with 12kW cooling capacity (Robur ACF-60LB). Khatri et al. [97] investigated the feasibility of using micro tri-generation systems for small village houses in India. For that purpose, they designed and constructed a set up which is based on the internal combustion engine

of 3.7kW typically used in agricultural sector of India. The refrigeration effect was achieved through an NH_3-H_2O vapour absorption refrigerator (Electrolux). Finally, 16kW double-effect absorption chiller provided by Broad was installed in test facilities of Carnegie Mellon University [98]. A micro co-generation system which provides driving heat for this chiller was designed with the main purpose to study the technical feasibility of using cogeneration systems at micro-scale level in buildings.

2.8. Technology cost

The cost of an absorption installation is directly dependant on the design of whole system and on choice of technology. Since the solar cooling and micro-CCHP have proved to be the most promising technologies for small capacity absorption machines, the economic aspects have been analysed with respect to these two technologies. One of the main task of ROCOCO project [99] was to identify the main costs in solar cooling systems and to try to reduce them. The investment cost distribution was assessed based on different case studies for both small-scale and large-scale installations. Figure 2.14 illustrates the average cost distribution in the case of small-scale solar cooling systems: 35% goes for pumps, fans, storage tanks and other type of auxiliary equipment; absorption chiller can contribute up to 30% of total cost; solar collectors make 20% and control system around 10%.

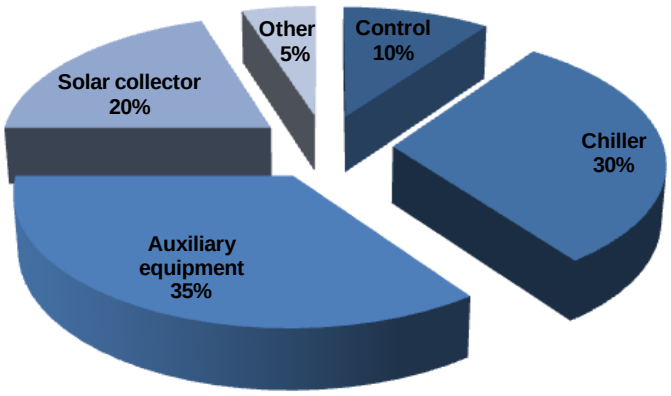

Figure 2.14 Investment cost distribution for small solar cooling systems

An example of a small-scale installation with real numbers can be found in the same report. The installation was located in Italy, with $20m^2$ solar collector field and

air-cooled absorption chiller. The cost and the share for each part of solar system are shown in Table 2.5. Significant savings have been achieved by avoiding storage tanks, cooling towers and back-up system.

Table 2.5 Investment cost of small solar system in Italy

Auxiliary equipment	5.573 €	19%
Solar collector	10.258 €	35%
Chiller (Rotartica 4.5kW)	9.535 €	32%
Control system	4.050 €	14%

A small-scale solar system with slightly higher cooling capacity and different design can be found in the paper of Dickinson et al. [100]. 72m^2 solar collector array and 35kW cooling capacity absorption chiller were installed in a government building in Phoenix, USA. A comparison with previously described system in Italy shows that different design with auxiliary equipment such as cooling tower and storage tank significantly increase the investment cost. On the other hand, if we compared the cost of these two systems per kW of produced cooling capacity, the US installation with 2886 €/kW$_c$ seems to be twice cheaper compared to 6537 €/kW$_c$ of the Italian installation.

Table 2.6 Investment cost of small solar system in the USA

Auxiliary equipment	29.300 $ (20.510 €)	20%
Solar collector	40.000 $ (28.000 €)	28%
Chiller (Yazaki 35kW)	20.000 $ (14.000 €)	14%
Control ,valves, piping	55.000 $ (38.500€)	38%

Also, approximately 30% should be added to the total sum for installation and mark-up. Finally, annual costs for maintenance, electricity and water consumption must be taken into account:

- Maintenance: 3.000 €
- Electricity: 800 € (based on 35kW cooling capacity chiller sample)
- Water consumption: 350 € (35kW cooling capacity chiller)

In order to decrease high investment cost, some companies have started the production of small pre-fabricated solar cooling systems called solar cooling kits. Solar cooling kit usually include: solar collectors, hot and cold storage, thermally driven chiller, cooler and system control. The cost of these kits in Europe is around 4000-4500

€/kW with the expectation to fall to 3000 €/kW in 2012 [75]. The cost of micro trigeneration technology can be analysed from the articles of Sugiartha et al. [83] and Moya et al. [84]. In their evaluation study of micro tri-generation system for supermarket applications in the UK, Sugiartha et al. used the micro gas turbine of 80kW$_e$ coupled with 12kW$_c$ absorption chiller. The installed cost of the MGT was 1009£ per kW of produced electricity with the operation and maintenance cost estimated to 0.0051£/kWh. The installed cost of the absorption chiller was 569£ per kW$_c$ with additional 40£/kW$_c$ per year for the operation and maintenance. Moya et al. analyzed a tri-generation system with 28 kW$_e$ MGT and a 17kW air-cooled ammonia-water absorption chiller (Robur ACF 60-00TK) installed in Central Forum building in Barcelona. The exhaust gases from MGT heat the thermal oil used to drive the absorption chiller which produces cooling effect. For that purpose, two additional heat exchangers were necessary: the exhaust gas/hot water and the exhaust gas/thermal oil heat exchanger. The installation cost of the system is presented in Table 2.7. The cost distribution from Figure 2.15 shows that absorption chiller participates with only 8% in total cost of the tri-generation system.

Table 2.7 Investment cost of the tri-generation system in Bcn

MGT Capstone C30	*51.408 €*
Exhaust gas/hot water heat exchanger	*3.500 €*
Exhaust gas/thermal oil heat exchanger	*7.578 €*
Absorption chiller	*9.000 €*
Material for the installation	*19.506 €*
Control system	*2.660 €*
Installation	*18.345 €*
Total cost	*111.997€*

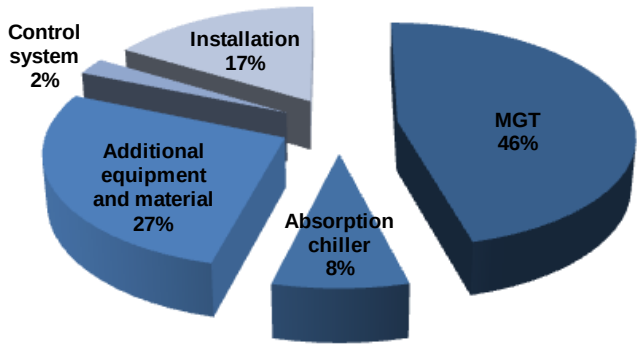

Figure 2.15 Cost distribution of the tri-generation system

From the economical point of view, both small-scale solar cooling systems and micro-CCHP with absorption chillers are worse than comparable conventional systems with compression chillers. Despite the relatively high energy savings on annual level, very high initial cost of these technologies makes them less favourable. Best practice examples in the case of small solar cooling installation show that 800-2600€ per year can be saved, depending on load hours, location and system design. Still, payback period is very long, around 20-30 years without any incentives. With incentives and also using these systems for DHW and space heating, payback period can be reduced to less than 10 years. The economic analysis from Moya et al. [101] can be taken as a reference for energy savings in the case of micro-CCHP. In the case of large residential building, annual energy savings are 12094€ with a payback period of 5.2 years. This is very close to the payback period for micro-CCHP system reported in Sugiartha et al. [102] which is around 6 years. Around 6 years is first-rate payback period under the current conditions and indicates a very good design of micro-CCHP system. More realistic scenarios are micro-CCHP systems with payback periods in range of 10-15 years. In addition to system design, payback period is directly dependant on the number of full load hours and on the ratio of gas-electricity price. If the current ratio of gas-electricity price increases from standard 0.3 to 0.4 or more, the payback period will be significantly reduced. This fact indicates that the right incentives are necessary factor to make both small-scale solar cooling and micro-CCHP closer to the conventional technology with compression chillers.

2.9. Regulations and incentives

It has become clear that small capacity absorption machine hardly will be able to compete with comparable compression machines in the near future if adequate promotions do not support their further development. This primarily refers to the integrated energy systems based on renewable energy sources which use absorption technology: CCHP and solar thermal systems. These systems have a great potential for saving primary energy (fossil fuels) and to reduce environmental impact.

EU promotes the use of renewable energy for heating and cooling in order to reduce primary energy dependency and decrease greenhouse gasses emissions.

Following the implementation of Directive 2009/28EC [103], EU member countries have developed their own strategies and introduced a range of incentives to meet the EU targets for 2020. A very exhaustive study on existing incentives in EU-27 countries has been reported by Cansino et al. [104]. According to the authors, the common types of incentives introduced in the EU countries are: subsidies, tax incentives, financial support and feed-in tariffs. Technologies based on renewable energy sources such as biomass, solar, and geothermal can benefit from public subsidies if they are used for heating and cooling purposes. The most subsidized technology is biomass micro-cogeneration followed by solar thermal technologies. The promotion of cogeneration is based on Directive 2004/8/EC of the European Parliament which promotes the high-efficiency cogeneration based on heat demand and potential benefits of the same with regard to saving primary energy, avoiding network losses and reducing greenhouse gasses emissions. Besides subsidies, there are also some regulations which demands implementation of renewable systems in new buildings. In Germany, there is a minimum use of 15% of renewable energy for all new buildings while in Spain all DHW installation have to be with solar thermal energy. Tax deduction, exemptions and reduced tax rates are other types of public instruments from which CCHP and solar thermal systems can benefit within the EU. In fact, at the moment there are no special incentives for CCHP systems but they can benefit from incentives for CHP systems bearing in mind that CCHP systems are/can be derived from CHP systems. One of the best examples for tax incentives is Sweden, where households can benefit from 30% tax credit when converting from direct electric heating and oil-based heating to systems based on cogeneration or heat pumps. Another example is Italy, where there is a possibility of reduced VAT (10% instead of 20%) for energy consumption if the refurbished house includes solar thermal system. Tax exemption from distribution and consumption taxes on natural gas is present in Spain to promote CHP, regulated by Royal Decree RD661/2007 [105]. The RD661/2007 promotes biomass green certificates, where the tariff is valid in the first 15 years and corrections apply after. Austria, Luxemburg and the UK have feed-in tariffs incentives for heating and cooling derived from renewable energy sources. Finally, low-interest loans are also type of incentives which has been offered, for instance, in Germany for the financing of solid biomass and solar thermal plants for heating and cooling.

Building certification programs like LEED (Leadership in Energy and Environmental Design) are another way to promote solar cooling and micro-CCHP systems opportunities. LEED certification, a program introduced by the US Green Buildings Council is a rating system for buildings which evaluates if the building is environmentally responsible, operationally efficient and in a healthy environment.

As can be seen, the majority of the energy policies and regulations differ from country to country due to different patterns of energy demand and supply, fuel prices, climate and environmental conditions. With respect to that, each country adapted policy measurements toward its own energy resources and adjusted them to the current situation. It is evident that progress has been made, but it is still necessary to put more efforts by making energy policies more consumer-friendly. Finally, of great importance is to harmonize policies at local, national and international levels in order to facilitate the further development of renewable energy based technologies, especially solar thermal and micro-CCHP technologies.

2.10. Potential and barriers

The potential on the field of primary energy savings and environmental benefits are the main advantages which encourage further development of small capacity absorption machines. Reduced electricity consumption and low CO_2 emission has been confirmed by numerous studies. Beside the space cooling and refrigeration purposes, it is also possible to use small capacity absorption machines for DHW production and space heating. Also, there is a possibility to use them in remote and isolated areas where the infrastructure does not meet energy requirements. Very promising application are supermarkets and small agro-food industry applications. Very intensive researches on this topic and numerous studies have pointed to solar thermal and micro-CHCP technologies as the main carriers for future development of small capacity absorption machines. It seems that these two technologies are the right path which can lead to the economic attractiveness of small capacity absorption machines, making them competitive with conventional compression machines. However, the problem is that the both solar thermal and micro-CHCP technologies are still under development. It is truth that several micro-CHP units such as gas micro turbines and fuel cells which can be

coupled with small absorption machines are now available at the market, but the cost is high. In the field of solar collectors has been made a great progress in the last few years which resulted in much accessible prices. Overall progress is evident; however, there are still lots of obstacles that impede the full expansion of small absorption machines. The main obstacle remains the high first cost and lack of serial production, which would inevitably lead to price reduction. The lower performance is another obstacle, small absorption machines are mainly single-stage with the COP lower than comparable compression units (0.7 compared to around 3). However, the first commercial small absorption double-stage unit looks promising with respect to the efficiency. There are many factors that affect the efficiency and effectiveness of the systems with small capacity absorption machines. Design and sizing are of great importance. The minimum solar fraction of around 50% is necessary that solar thermal system with single-stage absorption chiller starts saving primary energy. This indicates the need for increased number of hours operating at full load. Full load operation stands for micro-CHCP systems as well. The energy storage is another factor to which has been devoted a lot of research attention lately. In order to prevent inefficient systems, it is necessary to optimize the electricity consumption of external system components such as cooling towers. This is why the control is very important factor. On the other hand, the control also has to be simple in order to decrease the high first cost. Progress and cost reduction of electronic components for control should contribute to that. As already mentioned above, new opportunities have been introduced with small solar kits which make small absorption machines more accessible. The potential for further cost reduction of small solar kits has been presented by Mugnier [93]. The cost of solar collectors and storage could be lowered for 10% in the next 2-3 years. The cost reduction potential for (ab)sorption chillers is around 20% with new components, with possibility to increase up to 50% if serial production starts (more than 500 units). The price of the re-cooler could also decrease up to 50%. The price for installation can decrease up to 30% through standardized solar cooling kits. The control has the most promising potential for reduction, more than 60%.

Two very important factors for further development are lobbying and subsidies. The financial incentives for the installation of these systems are another important factor which may be a driving force for successful market penetration. However, maybe the

most important issue is to create a sense of responsibility among people about the fatal ecological consequences that can bring increasing use of electric cooling systems.

At the end, all the facts mentioned above indicate that small capacity absorption machines have a good potential for further development under the two emerging technologies such as solar thermal and micro-CHCP, but a lot of research work is ahead. Appropriate standards, test procedures and best practices guides together with intensified work on simulations, optimization and control strategies improvement are some of the needs which are necessary to accelerate the progress and to fill the gap with respect to the conventional systems.

Chapter 3

Multifunctional test bench

"A journey of a thousand miles must begin with a single step."
Lao Tzu

3.1. Introduction

For the purpose of performance analysis of different solar assisted and thermally driven technologies, an experimental test facility has been constructed at the laboratories of the University Rovira i Virgili (URV) in Tarragona, Spain. This, so-called "Multifunctional test bench" serves as a test stand for the scientific investigation of small-scale and mid-scale absorption equipment in particular, but also provides possibilities to test a variety of equipment used in HVAC systems, solar assisted air-conditioning and CHP application. A complete range of pilot scale equipment enables comprehensive testing of different units in order to select the most suitable technology for application of interest. Tests with thermally driven water-cooled[4] an air-cooled chillers and water-to-water and air-to-water heat pumps, electrically driven (vapour compression) water(air)-cooled chillers and water(air)-to-water heat pumps, Organic Rankin Cycle engines, fuel cells, gas micro turbines, internal combustion engines, multiple chillers operations, micro-cogeneration systems and evaporating desalination equipment are some of the operations which can be performed inside this multifunctional test bench. However, bearing in mind that the aim of this thesis is addressed to thermally driven chillers and heat pumps the main focus will be on absorption cooling and heating facilities.

The analysis of real benefits of equipment is usually performed by independent laboratories under conditions of operation based on predetermined standard. This ensures that the test was carried out under a certain quality requirements and the results obtained by this method are accurate. On the other hand, these tests are costly and time consuming. Normally, to balance these facts, almost all the equipment is analysed under

[4] The terminology is in accordance with [106]

the same conditions of operation in steady-state regime and with reduced number of tests. Standardization makes things easier when selecting the equipment type and size for particular system application, but only in the design stage. It is sufficient to choose type of equipment based on design demand and nominal conditions of the equipment, but it does not carry complete information about the equipment performance. Everyday practice confirms that the selection of appropriate equipment for a particular application can be very cumbersome task, when almost certainly the temperatures or thermal loads are not constant over time. This idea was one of the key factors in designing this multifunctional test bench. To create useful tool which will help to evaluate the benefits of both new designed equipment and equipment already existing on the market, analysing entire operating range and complying with existing standard at the same time. Complete performance map of the equipment, based on real data and taken under standardized procedure, might be useful in various ways: through simulation models and software packages, fault detection or for control purposes (e.g., model based control). In fact, a complete performance map of the equipment should be available always when it is likely to be employed in some cooling and heating systems application.

According to Gordon and Ng [107], when planning and designing test facility for conducting standard and application rating tests for chillers and heat pumps, two possible approaches can be considered, depending on one's needs. First approach is the black-box approach, where the chillers' (heat pump's) performance is inferred based on state measurements of external fluid circuits. In other words, the internal states of the refrigerant and solution are not measured and performance evaluation of the machine comes from steady state performance at a specified set of external flow rates and inlet/outlet temperatures. Second approach involves internal thermodynamic states of refrigerant and solution circuits as well as the state measurements of external fluid circuits. This, more complex feature, is applied when the computation of essential chillers' characteristics is needed and the black-box approach is insufficient. Values of the heat exchanger thermal conductance, working pair concentrations, internal process temperatures and flow rates are some of the measurements included in this intrusive approach. This additional information is necessary especially when designing and developing new equipment. By means of establishing the link between the states of

external fluids and system losses, the diagnostic capability can be used to adjust key component variables.

URV multifunctional test bench lies on both black-box and internal measurement approaches. Mainly, multifunctional test bench uses black-box approach to obtain performance evaluation of the chiller (heat pump) based only on external measurements. This type of experimental facilities is preferred in work with commercial equipment, when chillers are tested according to commercial standards. Also, the internal measurement approach is easily achievable using the same test bench equipped with some additional measuring equipment in order to define internal behaviour of the chiller (heat pump).

In general, there are two kind of standards developed for chillers and heat pumps:

(1) Commercial standards, which are issued by professional engineers society, industrial bodies or international institutes, and

(2) Statutory standards, which are issued by governmental organization

Commercial standards rely more on the thermal performance while statutory standards relate more to the mechanical integrity and robustness of the machine. Whereas the commercial standards deal with thermodynamic performance, full attention will be paid to this type of standards.

3.2. Absorption system standards

As mentioned above, standards play an important role in order to provide a valuable basis for machine evaluation prior to their release to the market, but also in applications, simulations and control issues. Among worldwide known and recognized institutions and standard issuing organizations such as American Society for Heating and Refrigeration Engineers (ASHRAE), the American Air-Conditioning, Heating and Refrigeration Institute (AHRI), the International Institute of Refrigeration (IIR), European Committee for Standardization (CEN), Australian Building Code Board (ABCB) there are only a few standards dealing with absorption systems. In particular,

there are only three available standards. First, issued by AHRI [108], which applies to water-cooled steam and hot-water operated water chilling units. Second, recommended by CEN [109, 110] for gas fired sorption air-conditioning and heat pump appliances with a heat input lower than 70kW. And third, JIS B 8622, the Standard for water-LiBr absorption refrigeration machines issued by Japanese Standards Association [111] which is beyond our limits due to language barrier.

3.3. AHRI/ANSI 560-2000

The AHRI/ANSI Standard 560-2000 applies to water-cooled single-effect steam chillers, water-cooled single-effect hot water chillers, water-cooled double-effect steam chillers, water-cooled double-effect hot water chillers, and water cooled double-effect direct-fired chillers with water-LiBr working pair.

Standard rating conditions:

- Entering condenser water temperature: 29.4 °C
- Condenser water flow rate: 0.065 L/s per kW of cooling (SE indirect fired), 0.072 L/s per kW (DE indirect fired, DE direct-fired)
- Condenser water-side fouling factor: 0.000044 m^2°C/W
- Evaporator leaving water temperature: 6.7°C
- Evaporator water flow rate: 0.043 L/s per kW
- Evaporator waterside fouling factor: 0.000018 m^2°C/W
- Tube-side fouling factor (steam): 0.000 m^2°C/W (indirect fired)
- Tube-side fouling factor (hot water): 0.00018 m^2°C/W (indirect fired)

Test Procedure

After installing the equipment in accordance with the manufacturer's instructions and non-condensables have been removed, start the system to reach steady state conditions within the following tolerances and instructions:

- The water flow rate in external circuits shall not deviate more than ±5% from the specified value
- The individual readings of water temperature in external circuits shall not vary from the specified values by more than 0.3ºC
- The leaving chilled water temperature, the entering absorber/condenser water temperature and the leaving hot water temperature shall be adjusted by an increment corresponding to the specified Field Fouling Allowance required for test
- Part-load tests for water chilling packages which have continuous capacity modulation must be taken within ± 2% of the full load at the specified part-load capacity
- Steam supply pressure shall be maintained within ±1.4kPa for SE and ± 14kPa for DE of the specified pressure
- Gas and oil heating values to be used for testing are as measured or verified by supplier. Flue gas back pressure shall be maintained within range specified by the manufacturer
- Chiller package shall be supplied with nameplate voltage and frequency

After steady-state conditions have been established at the specific set of conditions and within the defined tolerance, three sets of data shall be taken, at a minimum of 5 minute intervals, as simultaneously as possible.

Measurements to be recorded

a) Temperatures of water entering/ leaving components at each one of the external water circuits, [ºC]

b) Evaporator, absorber/condenser and generator water flow rate, [kg/s]

c) Heat Energy Input from one of the following:

- Steam consumption [kg/hr], steam supply pressure [kPa], steam supply temperature [ºC], steam condensate temperature [ºC]
- Hot water flow rate [kg/s], hot water supply temperature [ºC], hot water leaving temperature [ºC]
- Gas consumption [m3/hr], Higher Heating Value, HHV, gas pressure entering gas [kPa]

d) Water pressure drop in evaporator, absorber/condenser and generator (hot water fired units), [kPa]

e) Electric consumption, [kW]

f) Ambient temperature at test site, [ºC]

g) Barometric pressure at test site, [kPa]

h) Nameplate data, model and serial number of tested equipment

i) Date, place and time of test

Method for Simulating Field Fouling Allowance

Due to the fact that dirtiness at the surface of heat exchangers tends to reduce capacity and increase energy consumption, water-side fouling factor allowance represents an important factor when dealing with chillers (heat pumps). AHRI 560-2000 recommends the following procedure to analyse the effect of the fouling factor allowance on heat transfer surface:

The log mean temperature difference can be obtained from equation 3.1:

$$\mathrm{LMTD} = \frac{(t_s - t_{we}) - (t_s - t_{wl})}{\ln\left[\frac{t_s - t_{we}}{t_s - t_{wl}}\right]} = \frac{(t_{wl} - t_{we})}{\ln\left[\frac{(t_s - t_{wl}) + (t_{wl} - t_{we})}{t_s - t_{wl}}\right.} = \frac{R}{\ln\left(1 + \frac{R}{S}\right)} \tag{3.1}$$

The incremental log mean temperature difference (ILMD) is now determined using the equation 3.2:

$$ILMTD = ff_{sp}\left(\frac{q}{A}\right) \tag{3.2}$$

where:

t_{we} ,t_{w1}- entering/leaving water temperature

t_s- saturation temperature

ff_{sp} - specified field fouling allowance

q - component load

A - total heat transfer surface area

Next step is to calculate water temperature difference, needed to simulate the additional fouling (equations 3.3 and 3.4):

$$TD_a = S_{sp} - S_c \tag{3.3}$$

$$TD_a = S_{sp} - \frac{R}{e^z - 1} \tag{3.4}$$

where:

$$Z = \frac{R}{LMTD - ILMTD} \tag{3.5}$$

$$S_c = \frac{R}{e^z - 1} \tag{3.6}$$

S_{sp}, S_c - small temperature difference as specified/in cleaned condition

The water temperature difference is then added to the absorber/condenser entering water temperature or subtracted from the evaporator leaving water temperature to simulate the additional fouling factor.

Energy calculus and Heat Balance – Substantiating Test

The heat loads in the absorption chiller components can be calculated by general equation where q is equal to the product of water flow rate (or using the product of volumetric flow rate and density instead of mass flow rate), the water temperature difference between entering and leaving water and the specific heat of water (Cp) as shown in the following equation:

$$q = mC_p(T_e - T_l) = V\rho C_p(T_e - T_l) \tag{3.7}$$

In case when energy supply in generator comes from gas or other type of fuel, generator heat load is calculated according to equation 3.8:

$$q_G = m_F\,HHV \tag{3.8}$$

where:

m_F - fuel mass flow rate [kg/s]

HHV- Higher Heating Value [kJ/kg]

According to the Heat Balance Substantiating Test, all heat that enters the absorption unit should be equal to all heat that leaves. However, due to the heat losses or heat gains caused by radiation and convection may cause that overall heat balance differs from zero. The following equation 3.9 serves to calculate heat balance with omitted heat losses and gains:

$$HB = \frac{q_{hs} + q_{ev} - q_c}{q_c}\ 100\ [\%] \tag{3.9}$$

where:

q_{hs} - Input from heat source (generator heat load)

q_{ev} - Net cooling capacity (evaporator heat load)

q_c - Heat rejection to the cooling tower (absorber/condenser heat load)

In practice, heat losses caused by radiation and convection have the value that cannot be omitted. Therefore, for any test of water-cooled chiller to be acceptable, the heat balance (%) shall be within the allowable tolerance calculated by equation 3.10:

$$HB[\%] \leq 10.5\% - [0.07\ FL] + \left(\frac{833.3}{DT_{FL}\ FL}\right) \tag{3.10}$$

where:

FL - Full load

DT_{FL}- Difference between entering and leaving chilled water temperature at full load

Part-Load ratings

The intent of part load ratings is to permit the performance over a range of operating conditions. Energy efficiency of the absorption unit is determined through Coefficient of Performance (COP). COP is defined as a ratio cooling/heating capacity to the power input at any given set of rating conditions. Considering that chillers rarely operate at their maximum capacity, Integrated Part Load Value method was developed to provide consistent method for calculating single number part-load performance number for water-chilling products. This method requires that the unit efficiency be determined at 100%, 75%, 50%, 25% of standard ratings. The study of American Department of Energy [112], based on weighted average of 29 different cities across the USA with the most common building types and operations was used to develop a chiller

loading profile for a typical year. The resulting chiller loading profile is at 100% capacity about 1% of the time, 75% capacity about 42% of the time, 50% capacity about 45% of the time, and 25% capacity about 12% of the time. These constants are incorporated into the IPLV equation (3.11):

For COP:

$$IPLV = 0.01A + 0.42B + 0.45C + 0.12D \quad (3.11)$$

where:

A - COP at 100% capacity (condenser water at 29.4°C)

B - COP at 75% capacity (condenser water at 25.3°C)

C - COP at 50% capacity (condenser water at 21.1°C)

D - COP at 25% capacity (condenser water at 21.1°C)

IPLV provides the most accurate average chiller energy usage for evaluation of different chiller energy usage. IPLV becomes non-standard part load value (NPLV) method is used when the known parameters differ from standard ratings, having the manufacturers' recommended value.

3.4. EN 12309:2000

The European Standard EN 12309:2000 issued by CEN refers to gas-fired sorption air-conditioning and heat pump machines with heat input less than 70kW. Term sorption here covers the absorption and adsorption equipment. This standard applies only to machines with following characteristics: integral burner under the control of fully automatic burner control systems; closed refrigerant circuits in which the refrigerant does not come into direct contact with the fluid to be cooled (heated) and where mechanical means to assist transportation of the combustion air. Three different types of the machines can be distinguished by this standard depending on their primary function:

- Chiller: air-conditioning machine designed to provide cooling as primary function and may provide heating as a secondary function

- Chiller/heater: air-conditioning machine designed to provide cooling and heating both as primary function

- Heat pump appliance: heating machine utilizing a refrigerant to transfer heat from one medium to another at a higher temperature in order to contribute to the heating function also

Besides, depending on which heat transfer medium (air or water) is used for absorber/condenser, this standard denominates air-cooled and water-cooled machines. Part 1 of this standard specifies the requirements and test methods for the safe usage of this equipment. Whereas it covers only the gas-fired equipment, gases are classified into three families and divided into groups according to Wobbe index. Based on that, machines are classified according to the gases they use; the mode of evacuation of combustion products; temperature of their heat transfer media and their denomination. In addition, Part 1 covers all the relevant issue concerning construction, safety, marking, installation, work and maintenance of this equipment. This includes materials and methods of construction, thermal insulation, gas connection, soundness, operational safety in the event of fluctuation and interruption, requirements for adjusting, control and safety devices, ignition devices, transportation of combustion air and flue gasses, flame supervision system, operational requirements, test methods and technical instructions for installation and adjustment, use and maintenance and servicing.

To be in accordance with this standard, all heat inputs should be determined from the volumetric flow rate (V_0) or mass rate (M_0) which relate to the rate obtained with reference gas under reference test conditions (dry gas, 15ºC, 1013.25 mbar). The heat input (Q_0) can be calculated by one of following formulas (3.12a, 3.12b):

$$Q_0 = 0.278\, V_0 \times H_i (\text{or } H_s) \tag{3.12a}$$

$$Q_0 = 0.278\, M_0 \times H_i (\text{or } H_s) \tag{3.12b}$$

where:

V_0 - volumetric flow rate [m^3/h] obtained at reference conditions

M_0 - mass input [kg/h] obtained at reference conditions

H_i - net calorific value of the reference gas [MJ/m^3; MJ/kg]

H_s - gross calorific value of the reference gas [MJ/m^3; MJ/kg]

In practice, the values obtained in test do not correspond to these reference conditions so they should be corrected to bring them to the values that would actually have been obtained if these reference conditions had existed at the injector outlet (equations 3.12c and 3.12d).

$$Q_T = 0.278\, V_C \times H_i (\text{or } H_s) \tag{3.12c}$$

$$V_C = V_m \frac{p_a + p - p_w}{1\,013.25} \frac{288.15}{273.15 + t_g} \tag{3.12d}$$

where:

Q_T - heat input under the test conditions [kW]

V_C - volumetric flow rate [m^3/h] of dry test gas corrected to reference conditions

V_m - measured volumetric flow rate [m^3/h]

p_a - atmospheric pressure [mbar]

p - gas supply pressure at the gas meter [mbar]

p_w - partial vapour pressure [mbar]

t_g - gas temperature at the gas meter [ºC]

Part 2 of this standard relates to requirements and methods of test for the rational use of energy. Prior to start with rating tests, the test installation has to be designed in

such a way that all adjustments of set values, stability criteria and uncertainty of measurements can be fulfilled. This implies that all previous preparation must be in accordance with the Part 1 of the standard.

Test conditions for water or air-cooled liquid chillers and chiller/heaters

The tests for cooling mode have to be carried out under the environmental conditions and with the electrical power specified in Table 3.1.

Table 3.1 Environmental conditions and electrical power supply conditions

Machine	Measured quantities	Rating test
Water-cooled machine	Temperature	15ºC to 30 ºC
Air-cooled machine	Temperature	As the air inlet temperature
All machines	Voltage	Rated voltage

Rating test conditions for cooling capacity of the chillers are listed in Table 3.2. The manufacturer is obliged to declare cooling capacity together with gas utilization efficiency corresponding to test conditions (T1). If the manufacturer declares cooling capacity and gas utilization efficiency corresponding to test conditions (T2) or (T3), they shell also be verified.

Table 3.2 Rating test conditions for cooling capacity of chillers

Test condition	Type of machine	Test condition designation	Temperature at the absorber/ condenser [ºC]		Temperature at the evaporator [ºC]	
			inlet	outlet	inlet	outlet
T1	Water-cooled water chiller	W30/W7	30	35	12	7
T1	Water-cooled brine chiller	W30/B -5	30	35	0	-5
T1	Air/water heat pump Air-cooled water chiller	A35/W7	35	-	12	7
T2		A27/W7	27	-	12	7
T3		A46/W7	46	-	12	7
T1	Air/brine heat pump Air-cooled brine chiller	A35/B -5	35	-	0	-5
T2		A27/B -5	27	-	0	-5
T3		A46/B -5	46	-	0	-5

If a secondary function of the machine is heat recovery, where available heat from the machine whose primary function is cooling is used by means of an additional heat exchanger, the heat recovery capacity claimed by the manufacturer shall correspond to the appropriate test conditions given in Table 3.3.

Table 3.3 Rating test conditions for heat recovery capacity for chillers

Heat recovery water heat exchanger		
Inlet temperature		40 ºC
Outlet temperature		50 ºC
Condenser/absorber	Air Inlet Temperature	15 ºC
	Water Inlet Temperature	30 ºC
Evaporator	Water Outlet Temperature	7 ºC
	Brine Outlet Temperature	-5 ºC

These conditions are considered to be obtained and maintained under steady-state operating regime. Steady state regime implies that all measured quantities remain constant without having to alter set values. Permissible deviations of periodic fluctuations have to be in range with the deviations listed in Table 3.4. The duration of measurement in steady-state has to be at least 30 minutes, with a minimum of 2 minutes sequence for recording all meaningful data.

Table 3.4 Permissible deviation from set values for chillers

Measured quantity	**Permissible deviation of the arithmetic mean values from set values ±**	**Permissible deviation of the individual measured values from set values ±**
Liquid		
- inlet temperature	0.2 K	0.5 K
- outlet temperature	0.3 K	0.6 K
- flow (volume)	2 %	5 %
Air		
- inlet temperature (dry bulb)	0.5 K	1 K
- static pressure difference	-	10 %
Voltage	4 %	4 %

The cooling capacity as well as the heat recovery capacity can be determined using the formula (3.13):

$$Q = V_m \, \delta \, C_p \, \Delta t \qquad (3.13)$$

where:

Q - cooling/heat recovery capacity [kW]

V_m - volumetric flow rate of the heat transfer medium at inlet temperature [m^3/s]

δ - density of the heat transfer medium at inlet temperature [kg/m^3]

C_p - specific heat of the heat transfer medium at constant pressure at mean temperature of the heat transfer medium [kJ/kg K]

Δt - difference between inlet and outlet temperatures of the heat transfer medium [K]

The gas utilization efficiency (ηc) is determined by equation 3.14:

$$\eta_c = \frac{Q_C}{Q_T} \tag{3.14}$$

where:

Q_C - cooling capacity [kW]

Q_T - heat input of the burner under the test conditions [kW]

Standard specifies also similar procedure for testing air-cooled or water-cooled air conditioners as well as for machines in heating mode where both output measurements with and without defrosting are covered. Complete procedure and detailed explanation of the requirements for different gas-fired machines can be found in cited references.

Although at first sight seems that these standards are sufficient to cover whole field of absorption systems, simple analysis shows that still there are many uncovered topics. AHRI/ANSI 560-2000, as seen above, covers a wide area of water-cooled absorption chilling and chilling/heating units, both direct and indirect fired. However, this standard is not valid for air-cooled machines, heat pumps and exhaust gas fired applications. On the other hand, EN 12309-1&2:2000 covers this area but only for small-scale gas fired units. Hence the question raises how to treat indirect fired air-

cooled absorption chillers or heat pumps. What do happen with large-scale gas-fired absorption equipment or with NH_3-H_2O equipment? In addition, what to do with absorption refrigeration applications, non-standard units? All these facts indicate that there is still much room for research and improvement in this area. In practice, most of these issues are solved by seeking and adapting similar standards for vapour compression systems since this field is widely covered. URV multifunctional test bench can meet all the requirements specified by mentioned standards for testing absorption equipment, as will be seen in following sections.

3.5. Main components

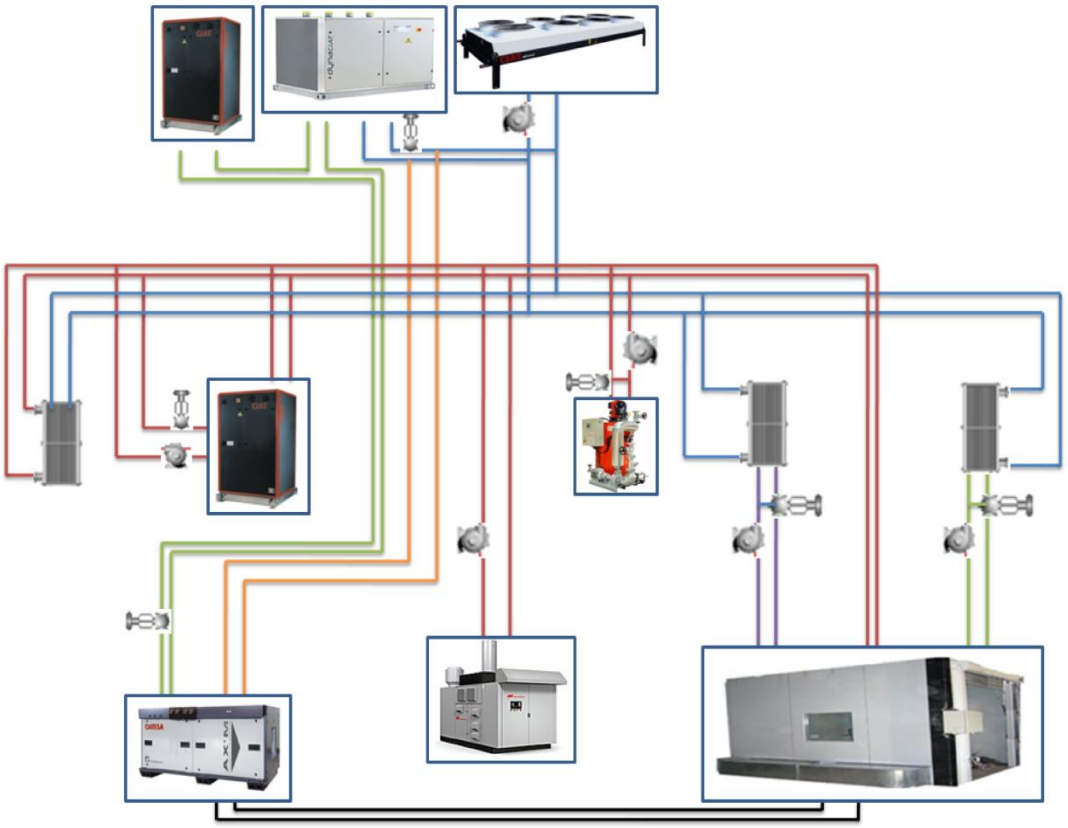

Figure 3.1 General scheme of the test bench

The primary goal of the multifunctional test bench is to provide experimental engineering data for the design, construction, operation and simulation of thermally driven systems and their components. The exclusive capabilities of the facility are often

applied to tests correlated to solar assisted air-conditioning applications and evaluation of renewable and other generation technologies. In particular, the emphasize is on work with (ab)sorption equipment in small-scale solar assisted air-conditioning and micro tri-generation systems. The multifunctional test bench consists of several major components in order to fulfil requirements for testing different equipment under different conditions of interest. Figure 3.1 shows the simplified scheme of the test bench with the most important pieces of equipment. Selection of the component and the way they are connected determine the operating mode necessary for particular test.

To provide necessary energy for the system activation, test bench dispose of one thermal fluid (hot oil) heater. Hot oil heater generates the heat which is required for ignition and smooth operation of the tested equipment. This heat is delivered to the equipment through the heat transfer fluid. Work with the hot oil heater is much more comfortable than work with solar collectors in laboratory conditions, for instance. This might not be true when transient behaviour of solar collectors is required, but certainly is true when testing equipment under wide temperature range in steady-state conditions. The time response for various set points is shorter whereas the heat supply is controlled and adjusted according to required conditions and not dependant on outside conditions as in case of the solar collectors. Nominal capacity of the gas-fired oil heater is 175kW and can work in a temperature range from 60 up to 300ºC. The heater is coupled with the gas burner Weishaupt WG 10 in a packaged boiler/burner unit. This package system permits capacity to be modulated in a range from 20% to 100% of nominal capacity. Technical characteristics of the thermal oil heater are listed in Table 3.5.

Table 3.5 Technical data for thermal oil heater Pirobloc GFT 010/20V

Nominal capacity [kW]	175	
Max operating pressure [bar]	7	
Max operating temperature [ºC]	300	
Thermal efficiency [%]	87-91	
Volume [l]	60	

Another possibility is to use gas micro turbine instead of oil fired heater. This option is generally used when it comes to experiments with Combine Heat and Power

applications. Table 3.6 shows natural gas micro turbine technical specification.

Table 3.6 Gas micro turbine Capstone C30

Fuel	LPNG
Rated output [kW]	28
Net efficiency LHV [%]	26
Exhausted gas temperature [ºC]	275
Fuel flow LHV [kW]	112
Exhausted heat energy [kW]	90.8
Exhausted gas flow [kg/s]	0.31

Table 3.7 Plate heat exchangers Alfa Laval

Type	M6M-FM11NBR	M6M-FM11NBR
Circuit	Chilled water	Cooling water
Number of plates	31	33
Max flow rate [kg/s]	15	15
Max temperature [˚C]	160	160
Max pressure [bar]	10	10
Flow principle	Parallel	Parallel

Two plate heat exchangers (Table 3.7) have the role of transferring the heat between the primary and secondary side of the test bench. Primary side here refers to external fluid circuits of the tested equipment while secondary side denotes heat dissipation circuit. One heat exchanger acts as heat source for chilled water circuit by means of transferring the heat from secondary side to the circuit while. On the contrary, second heat exchanger performs as heat sink by means of transferring the heat from cooling water circuit to secondary side. These heat exchangers are designed to handle efficiently the pressure difference that normally exists between the primary and secondary sides in heating and air-conditioning systems. Also, this type of heat exchangers allows temperature difference 0.5˚C between primary and secondary side. Beside these two heat exchangers, there is one more heat exchanger which forms part of secondary side. This brazed heat exchanger has a dual role. First, when it takes part of

application for desalination which is not discussed here since our focus on the absorption systems. Second role is to prevent gas burner shut off when heat demand of the tested appliance is lower than 20% of the burners modulating capacity. Consequently, excess heat is transferred through this heat exchanger from primary side (hot water) to secondary side allowing burner to work continuously at minimum capacity.

Dry cooler settled on the roof of the building is another important component of the multifunctional test bench. The main purpose of the dry cooler is to dissipate excess heat into the ambient air. Dry cooler consists of water to air coil and three fans, one with variable speed and two operating at constant speed. Dissipation capacity can be varied in a range between 10 and 100% of the nominal capacity by of controlling these three fans. Main characteristics of the dry cooler are listed in Table 3.8.

Table 3.8 Dry cooler CIAT Europe 2 9032 HI 920

Water flow rate [m^3/h]	9.5
Pressure drop [kPa]	67.8
Inlet/outlet temperature [˚C]	37/30
Air ambient temperature [˚C]	25
Thermal capacity [kW]	75

To test appliance under different ambient conditions, multifunctional test bench uses the environmental test chamber. This permits the user to simulate different temperature and humidity conditions which is of particular importance in experiments with air-cooled appliances. Manufacturer specifications are listed in Table 3.9.

Table 3.9 Environmental test chamber Telewig KZ/80

Dimensions [m]	3 x 3 x 3
Temperature range [ºC]	-20 - 100
Humidity range [%]	30 - 95
Temperature constancy [ºC]	± 0.3
Humidity constancy [%]	± 2.5RH

Table 3.10 Air handling unit CIATESA HYDRONIC AX M 45 CONFORT

Chilled water cooling coil with 12 rows	4ºC/9ºC
Cooling capacity [kW]	57.5
Water flow rate [m^3/h]	9.83
Hot water heater battery with 4 rows	45ºC/40ºC
Heating capacity[kW]	39.5
Water flow rate[m^3/h]	6.88
Hot water heater battery with 2 rows	80ºC/60ºC
Heating capacity[kW]	40.4
Water flow rate[m^3/h]	7
Fan air flow [m^3/h]	3500

Table 3.11 Vapour compression chiller DYNACIAT LG 350V

Heating capacity [kW]	126
Power input [kW]	22.3
EER	4.71
Cooling capacity [kW]	105.1
Power input [kW]	27.4
COP	4.4
Evaporator outlet T range [˚C]	-10 to +18
Condenser outlet T range [˚C]	+30 to +50
Evaporator flow rate [m^3/h]	11 to 34
Condenser flow rate [m^3/h]	10 to 26

Temperature and humidity inside the chamber are controlled by an air-handling unit (AHU) and one vapour compression chiller. Air-handling unit is connected through duct line to the test chamber on one side and to the vapour compression chiller via pipeline on the other. Simplified, required conditions inside the test chamber are controlled via air circulation through the air-handling unit. The vapour compression chiller situated at the roof enables smooth work of the air-handling unit by supplying the coils of the air handling unit with water at required temperature. AHU consist of one

cooling coil connected to vapour compression chiller, two heating coils and one fan which blows the air to the chamber and enables circulation. Nominal cooling capacity of the vapour compression chiller consisted of condenser, evaporator, throttling valve and two scroll compressors is 105kW. Chiller uses R410 refrigerant. Technical data for AHU and vapour compression chiller are given in Table 3.10 and Table 3.11, respectively.

Two hydraulic modules have been chosen in order to have enough static pressure available at a given water flow to overcome the pressure drop in the system. The expansion tanks within these units receive volume changes due to temperature changes in the water circuits. A pump within the module enables and supports the circulation of water circuits. Table 3.12 shows the main characteristics of hydraulic module.

Table 3.12 Hydraulic module CIAT MHJ 350

Water flow rate [m^3/h]	4-30
Operating range: cooling capacity [kW]	20-180
Buffer tank [l]	350
Expansion vessel [l]	30
Safety valve [bar]	4
Water filter [μm]	600

Four different Grundfos pumps were chosen to meet system requirements and enable smooth circulation of the fluid both on primary and secondary side. These pumps have implemented electronic speed control in order to achieve required flow rate in water circuits. Similarly, test bench uses three port valves with electro actuators (Siemens Activex SQX62) to control temperature in primary side circuits. Fitting material (valves, etc), pipes, ducts, electronic equipment and other peripheral material also take part of multifunctional test bench but for the sake of simplicity, detailed explanation is omitted.

In this way, different operating modes for testing required equipment become available by simple choosing different combinations of components, followed by

adequate pipelines arrangements and combination of valves. Following sections describe the most exploited operating modes when evaluating the performance of absorption machines.

3.6. Operating modes for absorption systems

3.6.1. Water-cooled absorption chiller

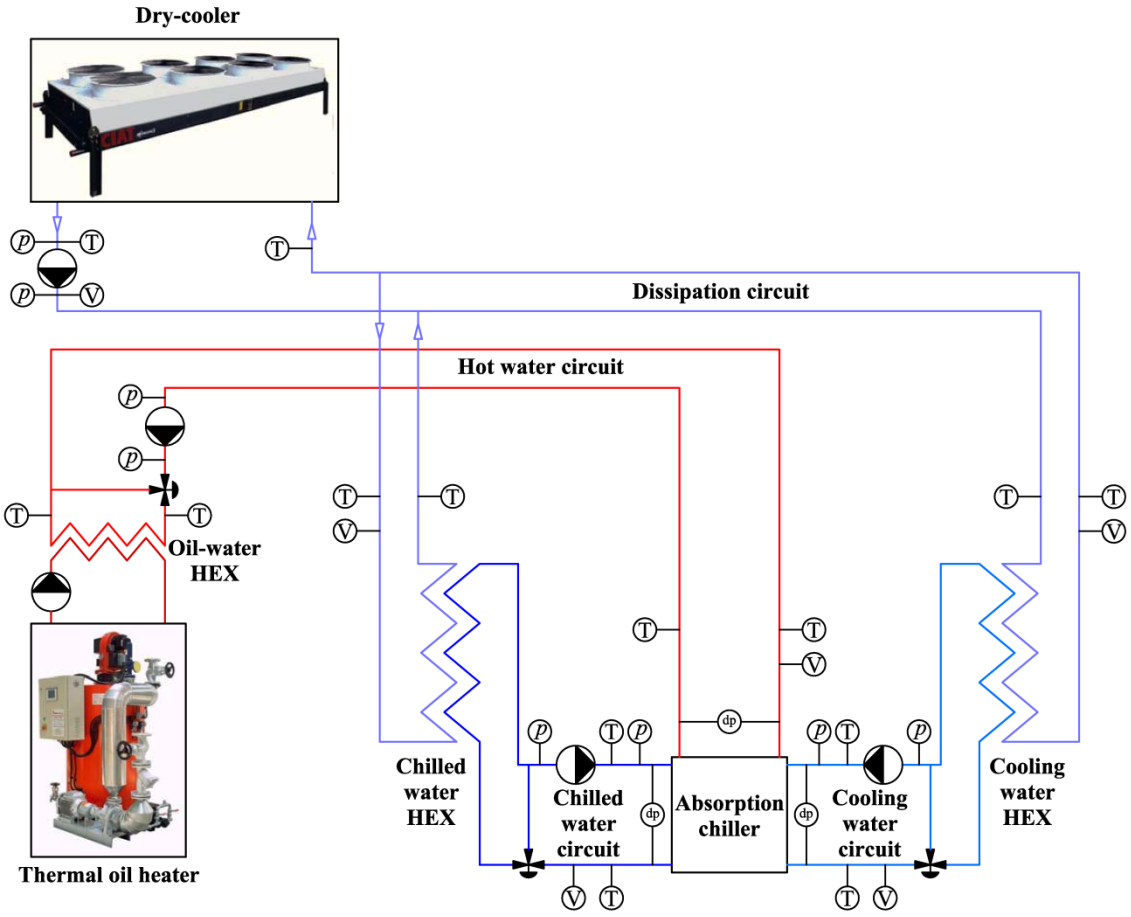

Figure 3.2 Test configuration for water-cooled absorption chiller

There are two possible configuration of the multifunctional test bench for testing water-cooled absorption chillers. The outside conditions, temperature difference between the loops of two heat exchangers (chilled and cooling water HEX) and the temperature levels used in particular test determine which configuration will be used. In majority of the cases, when the ambient temperature is not extreme, the absorption chillers are tested with configuration shown in Figure 3.2. A thermal oil heater provides

driving heat for the absorption chiller. The energy released by combustion of natural gas is used to heat the thermal oil, which circulates through one side of the oil/water heat exchanger. The oil/water heat exchanger transfers this heat to the water side and supplies the generator of the absorption chiller via the hot water circuit. The control of the hot water inlet temperature (inlet to the generator) is carried out in two steps. In the first step, temperature of the thermal oil heater is set approximately 5ºC higher than required hot water inlet temperature. In the second step, control system uses a PID controller, RTD sensor and transducer to correctly position the three-port valve. The RTD sensor monitors the actual temperature and feeds the information to the PID controller. The PID controller then sends a signal through a transducer to the valve, adjusting the actual hot water inlet temperature to the fixed set point. Fluctuation of the temperature controlled in this way is less than ±0.3˚C. Volumetric flow rate in the hot water circuit is controlled through pump by changing the pump frequency. In the chilled water circuit water leaving the absorption chiller passes through the chilled water heat exchanger where receives heat and then returns to the chiller. Similarly, in the cooling water circuit heat released by the absorber and condenser is removed by means of a cooling water circuit and cooling water heat exchanger. Two three-port valves with actuators, one in each circuit, controlled by PID controllers are used to the adjust evaporator outlet temperature and condenser inlet temperature. The recorded fluctuations are normally less than ±0.3˚C. Same as in the hot water circuit, flow rates are adjusted through pump frequency control. This type of control allows a wide range of the water temperatures and flow rates to be achieved during the tests. In the external, dissipation circuit, water stream with the heat transferred from the cooling water heat exchanger mixes with cooler water stream coming from the chilled water heat exchanger before entering the dry cooler. The dry-cooler releases excess heat to the ambient air through water to air coil unit. The excess heat is approximately equal to the heat supplied to the absorption chiller through hot water circuit. A following logic can prove that. If we neglect losses through the pipeline, the excess heat should be equal to difference between the heat released in cooling water heat exchanger and the heat supplied to the chilled water heat exchanger. These two heats are in fact thermal loads in the absorber/condenser and evaporator, respectively. Assuming that there are not heat

losses and performing Heat Balance Substantiating Test (the heat which enters the absorption unit is equal to the heat which leaves) we prove the hypothesis (3.15):

$$Q_{excess} = Q_{ac} - Q_{eva} = Q_{gen} \tag{3.15}$$

After leaving the dry cooler, cooled water of the dissipation circuit is pumped back to the cooling water heat exchanger maintaining the continuity of the process.

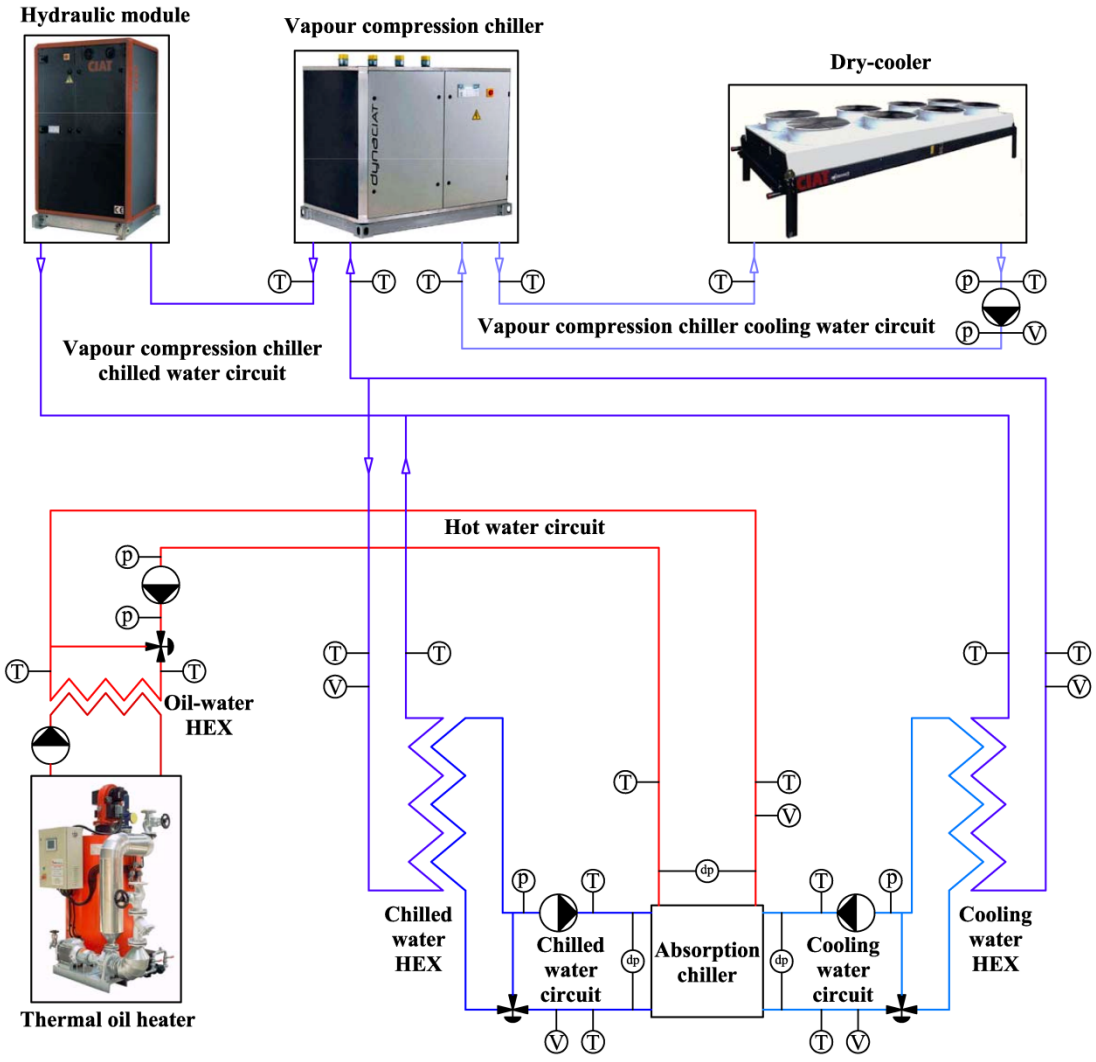

Figure 3.3 Test configuration for water-cooled absorption chiller in extreme conditions

The configuration shown in Figure 3.3 is used when outside conditions are extreme, as tends to happen in very hot summer days. The working principle is slightly modified with respect to the first configuration. Thermal fluid heater supplies the

driving heat to the absorption chiller via hot water circuit, while heat transfer between internal and external water circuits is performed through two heat exchangers. The main difference is use of vapour compression chiller to provide lower temperatures and therefore improved heat transfer. Water stream from two heat exchangers enters to the vapour compression chiller where heat is removed by means of evaporator coil. Cooled water than continues to the hydraulic module whose pump enables smooth circulation of the circuit. On the other side of vapour compression chiller, transferred heat is released by the condenser and rejected to the ambient air using dry cooler.

3.6.2. Air-cooled absorption chiller

The configuration for testing absorption chiller in air-cooled mode is somewhat more complex with respect to water-cooled mode since an additional air loop is necessary to maintain dissipation of the heat released from absorber/condenser. The necessary loop is created by changing the route of the pipeline and by employing two new components: air handling unit and environmental test chamber. This is shown in Figure 3.4. Same as in the configuration for the water-cooled chiller, thermal fluid heater supplies energy to the generator by means of hot water circuit and the chilled water heat exchanger performs as heat source for chilled water circuit feeding the evaporator with necessary energy. Now, the main challenge is how to handle heat dissipation of the absorber/condenser and to maintain the operating conditions stable. Normally, the air-cooled chiller contains an additional (or built-in) air coil unit to reject heat released by the absorber/condenser to the environment. Nevertheless, how to prevent accumulation of the heat since we are talking about controlled conditions of interest under closed environment? This is done by linking with the air-handling unit. Cold air from air handling unit, passing through duct and an opening with damper, enters to the chamber where it receives heat released by the absorber/condenser of the absorption chiller. Warm air then returns to the air handling unit passing through another duct line from the top of the test chamber delivering the heat to the cooling water circuit of the compression chiller. The openings at the bottom and at the top of the environmental test chamber equipped with appropriate air deflectors enable smooth circulation of the air. On the other side, water stream heated in the condenser of the compression chiller mixes with the cold water coming from chilled water heat

exchanger before entering to the dry cooler. After rejecting excess heat to the ambient, the water stream from the dry cooler forks in two streams, where one part goes to the compression chiller to receive heat in the condenser, and a second part proceeds to the chilled water heat exchanger to supply absorption chiller evaporator with necessary heat. Air temperature is controlled with PID controller through the air-handling unit while the control of hot and chilled water circuits remain the same as in configuration for water-cooled chillers.

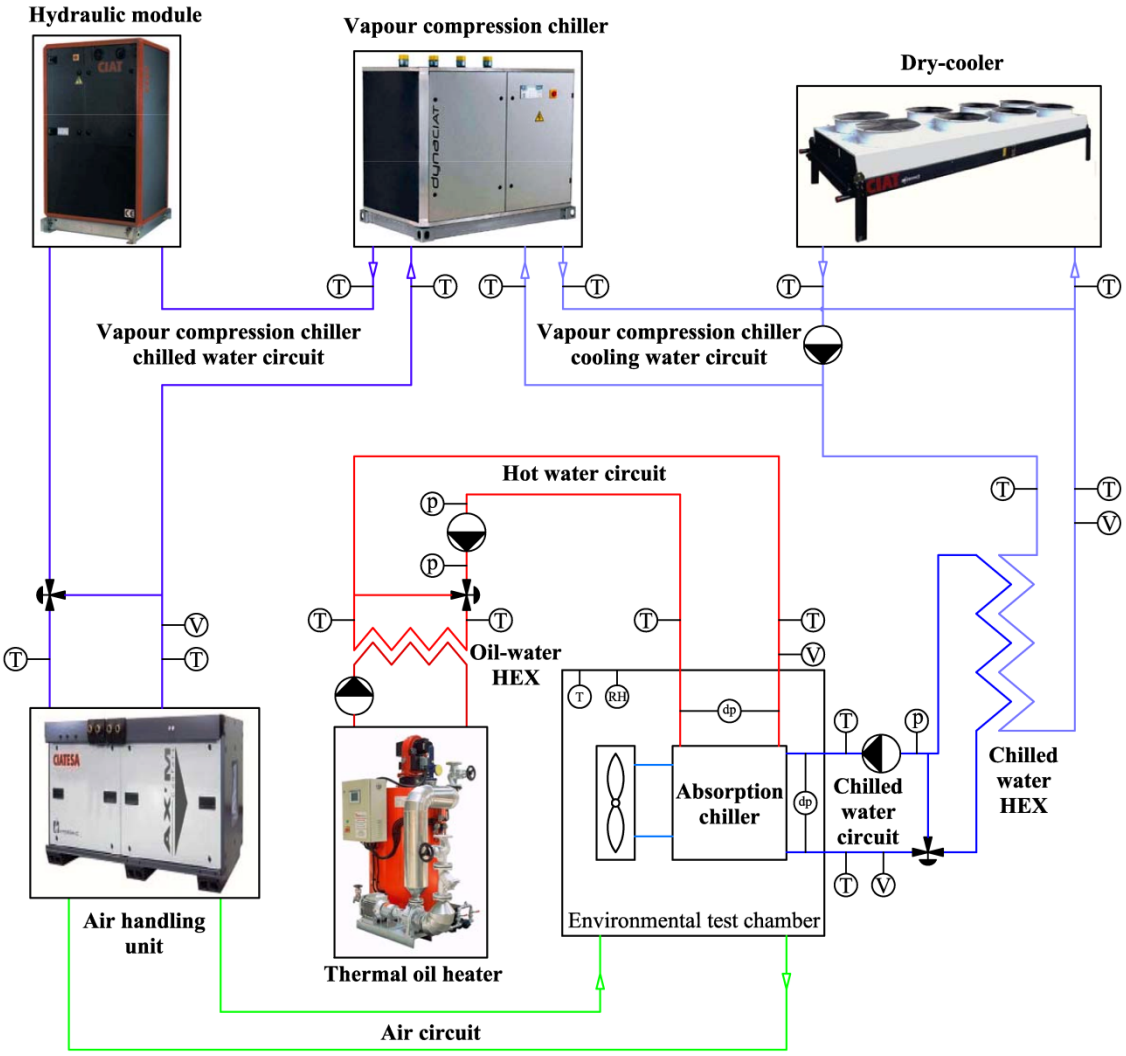

Figure 3.4 Test configuration for air-cooled absorption chiller

Another option is to test air-cooled absorption chiller under required conditions of interest but with possibility to vary relative humidity. This option is available by using configuration shown in Figure 3.5. Hot air coming from the test chamber enters to

the air-handling unit through air circuit to be cooled in a cooling coil which is connected to the evaporator of the compression chiller on the other side. Part of the condensed vapour is removed by a drainage system before passing the heating coil. The heating coil uses the heat released in the condenser of the vapour compression chiller to maintain the air temperature at required set point before returning to the test chamber.

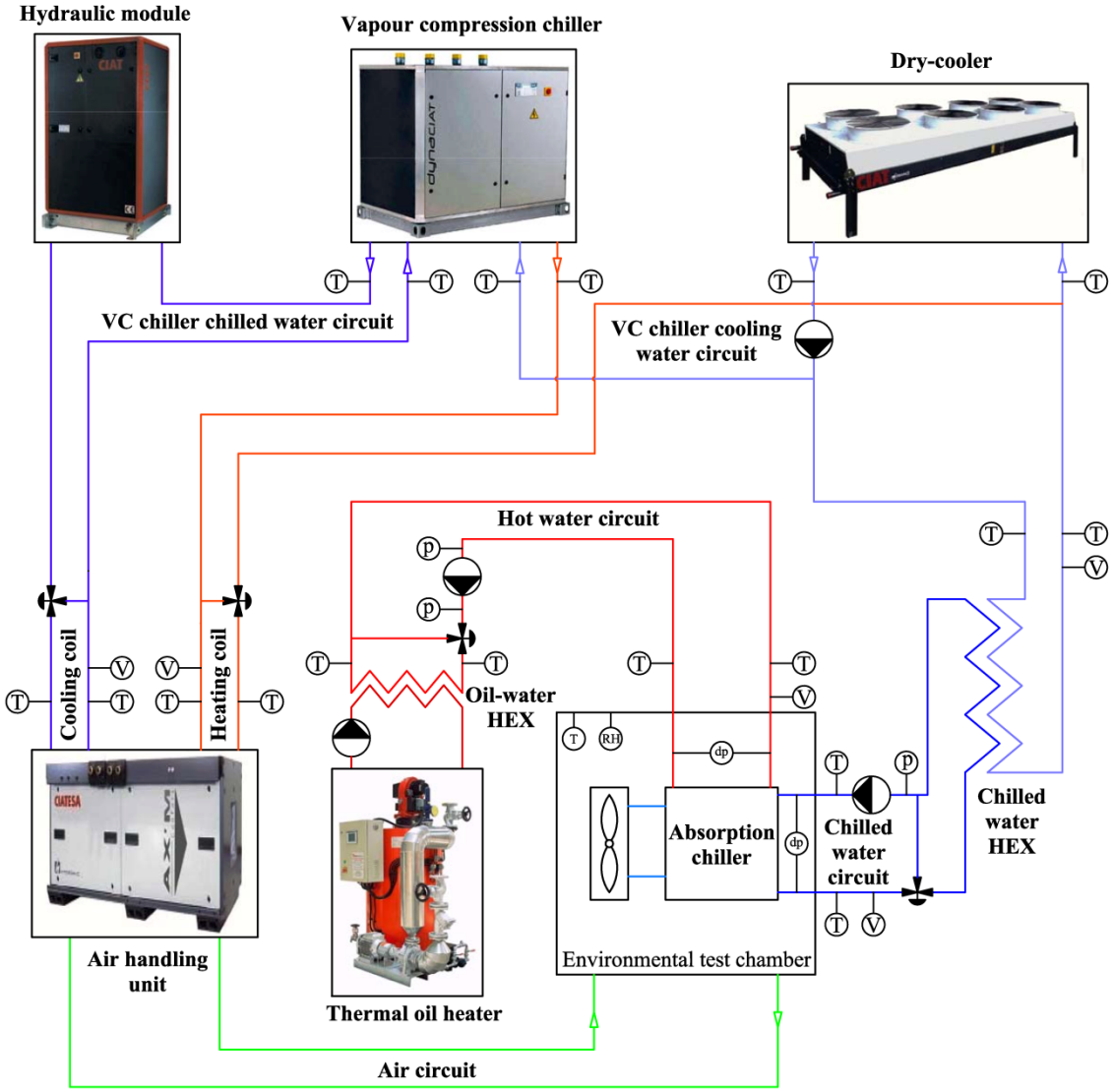

Figure 3.5 Test configuration for air-cooled chiller with variable humidity

3.6.3. Absorption heat-pump

The main difference between absorption chiller and heat pump is the final product. While in the absorption chiller the product is the refrigeration at the lowest temperature, in the absorption heat pump the product is heating at intermediate level

[23]. In addition, the useful heat should be produced at temperature level which permits its use in heating application. Since the absorption chillers and heat pumps operate between three temperature levels, increasing the temperature in the condenser/absorber will demand increase in evaporator temperature with constant driving temperature at the highest level (generator). According to these facts, the same configuration used for water-cooled absorption chillers (Figure 3.3) can be used to test the water-to-water absorption heat pumps. The only modification would be to change the controlled variable in the cooling water circuit. For the purpose of the heating application, the controlled variable should be absorber/condenser outlet temperature, which is easily achievable.

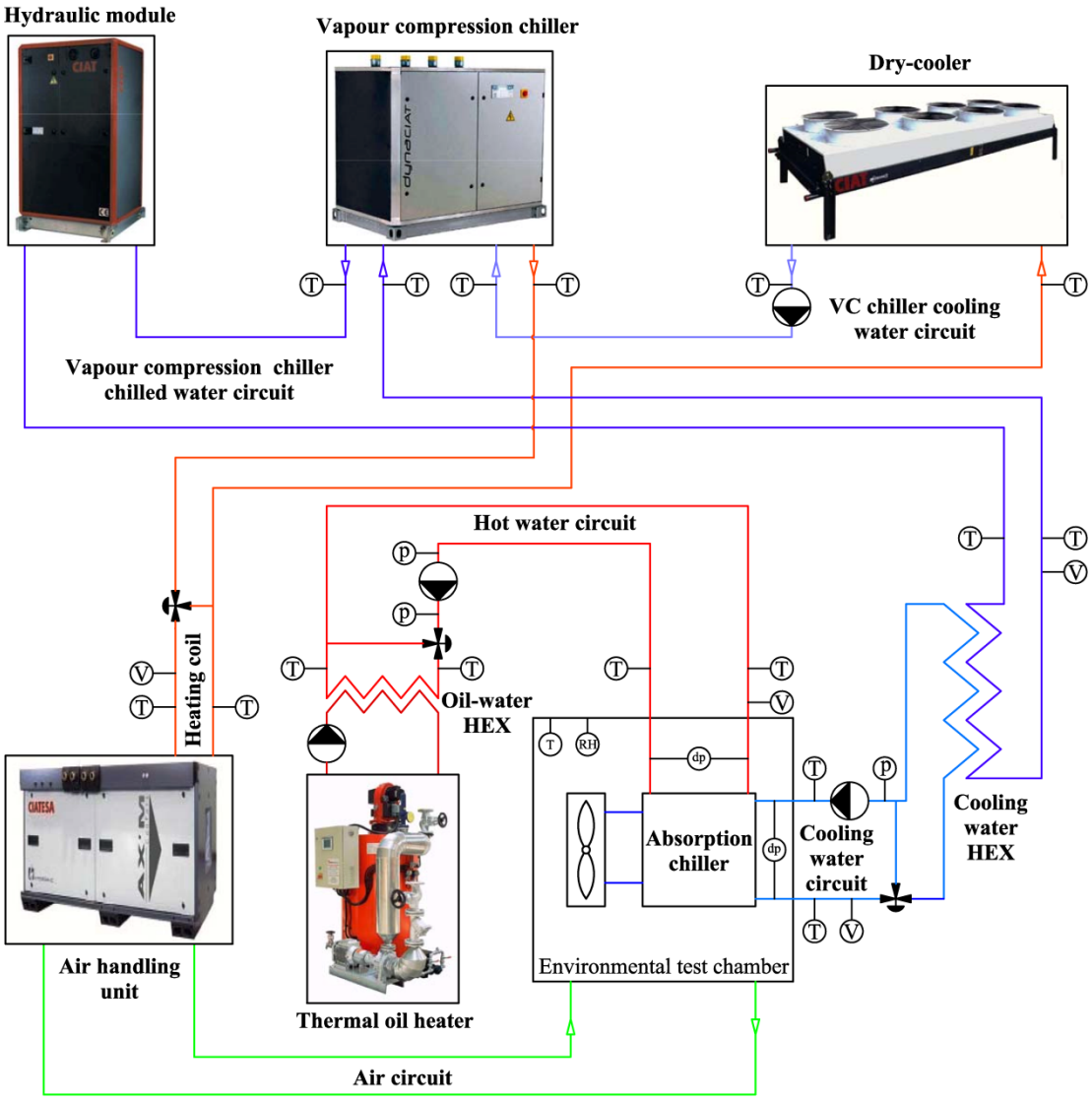

Figure 3.6 Test configuration for air/water absorption heat pump

Although air-to-water absorption heat pumps are rarely present at the market due to the limitations of the technology, configuration shown in Figure 3.6 allows testing the heat pumps even when outside air is used as heat source for the evaporator. The heat produced in the thermal oil heater and transferred through the hot water circuit drives the generator. Useful heat released from the absorber and condenser, which is now the main product to be used in heating applications (i.e. fan coils), is transferred through cooling water heat exchanger and water circuit to the compression chiller. The required ambient temperature is maintained inside the test chamber in a following way. After extracting the heat from ambient air inside the chamber to feed the evaporator, cooled air stream enters to the air-handling unit where receives necessary heat through the heating coil and returns to the chamber, maintaining the process continuous. The necessary heat in heating coil is provided by means of compression chiller condenser circuit.

3.7. Data acquisition

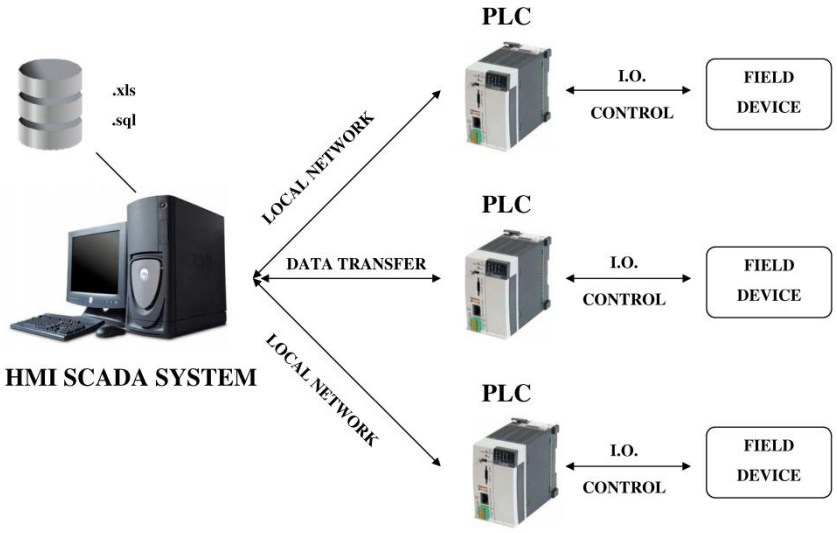

Figure 3.7 SCADA basic scheme

A small Supervisory Control and Data Acquisition (SCADA) system has been developed by CELECTRA Inc for the purpose of test operations in the multifunctional test bench. The SCADA system permits real time monitoring, data storage and real time control of each subsystem in the test bench. The last one implies that SCADA has

components of Distributed Control System by means of Programmable Logic Controllers (PLC), which are capable to execute autonomously simple logic processes. The basics of the SCADA system are shown in Figure 3.7.

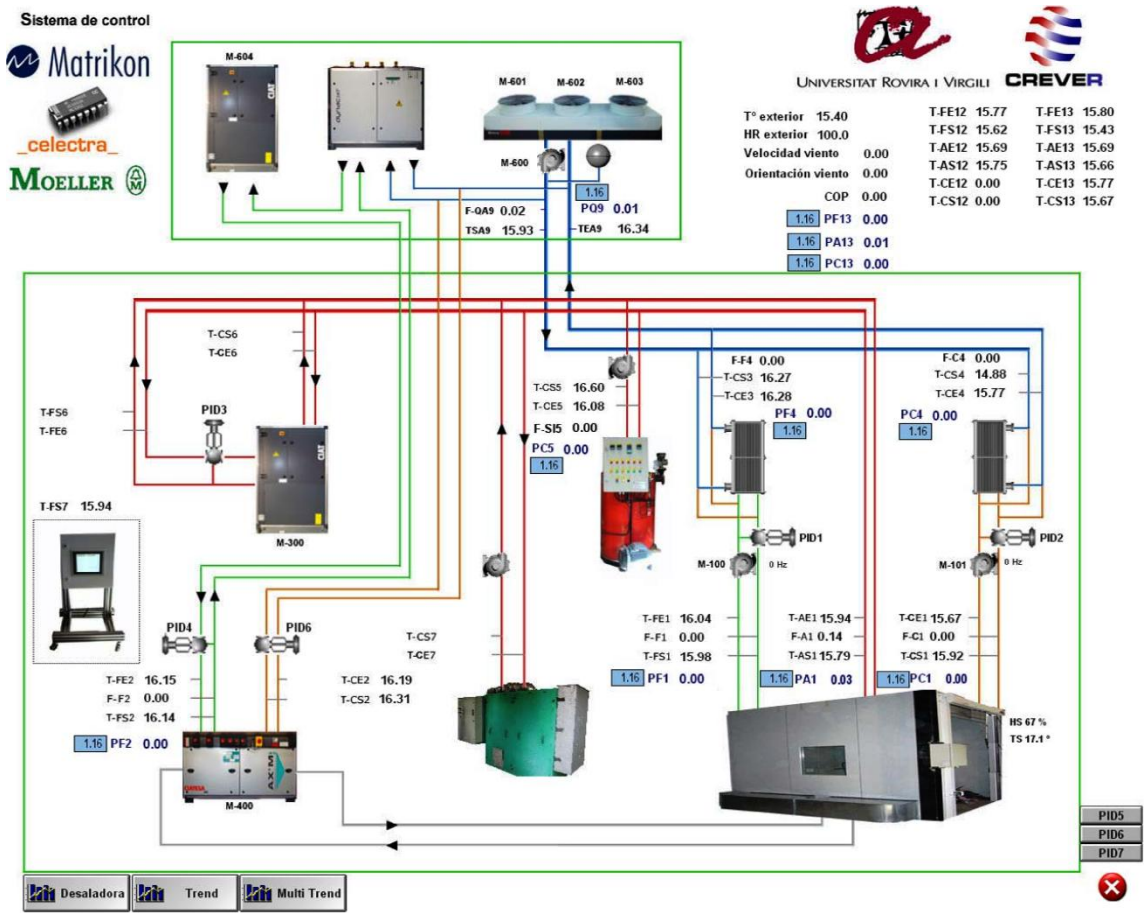

Figure 3.8 HMI of the multifunctional test bench

Control functions are performed by PLC in a way that it compares the measured quantity to the set point adjusting the controlled variable to match the required set point. Data acquisition begins when PLCs send information over the network to the SCADA. This is done through Matrikon OPC Server application where this information is translated into a standard OPC format. User interface and other application compatible with OPC such as trending application, spreadsheet and historian use it to read and write device data. With this automation control system, the test application can be started up, shut down, and adjusted automatically or manually through a computer. The only device which has to be started manually is the tested absorption appliance. The operating conditions can be displayed on a graphical user interface, and the measured

data can be stored for further analysis. The common name for this type of user interface is Human Machine Interface (HMI) as it allows the human operator to control and monitor the process. The HMI of the multifunctional test bench is a small and independent software package shown in Figure 3.8.

Parallel to the computer monitoring function shown above, the real time control function is also implemented in the HMI. Simple click on any of the device icons opens new tab with controlling parameters for the device. This allows us to change set point temperature in the air handling unit, temperature in the heat carrier circuits and to tune PID values for each controller. To increase dry cooler dissipation or to change volumetric flow rate by changing the frequency of the pump, etc. some of these examples are illustrated in Figure 3.9.

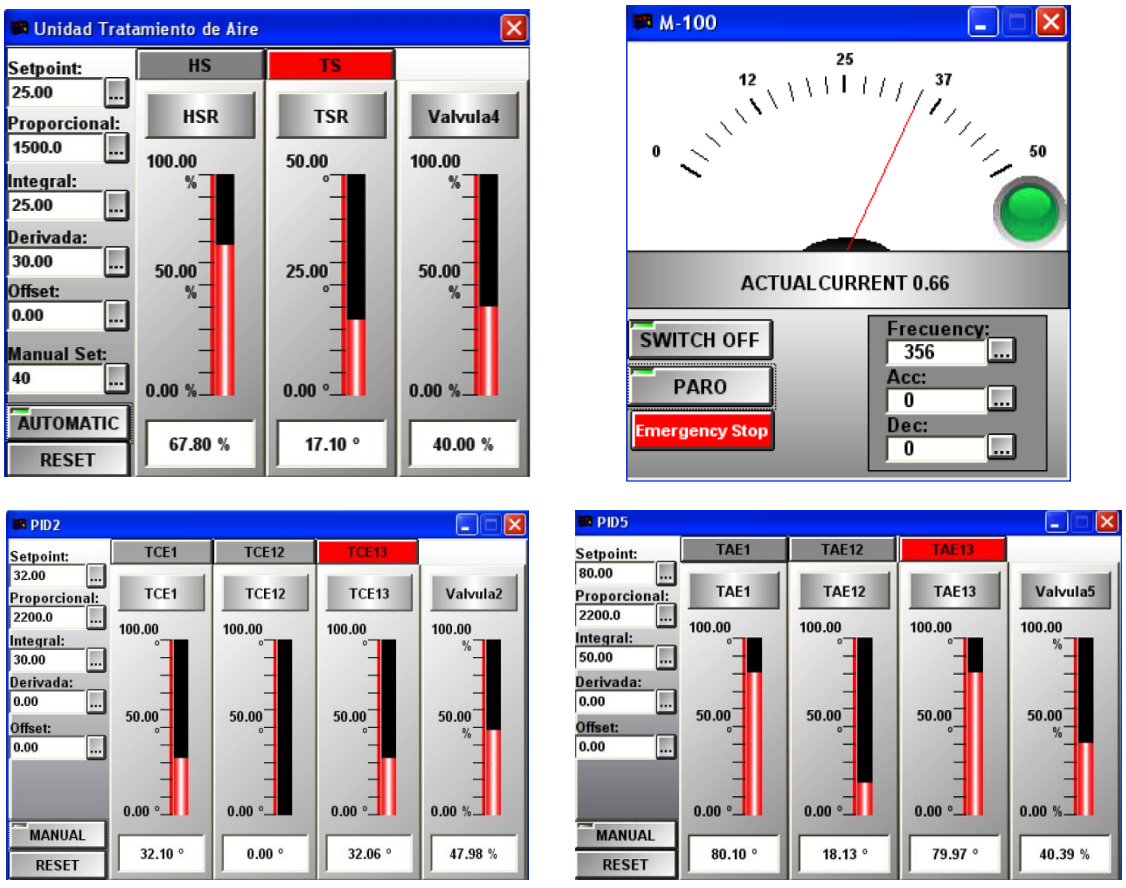

Figure 3.9 Control of the operational parameters through HMI

The main window of HMI presented in Figure 3.8 is directly linked to the system database and software program to provide on-line data visualization, process

historian platform and how often acquiring data. Depending on application in use, data visualization software can display up to 60 monitored parameters by simple marking on checkbox in front. Of course, this number is not final since it can be changed with requirements for additional sensors of some prototype or implementing some calculated quantities, for instance. The software plots historical data in various forms, such as trends, graphs and spreadsheets. One example of data trending charts is shown in Figure 3.10. Also important to mention is that the measurement data can be sampled in any time step range from a second to a year. To ensure rapid and efficient use of measurements results in further analysis, these data are stored in friendly format such as Excel spreadsheet.

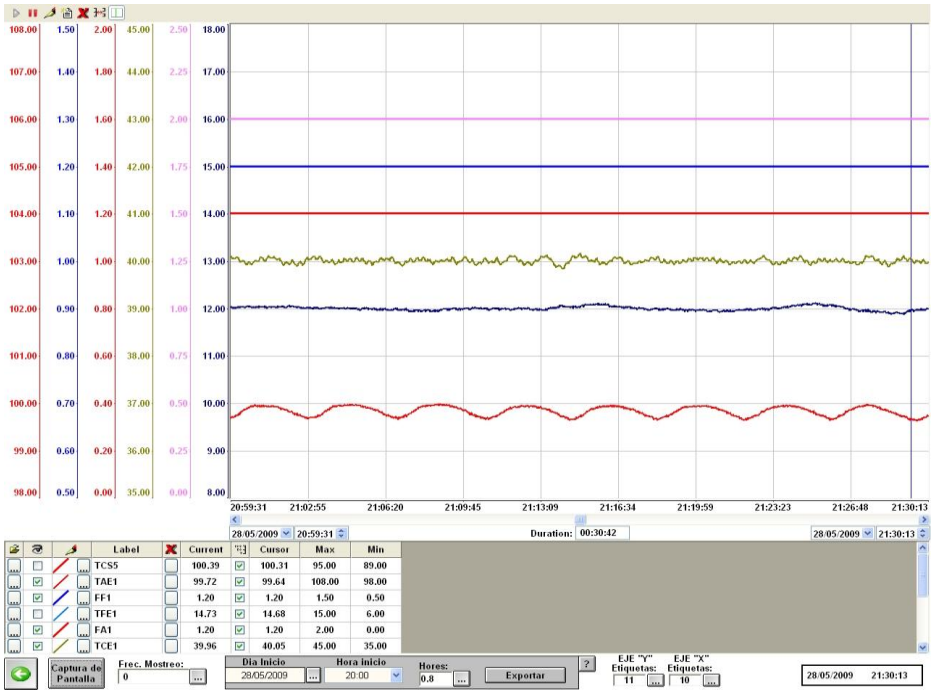

Figure 3.10 Trending chart for measured data

3.8. Instrumentation

Suitable instrumentation is very important in order to determine operating conditions of the absorption appliance and to evaluate its performance. In total, 36 PT100 resistance temperature detectors (RTD) with 2 and 3 wires form fixed part of the test bench. The RTDs are recognized as the most reliable standard available for

temperature measurement, more accurate than thermocouples and more suitable than thermistors for this kind of test application. All temperature sensors were chosen and installed according to recommended ASHRAE normative [113]. PT100 Class A comes with manufacturer accuracy of ±0.1ºC at zero ºC. The nominal resistance of a RTD is 100Ω at zero ºC. Equation 3.16 describes a nonlinear relationship between temperature and resistance:

$$R_T = R_0(1 + AT + BT^2 + C(T - 100)T^3) \quad (3.16)$$

where:

A=3.9083 10^{-3}

B=-5.775 10^{-7}

C=-4.183 10^{-12} below 0ºC, zero above 0ºC

Three Khrone Optiflux 1300 electromagnetic flowmeters are installed to measure the volumetric flow rate in the heat carrier water circuits of the tested absorption appliance. Electromagnetic flowmeters are the guarantee to measure the flow rate without disturbing the test bench operation. Beside these three, the test bench also has five ABB FXE4000-DE43F flowmeters placed in secondary circuits for monitoring all the flows within the facility. Both models have an accuracy of 0.5% of measured flow and both comply with ASME Standard MFC-16M-1995 [114]. An outdoor relative humidity sensor measures relative humidity inside the environmental test chamber and more than 20 pressure gauges mounted all over the test bench to ensure safe operation. To measure the outside conditions test facility consist of two devices placed at the roof of the laboratory building. For precise air humidity and temperature measurements, Siemens QFA3171+ AQF3100 outdoor relative humidity and temperature sensor is used. An anemometer and a vane, which form Young Wind Sentry Set, are used to measure the wind speed and wind direction.

Beside described instrumentation, some devices, which are not an integral part of the multifunctional test bench, can be mounted depending on type of the experiment performed. For instance, in experiments with absorption machines is always good to

know the pressure drops in water circuits or to measure electric consumption. In case of pressure drop measurements, available for use are the pressure transmitters SITRANS P or ROUSEMOUNT 3051. All pressure gauges are selected to meet the recommendations of ASME B40-100-2005 Standard [115]. Portable power analyser AR5 is the most suitable option when electric supply measurements are required. Table 3.13 shows the list of the test bench measuring instruments with the corresponding accuracy for each instrument.

Table 3.13 Instrumentation of the test bench

Model	Instrumentation	Variable measured	Range	Accuracy
PT100	RTD	Temperature	-50:200˚C	±0.1˚C at 0˚C
Khrone Optiflux 1300	Electromagnetic flowmeter	Volumetric flow rate	-25:220˚C	±0.5% of flow rate
ABB FXE4000-DE43F	Electromagnetic flowmeter	Volumetric flow rate	-20:60˚C	±0.5% of flow rate
Young 03002 Wind Sentry Assembly	Vane	Wind direction	360˚ mechanical 352˚ electrical	±5 º
	Anemometer	Wind direction	0:50 m/s	±0.5 m/s
Siemens QFA3171+AQF3100	Outdoor relative humidity and temperature sensor	RH	0:100% RH	±2% of RH
		Temperature	-40:70˚C	±0.1˚C at 0˚C
Siemens Sitrans P	Pressure transmitter	Differential pressure	0:600 mbar	±0.5% of max span
Rosemount 3051	Pressure transmitter	Differential pressure	0:2.5 bar	±0.15% of span
Circuitor AR5	Network analyzer	Electric power	5:45˚C	±1% of scale

As one can see from this Chapter, the multifunctional test bench is fully equipped test facility which complies with all recommended Standards for testing absorption equipment. Moreover, it meets the requirements for testing electrically driven liquid chilling packages, heat pumps and air-conditioners [116, 117]. All these facts make the multifunctional test bench very important and reliable tool for obtaining high-quality measurement data which are essential part of the modelling.

Chapter 4

Testing the performance of absorption chillers

"There is no such thing as a failed experiment,
only experiments with unexpected outcomes"
Richard Buckminster Fuller

4.1. Introduction

Large-scale absorption air-conditioning and refrigeration equipment have been present on the market for a long time, while the development of small-scale absorption chillers and heat pumps has intensified in the last decades which was triggered by rising concern about climatic change as well as with recent developments and progress in the field of solar energy and waste heat usage. This equipment has entered in early stage of standard production, designed for residential, commercial and industrial application. However, it is still in infancy and a lot of research efforts have to be made to be competitive with conventional systems. Therefore, experimental work is very important issue in order to improve this technology. Moreover, performance evaluation of the complete operating range is preferable for different application purposes. Most of the information are not available or are very scarce, especially when talking about commercial equipment. Despite the fact that the experimental work with the absorption machines is essential, there are just a few guidelines, standards and other expert recommendations. There is almost no standard procedure on how to test commercial (pilot either) absorption equipment just like there is no unique data treatment and analysis. Just to avoid misinterpretation, there are couple of standards about absorption appliances mentioned in previous Chapter, but there are mainly referring to standard rating conditions. Actually, one of the current objectives of IEA Annex 34 is to provide an unified basis for the development and revision of the standardisation framework to help thermally driven technologies to consolidate and further develop their market position [118]. Depending on end-user and purpose, scarce information is not enough. This fact is particularly expressed in the fields of simulation and control. Without

experimental data it is difficult to develop a correct model, and consequently, without the correct model, there is neither accurate simulation nor adequate control strategy.

Nowadays, more or less everything comes down to researcher experience and knowledge gained from other fields. Sometimes, the access to internal components is not always available and researchers can rely only on external measurements in that case. Also, a common practice in the literature is to present performance data coupled with external operating conditions. Precisely, the question of whether the external measurements are sufficient for complete characterization of the absorption equipment and whether the data are good enough for further exploitation in various applications was the motivation for making a simple procedure which would be a guideline for future testing. Consequently, the main purpose of this Chapter is to generate a simple procedure, based on existing knowledge and experience, to serve as a guide or best practice in dealing with small capacity absorption chillers and heat pumps. The procedure which will serve for performance evaluation of small capacity absorption chillers and heat pumps, based on external measurements only. The final outcome of that procedure will be a database which will serve for development of simple and accurate models which can be used in various applications. At the same time, the procedure will serve for validation of the novel test bench by testing the absorption machines through different operating modes. With respect to that, this Chapter is written as a kind of recapitulation, which contains all the stages that were passed in order to come to the final procedure. In the first stage the procedure was developed based on tests with Rotartica absorption machine. This machine was chosen due to its diversity to work in different operating modes. In the second stage, the firstly developed procedure was updated by adding some new elements in order to make it complete. In this stage, the tests were carried out with Pink absorption machine to show that the procedure is also applicable to small NH_3-H_2O chillers. The final test procedure contains several parts which will be explained in detail: how to plan the tests; which are important derived parameters for absorption machine and how to calculate them; how to develop detector for steady-state conditions; the uncertainty estimation and the analysis of the results with graphical and tabular display.

4.2. Stage one

4.2.1. Rotartica Solar 045

Figure 4.1 Rotartica Solar 045 and additional air-cooler for dry dissipation

As mentioned in the introduction, Rotartica Solar 045 (Figure 4.1) was the absorption machine which was chosen as case study to generate simple test procedure and to validate test bench. It is a single-effect hot water fired absorption machine which uses LiBr–H_2O as working fluid. The unit was designed both for wet and dry dissipation since it has an additional air-cooling unit which permits heat rejection directly to the environment. In addition, it can operate as both chiller and heat pump. The main technical information of the absorption unit is shown in Table 4.1.

Table 4.1 Technical data for Rotartica Solar 045

	Power [kW]	**Temperature [ºC]**			**Volumetric flow rate [m^3/h]**	
		min	**max**	**nominal**	**min**	**nominal**
Hot water circuit	7.2	80	108	90 (inlet)	0.6	0.9
Chilled water circuit	4.5			12 (outlet)	1.2	1.56
Cooling water circuit	11.7			40 (outlet)	1.5	1.98
Electric consumption	0.4					

The technological core of the machine is a rotary unit where all heat exchangers are located inside a hermetically sealed drum while rotating at approximately 400 revolutions per minute. However, use of rotational forces in absorption technology is not a new idea. In 1973, Pravda [119] patented a portable heat operated rotary heat pump for use in air-conditioning, particularly for cooling the passenger compartments in vehicles. It included a generator, absorber, condenser and evaporator, all mounted as a group. In 1984, Kantor [120] presented invention to provide a rotary inertial thermodynamic system and method in which the fluid flow is stable. One of the future objectives of the invention was to provide such a system which would be relatively compact, lightweight, uncomplicated, inexpensive and capable of operating under variety of conditions and in different environments. Ramshaw and Winnington [121] also presented an rotary assembly of absorption heat pump in which the vapour generator, the condenser and the absorber each include a wall across which the volatile component and liquid absorbent are flowing under the action of forces generated during the rotation of the assembly. The disclosure of Pravda [122] comprised a plurality of enclosed, interconnected components or chambers mounted for rotation in the rotary absorption heat pump. The radiator and the condenser were located concentric with the radial outboard of the absorber and absorber cooler and together with the generator these elements formed a group which is airtight and liquid tight. In addition, the disclosure was specially adapted to employ waste heat, radiator heat, solar heat or even heat obtainable by burning low cost hydrocarbons or other fuels. A couple of years later, the UK company Interotex Ltd. disclosed the patent of the double-effect absorption machine based on rotational principle [123]. The absorption machine comprised of a rotary assembly where all the components were interconnected to provide cyclic flow paths for a volatile fluid and an absorbent fluid. This assembly included a container associated with the flow paths of the volatile component for being charged with the fluid, storing an excess amount of volatile fluid collecting upstream of the evaporator exceeds a preset amount to adjust the concentrations of absorbent and volatile fluid. One of the novelties of the disclosure was a scoop (Pitot) pump arrangement for pumping and delivering it onto a surface of the evaporator. Finally, the licence for this technology was bought by Spanish spin-off company Rotartica S.A.

which finally released single-stage absorption machine Rotartica to the market [124], with some modifications.

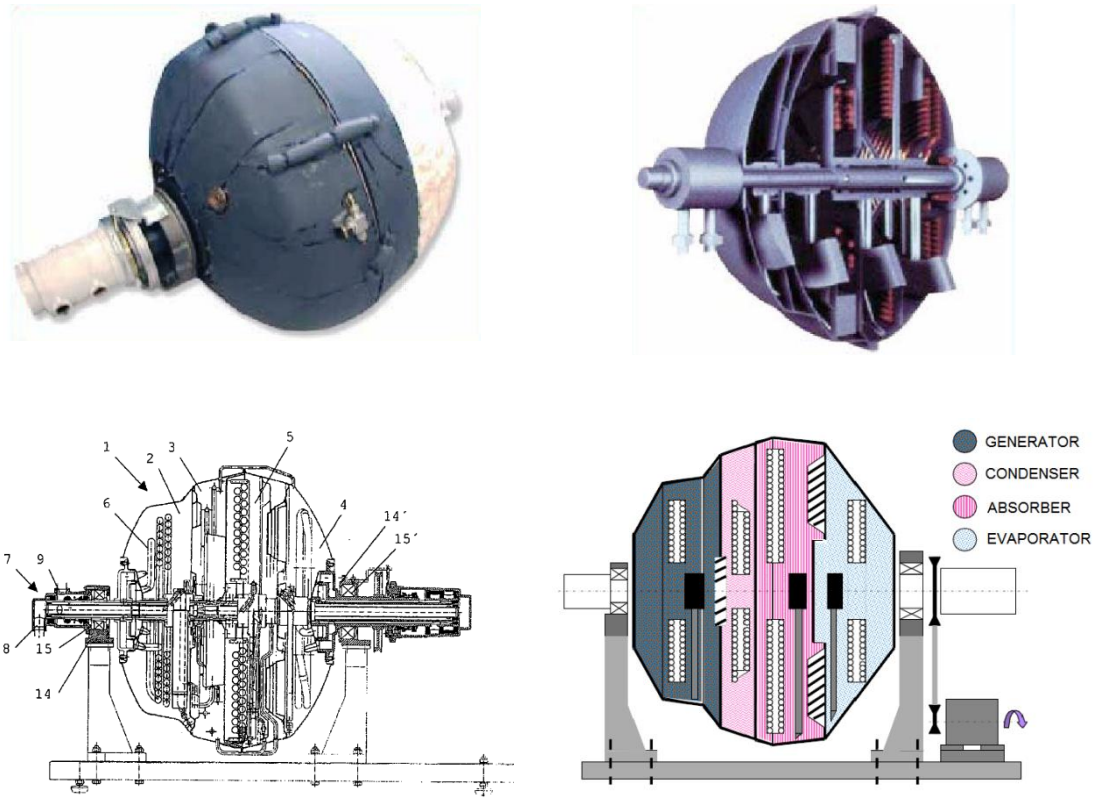

Figure 4.2 Rotary absorption assembly

Rotary absorption machine (Figure 4.2) can be activated by any thermal source. The invention comprises of a rotary unit divided in two sealed chambers. The generator (2) is in the form of spiral tube heat exchanger. Hot fluid from the thermal source flows inside the generator, while the external area is wet by the rich solution (rich with refrigerant) which is released as vapour after receiving the heat from the hot fluid. The refrigerant vaporized in the generator is condensed on the external area of the condenser, also in the form of spiral heat exchanger. A circular trough collects condensed liquid and trough refrigerant drainage pipe enters to the evaporator (4). The week solution on the external area of the absorber spiral tube (3) permits the cooling water of the dissipation circuit which flows inside the tube to remove excess heat. The cooling water runs sequentially through condenser and absorber in order to remove the heat from both processes. The evaporator is also a serpentine heat exchanger. The liquid refrigerant expands at lower pressure in the evaporator trough. Here, at lower pressure

and temperature, the liquid on the external area of the heat exchanger evaporates by means of the heat released by the chilled water which flows inside the tube. The solution heat exchanger (6) was designed and optimized particularly for this equipment. It is a plate heat exchanger made of stainless steel to minimise the corrosion and with dividing membranes with countercurrent flow to maximize the heat transfer. The solution pump is refreshment with respect to standard absorption equipment. It is a simple Pitot tube which hangs together with counterweight on a bearing placed on the axe of the unit. The kinetic energy of rotating fluid is converted to pressure energy; therefore no additional motors are needed for solution circulation. Internal control of the unit is provided in order to avoid any risk of damage. The absorbent concentration is self-regulating by storing a variable amount of liquid volatile component in the adequate container to meet the cycle requirements. If the risk of crystallization is detected, a mixture from the vapour generator is diverted to the solution heat exchanger to join the flow from the vapour absorber before entering to the solution heat exchanger. This increases the temperature of the flow entering the solution heat exchanger from absorber, which increases the temperature of the flow from the solution heat exchanger to the absorber and therefore preventing crystallization to occur. To avoid the damage during the start up and other extreme conditions, the generator disposes with one ON/OFF scoop pump with the preferential access to fluid in trough, thus reducing the possibility of the generator surface running dry. The use of rotational forces improves both heat and mass transfer rates inside the unit. Consequently, a thermal gradient between the evaporator and condenser is higher than in standard absorption equipment improving the efficiency of machine. Two major effects of the rotating absorption machine are: the good wetting of the heat exchangers, which is responsible for increase in both heat and mass coefficients; and the liquid film wetting these heat exchangers is extremely thin which facilitates the heat transfer from the liquid film to heat carrier liquid mediums. Process intensification of the heat and mass transfer characteristics in rotating absorption equipment was confirmed by several studies [125-127]. The process intensification and increased thermal gradient made this technology more favourable in a way that it can work without a cooling tower, thus preventing bacteria such as legionella from propagating.

Another advantage of the Rotartica is a possibility to provide heating at intermediate level, i.e. as a heat pump. All these advantages together with the possibility to work under different operating regimes (as water-cooled or air-cooled absorption chiller, heat pump, dissipation with or without cooling tower or with geothermal probe) as well as the use of solar energy for activation have made Rotartica interesting for various applications [128]. The novel absorption equipment has attracted several researchers to conduct their research studies on the performance of this machine. These studies were conducted on different models since the company was introducing some modification with each series released to the market.

The study presented by Zaltash et al. [129] showed that the air-cooled absorption chiller Rotartica 045v (air-cooled unit with integrated dry-cooler) is less efficient in warmer environments since the coefficient of performance (COP) decreases as ambient temperature increase. Also, study showed that the performance can be improved by increasing the temperature of the water supplied to the chiller or by increasing air flow. Izquierdo et al. [130] conducted experimental research of the same air-cooled chiller unit. The results showed that cooling power tend to decline with rising outdoor dry bulb temperatures. Monné et al. [131] carried out the trials at the University of Zaragoza concluding that cooling capacity improves as rotation speed of the drum increases. The experimental study of Agyenim et al. [132] about a solar system with Rotartica absorption chiller and a cold store showed good potential of the new concept of cold store to be integrated with existing and future housing stock. Labus et al. [133] published the experimental results of the water-cooled Rotartica operating both as chiller and as heat pump.

4.2.2. Measurement equipment and data acquisition system

The experimental variables measured in the testing were:

- Inlet and outlet temperatures of hot, chilled, and cooling water circuit
- Volumetric flow rates of hot, chilled, and cooling water circuit
- Pressure drop in each circuit
- Electric consumption of the machine

The measurement equipment used in the tests: RTD temperature sensors, electromagnetic flowmeters, pressure transmitters and portable power analyzer (used to measure electric supply needed for shaft work of the absorption machine drum) has been already described in detail in Section 3.8 of previous Chapter. All measured quantities were converted into electric signals and controlled by a programmable logic controller (PLC). PLC communicates over a network to the computer running a SCADA (Supervisory Control and Data Acquisition). The software allows visualizing and memorizing all parameters examined with the possibility to choose how often acquiring data.

4.2.3. Experimental procedure and test conditions

First, the set point temperature of the thermal oil heater was set to the desired value and all the components of the test bench were powered on. The flow rates of external water circuits were set by adjusting pumps frequency. Hot water inlet temperature, chilled water outlet temperature, and cooling water inlet temperature were set to desired value. Next, when all the parameters were set and controlled from the computer board via SCADA software the absorption machine was powered on.

It takes approximately 60 minutes from the moment when the oil heater was ignited until the moment when the system reaches set conditions. Time period between the moment when drum starts to rotate and the moment when the unit reaches steady-state conditions is around 30 minutes. It was assumed that machine operates in steady-state if the fluctuations of all controlled parameters were less than 4% of set point values. After reaching the steady-state, the data were collected for a period of 30 minutes in 1s intervals (interval can be set to 5s or 10s in order to reduce data storage). Changing any of the parameters, the system would need approximately 20-30 min to reach new steady-state conditions. The data were then exported into an Excel spreadsheet file for data reduction and further analysis.

The tests in cooling mode were carried out in two steps. In the first step the performance evaluation of the absorption machine was conducted by varying the flow rate of hot water circuit (0.9; 1.2; 1.4 m^3/h) at different chilled water flow rates (1.2; 1.6; 2:0 m^3/h) and cooling water flow rates (1.5; 2.0; 2.5 m^3/h). The temperatures of

inlet hot water, outlet chilled water, and inlet cooling water were kept constant at nominal conditions (90ºC; 12 ºC; 35 ºC).This step was necessary in order to explore the influence of flow rates on the machine performance and depending on the analysis of obtained results to choose the suitable flow rates for the tests where the temperature was changed.

In the second step the flow rates were kept constant at selected values for which absorption machine showed the best results during the first step. Here, the performance was measured by varying the temperatures of hot, chilled, and cooling water. In the tests when machine was operating in cooling mode (chiller), controlled parameters were inlet hot, outlet chilled, and inlet cooling water temperatures. Temperature ranges were chosen to cover the entire range of temperatures which is of interest in different applications (solar cooling, CCHP) while at the same time they have been consistent with the range that is determined by the manufacturer's design.

Similarly, the tests in heating mode (heat pump) were conducted to explore the influence of temperatures in external circuits on heat pump performance. Actually, the idea was to explore the range in which Rotartica can operate as heat pump since it had not been done before (at least manufacturer did not publish this information). In this case, the controlled temperatures were inlet temperature of hot water, inlet temperature of chilled water, and outlet temperature of cooling water (which is of interest for heating elements, i.e. fan-coils).

4.2.4. Data modelling

The thermal load of the evaporator was calculated by using equation 4.1:

$$\dot{Q}_{eva} = \dot{V}_{chw} \cdot \rho_{chw} \cdot Cp_{chw}(T_{chw,in} - T_{chw,out}) \quad (4.1)$$

where $\dot{V}_{chw}$ is the volumetric flow rate of the chilled water circuit, ρ_{chw} is the density and Cp_{chw} is the specific heat of water at constant pressure. The last two parameters were calculated based on the average value of the inlet and outlet temperatures of chilled water, $T_{chw,in}$and $T_{chw,out}$. In case when fluid in external heat carrier is different

(i.e. glycol), the fluid properties from adequate table or software package must be applied. Similarly, the generator load was calculated by using equation 4.2:

$$\dot{Q}_{gen} = \dot{V}_{hw} \cdot \rho_{hw} \cdot Cp_{hw}(T_{hw,in} - T_{hw,out}) \quad (4.2)$$

The absorber and condenser loads were calculated as single load since the common practice in absorption machines is that the same external water circuit is used for both components. This is described by equation (4.3):

$$\dot{Q}_{ac} = \dot{V}_{cw} \cdot \rho_{cw} \cdot Cp_{cw}(T_{hw,out} - T_{hw,in}) \quad (4.3)$$

In case when chiller has to be tested in air-cooled mode[5] (absorber and condenser coupled with air-cooler) the same equation can be used if it is possible to measure from water side. Otherwise, the measurements should be performed on the air side.

Three different indicators were used to evaluate the performance of the absorption machine operating as chiller: thermal coefficient of performance (COP), energy efficiency ratio (EER) and overall coefficient of performance. Thermal COP assesses only thermal performance as ratio of cooling capacity to heat supplied to the generator for activation (equation 4.4):

$$COP_{chiller,th} = \frac{\dot{Q}_{eva}}{\dot{Q}_{gen}} \quad (4.4)$$

The electricity use of the chiller was assessed by Energy Efficiency Ratio (EER[6]) including electricity consumption necessary for drum rotation (necessary for solution circulation, valves and internal controller of the machine). The parasitic electricity consumption of external circuits' equipment such as pumps and fans is not taken into account. The EER was thus defined as ratio of cooling capacity to the electricity consumption of the absorption chiller by equation 4.5:

[5] This is only informative since air-cooled mode tests were not performed

[6] In literature, some authors like to use term electrical COP ($COP_{el} = \frac{\dot{Q}_{eva}}{E}$) instead of EER

$$EER_{chiller} = \frac{\dot{Q}_{eva}}{\frac{E}{\eta}} \tag{4.5}$$

Here, E is the electrical consumption measured by power analyser AR5 and η is the overall generating efficiency of the Spanish electricity system taken to be equal to 0.33 according to best practice standard.

Overall COP was used to assess performance by including both electrical consumption and heat supplied to the generator into one equation (4.6):

$$COP_{chiller,all} = \frac{\dot{Q}_{eva}}{\dot{Q}_{gen} + \frac{E}{\eta}} \tag{4.6}$$

The same indicators were used to assess the performance of the machine when it operates as heat pump, with difference that now useful heat generated in absorber and condenser was used in the numerator instead of cooling capacity (equations 4.7-4.9):

$$COP_{hp,th} = \frac{\dot{Q}_{ac}}{\dot{Q}_{gen}} \tag{4.7}$$

$$EER_{hp} = \frac{\dot{Q}_{ac}}{\frac{E}{\eta}} \tag{4.8}$$

$$COP_{hp,all} = \frac{\dot{Q}_{ac}}{\dot{Q}_{gen} + \frac{E}{\eta}} \tag{4.9}$$

Finally, an energy balance equation (4.10) was applied to main components of the absorption heat pump to calculate the heat losses to the surroundings:

$$\dot{Q}_{eva} + \dot{Q}_{gen} = \dot{Q}_{ac} + \dot{Q}_{loss} \tag{4.10}$$

It should be mentioned that the performance of absorption machine only was evaluated. If the electrical consumption of external circuit components was taken into account, the performance indicators would be smaller. The electricity use for pumps and fans in external circuits is dependent on many factors such as the hydraulic layout of the system, component size and how the system is controlled. In that case is more appropriate to use other indicators such as Primary Energy Ratio (PER), Seasonal Energy Efficiency Ratio (PER), etc to assess the performance of whole system with all the components at seasonal level. More information about this can be found in Appendix A.

4.2.5. Uncertainty estimation

The evaluation of experimental uncertainties was carried out in accordance with United Kingdom Accreditation Service [134] guideline[8] for the expression of uncertainty in measurement. Type B evaluation of standard uncertainty was evaluated by judgement based on available information on the possible variability of input quantities. When the uncertainties of heat loads were evaluated, the following input quantities were taken into account: inlet and outlet temperatures of external circuits, volumetric flow rate, density, and specific heat capacity. Uncertainty contribution for temperature and volumetric flow rate was calculated as a combination of different sources of uncertainty: repeatability, accuracy of the instrument and resolution of the instrument. Repeatability was estimated as the standard deviation of the measured input quantity using the following equation (4.11):

$$u_1(x) = \sqrt{\frac{\sum_{i=1}^{n}(X_i - \bar{X})^2}{n(n-1)}} \tag{4.11}$$

Values for the accuracy and resolution were adopted from the equipment catalogue. To calculate uncertainty contribution for density and specific heat, uncertainties were assigned to reference data taken from NIST homepage. To resume, when all uncertainty sources for each input quantity were determined, they were multiplied by their probability distribution and summed to calculate the uncertainty contribution. Sensitivity coefficient (c_i) was calculated as the partial derivative of the

model function with respect to input quantity. Afterward, using the law of propagation of uncertainty the combined standard uncertainty was calculated using equation 4.12:

$$u(y) = \sqrt{\sum_{i=1}^{n} c_i^2 u_i^2 (y_i)} \tag{4.12}$$

The last step was to calculate expanded uncertainty by multiplying the standard uncertainty by a coverage factor k = 2, which for a normal distribution corresponds to a coverage probability of approximately 95%. More details can be found in Appendix B.

4.2.6. Results and Discussion

4.2.6.1. Chiller mode performance

First set of tests was used to analyse the influence of the external flow rates on both chillers' performance and pressure drop at nominal operating temperatures. This analysis might be useful in various ways: helps to determine the range of operating flow rates, to see what is the real effect of flow rates and is there any sense to vary flow rates in some application for control purpose (or just to use constant flow pumps) and also to show if any trade-off is necessary.

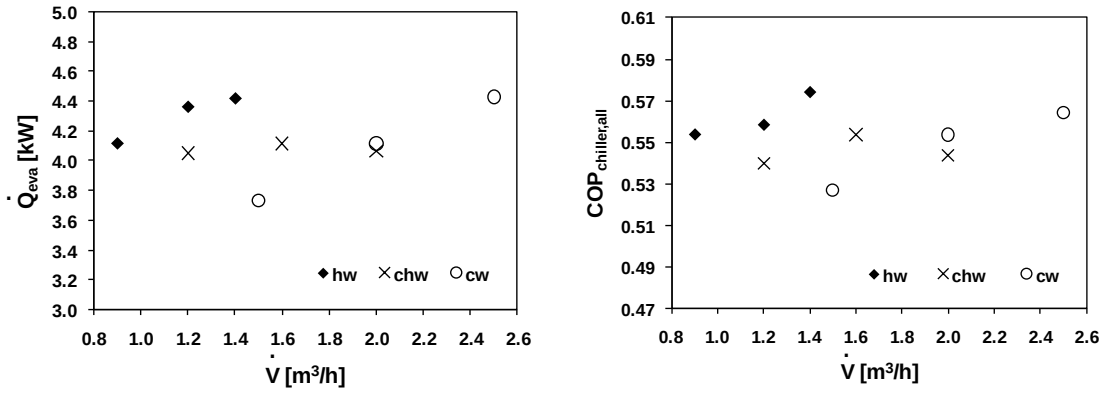

Figure 4.3 Volumetric flow rate vs. performance

Figure 4.3 shows that the chillers' performance improves as the hot water and cooling water flow rates increase while chilled water flow rate has a very small

influence. The highest influence is clearly visible in the cooling water circuit. One of the reasons for this lays in a fact that the cooling water circuit has the widest flow rate range due to the manufacturer's design. As it was expected, the pressure drop increases as the flow rate increases. This is shown in Figure 4.4. Again, the maximum values appeared in the cooling water circuit, which is reasonable because the flow rate in this circuit was the highest. One of the consequences is that normal work of the external circuit pump might be affected by this pressure drop increment. This can be avoided by stabilizing the system operation which results in slightly lower system performance. For that reason, in the following tests dealing with the influence of external circuit temperatures the adopted values for hot, chilled, and cooling water flow rates were 1.2, 1.2, and 2.0 m^3/h, respectively. The results of the flow rate analysis lead to a conclusion that in absorption machines, where a permissible range is very narrow, the influence of flow rate is very small. This further indicates that there is no point to use variable speed pumps to control the capacity by changing the flow rate, because the effect is small. At the same time, significant savings can be obtained by using cheaper equipment.

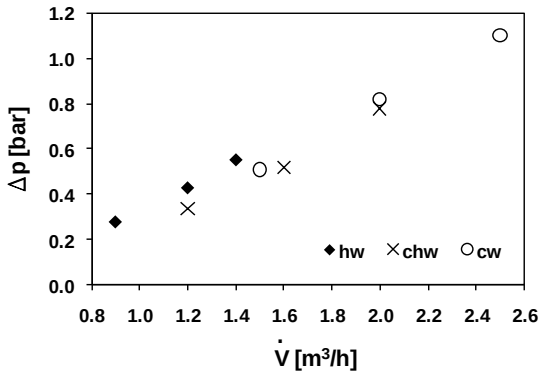

Figure 4.4 Volumetric flow rate vs pressure drop

In the second set of the tests, the performance of the absorption chiller was evaluated by varying the temperatures of external circuits. Table 4.2 shows the summary of the tests with detailed datasets for different operating conditions at constant flow rates. Figure 4.5 illustrates the performance of chiller operation mode with inlet hot water temperature set to 90ºC at different chilled water and cooling water temperatures. The best performance is achieved at higher values of chilled water outlet temperature and lower values of inlet cooling water temperature. Also, the tests with $T_{hw,in}$ at 80ºC and 100ºC showed that the higher performance can be achieved as the hot

water temperature increases. Heat balance was performed by using equation 4.10. Recalculated in percentage, as heat loss divided by heat input in the evaporator and generator is multiplied by 100, it gives an average value less than 6%. This indicates a very acceptable heat balance with only a small amount of heat lost in the process. Recorded electrical consumption of the absorption chiller varies between 300W and 340W. The uncertainty in the case of chilling capacity is in the range between ±0.26 and ±0.31kW and in the case of overall COP between ±0.04 and ±0.07.

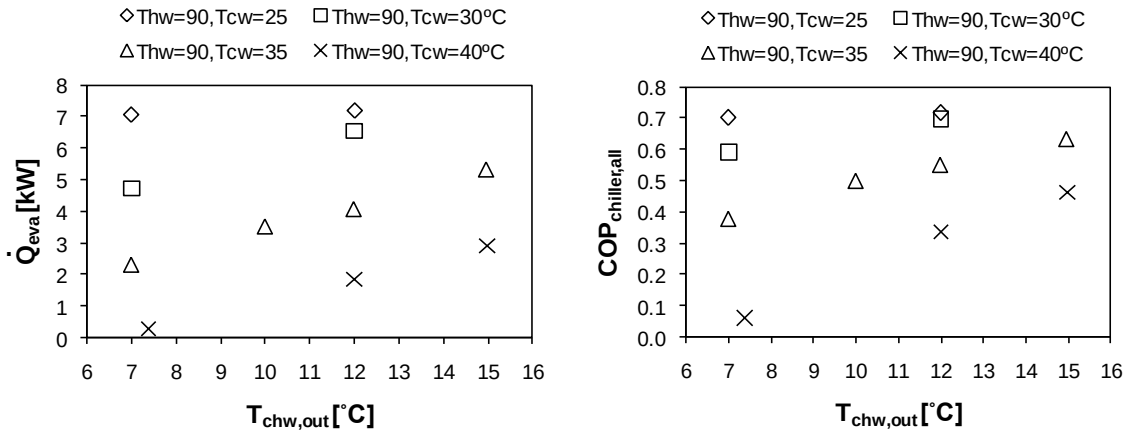

Figure 4.5 Chilled water outlet temperature vs. performance at $T_{hw,in}$=90ºC

Table 4.2 Test conditions

No	**Chiller mode**						**Heat pump mode**					
	$T_{chw,in}$	$T_{chw,out}$	$T_{cw,in}$	$T_{cw,out}$	$T_{hw,in}$	$T_{hw,out}$	$T_{chw,in}$	$T_{chw,out}$	$T_{cw,in}$	$T_{cw,out}$	$T_{hw,in}$	$T_{hw,out}$
1	17.2	12.0	25.0	32.1	80.0	73.6	15.0	13.1	36.5	40.0	85.0	81.0
2	15.5	12.0	30.0	35.1	80.1	75.2	18.0	15.2	35.6	40.0	85.0	80.2
3	12.0	7.0	25.0	32.2	90.0	83.2	20.0	16.6	35.0	40.0	85.0	79.7
4	17.1	12.0	25.2	32.6	90.0	82.9	18.0	17.4	43.3	45.0	85.0	82.4
5	10.4	7.0	30.0	35.3	90.0	84.7	20.0	18.8	42.6	45.0	85.0	81.9
6	16.7	12.0	30.0	36.7	90.0	83.7	25.0	22.3	41.0	45.0	85.0	80.6
7	8.7	7.0	35.0	38.3	90.0	86.1	18.0	14.4	34.4	40.0	90.0	84.1
8	12.5	10.0	35.0	39.3	90.0	85.4	20.0	16.0	34.0	40.0	90.0	83.4
9	14.9	12.0	35.0	39.8	90.0	85.1	25.0	19.5	32.9	40.7	90.0	82.4
10	18.8	15.0	35.0	40.8	90.0	84.4	15.0	14.3	43.0	45.0	90.0	86.9
11	7.6	7.4	40.0	41.7	90.0	87.4	18.0	16.4	42.0	45.0	90.0	86.1
12	13.3	12.0	40.0	42.9	90.0	86.6	20.0	17.9	41.4	45.0	90.0	85.7
13	17.1	15.0	40.0	43.7	90.0	86.0	25.1	21.5	39.4	45.0	89.7	83.9
14	11.3	7.0	30.0	37.0	100.0	92.9	15.0	11.7	34.7	40.0	95.0	88.9
15	18.1	12.0	30.0	38.6	100.0	92.0	18.0	13.5	33.4	40.0	95.0	87.9
16	8.9	7.0	35.0	39.9	100.0	93.7	20.0	15.0	32.9	40.0	95.0	87.5
17	16.3	12.0	35.0	41.7	100.0	93.3	15.0	13.2	41.6	45.0	95.0	90.7
18	7.3	7.0	40.0	43.2	100.0	95.0	18.0	15.4	40.7	45.0	95.0	89.9
19	14.6	12.0	40.0	44.6	100.0	94.8	20.0	16.8	39.9	45.0	95.0	89.4
20							25.0	20.1	38.0	45.0	95.5	88.2

4.2.6.2. Heat pump mode performance

During the winter, when outside temperature is low, the rejected heat from the absorber and condenser can be used to provide heating to certain space. The tests for absorption heat pump were conducted in a similar way as in the case of chiller with difference that now the controlled parameters are chilled water inlet temperature and cooling water outlet temperature. This is a requirement in most applications since the cooling water outlet temperature is the one which enters to the heating element (fan-coil). The temperature range of inlet hot water was chosen for applications which operate with back up heater, whereas solar collectors cannot always guarantee enough heat and smooth work during the winter. The temperature range of outlet cooling water was chosen to satisfy higher temperature levels required for heating applications. The temperature level of the chilled water also had to be higher, which was a direct consequence of dependence between the internal temperature levels within the absorption process.

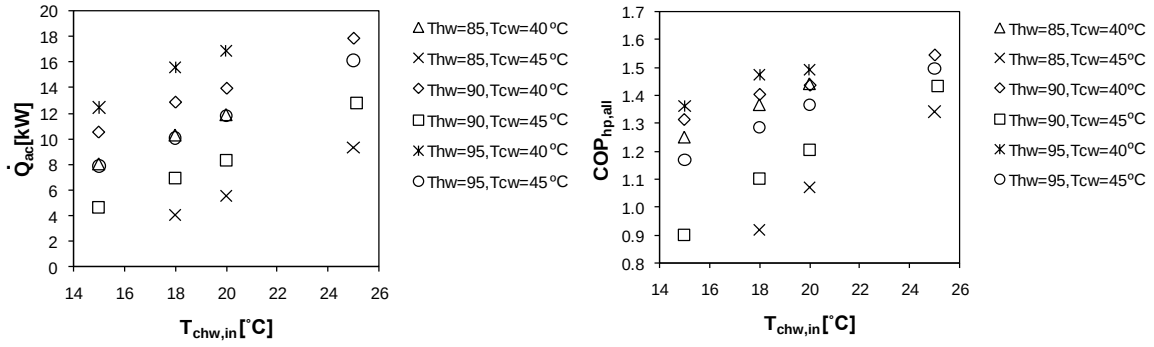

Figure 4.6 Inlet chilled water temperature vs. performance HP

The tests in heat pump mode were analysed by using the same approach as in the tests in cooling mode. All the temperatures measured during the tests in heat pump mode are presented in Table 4.2. Figure 4.6 shows performance of the heat pump at different values of hot water inlet temperature (85ºC, 95ºC and 95ºC), chilled water inlet temperature (between 15ºC and 25ºC), and cooling water outlet temperature (40ºC and 45ºC). Both useful heat and $COP_{hp,all}$ have the rising trend as the hot water temperature and chilled water temperature increase. The same values decrease as the outlet cooling temperature increases from 40ºC to 45ºC. The best achieved overall COP for heating

has value close to 1.6 (Figure 4.6). The value of thermal COP is slightly higher, around 1.7. Some additional tests were conducted in order to explore the limits of the outlet cooling water temperature. In the test when T_{hw}=90ºC, T_{cw}=48ºC and T_{chw}=20ºC the recorded useful heat was 4.39kW and corresponding $COP_{hp,all}$ equal to 0.87. The poor performance as well as the difficulty to maintain steady-state conditions indicates that around 48ºC would be limiting temperature for heating applications. Analysis based on pressure drop confirmed that change of temperatures in external circuits has negligible influence on pressure drop. Recorded electrical consumption of the absorption heat pump varies between 300 and 340 W, same as in the case of chiller. Heat balance gives averaged value for heat loss of around 0.5kW or less than 7%. Again, error analysis confirmed that all the calculated quantities are in the range of estimated uncertainties.

4.3. Stage two

A procedure which contains all the necessary elements to describe the absorption machine behaviour in steady-state conditions with sufficient accuracy was established in the Stage one. The procedure, based only on external manipulable parameters, provides sufficient information to understand behaviour of the absorption machine in different operating modes which can be useful in various applications of interest. The previous experience and knowledge generated in the field of experimental research were used for its establishment. At the same time, the tests performed in the Stage one served to validate two operating modes of the multifunctional test bench: chiller and heat pump modes.

However, the wish was to improve the test procedure, making it the more robust, especially in the field of steady-state identification. Therefore, extensive literature review has been carried out on methods of steady-state identification, in order to develop a steady-state detector which will help in creation of high quality database. Another question appeared with regard to our objective of creating database(s) which will be used for the modelling of absorption machines: which is the number of samples (number of different steady-state conditions) required to obtain precise estimate of the absorption machine empirical model developed on experimental data? According to [135], "*if the relationship between the input and output parameters of the model is not*

very strong, a small sample (<15) may not be large enough to detect it. Also, small samples do not provide a very precise estimate of the strength of the relationship, which is measured by adjusted coefficient of determination R^2. If a precise estimate is needed, larger samples (typically 40 or more) should be used." Also, the idea was to show that procedure is also applicable to small ammonia-water chillers. The following part describes the improved procedure with all the changes from the original procedure, illustrated by the example of small NH_3-H_2O absorption chiller.

4.3.1. Pink chilli PSC 12

A 10kW cooling capacity single-effect ammonia-water absorption chiller prototype was developed by Joanneum Research in cooperation with the company Pink GmbH in Austria. One of the innovations during the design stage was a newly developed membrane solution pump. This prototype was used within the EU project PolySMART where the chiller was coupled with the biomass driven Stirling engine at a modern winery in southern Austria [136]. The licence was bought by the German company SolarNext which distributes this chiller since the end of 2006. Since then, several prototypes of Pink chilli PSC have been developed with constant work on improvement and optimisation. These prototypes were tested in different locations around the Europe in order to analyse the behaviour of the prototypes in solar assisted air-conditioning systems. Based on different test stands, the analysis showed that the chiller can reach a wide range of operating temperatures. According to Jakob et al. [137], the chiller can reach evaporator outlet temperatures from 15ºC to -5ºC, at hot water inlet temperatures from 75ºC to 115ºC and cooling water temperature range of 24ºC to 40ºC. It can be cooled with wet cooling tower or dry cooler.

Figure 4.7 Pink chilli PSC 12

The absorption unit used in our tests was chilli PSC 12, shown in Figure 4.7. The standard model chilli PSC 12 in nominal conditions reaches thermal COP of around 0.65. Table 4.3 shows the specification data according to manufacturer's catalogue. However, the chiller used in our tests was modified version of chilli PSC 12 with lower concentration of ammonia in order to operate at lower chilled water temperatures. In practice, this modification completely changes the operation of the absorption chiller. Also, since the manufacturer did not provide technical data for modified version, the performance evaluation was necessary to determine the operating range of the chiller.

Table 4.3 Technical data for Pink chilli PSC 12

	Power [kW]	**Temperature [ºC]**		**Volumetric flow rate [m^3/h]**	
		Fan-coil	***Chilled ceiling***	***Fan-coil***	***Chilled ceiling***
Hot water circuit	18.2	85 (inlet)	75	2.2	2.2
Chilled water circuit	12	15 (outlet)	15	1.7	3.4
Cooling water circuit	28.2	24 (inlet)	24	4.8	4.8
Electric consumption	0.4				

4.3.2. Measurement equipment and data acquisition system

The instrumentation and data acquisition system used for experiments with Pink absorption chiller have already been explained in Section 4.2.2. It was also possible to measure two additional parameters, generator and absorber pressures, since the absorption chiller disposes of two manometers indicating pressure levels.

4.3.3. Experimental procedure and test conditions

The experimental procedure was the similar to one explained in Section 4.2.3. First, the following conditions were chosen as the starting point: chilled water outlet temperature at 7ºC, cooling water inlet temperature at 27ºC and hot water inlet temperature at 85ºC, chilled water flow rate 3.4 m^3/h, cooling water flow rate 4.8 m^3/h and hot water flow rate 2.24m^3/h. The reason for higher cooling water inlet temperature lies in fact that nominal temperature according to Table 4.3 could not be achieved since

the operation of the chiller was very unstable and it was not possible to maintain steady-state conditions. Next step was to investigate the influence of flow rates on performance and pressure drops in the external circuits. Starting from the chosen conditions, the flow rates in each circuit were changing (25% and 50% in both directions when the pump frequency allowed). Third step was to obtain complete performance map for the fan-coil applications. Using the fixed flow rates ($\dot{V}_{chw}$ = 1.72m^3/h, $\dot{V}_{cw}$ = 4.8m^3/h and $\dot{V}_{cw}$ = 2.24m^3/h) and water as fluid in the external circuits, the performance was determined by varying the temperatures: the chilled water outlet temperature in range 5-12ºC, the cooling water inlet temperature in range 27-35ºC and the hot water inlet temperature in range 80-100ºC. In addition, the performance evaluation of the chiller was conducted using the brine (38% concentration of ethylene glycol) in the chilled fluid circuit in order to investigate the operation of the chiller at temperatures near and below 0ºC. For that purpose, the flow rate in the chilled fluid circuit was fixed at 3.4m^3/h, since the chiller operation became unstable at lower temperatures. In this case the performance evaluation of the absorption chiller was conducted by varying chilled fluid temperature from -3ºC to 12ºC at different inlet cooling water temperatures (25; 27; 30; 35ºC) and different inlet hot water temperatures (75; 85; 95ºC).

The duration of the steady-state tests was according to CEN standards, not less than 30 minutes and with readings every 5s.

4.3.4. Data modelling

Data modelling was carried out in the same way as in Section 4.2.4. The values for the density and the specific heat of the external circuit fluid were taken from appropriate table when test conditions required operation with glycol mixture.

4.3.5. Steady-state identification

Off-line steady-state detector was developed to identify steady-state regions of the performed tests. The idea for its development was found in the paper of Kim et al. [138], where the authors developed the steady-state detector for fault detection and diagnosis of vapour compression system based on moving window average of seven selected variables. Steady-state detector for compression system was modified in order

to correspond to absorption systems. Several improvements were added to new steady-state detector. These improvements refer to the additional data filter which eliminates remaining transient periods caused by time delays when changing from one steady-state to another and two additional checks to confirm steady-state conditions. In detail procedure for development of absorption system steady-state detector as well as comprehensive literature review are provided in Appendix C.

4.3.6. Uncertainty estimation

The estimation of uncertainties was realized in the same manner already explained in Section 4.2.5. In addition, the uncertainty estimation can serve as additional check for our steady-state detection process. After calculation of uncertainty for the derived variables (loads, COPs), the minimum and the maximum values of the readings (of the derived variable) within the observed steady-state interval should be within the calculated uncertainty bounds from the average value.

4.3.7. Automation of the procedure

The entire procedure described above can be (semi)automated in a way illustrated in Figure 4.8.

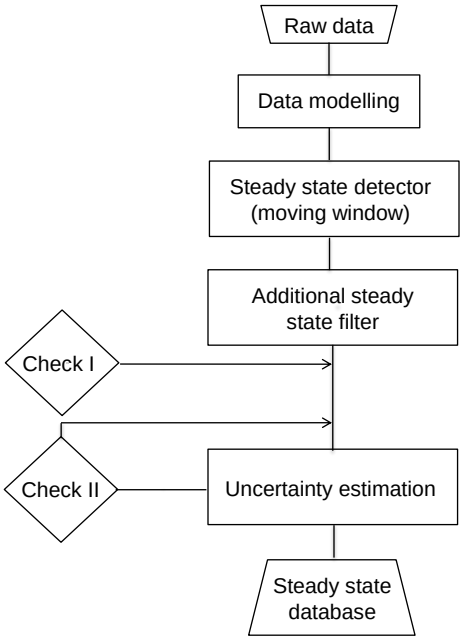

Figure 4.8 Test procedure flowchart

4.3.8. Results and Discussion

4.3.8.1. Chiller mode performance

First set of tests was used to analyze the influence of the external flow rates on both chillers' performance and pressure drop at nominal operating temperatures. As can be seen from Figure 4.9 and Figure 4.10 the influence of flow rates is more expressed than in the case of Rotartica absorption machine. This is due to the fact that permissible ranges for flow rate variation are much wider than in the first case. The trends are also similar as in the case of Rotartica. Chilling capacity increases as the cooling water flow rate or the hot water flow rate increase. On the other hand, an increase of the chilled water flow rate causes small drop in the performance. This type of analysis is very common when it is necessary to determine the flow rates for particular application. Working with lower flow rates in chilled water circuit is suitable for fan-coil applications since higher temperature difference between the inlet and outlet can be obtained, while lower temperature difference is more suitable for chilled ceilings, for instance. Flow rate influence on pressure drop illustrated in Figure 4.10 shows linear trend, increasing as the flow rate increase. The comparison with manufacturer data showed a very big discrepancy. Pressure drop in the chilled water circuit was twice lower while, on the other hand, the pressure drop in the cooling water circuit was twice higher. At nominal flow rate of 4.8m^3/h in the cooling water circuit, the pressure drop reached the value of 1.4bar. Only the hot water circuit indicated the pressure drop close to the manufacturers'.

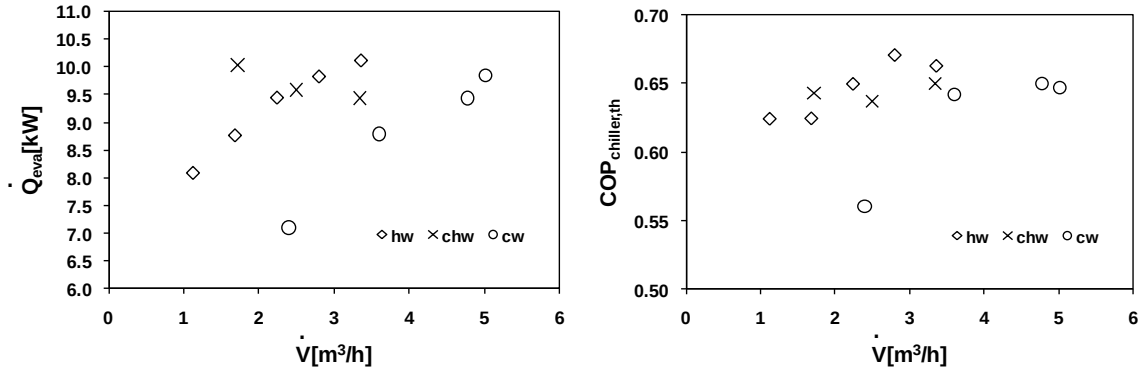

Figure 4.9 Volumetric flow rate vs. performance

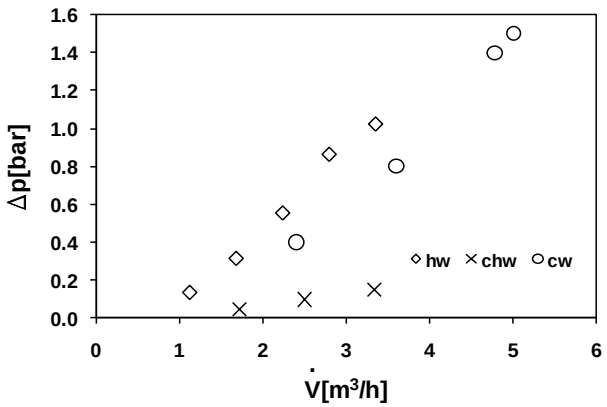

Figure 4.10 Volumetric flow rate vs. pressure drop

This analysis showed that flow rates can have a significant impact on chilling capacity which further implies that they could be used to control (or to adjust) the chilling capacity by using variable frequency pumps. However, as mentioned before, this is not common practice in the case of small capacity absorption chillers since the cost increases. The most common practice is to work with fixed flow rates while the capacity control is performed by adjusting external circuit temperatures.

The second set of tests was conducted to explore the whole temperature range of the chiller for fan-coil applications. For that purpose, the flow rates were maintained constant: chilled water flow rate at 1.7m^3/h, cooling water flow rate 4.8m^3/h and hot water flow rate 2.24m^3/h. Although the cooling water flow rate has a higher pressure drop than it should, this value was adopted due to manufacturer's recommendation. The chilled water temperature was varied in range 5-12ºC, which is suitable range for fan-coils. The inlet cooling water temperature was varied from 27-35ºC. Operation at temperatures lower than 27ºC was not possible, at least not with selected flow rate in chilled water circuit, since the machine could not reach steady-state conditions. This is a direct consequence of lower ammonia concentration. The lower limit for hot water inlet temperature was 80ºC and upper limit was explored up to 100ºC. Operation at temperatures higher than 100ºC brings the risk of chiller's breakdown due to the pressure blockade at the generator of 15bars which was set by manufacturer. Nearness of the critical pressure was the reason while some of the tests were not realized at 100ºC and higher inlet cooling water temperatures. As can be seen from Figures 4.14-4.16, all the trends were coherent and logical: the chilling capacity increased as the outlet chilled

water temperature increased; decreased as the inlet cooling water temperature increased and increased as the inlet hot water temperature increased. The thermal COP followed the same trend. In total, 138 steady-state points were obtained. The chilling capacity covered by these tests was in the range of 0.49-15.23kW. Thermal COP varied from 0.11-0.76. The average electrical consumption of the absorption chiller needed for solution pump work was around 620W_e. Energy Efficiency Ratio varied from 0.27 to 7.98. After performing heat balance, the average heat loss was found to be less than 5%. The uncertainty analysis showed that the uncertainty in the case of chilling capacity was in the range between ±0.53 and ±0.71kW and in the case of thermal COP between ±0.04 and ±0.15. The exhaustive summary of the tests can be found in Appendix D.

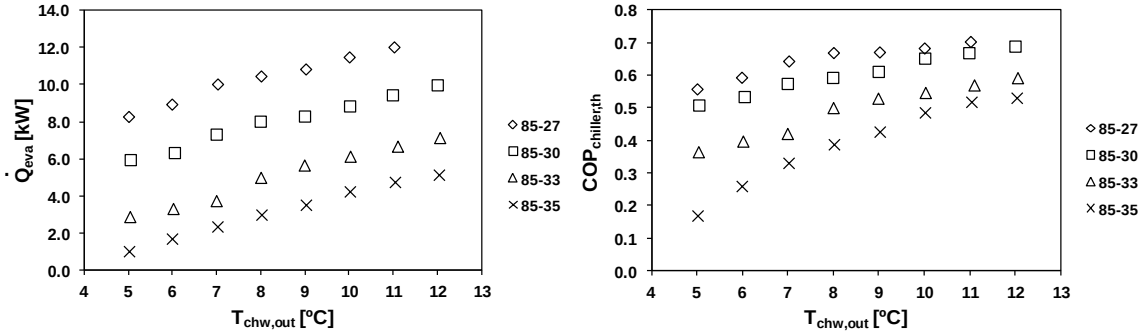

Figure 4.11 Chilled water outlet temperature vs. performance at $T_{hw,in}$=85ºC

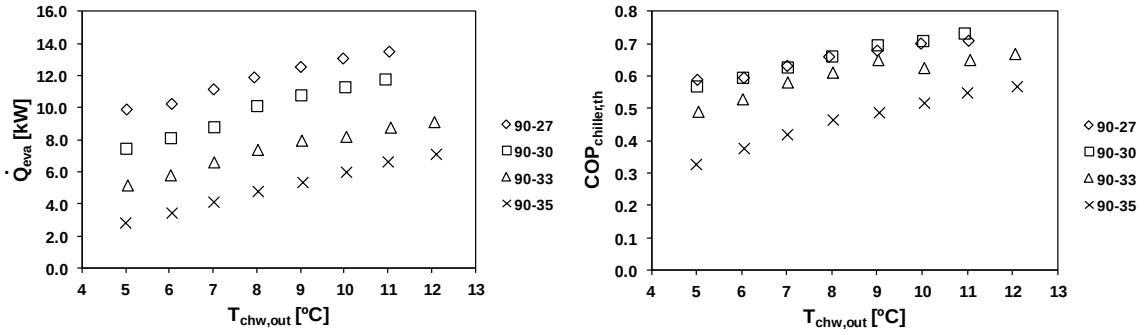

Figure 4.12 Chilled water outlet temperature vs. performance at $T_{hw,in}$=90ºC

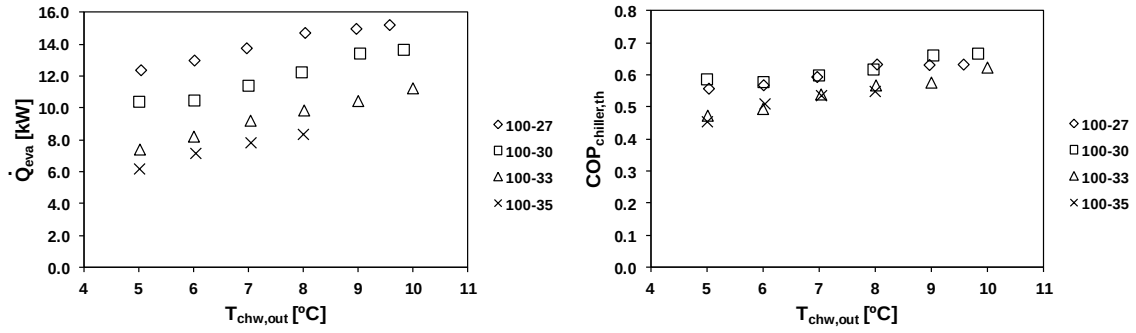

Figure 4.13 Chilled water outlet temperature vs. performance at $T_{hw,in}$=100ºC

The last set of tests was performed to evaluate the performance of the absorption chiller including wider range of temperatures, especially in the cooling water and chilled fluid circuit. In order to operate at temperatures below 0ºC, the chilled fluid circuit was filled with brine (38% concentration of ethylene glycol). To avoid unstable operation of the absorption chiller at lower chilling temperatures, the flow rate in chilled fluid circuit was increased to 3.4m^3/h. The tests included three levels of inlet hot water temperatures (75; 85; 95ºC), at different inlet cooling water temperatures (25; 27; 30; 35ºC) and outlet chilled fluid temperature (-3ºC to 12ºC). The tests at inlet hot water temperatures of 85ºC and 95ºC were additionally extended to inlet cooling water temperature of 20ºC. The special interest was to see what will be performance at temperatures near and below 0ºC. These temperatures are interesting for applications such as wine cellars, breweries, or trawling fishing vessel. Figures 4.17-4.19 show the summary of the results. Again, the absorption chiller behaviour was in agreement with common trend. Chilling capacity increased when the hot water or chilled fluid temperatures were increased and decreased when cooling water temperature was increased. The comparison with the tests performed with pure water as chilling fluid under the same temperature conditions showed that the chilling capacity was lower. There are two reasons for that. First, from the tests with flow rate it could be seen that the chilling capacity decreases as the chilled fluid flow rate increases. And second, the concentration of the anti-freeze agent (ethylene glycol) affects the heat transfer rate. The lowest temperature at which the chiller could operate under the steady-state conditions was -3ºC. Decreasing the outlet chilled fluid temperature more the chiller maintained steady-state conditions just for a very short period of time and then started with large

oscillations. Decreasing the cooling water inlet temperature to 20ºC, the performance significantly improved as can be seen in Figures 4.18 and 4.19. On the other hand, this reduced the range of the outlet chilled fluid temperature. For example, at $T_{hw,in}$=95ºC the upper limit is 5ºC (Figure 4.16). In total 67 tests conducted in steady-state conditions cover the chilling capacity range of 0.77-13.4kW with the thermal COP range of 0.19-0.75. The average recorded electrical consumption was 600W_e. EER varied between 0.45 and 7.62. Average heat loss was less than 6%. Calculated uncertainties in the case of the chilling capacity varied between ±0.55 and ±0.79kW while in the case of thermal COP between ±0.04 and ±0.15.

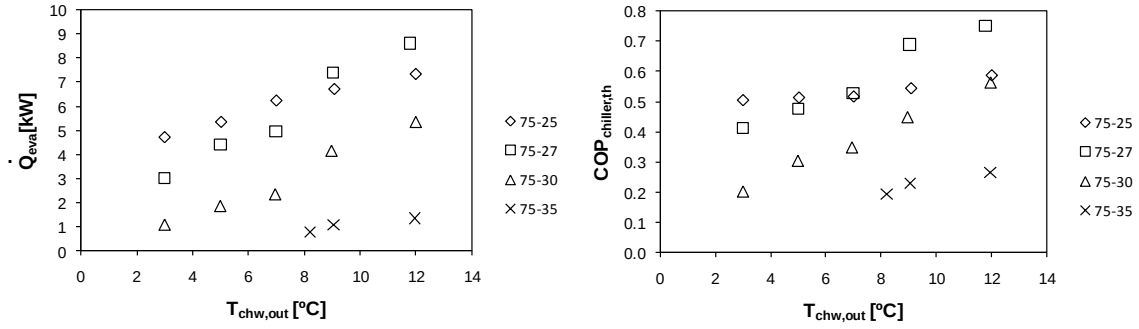

Figure 4.14 Chilled fluid outlet temperature vs. performance at $T_{hw,in}$=75ºC (EG)

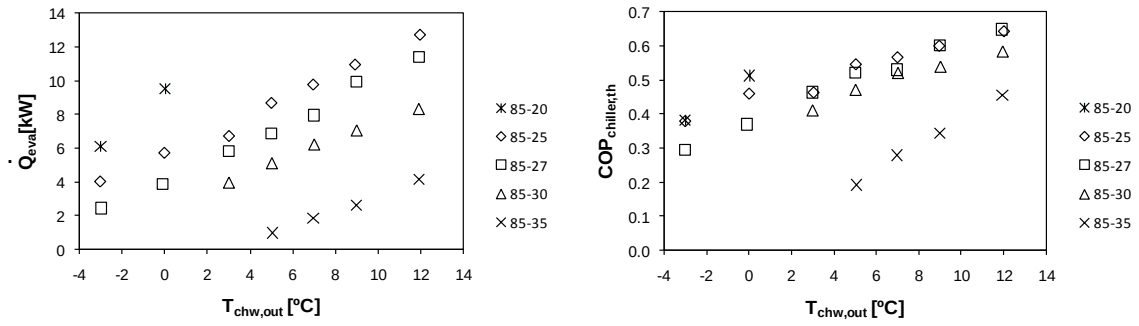

Figure 4.15 Chilled fluid outlet temperature vs. performance at $T_{hw,in}$=85ºC (EG)

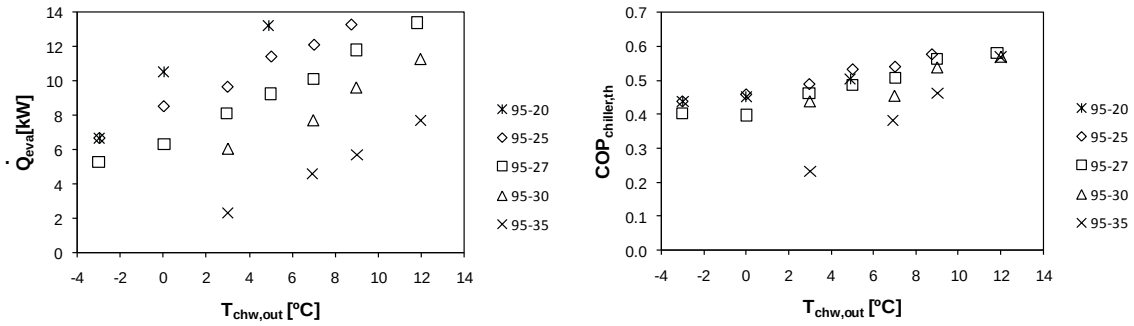

Figure 4.16 Chilled fluid outlet temperature vs. performance at $T_{hw,in}$=95ºC (EG)

4.4. Conclusions

A comprehensive procedure for testing absorption machine performance under the steady-state conditions has been developed based on the tests with two different small capacity commercial units. By monitoring only external measurable parameters, this procedure allows the creation of the complete performance map for absorption machines based on highly accurate data. A step by step procedure was explained in details: how to collect the data, which are the important indicators and how to calculate them, how to estimate the uncertainties of the calculated variables, how to develop a steady-state detector and result analysis. Off-line steady-state detector for absorption chillers was developed based on analogy with steady-state detector for vapour compression chillers using the moving window average. Small capacity H_2O-LiBr absorption machine Rotartica was tested both as chiller and as heat pump. A complete operating range for fan-coil applications was explored using the tests with another small capacity chiller which operates with NH_3-H_2O (Pink). Also, the same chiller was tested for low temperature application by using the brine in chilled fluid circuit. The obtained data were used to form the database which will further be used for model development. At the same time, the tests explained in this Chapter served to validate the functionality of the multifunctional test bench.

Chapter 5

Modelling methods

"All models are wrong, but some are useful."

George E. P. Box

5.1. Introduction

A model can be considered as a mathematical description of a physical state or process. This mathematical description helps us to think about the process and its mechanisms, so we can better comprehend the results. The model can further be used to improve the process or system based on analysis of simulated data.

Generally, there are two types of models: mechanistic and empirical [139]. Mechanistic models provide an insight into a physical process or system while the empirical models describe the general shape of dataset for an observed process or system which is tried to model.

With respect to absorption chiller modelling, both mechanistic and empirical approaches are present in the literature. Mechanistic or more precisely thermodynamic models were reported by various authors. Joudi and Lafta [140] developed the thermodynamic model of H_2O-LiBr absorption system based on detailed mass and energy balances and the heat and mass transfer relationships for the cycle components. Similarly, Kaynakli and Kilic [141] did the theoretical study on performance of H_2O-LiBr absorption system. Using the thermodynamic analysis of absorption cycle, the authors investigated the influences of operating temperature and heat exchanger effectiveness on the thermal loads of the components and COP. Silverio and Figueiredo [142] used thermodynamic approach for steady-state simulation of an ammonia-water absorption system. The thermodynamic state relations and the equations for the pressure drops and the heat transfer coefficients were solved using the solution algorithm based on Substitution Newton Rapshon method. Grossman and Zaltash [143] developed modular simulation tool for absorption systems called ABSIM which makes possible the investigation of various absorption cycle configurations working with different

fluids. Based on a user-supplied cycled diagram, working fluid specification and given operating conditions, ABSIM calculates the internal state points and thermal loads of the components. This is enabled through the subroutines which contain the governing equations for each component of the cycle. Garimella et al. [144] used ABSIM to model and to evaluate the performance of a Generator Absorber heat eXchanger (GAX) heat pump. However, thermodynamic models are very demanding since they require comprehensive knowledge of the absorption cycle including all internal state points. The model needs lots of input parameters such as heat transfer coefficients (U) and heat transfer areas (A) of heat exchangers, solution flow rate, working fluid properties and water side flows and temperatures as well as some additional assumptions for convenience of modelling. In most of the cases, especially with commercial units, the internal parameters are not available. This is the reason why thermodynamic models are more adequate during the design stage of absorption equipment [145]. The computation time in simulation software packages is very long since these models require a lot of simultaneous iterations. The annual simulations of different systems on hourly time step basis are more than evident proof for that fact. Thus, there is a need for simple models which can provide sufficiently good representation of the absorption machine behaviour based only on available external parameters (experimental measurements or manufacturer catalogue data). Simple models can easily be incorporated in simulation programs or used for fault detection and control. Contrary to the mechanistic models, the empirical and semi-empirical models require less time and effort to develop and computation time is much shorter when they are built-in simulation programs. The parameters and fitting coefficients of the models are determined by using the regression method or minimizing algorithms applied to a dataset obtained from manufacturer catalogue or experimental measurements.

The studies about development of empirically based models for absorption equipment have been reported by several authors. Gordon and Ng [146] developed a general model for predicting absorption chillers performance. The model lays both on physical and empirical principles. The physical principles that govern the performance of the absorption chiller are fitted to the experimental or manufacturer data by using a regression method. Ziegler and co-authors [15, 147] developed a model which predicts the performance of the absorption chiller by two simple algebraic equations: one for

cooling capacity and one for driving heat input. Labus et al. [148] used the empirical approach to model absorption chillers based on manufacturers curves in order to investigate the energy savings when different absorption configurations were applied in chiller plant. The Artificial Neural Networks (ANN) have also been used for absorption chiller modelling. ANN models belong to the black-box approaches where the estimated parameters of the model have no physical interpretations. ANN approach for performance analysis of an absorption chiller was proposed in the study of Sozen and Akcayol [149]. The ANN model employed only working temperatures of four components as input parameters in order to predict the performance of the chiller. Another study where the ANN were used for modelling of steam fired double effect absorption chiller is reported by Manohar et al. [150].

Regardless the numerous studies on the modelling of absorption equipment, literature review shows that there is a huge gap when it comes to comprehensive comparative studies on different modelling techniques for predicting absorption equipment performance. The studies which would evaluate the capability of the models to predict energy performance in a similar way as Lee and Lu [19] did in their study on vapour-compression chillers.

Consequently, the main aim of this Chapter is to present a comparative evaluation of different modelling approaches for predicting the performance of small absorption chillers. The comparative evaluation which can serve as a reference when there is a need for simple, but accurate models of absorption chillers as in the case of simulation software packages. The simple chiller models with minimum input parameters which will facilitate the annual simulations of complex building systems having a high level of performance prediction at the same time. Also, this Chapter aims to provide the statistical explanation which may help in selecting the appropriate model.

For that purpose, five different absorption chiller models were examined: First Law of Thermodynamics model, the adapted Gordon-Ng model, the adapted characteristic equation model, the artificial neural networks model and the multivariate polynomial model.

5.2. Database for modelling

Two datasets of tests described in previous Chapter and manufacturers' catalogues were used as a base for modelling. First dataset was obtained in tests with Rotarica absorption chiller and consists of 19 steady-state points. This sparse dataset tries to cover very wide temperature operation range of the chiller: inlet hot water temperature 80-100ºC, inlet cooling water temperature 25-40ºC and outlet chilled water temperature 7-15ºC. Second dataset refers to Pink absorption chiller and consists of 138 steady state points obtained when the chiller was tested for fan-coil applications. This detailed dataset covers the following temperatures ranges: inlet hot water temperature 80-100ºC, inlet cooling water temperature 27-35ºC and outlet chilled water temperature 5-12ºC. In both cases, the external circuits flow rates were maintained constant and with respect to that, the developed models also assume operation with constant flow rates. The obvious difference in datasets between two chillers was made on purpose, in order to investigate the effect on prediction results of the models as well as on statistical indicators.

5.3. Models

5.3.1. Thermodynamic model (TD)

The thermodynamic model was developed based on methodology which is normally applied at design stage of absorption chiller and using data from manufacturer's catalogue. The design stage model is used to analyze the behaviour of absorption chiller with respect to characteristics of each component; internal conditions of the cycle and conditions of external heat carrier circuits. This implies assumption of some internal parameters when defining the governing equations for each component in absorption cycle in order to obtain the required chilling capacity. Beside this assumption, some additional assumptions within the absorption cycle are usually used for convenience in modelling.

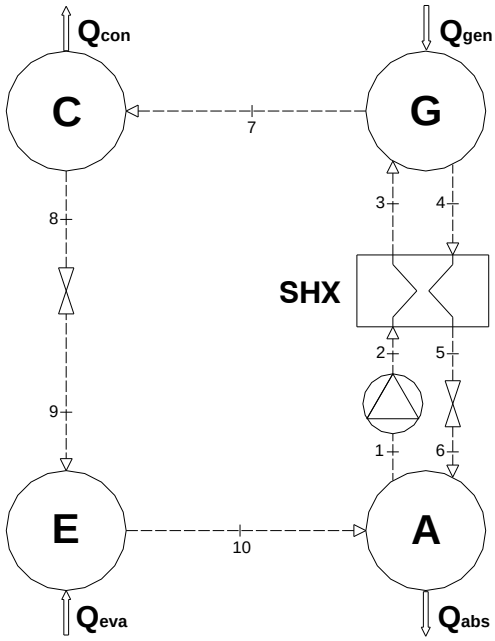

Figure 5.1 SE absorption cycle- internal states

With reference to Figure 5.1, these assumptions are:

- at points 1, 4 and 8 there is only saturated liquid; at point 10 there is only saturated vapour
- there are no pressure drops except through the solution pump and throttling devices
- vapour flashes as liquid passes through throttling devices
- refrigerant flow is constant
- throttling devices are isenthalpic
- there are no jacket heat losses
- solution pump is ideal (isentropic)

Based on these assumptions and using the fluid properties for corresponding working pair, a steady-state absorption chiller model can be written by performing mass and energy balances for each component. The internal conditions such as pressures, temperatures and flow rates can be calculated once when the system of equation is set and absorption cycle closed. The governing equations of absorption chiller components without external circuit balances are presented in equations 5.1 to 5.20:

Generator:

$$\dot{m}_3 = \dot{m}_4 + \dot{m}_7 \tag{5.1}$$

$$\dot{m}_3 x_3 = \dot{m}_4 x_4 \tag{5.2}$$

$$\dot{Q}_{gen} = \dot{m}_4 h_4 + \dot{m}_7 h_7 - \dot{m}_3 h_3 \tag{5.3}$$

Condenser:

$$\dot{m}_7 = \dot{m}_8 \tag{5.4}$$

$$\dot{Q}_{con} = \dot{m}_7 (h_7 - h_8) \tag{5.5}$$

Evaporator:

$$\dot{m}_9 = \dot{m}_{10} \tag{5.6}$$

$$\dot{Q}_{eva} = \dot{m}_9 (h_{10} - h_9) \tag{5.7}$$

Absorber:

$$\dot{m}_1 = \dot{m}_6 + \dot{m}_{10} \tag{5.8}$$

$$\dot{m}_6 x_6 = \dot{m}_1 x_1 \tag{5.9}$$

$$\dot{Q}_{abs} = \dot{m}_{10} h_{10} + \dot{m}_6 h_6 - \dot{m}_1 h_1 \tag{5.10}$$

Throttling valves:

$$h_5 = h_6, \qquad h_8 = h_9 \tag{5.11} \tag{5.12}$$

Solution pump:

$$W = \dot{m}_2 h_2 - \dot{m}_1 h_1 \tag{5.13}$$

Solution heat exchanger:

$$\dot{m}_2 = \dot{m}_3, \qquad \dot{m}_4 = \dot{m}_5 \tag{5.14) (5.15}$$

$$x_2 = x_3, \qquad x_4 = x_5 \tag{5.16) (5.17}$$

$$\dot{Q}_{shx} = \dot{m}_1 (h_3 - h_2) \tag{5.18}$$

$$\dot{Q}_{shx} = \dot{m}_4 (h_4 - h_5) \tag{5.19}$$

Coefficient of performance:

$$COP = \frac{\dot{Q}_{eva}}{\dot{Q}_{gen} + W} \tag{5.20}$$

The input parameters for the model of absorption cycle shown in Figure 5.1 are represented in Table 5.1. Since we disposed only with the manufacturers' catalogue data, some initial guesses were necessary. These guesses refer to the internal operating temperatures of four components and efficiency of the solution heat exchanger.

Table 5.1 Input parameters assuming pinch temperatures

Parameter	**Nomenclature**
Absorber temperature	T_1
Generator temperature	T_4
Condenser temperature	T_8
Evaporator temperature	T_{10}
Solution heat exchanger effectiveness	ε_{shx}

Based on experience reported in the literature, "pinch" temperatures for each component and effectiveness of solution heat exchanger were assumed. Having these input data defined, the absorption cycle can be closed. The modelling of the cycle was done in Engineering Equation Solver (EES). EES is an iterative solver which includes the properties of the fluid mixtures and therefore facilitates the modelling. Once when the cycle was closed, the model was upgraded with the parameters from external fluid

circuits (temperatures and flow rates) using manufacturers' catalogue. This was done by adding the heat balance equations for each component from water side. Figure 5.2 and Figure 5.3 illustrate complete H_2O-LiBr and NH_3-H_2O cycles with external circuit state points.

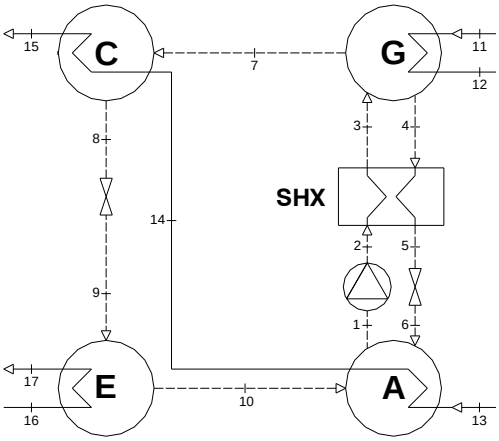

Figure 5.2 H_2O-LiBr cycle with external heat flows

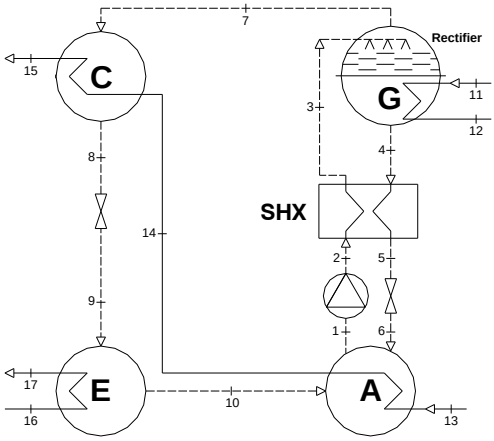

Figure 5.3 NH_3-H_2O cycle with external heat flows

At this step was possible to simulate the behaviour of absorption chiller at nominal conditions. The next step was to adjust all the component loads to values reported by manufacturer by performing parametric optimization of pinch temperatures and solution heat exchanger effectiveness. After obtaining the optimal pinch temperatures, we approached to the calculation of the UA values by applying equations 5.21 and 5.22:

$$UA = \frac{\dot{Q}_k}{\Delta T_{lm}} \tag{5.21}$$

$$\Delta T_{lm} = \frac{\left(T_{h,1} - T_{c,1}\right) - \left(T_{h,2} - T_{c,2}\right)}{\ln \frac{\left(T_{h,1} - T_{c,1}\right)}{\left(T_{h,2} - T_{c,2}\right)}} \tag{5.22}$$

where h and c refer to the hot and cold sides, respectively, k depicts component and ΔT_{lm} is the log mean temperature difference.

Finally, the pinch temperatures in the program code were replaced with estimated UA values as input parameters, obtaining the model which can predict the

performance of absorption chiller by using external temperatures and flow rates as input parameters. The same methodology was applied to both chillers (Rotartica and Pink), by using the appropriate fluid properties and adapting the equations for both H_2O-LiBr and NH_3-H_2O cycles. Although this backward methodology might look too approximate, unfortunately, this is the only way to model the absorption process using thermodynamic principles when there is no information about the internal states of the machine. The other shortage of the model is constant UA values approach which is not quite correct, since the UA values vary at different operating conditions. However, this approach is quite common for rough estimation of absorption chiller performance. More details about the absorption cycle modelling as well as the detailed governing equations for different cycles can be found in [23].

5.3.2. Adapted Gordon-Ng model (GNA)

A general thermodynamic model for absorption chillers developed by Gordon and Ng [146] is actually a combination of mechanistic and empirical approaches. According to the authors, the dominant irreversibility of the absorption chillers is finite-rate mass transfer. The losses due to the finite-rate mass transfer can therefore be approximated as temperature independent. The original model was based on external input parameters of four main components (generator condenser, evaporator and absorber), assuming that manufacturers' catalogues provide the operating conditions for each one of them. However, the current manufacturers' practice is to provide operating curves based on three circuits, i.e. treating absorber and condenser as one component. The main reason for that is the series arrangement of the absorber and condenser in majority of the commercial absorption chillers. Therefore, the original model was modified to correspond to the actual situation, considering the absorber and condenser as one heat exchanger.

Staring from the First law of thermodynamics, the energy balance of the absorption chiller can be expressed by equation 5.23:

$$\dot{Q}_{gen} + \dot{Q}_{eva} - \dot{Q}_{abs} - \dot{Q}_{con} = 0 \tag{5.23}$$

Since the absorber and condenser are treated as one component, equation 5.23 can be rearranged to:

$$\dot{Q}_{gen} + \dot{Q}_{eva} - \dot{Q}_{ac} = 0 \tag{5.24}$$

The entropy balance which takes into account the dominant irreversibility can be approximated by equation 5.25:

$$\Delta S = \frac{\dot{Q}_{ac} - \dot{q}_{ac}^{loss}}{T_{ac}} - \frac{\dot{Q}_{gen} - \dot{q}_{gen}^{loss}}{T_{gen}} - \frac{\dot{Q}_{eva} - \dot{q}_{eva}^{loss}}{T_{eva}} = 0 \tag{5.25}$$

Here, $\dot{q}^{loss}$ denotes losses from all sources other than finite-rate heat transfer. The heat transfer process was approximated as isothermal, due to the common practice in heat exchangers to adopt process-averaged values for absolute temperatures T_{eva}, T_{ac}, T_{gen} . Rearranging the equation 5.25 and expressing in terms of $\dot{Q}_{ac}$ yields

$$\dot{Q}_{ac} = T_{ac}\left[\frac{\dot{Q}_{gen} - \dot{q}_{gen}^{loss}}{T_{gen}} + \frac{\dot{Q}_{eva} - \dot{q}_{eva}^{loss}}{T_{eva}}\right] + \dot{q}_{ac}^{loss} \tag{5.26}$$

Inserting equation 5.26 into equation 5.24 yields

$$\dot{Q}_{gen} + \dot{Q}_{eva} - T_{ac}\left[\frac{\dot{Q}_{gen} - \dot{q}_{gen}^{loss}}{T_{gen}} + \frac{\dot{Q}_{eva} - \dot{q}_{eva}^{loss}}{T_{eva}}\right] + \dot{q}_{ac}^{loss} = 0 \tag{5.27}$$

Now, by solving equation 5.27 for $\dot{Q}_{gen}$, it can be obtained

$$\dot{Q}_{gen} = \dot{Q}_{eva}\left[\frac{T_{ac} - T_{eva}}{T_{eva}}\right] \cdot \left[\frac{T_{gen}}{T_{gen} - T_{ac}}\right] + \left[\frac{T_{gen}}{T_{gen} - T_{ac}}\right] \cdot \left[\dot{q}_{ac}^{loss} - \dot{q}_{eva}^{loss}\frac{T_{ac}}{T_{eva}} - \dot{q}_{gen}^{loss}\frac{T_{ac}}{T_{gen}}\right] \tag{5.28}$$

By introducing the COP and dividing both sides of equation 5.28 by $\dot{Q}_{eva}$

$$COP = \frac{\dot{Q}_{eva}}{\dot{Q}_{gen}} \tag{5.29}$$

$$\frac{1}{COP} = \left[\frac{T_{ac} - T_{eva}}{T_{eva}}\right] \cdot \left[\frac{T_{gen}}{T_{gen} - T_{ac}}\right] + \left[\frac{1}{\dot{Q}_{eva}}\right] \cdot \left[\frac{T_{gen}}{T_{gen} - T_{ac}}\right] \cdot \left[\dot{q}_{ac}^{loss} - \dot{q}_{eva}^{loss}\frac{T_{ac}}{T_{eva}} - \dot{q}_{gen}^{loss}\frac{T_{ac}}{T_{gen}}\right] \quad (5.30)$$

Using the equation 5.30, the final form can be expressed as:

$$\frac{1}{COP} = \left[\frac{T_{ac}^{in} - T_{eva}^{out}}{T_{eva}^{out}}\right] \cdot \left[\frac{T_{gen}^{in}}{T_{gen}^{in} - T_{ac}^{in}}\right] + \left[\frac{1}{\dot{Q}_{eva}}\right] \cdot \left[\frac{T_{gen}^{in}}{T_{gen}^{in} - T_{ac}^{in}}\right] \cdot \left[\dot{q}_{ac}^{loss} - \dot{q}_{eva}^{loss}\frac{T_{ac}^{in}}{T_{eva}^{out}} - \dot{q}_{gen}^{loss}\frac{T_{ac}^{in}}{T_{gen}^{in}}\right] \quad (5.31)$$

According to Gordon and Ng approximation, the finite-rate mass transfer is roughly temperature independent. With respect to that, the losses in the evaporator $\dot{q}_{eva}^{loss}$ can be neglected, and the other two terms $\dot{q}_{gen}^{loss}, \dot{q}_{ac}^{loss}$ can be viewed as constant characteristic of particular chiller. COP can be expressed as (5.32):

$$\frac{1}{COP} = \left[\frac{T_{ac}^{in} - T_{eva}^{out}}{T_{eva}^{out}}\right]\left[\frac{T_{gen}^{in}}{T_{gen}^{in} - T_{ac}^{in}}\right] + \left[\frac{1}{\dot{Q}_{eva}}\right]\left[\frac{T_{gen}^{in}}{T_{gen}^{in} - T_{ac}^{in}}\right]\left[\alpha_1 - \alpha_2\frac{T_{ac}^{in}}{T_{gen}^{in}}\right] \quad (5.32)$$

where α_1 and α_2 are the regression parameters to be fitted and at the same time the constants which characterise the entropy generation of particular chiller. Considering that a plot of $[\frac{T_{ac}^{in}}{T_{gen}^{in}}]$ against $\left[\frac{T_{gen}^{in} - T_{ac}^{in}}{T_{gen}^{in} \cdot COP} - \frac{T_{ac}^{in} - T_{eva}^{out}}{T_{eva}^{out}}\right]\dot{Q}_{eva}$ leads to a straight line, α_1 and α_2 were calculated as the intercept and slope of this line using linear regression. Bearing in mind that latter analysis compares different modelling approaches by means of the deviations between the experimental and modelled heat loads, the final equation of GNA model was rearranged. Thus, in order to evaluate GNA model the equation 5.32 was rearranged to obtain $\dot{Q}_{eva}$ while $\dot{Q}_{gen}$ can be calculated from equation 5.29.

Finally, $\dot{Q}_{eva}$ and $\dot{Q}_{gen}$ as function of T_{eva}^{out} ,T_{ac}^{in} , T_{gen}^{in}[7] and COP can be expressed by equations 5.33 and 5.34:

$$\dot{Q}_{eva} = \frac{B}{\frac{1}{COP} - A} \tag{5.33}$$

$$\dot{Q}_{gen} = \frac{B}{1 - A \cdot COP} \tag{5.34}$$

where

$$A = \left[\frac{T_{ac}^{in} - T_{eva}^{out}}{T_{eva}^{out}}\right]\left[\frac{T_{gen}^{in}}{T_{gen}^{in} - T_{ac}^{in}}\right] \tag{5.35}$$

$$B = \left[\frac{T_{g}^{i}}{T_{g}^{i} - T_{ac}^{i}}\right]\left[\alpha_1 - \alpha_2 \frac{T_{ac}^{i}}{T_{g}^{i}}\right] \tag{5.36}$$

5.3.3. Adapted characteristic equation method $\Delta\Delta t$'

Ziegler et al. [15] developed an approximate method for modelling absorption chillers which is able to represent both cooling capacity and driving heat input by simple algebraic equations. These equations are expressed as a function of so-called characteristic temperature function ($\Delta\Delta t$), which depends on the average temperature of the external heat carrier fluids. One of the main assumptions is that the heat transfer processes in absorption chillers dominate their behaviour. Starting from the heat transfer equations in the four major components where the transferred heat is related to the driving temperature difference in the heat exchangers and by combining them with Duhring's rule the authors determine the relationship between the external temperatures. The relationship of the total heat transfer between the absorption chiller and the ambient is proportional to a characteristic temperature difference as it can be seen in equation 5.37:

[7] For the sake of clarity in modelling, this Chapter has a slightly modified nomenclature. External fluid circuits indexes are replaced by indexes that correspond to absorption chiller components: $T_{eva}^{out} = T_{chw,out}$, $T_{ac}^{in} = T_{cw,in}$ and $T_{gen}^{in} = T_{hw,in}$.

$$\Delta\Delta t = \left(T_{gen} - T_{abs}\right) - R(T_{con} - T_{eva}) \approx T_{gen} - (1 - R)T_{ac} + RT_{eva} \quad (5.37)$$

In this way, a complex response to all external heat carrier temperatures is reduced to a linear function of heat flow and the external temperatures. R is a constant between 1.1-1.2 used to relate the slope of vapour pressure line to the one of pure water.

Simple linear correlation is very convenient, but it has been found that the predicted performance of the cooling capacity deviates considerably of linear behaviour, for instance, at high driving temperatures, due to higher internal losses. With respect to that, an adapted characteristic equation method was proposed by Kuhn and Ziegler [151]. In this improved model, a numerical fit of catalogue or experimental data is used to improve the characteristic equation. Thus, adapted characteristic temperature function ($\Delta\Delta t'$) takes the form (5.38):

$$\Delta\Delta t' = T_{gen} - a \cdot T_{ac} + e \cdot T_{eva} \quad (5.38)$$

And the linear characteristic equation for component loads with (5.39):

$$\dot{Q}_{(k)} = s' \cdot \Delta\Delta t' + r \quad (5.39)$$

Combining equations 5.38 and 5.39 yields one correlation (5.40) which represents the thermal performance of the components in function of external arithmetic mean temperatures of the generator (T_{gen}), absorber-condenser (T_{ac}) and evaporator (T_{eva}), when the external flow rates are constant.

$$\dot{Q}_{(k)} = s' \cdot T_{gen} - s' \cdot a \cdot T_{ac} + s' \cdot e \cdot T_{eva} + r \quad (5.40)$$

The four parameters (s', a, e and r) are estimated by using the multiple linear regression algorithm to fit the catalogue or experimental data. This algorithm chooses regression coefficients to minimise the residual sum of squares. The analyses of Puig et al. [152] confirmed the capability of $\Delta\Delta t'$ method to obtain good results and also better accuracy than the original method ($\Delta\Delta t$). Finally, by combining the obtained characteristic functions (5.40) with equations for external arithmetic mean temperatures

(5.41)-(5.43) and with external energy balances (5.44)-(5.46), it results in a system of six equations with six unknowns which can easily be solved. The developed model requires only three temperatures (one from each of the external circuits) and fixed flow rates of external heat carriers to predict the performance of the absorption chiller or heat pump.

$$T_{eva}^{in} = 2 \cdot T_{eva} - T_{eva}^{out} \tag{5.41}$$

$$T_{gen}^{out} = 2 \cdot T_{gen} - T_{gen}^{in} \tag{5.42}$$

$$T_{ac}^{out} = 2 \cdot T_{ac} - T_{ac}^{in} \tag{5.43}$$

$$\dot{Q}_{eva} = 2 \cdot m_{eva} \cdot C_{p_{eva}} \cdot (T_{eva} - T_{eva}^{out}) \tag{5.44}$$

$$\dot{Q}_{gen} = 2 \cdot m_{gen} \cdot C_{p_{gen}} \cdot (T_{gen}^{in} - T_{gen}) \tag{5.45}$$

$$\dot{Q}_{ac} = 2 \cdot m_{ac} \cdot C_{p_{ac}} \cdot (T_{ac} - T_{ac}^{in}) \tag{5.46}$$

Despite this method is based on numerical fit to experimental or catalogue data, it would not be right to classify it just as black-box. Just as in the case of GNA model, term semi-empirical would be more appropriate knowing that these equations contain the thermodynamic information of the absorption system in simplified form.

5.3.4. Multivariate Polynomial Regression (MPR)

The MPR models belong to the black-box group of models, which do not carry the information about the physical processes incorporated in the model structure. MPR models are very effective tool for describing complex non-linear relationships between input and output variables without any consideration what occurs within the black box. The parameters for the MPR model are calculated by fitting to experimental data in a manner that determines a minimum squared error polynomial for given data. Due to their simple structure, MPR models have been applied in various fields such as forecasting, control, optimization, fault detection and diagnosis [19, 153, 154]. A typical polynomial regression model contains the squared and higher order terms of the

estimator variable. Normally, the higher order MPR models offer better accuracy of prediction. However, high-order MPR can become impractical due to its prohibitive number of parameters. One of the common techniques in the case of the high order MPR models with large number of parameters is to reduce the model by retaining only those parameters that are statistically significant. Also, excessive polynomial order for a relatively small database may worsen data interpolation. These are the some of the reasons why it has been decided to apply 2nd order polynomials to forecast absorption chiller performance. Thus, the MPR models were developed to calculate the thermal loads of the absorption chiller by using the measurements of external circuits: generator inlet temperature, absorber/condenser inlet temperature, and evaporator outlet temperature. The generalized 2nd order model in case of absorption chillers can be represented by equation 5.47:

$$\dot{Q}_{(k)} = \beta_{0,k} + \beta_{1,k}T_{gen}^{in} + \beta_{2,k}T_{ac}^{in} + \beta_{3,k}T_{eva}^{out} + \beta_{4,k}T_{gen}^{in} \cdot T_{ac}^{in} + \beta_{5,k}t_g \cdot T_{eva}^{out} + \beta_{6,k}T_{ac}^{in} \cdot T_{eva}^{out} + \beta_{7,k}\left(T_{gen}^{in}\right)^2 + \beta_{8,k}\left(T_{ac}^{in}\right)^2 + \beta_{9,k}(T_{eva}^{out})^2 \quad (5.47)$$

The above model has ten coefficients, which need to be fitted from experimental data. These coefficients, as mentioned before, have no physical meaning and therefore cannot be interpreted in physical terms.

5.3.5. Artificial Neural Networks (ANN)

ANN models also belong to group of black-box models. Since their origins in the 1940s [155] and the first Perceptron model developed by Rosenblatt, artificial neural networks (ANN) have gone from almost being abandoned to a highly promising technology. In the last two decades ANN are experiencing a huge expansion and now it has been recognized as a good tool for modelling, identification and control in steady state and dynamic systems [156, 157]. These models have several advantages: there is no need to make assumptions about the nature of underlying structures, to take into account the non-linearity of the system, and correlations between variables. Because of their simplicity to solve non-linearity and complicated problems in complex systems in a straightforward fashion, they have been used in a variety of renewable energy system applications [158]: from solar radiation, wind speed prediction and the modelling of

solar steam generators, through photovoltaic systems to energy optimization and the prediction of the energy consumption of a passive solar building. In the last few years, feed-forward neural networks with back-propagation have found their place in the field of absorption systems and their applications [17, 159-161] .

ANN were inspired by the human brain as the centre of the human nervous system. The brain is principally composed of a very large number of neurons, which are massively interconnected. Like the human brain, a neural network is an adaptive system which can be trained to perform a particular function or behaviour on the basis of input and output information that flows through the network. The connections (weights) between the elements can be adjusted to model complex relationships between inputs and outputs or to find patterns in data. The structure of ANN model is illustrated in Figure 5.4.

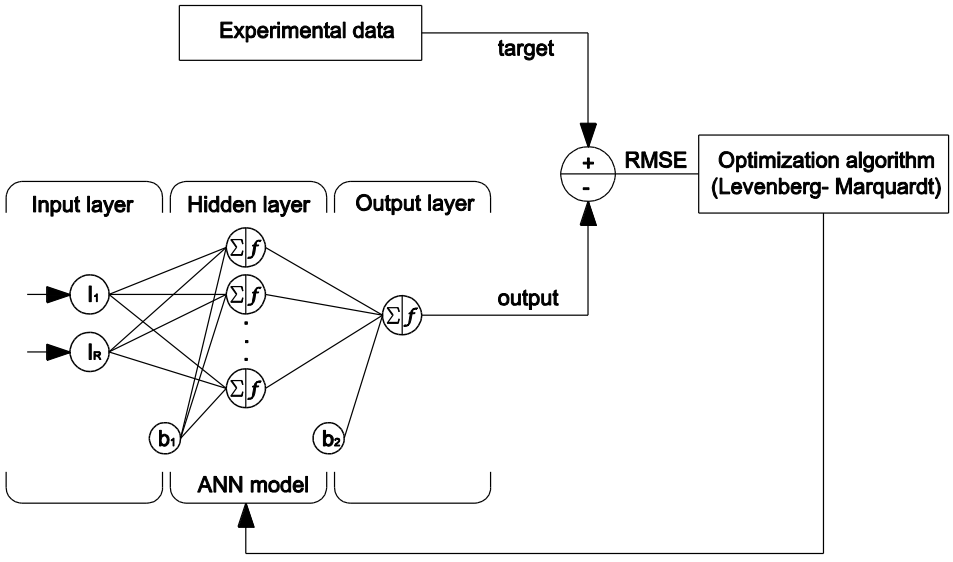

Figure 5.4 ANN structure

There are many types of ANN architectures in the literature; however, the most common network structure used for prediction is the multi-layer feed-forward network with back-propagation. In feed-forward networks, signals flow forward from inputs, through one or more hidden layers of sigmoid neurons before reaching the output layer of linear neurons. Back-propagation is a gradient descent algorithm. The difference between the obtained network output and the desired output (target) is compared and

iterated until the output reaches the prescribed tolerance value. The Levenberg-Marquardt algorithm of optimization was proved to be the optimal solution to minimize the error [162]. The error is calculated as the difference between the target output (t) and the network output (net) for N data, minimizing a Root Mean Square Error (RMSE) in the following way (5.48):

$$\mathrm{RMSE} = \sqrt{\frac{1}{\mathrm{N}}\sum_{\mathrm{i}=1}^{\mathrm{N}}(\mathrm{t(i)} - \mathrm{net(i)})^2} \tag{5.48}$$

Since there is no explicit rule to determine the topology of ANN (the number of neurons in the hidden layer or the number of hidden layers) the trial and error method is usually applied to find the best solution.

5.4. Results and discussion

5.4.1. Model parameters

5.4.1.1. TD

Table 5.2 shows estimated parameters for H_2O-LiBr absorption chiller Rotartica, after applying the backward methodology with pinch temperatures. These parameters were estimated based on the nominal operation conditions, taken from manufacturer's catalogue.

Table 5.2 Estimated input parameters for TD model-Rotartica

UA_c [kW/K]	0.9387
UA_g [kW/K]	1.423
UA_a [kW/K]	2.236
UA_e [kW/K]	0.7881
ε_{shx}	0.669

In case of the NH_3-H_2O chiller Pink, the manufacturers' catalogue was useless, since the nominal operating conditions do not cover this particular model with lower ammonia filling. Therefore, as base points for backward modelling were taken the steady state points from our tests at various temperature levels. This was necessary since ammonia water cycle is very sensitive with respect to the UA values. The estimated UA values can be applied only for a narrow temperature range around the

point used for backward modelling, otherwise, the EES program code cannot iterate. This fact implies the repetition of the backward modelling process at various temperature levels, in order to be able to simulate the whole selected range. Table 5.3 shows one set of the estimated input parameters for Pink chiller under following temperature conditions: T_{gen}^{in}=100ºC, T_{eva}^{out} =7 ºC and T_{ac}^{in} =33ºC .

Table 5.3 Estimated input parameters for TD model-Pink

UA_c [kW/K]	10.72
UA_g [kW/K]	2.146
UA_a [kW/K]	8.458
UA_e [kW/K]	2.238
ε_{shx}	0.9

5.4.1.2. GNA

Two linear regression coefficients for the GNA model, α_1 and α_2, were obtained after performing numerical fit on experimental datasets. Table 5.4 shows these coefficients for two observed absorption chillers, Rotartica and Pink.

Table 5.4 GNA model coefficients

Coefficient	Rotartica	Pink
$\boldsymbol{\alpha_1}$	16.5931	36.524
$\boldsymbol{\alpha_2}$	18.7232	41.5269

5.4.1.3. ΔΔt'

The same experimental datasets were applied for $\Delta\Delta t'$ method. Multiple linear regression fit resulted in the following coefficients for characteristic functions of absorption chillers (Table 5.5):

Table 5.5 Multiple linear regression fit parameters ($\Delta\Delta t'$)

	Rotartica				Pink			
	s'	$s'a$	$s'e$	r	s'	$s'a$	$s'e$	r
$\dot{Q}_{eva}$	0.1937	0.504	0.4498	0	0.6822	1.0057	0.3801	1.6396
$\dot{Q}_{ac}$	0.4422	0.989	0.7084	0	1.2698	2.3951	1.0347	0
$\dot{Q}_{gen}$	0.234	0.464	0.2614	0	0.5662	1.3066	0.5947	0

5.4.1.4. MPR

In the case of MPR models, Table 5.6 shows the regression fitting parameters ($\beta_{i,k}$) for the different heat loads (k) when 2nd order polynomial fit was applied on experimental data of two absorption chillers.

Table 5.6 Fitting coefficients for MPR models

	Rotartica			Pink		
(k)	$\dot{Q}_{eva}$	$\dot{Q}_{ac}$	$\dot{Q}_{gen}$	$\dot{Q}_{eva}$	$\dot{Q}_{ac}$	$\dot{Q}_{gen}$
β_0	82.0437	74.3823	-5.7974	6.818	65.3225	28.7061
β_1	-1.4152	-1.1981	0.2534	0.3703	0.3092	0.5642
β_2	0.1191	-0.3936	-0.6578	-1.4329	-4.4372	-3.037
β_3	-2.8436	-1.3507	1.3166	1.113	0.2036	-0.5002
β_4	-0.0042	-0.0017	0.0033	0.0122	0.0159	0.0079
β_5	0.029	0.0155	-0.0094	0.0014	0.0095	0.0048
β_6	0.0128	0.0055	-0.01	-0.0076	0.0117	0.0184
β_7	0.0075	0.008	-0.0002	-0.0025	-0.0001	-0.0019
β_8	-0.0046	-0.0053	0.001	-0.0081	0.0146	0.0187
β_9	0.0052	0.018	0.0073	-0.0217	-0.0172	-0.0009

5.4.1.5. ANN

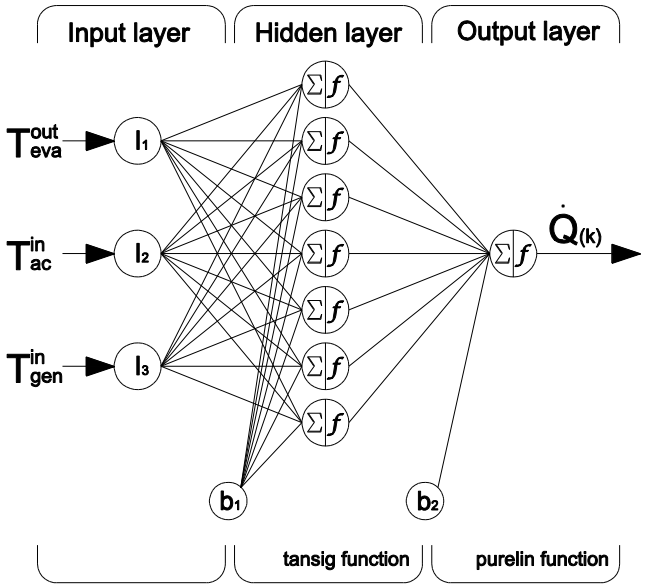

Figure 5.5 ANN topology

ANN models for two absorption chillers were developed by using MatLab software environment. By applying trial and error method rule to determine the number of neurons in the hidden layer and the number of hidden layers, the adopted topology for ANN models was (3-7-1) in both cases (Rotartica and Pink), as illustrated in Figure

5.5. One input layer with three variables, one hidden layer with seven neurons and one output layer with one output: a component load (three different models for $\dot{Q}_{eva}$, $\dot{Q}_{ac}$ and $\dot{Q}_{gen}$ of each of the absorption chillers). The training of the ANN was based on error back propagation technique using the Levenberg-Marquardt algorithm of optimization. The input parameters were normalized in the [0.2, 0.8] range. A hyperbolic tangent sigmoid function (*tansig*) was used in the hidden layer and the linear transfer function (*purelin*) was used in the output layer. To test the robustness and predict the ability of the models, the experimental database was split: a total of 70% was used for training, 20% for validation and 10% for testing.

The ANN absorption chiller models for calculating thermal loads are given by the general equation (5.49):

$$\dot{Q}_{(k)} = \sum_{1}^{J}\left[LW_{(1,J)}\left(\frac{2}{1+\exp\left(-2\left(\sum_{1}^{R} IW_{(J,R)} I_R + b_{1(J)}\right)\right)} - 1\right)\right] + b_2 \qquad (5.49)$$

where I is the input, R is the number of the input (R=3), b_1 are biases in the hidden layer, b_2 are biases in the output layer, J is the number of neurons in the hidden layer (J=7), and IW and LW are the weights in the input and output hidden layer, respectively. Tables 5.7 and 5.8 show the coefficients for ANN simulations of two absorption chillers obtained during the training stage.

Table 5.7 ANN coefficients-Rotartica

Input weights								
IW($\dot{Q}_{eva}$)			**IW($\dot{Q}_{ac}$)**			**IW($\dot{Q}_{gen}$)**		
9.5922	1.1127	-2.8749	3.0643	-1.1805	-8.3213	6.9474	-5.2149	8.213
-2.2934	1.9244	-9.3767	0.5297	-0.8164	0.8397	0.2142	-7.4426	-7.6131
-6.9985	1.3332	4.1288	-1.8697	1.5584	9.1415	-5.6933	4.2097	7.1662
-7.0962	3.5343	3.175	1.5803	-2.9252	12.2998	10.37	3.3326	3.173
5.1588	-10.0578	20.6436	10.6704	12.1474	2.63	6.2784	-7.5392	3.4556
-0.7916	1.9889	-0.9441	4.8713	-2.2103	-12.8595	0.8029	-1.7402	1.0614
6.0008	5.0222	10.4135	0.2361	-8.5725	-0.8526	10.3616	-1.3676	-3.5351
Output weights								
LW($\dot{Q}_{eva}$)	-3.1826	-1.5257	1.9204	-1.8471	-1.154	-6.3839	-3.8225	
LW($\dot{Q}_{ac}$)	-4.9422	18.126	-0.4172	5.7982	-1.0357	2.9972	1.6144	
LW($\dot{Q}_{gen}$)	0.3898	-2.6433	0.7111	-1.3186	0.9854	5.9236	-0.2167	
Biases in input layer				**Biases in hidden layer**				

$b1(\dot{Q}_{eva})$	$b1(\dot{Q}_{ac})$	$b1(\dot{Q}_{gen})$	$b2(\dot{Q}_{eva})$	$b2(\dot{Q}_{ac})$	$b2(\dot{Q}_{gen})$
-9.0668	-6.3762	8.1163	5.7146	8.6907	5.4579
6.9072	-0.4734	-0.3853			
-6.8933	-1.4607	-6.4215			
-3.8973	11.4221	-2.7785			
-10.6053	-7.3175	-3.4482			
-0.1994	-0.3095	0.2362			
0.9475	5.627	-3.074			

Table 5.8 ANN coefficients-Pink chilli12

Input weights								
$IW(\dot{Q}_{eva})$			$IW(\dot{Q}_{ac})$			$IW(\dot{Q}_{gen})$		
-2.6842	-26.2414	40.2259	1.3136	-4.368	-2.9482	4.0929	36.7107	28.4331
27.994	37.8786	151.8244	-1.6348	3.5549	-6.8414	-0.617	2.0084	-4.4218
4.5898	1.0661	1.0163	-3.1738	-0.4494	3.5448	14.3784	-4.0429	-11.2227
0.4744	-2.2865	-7.902	-3.85	-1.5356	-7.2797	-0.8131	2.9104	-7.6695
2.0043	14.9552	27.8277	-0.6074	1.2485	-0.0293	-14.7601	29.0476	-43.4843
3.0631	3.4876	-3.0904	1.0057	-11.3297	-5.0261	-3.305	1.8499	13.8269
0.6453	-1.4337	0.9214	0.2914	-0.8686	6.4158	-0.6262	9.0005	-9.7543
Output weights								
$LW(\dot{Q}_{eva})$	-0.6507	-0.4582	1.1899	-1.0693	0.616	-0.9387	10.0674	
$LW(\dot{Q}_{ac})$	-3.5228	-3.8286	1.8483	0.8719	-27.8663	-1.233	4.1751	
$LW(\dot{Q}_{gen})$	-0.4252	-18.2436	0.4097	9.6199	-0.3298	-1.5636	-1.9776	
Biases in input layer				**Biases in hidden layer**				
$b1(\dot{Q}_{eva})$	$b1(\dot{Q}_{ac})$	$b1(\dot{Q}_{gen})$	$b2(\dot{Q}_{eva})$	$b2(\dot{Q}_{ac})$	$b2(\dot{Q}_{gen})$			
-7.5266	2.1264	-22.9476	6.993	23.9447	12.8346			
-73.789	0.5695	1.0747						
-2.7049	1.3703	1.3844						
3.5951	11.9184	2.0647						
-33.3159	-0.1494	3.6732						
-1.984	9.4941	-10.9156						
0.0916	-3.7636	5.1815						

5.4.2. Evaluation of the models

5.4.2.1. Simple comparison

The models of two absorption chillers developed with different modelling approaches show a great diversity of simulated results. Figure 5.6 shows the comparison of the catalogue data, tests and simulations results in the case of Rotartica absorption chiller. Chilling capacity is represented as a function of the chilled water outlet

temperature at T_{hw}^{in} =90ºC and T_{cw}^{in} =35ºC. One of the differences which are visible from the Figure 5.6 is that the experimental values for chilling capacity are lower than the catalogue values. At first sight, one of the facts which might cause that is flow rates of chilled water (0.43 kg/s) and cooling water (0.55 kg/s) circuits which differ from nominal values (0.44 kg/s for chilled water and 0.56 kg/s for cooling water). On the other hand, the sensitivity analysis from Chapter Four indicates that the influence of flow rates in a narrow range such is the case with Rotartica does not affect the performance of the absorption chiller significantly. This drives to a conclusion that the real performance of the machine is lower than the one reported by manufacturer. Also, it can be seen that data obtained from thermodynamic simulation are in close agreement with catalogue data. The matching of TD model outputs to catalogue data stems from a fact that model parameters were estimated by using the nominal conditions specified at the manufacturer catalogue. The discrepancy between the simulation and catalogue data increases moving away from this curve, which is the same as moving away from nominal conditions. The reason for that is that the UA values are not constant as we assumed. The disadvantages of the thermodynamic models with constant UA values were also reported in the study of Kim and Infante Ferreira [163].The discrepancy of the TD model to the experimental data is even more expressed. Conversely, the empirically-based models of the absorption chiller have very good agreement with experimental data, with exception of GNA model. Obviously, the reason for the good agreement between the experimental data and the empirical models is that experimental data were used to fit the models parameters.

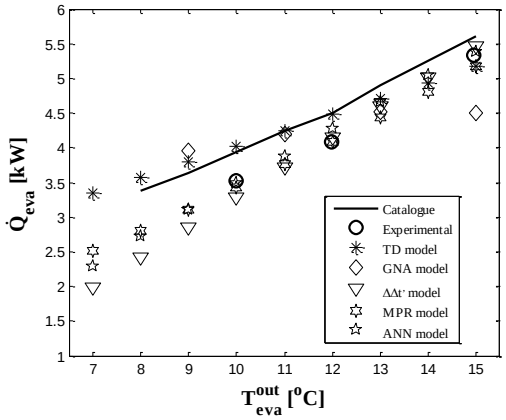

Figure 5.6 Comparison of the catalogue and experimental data with data obtained by simulation-Rotartica

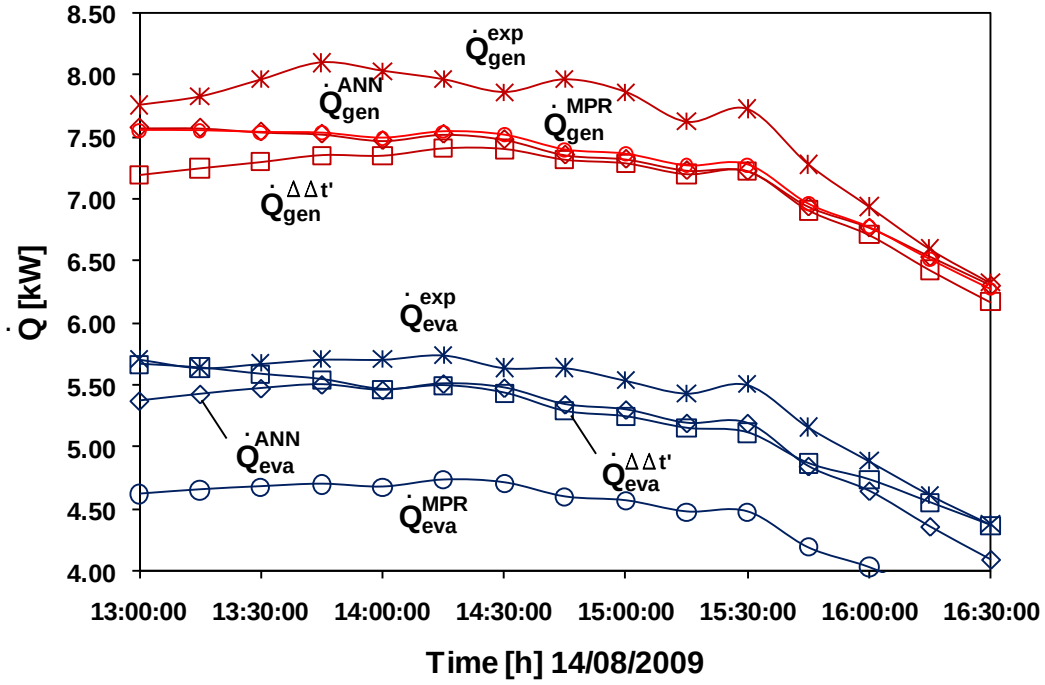

Figure 5.7 Rotartica-cross validation of empirical models with experimental data from Evola et al. (2010)

In order to validate our models, three empirical models which showed close agreement with experimental data, ΔΔt', MPR and ANN, were compared with independent experimental data of other authors for the same absorption machine in a small solar-assisted installation. Figure 5.7 shows the comparison with the 3.5 hours profile reported by Evola et al. [164] which indicates that majority of compared empirical models have very good prediction capability. With exception of the MPR model prediction for chilling capacity, the highest deviation of other models is around 9%. Moreover, the mean deviation is less than 5% which indicates that these models can be more than suitable for simulation tools. However, this has to be taken with a dose of caution. As explained before, the empirical models were developed with poor dataset. It is very difficult, if not impossible, to develop a model which will be able to predict the behaviour of any system accurately based on small data samples. Simply, that kind of model does not dispose with enough information to establish the correlations properly. It can establish the correlations which are only valid for the range of data (or points) used for modelling. Moving away from that range the model will deviate radically. Therefore, the only logical explanation for the observed case is that the profile used for comparison was close to the data used for modelling.

In the case of Pink absorption chiller, catalogue data were not available since the model is not from standard series (lower ammonia filling). Therefore, all the models were developed based on experimental datasets. This includes the estimation of UA values for TD model. The main difference with respect to the Rotartica is that these models were developed on comprehensive datasets which completely cover the range of the chiller for fan-coil applications. Figure 5.8 shows the comparison of the tests and simulations at T_{hw}^{in} =85ºC and T_{cw}^{in} =27ºC. Same as in case with Rotartica, TD and GNA models showed lower prediction results when compared to other three models. The main reason for deviation of the TD model still remains the fact that UA values are not constant. ΔΔt', MPR and ANN shows very close agreement with experimental data. Another interesting detail which can be seen in Figure 5.8 is that now the difference in prediction capabilities between these three models is much smaller than in case of Rotartica. This is direct consequence of the large number of data used for model development.

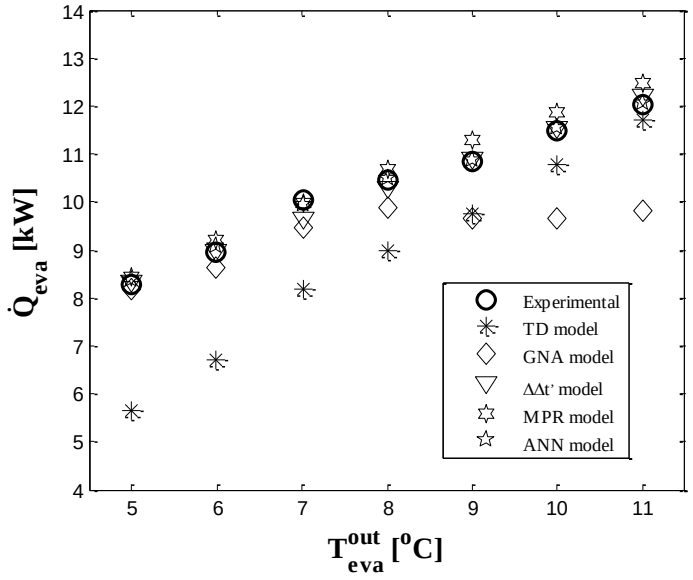

Figure 5.8 Comparison of the experimental data with data obtained by simulation-Pink

Unfortunately, cross validation of the models with independent data reported by other authors was not possible due to lack of information.

5.4.2.2. Statistical indicators

The goodness-of-fit of models is usually evaluated in terms of the statistical indicators. The statistical performance analysis of different developed models was conducted including several statistical indicators: the residual sum of squares (SS_{res}), the coefficient of determination (R^2), the root mean square error (RMSE), the coefficient of variation (CV), the mean absolute difference ($|\bar{\epsilon}|$), the maximum residual (ϵ_{min}) and the minimum residual (ϵ_{min}).

The most common parameters to check how close the predicted values are to observed data are the residual sum of squares and the coefficient of determination. Residual is unexplained variation after fitting a model explained through the difference between the value predicted by the model (y_i) and the associated observed value ($\hat{y}_i$) (5.50). The sum of the squares of these differences is called the residual sum of squares (5.51) and can be understood as a measure of the discrepancy between the data and an estimation model. A smaller SS_{res} indicates better fit to the observed data.

$$\epsilon_i = y_i - \hat{y}_i \tag{5.50}$$

$$SS_{res} = \sum_{i=1}^{N} {\epsilon_i}^2 \tag{5.51}$$

The coefficient of determination is another parameter which quantifies the goodness of fit. The R^2 can be calculated from the residual sum of squares and the total sum of squares (SS_{tot}) by using equation 5.52:

$$R^2 = 1 - \frac{SS_{res}}{SS_{tot}} \tag{5.52}$$

$$SS_{tot} = \sum_{i=1}^{N} \hat{y}_i - \bar{y}_i \tag{5.53}$$

R^2 can be interpreted as a statistical measure of how well a model prediction approximates the observed data. An R^2 of 1.0 would indicate that model prediction

perfectly fits the observed data. However, the statistical analysis cannot rely only on R^2, no matter how a fit is reasonable. It should be interpreted together with other model parameters which may have values that make no sense or the confidence intervals may be too wide.

An illustration of how close the model prediction is likely to be to the parametric mean can be done by using confidence limits (CL), the values at the upper and lower end of the confidence interval. Usually, the model best fit parameter values are evaluated by using 95% confidence interval. Simplified, it means that 5% of the predicted values are expected to fall outside the confidence limits. If the confidence limits are reasonably narrow, it can be said that the best fit parameter values are determined with a reasonable certainty. The 95% confidence limits can be estimated by using the equation 5.54:

$$\mathrm{CL} = \mathrm{BestFit} \pm t^{*} \cdot \mathrm{RMSE} \tag{5.54}$$

t^{*} is the constant which comes from t distribution, and depends on the desired confidence distribution and the numbers of degrees of freedom. The RMSE is statistical indicator which measures the precision of the model and can be calculated as the square root of the variance of the residuals (equation 5.55). RMSE indicates the absolute fit of the model to the observed data.

$$\mathrm{RMSE} = \sqrt{\frac{1}{N}\sum_{i=1}^{N} \epsilon_i{}^2} \tag{5.55}$$

Five different models of Rotartica absorption chiller are compared in Figure 5.9 through the predicted chilling capacity and driving heat input ($\dot{Q}_{eva}$and $\dot{Q}_{gen}$). R^2 and CL (in the form of dashed lines) of each model are shown as parameters that allow the comparison of the predictive capabilities. The statistical parameters indicate that better accuracy can be obtained from the pure black-box models rather than the thermodynamic and semi-empirical models. R^2 of TD model (both for $\dot{Q}_{eva}$and $\dot{Q}_{gen}$) is greater than 0.90, indicating a good fit. On the other hand, Figure 5.9a and Figure 5.9f

show that most of the predicted values lie above the diagonal which indicates the best fit. This means that the TD model overestimates $\dot{Q}_{eva}$and $\dot{Q}_{gen}$ because it does not take in account pressure drops, heat leaks, and other irreversibilities. In contrast of the TD model, the predicted values of heat loads obtained by the GNA lay around the diagonal, due to fact that the GNA takes into account the process irreversibilities through the 2nd Law of Thermodynamics. When comparing R^2, GNA performs worse than TD model, but in terms of precision GNA performs better than TD because GNA shows narrower confidence levels (RMSE of GNA is lower than RMSE of TD). ΔΔt' approach predicts chiller's behaviour much better than the previous two, but the best fits are obtained using ANN and MPR modelling (R^2 > 0.99). However, it was not possible to estimate the confidence levels in the case of ANN model. The number of ANN coefficients was higher than the number of the observed data used for model development. This led to a negative value of degrees of freedom, which is unacceptable from statistical point of view. This fact further questioned the reliability of other empirical models with respect to the small sample used for modelling. Small samples do not provide very precise estimate of the strength of the relationship, which is measured by R^2. This is the reason why majority of statistical software packages recommend larger samples (>40) for precise estimate [135]. Therefore, in terms of precision, neither one of the empirical models is reliable. The poor dataset did not provide enough information to models to cover properly whole range of operating conditions. This confirms the explanation given in Section 5.4.2.1 about the good results of validation with independent data. The independent data taken from the daily profile coincided with the range for which the models had the most input data. This further indicates that these models can be useful, but only within a narrow range around the input data used. Moving away from these points, the reliability of these models decreases because the relationships within the models are not strong enough.

Figure 5.10 shows the comparison between the measured and predicted evaporator and generator loads in the case of Pink absorption chiller. The first conclusion which arises from the scatter plots is that empirical models improve with increased number of samples. The improvement can be observed through the values of R^2 and CL. In case of TD modelling approach, $R^2(\dot{Q}_{eva})$ is higher than in the previous case (Rotartica) as a direct consequence of the higher number of UA values used during

simulations. Likewise, it can be seen that $R^2(\dot{Q}_{gen})$ is lower than in the previous case. The UA values are also the reason for this. At a certain temperature level, the model behaves well at point where the UA values were estimated by backward modelling. Moving away from that point the model starts to deviate and also has problems to converge due to the high sensitivity of NH_3-H_2O cycle to the UA values and to the fluid properties. The correct way would be to estimate UA values for each point in order to obtain greater accuracy. But that is not an option, first, because it significantly lengthens the time of modelling, and second, such a methodology would be difficult to integrate into software packages or in control. Figure 5.10b and Figure 5.10g show that statistical indicators of GNA also improved. Prediction improved due to the linear regression coefficients obtained from larger data samples. The last three approaches ($\Delta\Delta t'$, MPR and ANN) show the best statistical parameters. Compared to the previous case it can be seen that R^2 of $\Delta\Delta t'$ considerably increased. The high R^2 and narrow CL indicates excellent predictive power of all three approaches (R^2~0.99). Among them, the narrower CL ranges and highest R2 values (>0.998) were obtained with ANN modelling approach.

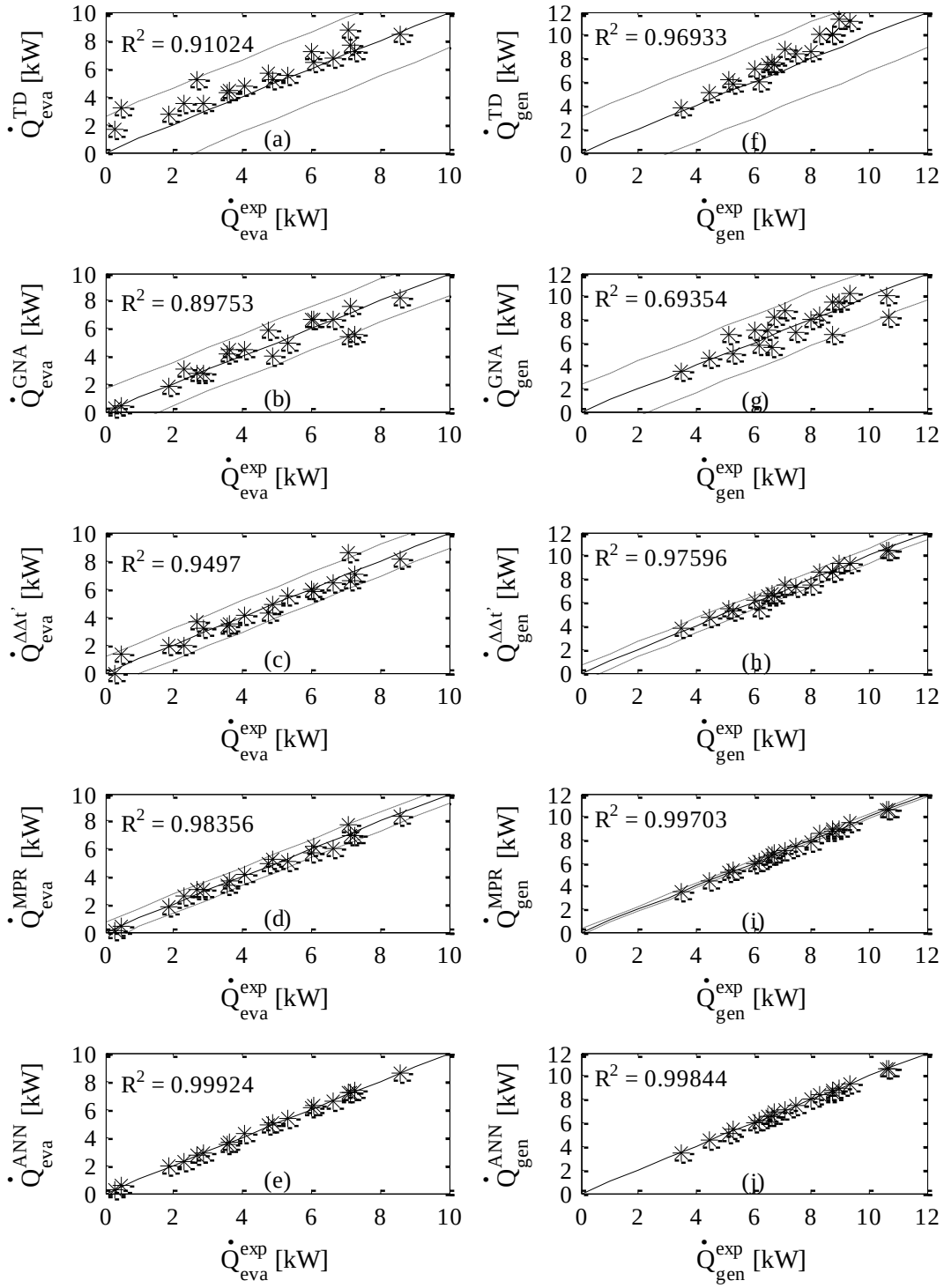

Figure 5.9 Comparison between the measured and predicted evaporator and generator loads-Rotartica

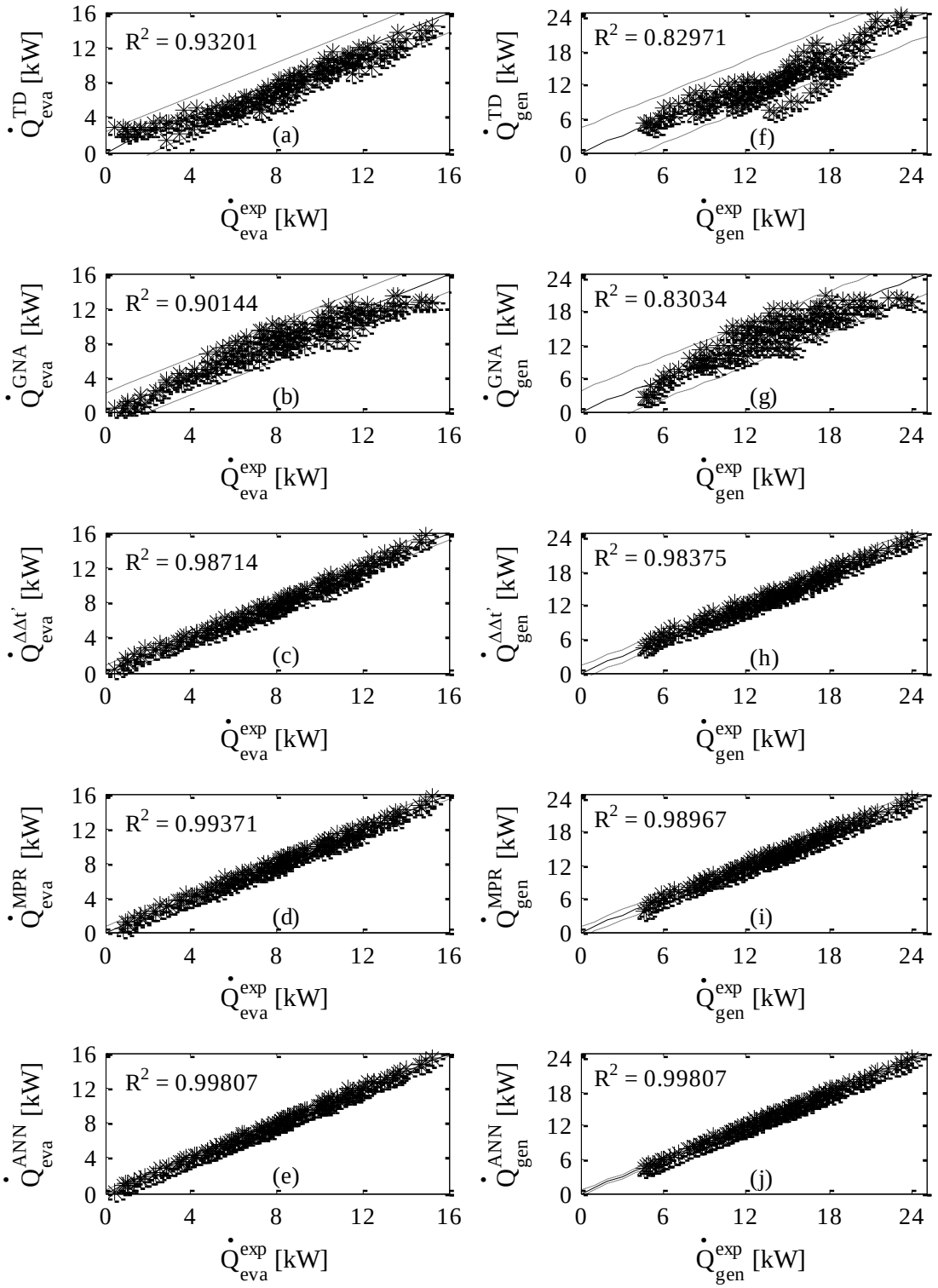

Figure 5.10 Comparison between the measured and predicted evaporator and generator loads-Pink

The CV indicator can be used for better visualization of the predicting capabilities using different modelling approaches. Coefficient of variation of the root

mean square error is a normalized measure of dispersion of probability distribution. CV is defined as RMSE divided by dependant variable mean (5.56).

$$CV = \frac{RMSE}{\bar{y}_i} \cdot 100\ [\%] \tag{5.56}$$

The CV values for five different modelling methods in the case of Pink absorption chiller are illustrated in Figure 5.11. If we assume that around 10% deviation of CV is acceptable to get a satisfactory prediction, it is clear that the developed TD and GNA models cannot pass this threshold. On the other hand, the calculated CV values of ΔΔt', MPR and ANN are lower than 5% which is more than satisfactory. Again, the ANN method obtained the best CV indicators (<2%).

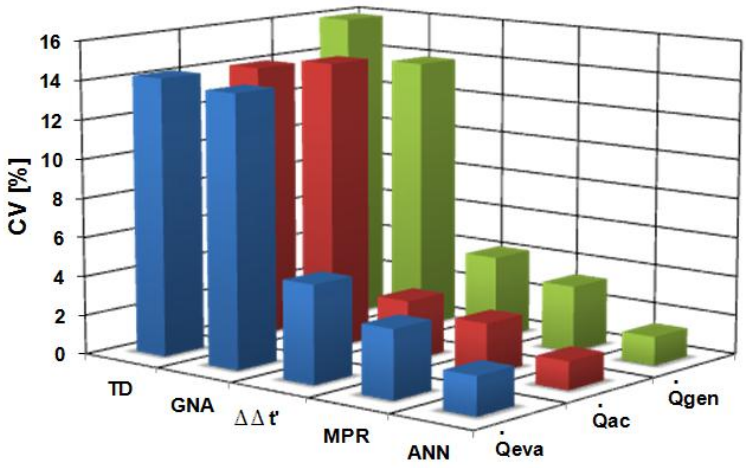

Figure 5.11 CV values-Pink

To give a better view of goodness of fit, three additional parameters were also included in analysis. Maximum residual and minimum residual might be useful to see the range of the differences while the mean absolute difference shows the overall magnitude of the differences between predictions and simulations (5.57).

$$|\bar{\epsilon}| = \frac{1}{N}\sum_{i=1}^{N}|\epsilon_i| \tag{5.57}$$

Table 5.9 and Table 5.10 show the summary of all the statistical indicators of the models after applying different modelling methods on two absorption chillers.

Table 5.9 Statistical indicators-Rotartica

Parameter	Load	TD	GNA	ΔΔt'	MPR	ANN
R^2	$\dot{Q}_{eva}$	0.9102	0.8975	0.9496	0.9836	0.9992
	$\dot{Q}_{ac}$	0.9767	0.8028	0.9893	0.9947	0.9971
	$\dot{Q}_{gen}$	0.9693	0.6743	0.9756	0.997	0.9984
RMSE	$\dot{Q}_{eva}$	1.1041	0.7417	0.5202	0.297	0.0645
	$\dot{Q}_{ac}$	1.6016	1.8644	0.4343	0.3066	0.2265
	$\dot{Q}_{gen}$	1.3096	1.0992	0.3011	0.1049	0.0778
CV [%]	$\dot{Q}_{eva}$	24.5393	16.4839	11.562	6.6018	1.4346
	$\dot{Q}_{ac}$	13.0487	15.1901	3.5382	2.4977	1.8455
	$\dot{Q}_{gen}$	18.001	15.1101	4.1386	1.4416	1.0695
SS_{res}	$\dot{Q}_{eva}$	23.1614	10.451	5.1417	1.6763	0.0792
	$\dot{Q}_{ac}$	48.7377	66.0467	3.5833	1.7857	0.9749
	$\dot{Q}_{gen}$	32.5837	22.9583	1.7223	0.209	0.115
ϵ_{min}	$\dot{Q}_{eva}$	-2.63	-1.12	-1.48	-0.71	-0.16
	$\dot{Q}_{ac}$	-3.05	-2.37	-1.49	-0.75	-0.10
	$\dot{Q}_{gen}$	-2.35	-1.67	-0.45	-0.24	-0.16
ϵ_{max}	$\dot{Q}_{eva}$	0.23	1.70	0.60	0.55	0.12
	$\dot{Q}_{ac}$	-0.30	4.52	0.76	0.35	0.52
	$\dot{Q}_{gen}$	0.16	2.57	0.68	0.18	0.23
$\lvert\bar{\epsilon}\rvert$	$\dot{Q}_{eva}$	0.84	0.55	0.38	0.23	0.04
	$\dot{Q}_{ac}$	1.46	1.42	0.27	0.27	0.18
	$\dot{Q}_{gen}$	1.17	0.85	0.24	0.08	0.05

Table 5.10 Statistical indicators-Pink

Parameter	Load	TD	GNA	ΔΔt'	MPR	ANN
R^2	$\dot{Q}_{eva}$	0.932	0.9014	0.9871	0.9937	0.9981
	$\dot{Q}_{ac}$	0.9075	0.8547	0.993	0.9949	0.9985
	$\dot{Q}_{gen}$	0.8297	0.8303	0.9838	0.9897	0.9981
RMSE	$\dot{Q}_{eva}$	1.138	1.1128	0.4002	0.2799	0.1569
	$\dot{Q}_{ac}$	3.2085	3.3503	0.7007	0.5973	0.3285
	$\dot{Q}_{gen}$	2.2028	1.9311	0.5888	0.4669	0.2021
CV [%]	$\dot{Q}_{eva}$	14.1775	13.8627	4.9853	3.4873	1.9543
	$\dot{Q}_{ac}$	14.0231	14.6427	3.0625	2.6105	1.4357
	$\dot{Q}_{gen}$	15.9372	13.971	4.2597	3.3777	1.4622
$SS_{res}[10^3]$	$\dot{Q}_{eva}$	0.1787	0.1709	0.0221	0.0108	0.0034
	$\dot{Q}_{ac}$	1.4207	1.549	0.0678	0.0492	0.0149
	$\dot{Q}_{gen}$	0.6697	0.5146	0.0478	0.0301	0.0056
ϵ_{min}	$\dot{Q}_{eva}$	-2.39	-2.20	-0.94	-0.66	-0.50
	$\dot{Q}_{ac}$	-2.31	-5.49	-1.84	-1.59	-0.77
	$\dot{Q}_{gen}$	-2.47	-4.35	-1.52	-0.99	-0.78
ϵ_{max}	$\dot{Q}_{eva}$	2.63	3.05	0.98	0.76	0.39
	$\dot{Q}_{ac}$	9.50	9.56	1.86	1.69	0.85
	$\dot{Q}_{gen}$	6.85	4.19	1.19	1.08	0.58
$\lvert\bar{\epsilon}\rvert$	$\dot{Q}_{eva}$	0.92	0.87	0.31	0.22	0.12
	$\dot{Q}_{ac}$	2.46	2.66	0.55	0.46	0.26
	$\dot{Q}_{gen}$	1.64	1.55	0.48	0.38	0.14

5.4.2.3. AIC_c and BIC analysis

In terms of complexity, some of the developed models are more complex than others; therefore, they have to be compared in order to select the appropriate one. On the other hand, the comparisons between the models only make sense if the best fits of the models are sensible. If all the models fit the data with sensible best fit values, next step is to compare their goodness of fit by using sum of squares. If the simpler model has lower residual sum of squares, which is not the common practice, the use of more complex models make no sense. Otherwise, further statistical analysis is necessary to select the most appropriate model. The statistical analysis usually used in the case of nested models (when one model is a simpler case of the other) is the extra sum of squares test (F-test). The comparison of non-nested models, which is our case, with F-test is not appropriate. When comparing non-nested models there are two criteria which

can be used: Akaike's Information Criterion (AIC) or Schwarz-Bayesian Information Criterion (BIC). The AIC can be termed as a measure of the goodness of fit of any estimated statistical model. The BIC is a type of model selection among a class of parametric models with different numbers of parameters. The difference between AIC and BIC is that the penalty term for the number of parameters in the model is larger in BIC than in AIC. Both criteria were applied to compare developed models. AIC_c is a second order AIC with a greater penalty for extra parameters and can be calculated by using equation 5.58:

$$AIC_c = N \cdot \ln\left(\frac{SS_{res}}{N}\right) + 2K + \frac{2K(K+1)}{N-K-1} \tag{5.58}$$

Similarly, BIC is defined by equation 5.59:

$$BIC = N \cdot \ln(SS_{res}) + K \cdot \ln(N) \tag{5.59}$$

where N is the number of data points, K is the number of the model parameters and SS_{res} is residual sum of squares. The interpretation of the results in both tests is the same: the model with lower value is more likely to be selected. AIC_c and BIC analysis results of all models developed for Pink absorption chiller are presented in Tables 5.11 and 5.12, respectively. The analysis also included TD and GNA models, although they should be discarded after goodness of fit comparison. As can be seen, both AIC_c and BIC results are in agreement with the goodness of fit results, recommending the most complex model to be adopted (ANN).

Table 5.11 AICc-Pink

Model	$\dot{Q}_{eva}$	$\dot{Q}_{ac}$	$\dot{Q}_{gen}$
TD	62.1847	348.2604	244.4674
GNA	33.5811	337.7877	185.7174
ΔΔt'	-244.477	-91.9774	-140.016
MPR	-329.679	-120.502	-188.498
ANN	-412.86	-208.874	-342.941

Table 5.12 BIC-Pink

Model	$\dot{Q}_{eva}$	$\dot{Q}_{ac}$	$\dot{Q}_{gen}$
TD	774.8	1060.9	95 .
GNA	719.3	1023.5	871.4
ΔΔt'	446.9	596.6	548.5
MPR	377.8	587	519
ANN	346.1	550.1	416

5.5. Conclusions

In this Chapter a comprehensive comparison of different methods for steady state modelling of small capacity absorption chillers was presented. Using both mechanistic and empirical approaches, the models were developed based on experimental data from our test bench and manufacturer catalogue. All the models, with exception of TD which required some additional assumptions, were based only on the measurements of external water circuits. Five different methods (TD, GNA, ΔΔt', MPR, ANN) were applied to model two commercial absorption chillers, one with small dataset (Rotartica) and other with large dataset (Pink), in order to investigate the influence of database size on the prediction of the models. The analysis showed that models developed with small dataset are not reliable and statistically correct, since small datasets are insufficient to form strong relationships within the models. On the other hand, the models created with large dataset which completely covers the operating range of the absorption chiller showed very high level of predicting capabilities. With respect to that, it is very important to emphasize the significance of comprehensive and accurate data sets in order to map properly the whole performance range. Reliable data (reconciled measurements, accurate sensors, true steady-state data, etc.) reduce the effect of random errors in data fitting. The results confirmed that TD method is more suitable for design phase of absorption equipment and not for simulation packages due to its complexity and numerous iterations which can cause problems in annual simulations. The constant UA values are not an appropriate approach, because the deviations increase significantly moving away from the nominal conditions. This is clearly visible through the poor statistical indicators such as R^2 and CV. Although the GNA neither represents all the operating range with high accuracy, it is still used in some simulation programs due to its simplicity. This is justified by a fact that on a whole year hourly simulation, these deviations will most probably equal out to a great extent. However, the results of statistical analysis indicate that more appropriate would be to use another three methods in order to obtain better accuracy. Excellent statistical indicators (R^2 around 0.99, CV lower than 5% and narrow CL) clearly show that any of the three different methods (ΔΔt', MPR and ANN) is suitable for the performance prediction of absorption systems, but also for other purposes: control and monitoring, fault detection, and optimization.

Nevertheless, the best prediction was obtained with the ANN method with R^2>0.998 and CV<2%. The comparison of the models with AIC_c and BIC statistical tests confirmed that ANN was the most suitable method to model Pink absorption chiller.

Chapter 6

Optimal control

"However beautiful the strategy, you should occasionally look at the results."
Winston Churchill

6.1. Introduction

The control of HVAC systems has been a very active area of research and development for many years. The progress of computer science and increasing availability of control devices together with the growing concern on energy and cost efficiency made that field of supervisory control become very attractive. Supervisory control, also called optimal control, is the high level control which uses the optimization techniques to find the most efficient settings for all the local controllers in terms of minimizing the overall system energy input or operating cost. There are different categories of supervisory control depending on used method. In this research, the attention was paid to the model-based supervisory control. Two main components of this control are the model and the optimization technique. The main function of the model is to predict the system performance (or cost), as well as the system response to the changes of control settings. On the other hand, the main function of the optimization technique is to seek the optimal control settings in order to make the system more efficient.

The main aim of Chapter 6 is to provide an insight of possible control strategies for absorption chillers by using optimal control. For that purpose, two control strategies were developed based on black-box models (ANN) using MatLab. Black-box models are very suitable for supervisory control due to its simplicity and lower computational costs when compared to physical models. However, they are only reliable for the operating points within the range of covered data. The first developed strategy was neural network inverse (ANNi) which allows selecting the parameters for the optimal performance of the absorption chiller in order to achieve the required cooling capacity. Second developed strategy couples ANN with Genetic Algorithms as optimization

technique to find the optimal operating conditions in order to optimize the performance of the small system with absorption chiller. In addition, the existing achievements in the field of control for absorption systems are provided to complete the image of these systems.

6.2. Control strategies for absorption systems

The control of absorption chillers can be divided into two types: internal and external. The internal control is usually determined by the manufacturer's design with the main function to maintain the internal parameters (concentrations, flow rates, pressures, temperatures) within the limits, which enable the smooth operation and prevent the risks of damage. The absorption chiller is usually part of a larger system where the changes in the external circuits affect the operation of the absorption chiller. The external control of the absorption chiller deals with the parameters of the external circuits in order to satisfy the cooling demand. This indicates a direct correlation between these two types of control. The most relevant manipulable parameters to control an absorption chiller externally are: hot medium inlet temperature and mass flow rate, cooling medium inlet temperature and mass flow rate and chilling medium outlet temperature and mass flow rate. The hot fluid inlet temperature depends on the control of the heat supply system while the outlet temperature is a result of the momentary heat flow in the generator. The cooling medium inlet temperature depends on the heat dissipation component and its performance while the outlet temperature is a result of the momentary heat flow in the absorber and condenser. The inlet temperature of the chilling medium is the parameter which depends on chilling medium distribution system and cannot be influenced. The outlet temperature of the chilling medium is the result of the cooling demand and necessary temperature for the particular application. Usually, this temperature is within certain limits to allow satisfactory operation of the chilling distribution system.

The absorption systems explained in the patents of Mann [165] and Anderson [166] had control which employed two separate temperature sensors, one to sense the temperature of the fluid entering the system and another to sense the temperature of the fluid medium after it has been chilled. The control was adapted to vary the refrigeration

capacity of the system in response to varying load conditions and not in response to changes in internal conditions in the refrigeration system itself. The disadvantage of this control was that if there was any malfunction in the refrigeration system, the control system would have resulted in maximum energy input to the refrigeration system, as an attempt to compensate the malfunction. The fuzzy logic rules for a PID controller in a control system for an absorption refrigerator were introduced by Ogawa et al. [167]. The controlled system was adapted to subject the outlet temperature of the chilling medium to fuzzy logic control adjusting the amount of heat supplied to the generator. Yeung et al. [168] described a simple control mechanism for chilled and cooling medium (water) temperatures in a solar air-conditioning system in Hong Kong. The control mechanism monitored the chilled water temperature and when it dropped below the set point, the hot water supply to the chiller was cut off. The cooling water temperature was controlled with a differential controller in on-off mode. The fan of the wet cooling tower switched on when the cooling tower sump temperature exceeded 29.5°C and switched off at temperatures below. This control strategy resulted in a fluctuating operation of the chiller with increased thermal losses due to a higher number of start-up and shut-down procedures. Li and Sumathy [66] reported on the performance of a solar powered absorption air conditioning system with a partitioned hot water storage tank. They used an active control of the hot water feed-in position into the storage tank, depending on available solar and tank temperatures. The goal of this setup was an earlier chiller start-up in the morning due to a reduced storage tank volume. The solar pump had no variable flow control and was operated only in differential on-off mode. The cooling tower was a wet cooling tower with a differential on-off controller for the fan. The storage tank was partitioned into two parts. This study showed that the total solar cooling COP could be increased by approx. 15% compared to the traditional whole-tank mode. Conventional absorption chiller control logic was embodied again in the disclosure of Jenkins [169]. A control input for the absorption chiller was the heat supply controlled by a capacity valve, which was in turn controlled by a PI controller. The controller was controlled by a non-linear function. Optimal supervisory control investigation of the equipment in a cooling plant with double effect absorption chiller was carried out by Koeppel et al. [170] in order to minimize the total operating cost. They developed a simplified strategy for cooling tower fan control for absorption

cooling plants that involves the determination of a linear relationship between a set point for cooling tower supply water temperature and ambient wet-bulb temperature. The optimization algorithm was formulated as a TRNSYS component model in which the inputs were the control variables and the objective function. The application of this simple strategy resulted in savings that were nearly identical to the optimization results. Chow et al [171] developed a control strategy for the optimal use of fuel and electricity for a direct-fired absorption chiller system. Multivariable model-based method of supervisory control was applied by coupling ANNs with genetic algorithms (ANN ability to learn complex nonlinear mapping together with the GA ability to search the global optimum). The results from this study showed that considerable amount of energy can be saved since such supervisory controller allows an overall consideration of the interactions among the systems and their controlled variables. The possibility of supervisory and optimal control strategies of HVAC systems were explained comprehensively by Wang and Ma [172].

According to Henning [13], there are two main control modes to control absorption cooling systems depending on application purpose. The first mode is a heat-guided mode characterized by a direct transformation of the available supply heat into cold. There is neither active control of the chilled fluid temperature nor cooling capacity; as long as there is sufficient heat to drive the absorption chiller, the cold is produced. There are two possible variations of this mode, with or without heat storage tank. Without a heat storage tank, only a thermal inertia of the chiller and building causes temporal delays since there is a direct link between heat supply (i.e. solar collectors) and cold supply to the building. The cold can be produced fast but without limitation of its quantity. This can lead to very low inlet temperature of chilled water, which can cause freezing of the evaporator, and to frequent transient load operations, which leads to the conclusion that this mode is not suitable for air-conditioning purposes with a steady demand of cold. The second mode is cold-guided mode, where the chilling medium temperature is set to fulfil the cooling demand. This mode requires a constant amount of heat supplied to the generator. The constant heat supply can be obtained in various ways with respect to the cooling system design and to the absorption chiller type. The chilled water temperature can be controlled by adjusting either hot or cooling water inlet temperature of the absorption chiller.

The control of large-scale absorption chillers is normally provided through the hot medium circuit. Usually, when designing a control strategy of an absorption chiller in air-conditioning applications the primary objective is to control the capacity by maintaining the temperature of the chilling fluid leaving the evaporator. The internal control system compares the temperature of the leaving fluid to the set point and adjusts the amount of solution supplied to the generator by adjusting heat input to the generator. The combination of solution temperature and concentration determines the temperature at which the refrigerant vaporizes in the evaporator. Varying the temperature at which the refrigerant boils in the evaporator changes the capacity of the absorption chiller. Thus, in order to control the capacity of the chiller to meet the ever-changing system loads, either the solution temperature or the solution concentration must be varied. A common method to vary the temperature of the solution is to vary the amount of absorbent solution delivered to generator. The most common ways are to use throttling valve or a bypass valve. More expensive way is to use adjustable frequency drive to vary speed of the generator pump motor, thus reducing the flow of the solution to the generator. In order to vary the solution concentration, absorption chillers vary the heat input to the generator. Nowadays, almost all large-scale absorption chillers are equipped with a microprocessor-based control panel that monitors and controls all operations of the machine [173-175]**.** The common way to control large capacity absorption chillers is through the modulating energy valve. In response of outlet chilled water temperature, the valve close, which reduces the heat input to the generator. There are two variation of this control, depending on manufacturer's design. The first variation can be seen, for instance, at YORK steam and hot water chillers which are equipped with control valves capable of modulating steam or hot-water flow continuously from 10-100%. The second variation is when hot water control valve adjusts the hot water inlet temperature in order to maintain chilled water temperature [175]. Using the energy valve as sole method of control would cause the slow response of the chiller to a capacity change. By varying the solution flow rate, especially with the use of adjustable frequency drives, recent chiller designs are now able to react much faster to ever-changing load and cooling water conditions. Similarly, in direct-fired absorption chillers the amount of heat input to the generator is varied by modulating the capacity of the burner. Between 30 and 100

percent of cooling capacity the burner firing rate is adjusted to meet the cooling load. Below 30 percent the burner is cycled [176].

The temperature of the cooling water (cooling tower circuit) also has a significant impact on the operation of absorption chillers. In order to provide stable control of the cooling water temperature, a cooling tower bypass is typically recommended. In some new chillers and control designs, variable speed drives are used to vary the flow of the solution, allowing the chiller to maintain tight control in situations where the cooling water temperature may be highly variable. However, modulating control kit increases the installation cost of the chiller and that is the main reason why large number of installed chillers operate only with simple ON-OFF control strategy. A study of Perez de Vinaspre et al. [177] gives an example of ON-OFF control strategy for direct-fired double effect absorption chiller (Yazaki). The signal from the thermostat starts the burner and the chiller operates until it reaches the target impulsion temperature of 7ºC. After reaching that point, the operation stops and starts again when the return temperature of the primary circuit is above the target temperature (10ºC) due to an increase of the building thermal load. However, due to the low demand for air-conditioning of the building with respect to the chilling capacity of the absorption chiller, the on/off cycles were frequent and short. The average chilling capacity was 63% of nominal value and 59% of scheduled time the chiller was on standby. These facts point out the significance of absorption chiller sizing in ON-OFF control strategy.

In contrast to large-scale absorption chillers, which have been present at the market for a long time, the interest for small-scale absorption chillers has been found recently. With only a few commercial units and with small number of expert groups working in this research field, the control issues are still in the phase of development. The usual control for small capacity absorption chillers is ON-OFF operation [178, 179]. The main problem for this type of the control is thermal inertia. When the chiller is turned off it cools down and if the following ON period is delayed by the thermal inertia the negative effect is visible in large reduction of COP. Two other possible control strategies were considered by the same author. The first strategy used the hot water inlet temperature to modulate the capacity of the chiller. This allowed the modulation of more than 50% of the chilling capacity. The second control strategy was

to actuate on hot water flow rate. A lower rate of the generator raised the temperature difference between the inlet and outlet of the generator with an overall lower mean temperature. The effect on the whole was less pronounced than in the first strategy, but it had the advantage of fully using the available temperature level without an inefficient mixing to produce lower temperatures. Finally, Lazzarin considered the option to use both strategies. However, the results showed that the penalisation was unavoidable whenever the machine is modulated to meet directly the cooling demand.

The catalogues of the commercial units [180-182] show that most of small capacity absorption chillers are controlled either by simple ON-OFF cycling or by modulating valve in the hot water circuit. It is also possible to modulate flow rates of hot and cooling medium circuits but this option is limited for some chillers [181] due to very narrow range of the flow rates permitted by manufacturer design. If the flow rates limits are exceeded, the internal control normally turns off the chiller to prevent any damage. Once when absorption chiller is started, it will operate automatically and remain in operation as long as there is a cooling demand. The hot water circuit pump or bypass valve is cycled ON and OFF to control the flow or temperature of the heat medium through the generator in response to the chilled water temperature. When the chilled water temperature reaches the required level, the solution dilutes and the pump in the chilled water circuit stops. The temperature than starts to rise and when it reaches the differential temperature parameter added to the set point the chiller turns on again. The set points of manipulable heat medium temperatures are adjustable only in ranges prescribed by manufacturer.

The facts exposed above indicate that small capacity chillers are in general installed to work at full load operation in order to have higher efficiency. On the other hand, this reveals the fact that the simple control of the absorption chiller is not enough. The design of whole system together with control strategy of all the system components is crucial in order to obtain efficiency comparable to the conventional systems. The design and control strategy in a cooling system with various components (cold and hot storage tanks, solar circuit, back up heater, cooling tower or air condenser and terminal units) should be conducted carefully in order to be cost-effective and efficient. The control of a cooling system can be done in various ways, depending on application and

purpose. Therefore, all aspects relevant for the optimum system performance should be considered. The following literature references describe previous and contemporary research on small scale absorption chillers control strategies.

If the absorption chiller is a part of solar assisted air conditioning system, automation and control become more complex. In order to be competitive with conventional systems, the electricity savings in solar systems must be sufficient to justify the cost of the overall system. In that term the use of solar energy gathered by solar collectors has to be maximized. The usage of solar collectors invokes another issue: energy storage to extend operational hours of the system. Melendez-Gonzalez et al. [183] in their patent described in detail several control strategies for solar assisted air conditioning systems. Different aspects were included in this disclosure: if there is enough solar radiation and when to turn on a back-up boiler, the control sequence for different components, use of energy storage tank, use of air cooler instead of cooling tower for small capacity chillers, complete automation of the system. Storenkamer et al. [184] used TRNSYS environment to develop a control strategy for a 10kW absorption chiller in the solar cooling system of an office building in Berlin, Germany. The control strategy of the system was a combination of an on-off- and P-control in the solar and storage loop and a PI-control for the external heat mediums of the chiller. Two continuously variable three-port mixing valves controlled the supply temperature of hot and cooling water of the chiller, thereby providing the necessary control of the chilling capacity. The generator circuit pump switched on when the top temperature of the hot storage tank exceeded the set point for the minimum operating temperature of the chiller and switched off when the top temperature of the storage fell below 65°C. The outlet temperature of chilled water which fed the chilled ceiling panels was supplied at 15°C by controlling the three-port mixing valve in the generator circuit. Performance control of the chiller could also be reached via a combination of mass flow and temperature control of the external heat mediums but was limited due to reduced overall heat transfer coefficients of the chiller at lower flow speeds. The TRNSYS type for absorption chiller was developed by using the characteristic equations for absorption chillers as described by Ziegler et al. [185]. Lazzarin in his paper [186] analyzed characteristics arrangements of solar cooling plants. The paper emphasizes the importance of well sized storage system with hot and cold section in order to optimise

solar collector performance, reducing the installed chiller capacity which is an expensive item in the overall plant cost. The author concluded that it is possible to modulate well capacity control of the absorption chiller by the hot medium manipulable parameters (inlet temperature and flow rate) if the hot and cold storage are well designed and controlled by their own circuits. Kolenbach [187] in his PhD thesis described three control strategies using the mass flow rate in the hot water (solar) circuit of a solar cooling system: differential on/off, radiation-based and temperature-difference-based strategies. Usually, the mass flow rate of the heat transfer medium in the solar circuit is the controlled variable and the outlet temperature of the solar field is the measured variable. From most of the studies it can be concluded that a differential on/off operation of the main external circuit pumps should be avoided. Although such a control is simple to install and to operate, the system performance decreases due to frequent on/off operation of the chiller and therefore cannot be justified only with the simplicity. The conclusion which can be drawn is that a mass flow and/or temperature control should be installed in the external circuits. When talking about the control of the cooling water temperature, Kohlenbach gave an overview on control possibilities (Figure 6.1). In configuration (1), the cooling water inlet temperature into the chiller is controlled via the speed of the cooling tower fan using a frequency inverter while the cooling water mass flow rate is kept constant; in configuration (2), the cooling water inlet temperature into the chiller is controlled via a three-port valve that mixes warm return water from the chiller with cold feed water from the cooling tower; and in configuration (3), the cooling water inlet temperature into the chiller is controlled via the pump speed of the cooling water pump using a frequency inverter while the cooling tower fan speed is kept constant.

If the purpose of a solar cooling system is to provide a defined chilling capacity at preferably low electrical energy consumption, then the cooling water temperature set point should be kept as high as possible. Otherwise, if the purpose of a solar cooling system is to provide maximum chilling capacity and if the electrical power consumption is of secondary importance, then the cooling water temperature set point should be kept as low as possible.

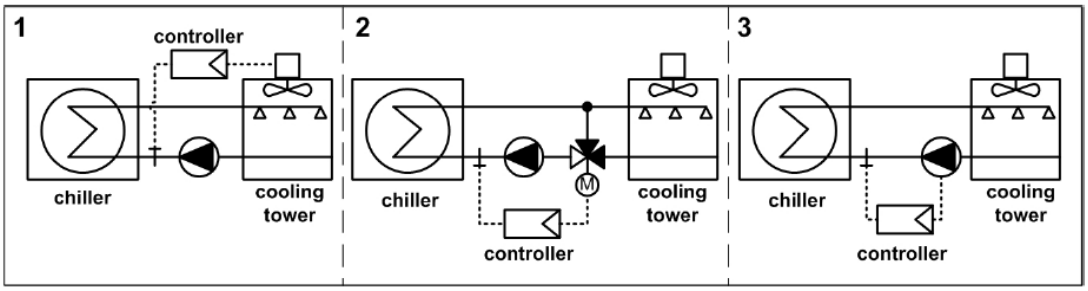

Figure 6.1 Control strategies for cooling water circuit

The chilled water temperature of an absorption chiller can be controlled by using different strategies. The most common strategy is the control of the hot water inlet temperature during chiller's operation with constant cooling water inlet temperature as shown in Figure 6.2. A three-port valve is used to mix the cold return flow from the generator with the supply flow of temperature from the hot water source. The valve recirculation is controlled in such a way that the hot water temperature entering the chiller in combination with inlet temperatures of cooling water and chilled water results in the desired chilled water outlet temperature. At constant cooling and chilled water input temperatures, the reduction of the external heat input into the generator results in a decrease of vapour mass flow to the condenser and thus a lower concentration of the solution leaving the generator. The lower solution concentration reduces the capacity of the absorber and less vapour mass flow can be absorbed. This results in decrement of the evaporator heat flow and a rise of chilled water outlet temperature.

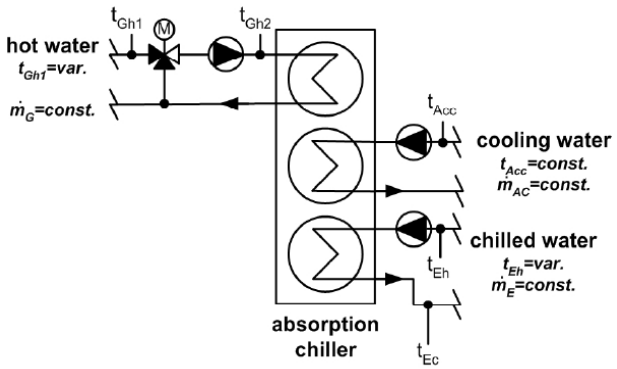

Figure 6.2 Control through the hot water circuit

A second possibility is the control of the cooling water inlet temperature during chiller operation with constant hot water inlet temperature as shown in Figure 6.3. A

three-port valve is used to mix the warm return flow from the condenser with the cold supply flow of temperature from the cooling water source. The valve recirculation is controlled in such way that the cooling water temperature entering the chiller in combination with inlet temperatures of hot water and chilled water results in the desired chilled water outlet temperature. For constant hot and chilled water inlet temperatures as well as mass flows, an increase in cooling water temperature decreases the absorber capacity; therefore less water vapour can be evaporated in the evaporator. The heat flow decreases and the chilled water outlet temperature increases.

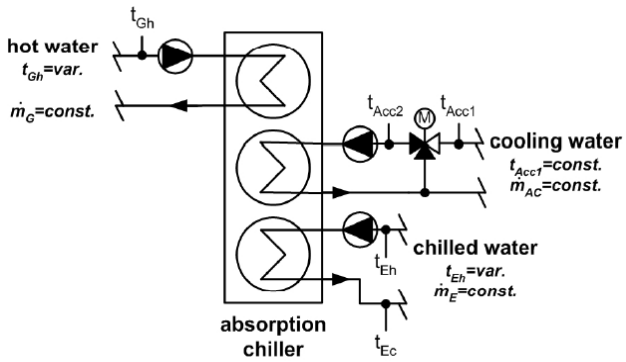

Figure 6.3 Control through the cooling water circuit

A combination of both hot and cooling water based strategies can also be used. If the hot water inlet temperature is not sufficient for a given chilling load, the cooling water temperature can be lowered in order to reach the desired chilled water temperature. The optimum combination of hot and cooling water control depends on the user-specified conditions.

Clauß et al. [188] presented the strategy based on the characteristic equation model which determines the required cooling water temperature. If the hot water temperature is not high enough for a given chilling load, cooling water temperature is lowered and vice versa, when the driving temperature is high cooling water temperature is increased. In the parametric study of Kuhn et al. [189] TRNSYS simulations were carried out in order to compare control strategies for the absorption chiller. Conventional control by hot water adjustment was compared with a new control method by cooling water adjustment. In conventional control, the system controls chilling capacity within the set point plus the deadband by sensing the outlet chilled water and

regulating the hot water control valve via a mechanically linked actuator motor. Cooling water adjustment was done by using the characteristic equation model to find a governing temperature of inlet cooling water for PID controller. The results showed that the new strategy provides stable chilled water outlet temperature and also decreases parasitic electricity consumption of auxiliary equipment with respect to the conventional strategy. Characteristic equation was used again by Albers et al. [190] as a tool for improving part load behaviour of 35kW commercial absorption chiller. The information which is coded in the characteristic temperature function allows replacing a change in driving temperature against the change in cooling water temperature. This gives rise to the possibility to optimize the electricity consumption of the cooling tower fans and pumps against the temperature of the driving heat which will in turn influence the collector efficiency. This control strategy requires the combined control of generator and cooling water circuit, which is not common practice. Pietrushka et al. [191] analysed seven cases with different control options for a 15kW H_2O-LiBr absorption chiller system. The results of a simulation showed that a fan speed control of the cooling tower ventilator as well as a ΔT-control of the cold distribution system are essential to obtain a high electrical COP of the system. The best overall efficiency was obtained when the generator temperature was allowed to vary between 70°C and 90(95)°C at the lowest possible set point for the absorber inlet temperature. Zetzsche et al. [192] in their study involved ice storage in a solar plant with 10kW absorption chiller. On the building side, the control parameter was the inlet water temperature into the rooms followed by sensor for relative humidity. When the dew point was reached, the sensor provided a signal to the controller and the flow through the chilled ceiling of this particular room stopped. On the solar plant side, absorption chiller was directly fed from solar collectors without any control. Consequently, the chiller started to operate when the minimum required hot water inlet temperature was available. The evaporation in the generator started when a certain temperature level was reached. If the required temperature level was not available, the outlet temperature of the generator was almost equal to the inlet temperature. A stored program control unit controlled the chiller. This control unit switched all pumps and the dry cooling tower on and off while the internal valves were regulated in such a way that COP was always at maximum.

The examples exposed above show that absorption chillers can be controlled in various ways. The main problem which impedes direct control of the absorption chillers is thermal inertia, the capability of the absorption cycle to store the energy. This is more expressed in the case of large capacity absorption chillers due to their size and large heat exchangers. The control in this case is through hot medium circuit by modulating the capacity of the burner or by modulating valve with respect to chilled water outlet temperature. The control prevents chiller to shut down and to avoid delay which would cause new start of the same. Otherwise, chiller would be working with simple ON-OFF cycling control which would decrease the overall performance as seen in the case study of Perez de Vinaspre et al. [177]. On the other hand, in the case of small capacity absorption chillers, small size and the possibility of using compact heat exchangers significantly reduce the solution charge and consequently the effect of thermal inertia. The response of these chillers to changes of external circuits inlet conditions is much faster in comparison with large capacity chillers. Some studies and experience in work with small capacity absorption chillers can confirm that their response can be very fast (especially units up to 15kW capacities). The control of these chillers can also be performed in several ways as seen above, but the results of various studies, as well as best practice, recommend four possible strategies. The first is conventional method by adjusting the hot water inlet temperature in order to control the outlet chilled water temperature. The second method is to control the inlet cooling water temperature to maintain the chilled water set temperature at required part load operation when hot water temperature is constant. The adjustment can be done by using the frequency inverter or three port valve, depending on heat dissipation component (cooling tower, dry cooler). The third and maybe the optimum method is a combination of both hot and cooling water based strategies. However, user-defined conditions determine the optimum combination of hot and cooling water control. The control of the absorption chillers by adjusting flow rates is not recommendable whereas the modulation of the cooling capacity is too small due to narrow ranges which come with manufacturer's design. The realization of any of the three control strategies requires a controller for maintaining the set temperature. In a practical application, the correct parameters of such a controller have to be identified for stable system operation. This requires a proper model of the chiller which will be implemented in the controller through the

transfer function. A whole system design and sizing is another important parameter beside the absorption chiller control strategy, in order to be high efficient and therefore cost competitive. Nevertheless, special care has to be given to the electrical consumption of the parasitic equipment (pumps and fans). Sometimes, when cooling demand is very low and absorption chiller works at lower part loads, electrical consumption of these devices may decrease electrical COP significantly. In that case ON-OFF control is the correct choice in order to increase the overall efficiency.

6.3. Artificial Neural Network Inverse (ANNi)

The main idea of ANNi methodology is to use the neural network model by coupling it with the optimization algorithm to find the optimal input values for the required output. Therefore, ANNi can be considered as model-based method of supervisory control, in which the values of the manipulable parameters are obtained by solving an on-line optimization problem to obtain the required output [193, 194]. The term inverse indicates that the direction of the ANN/optimization algorithm combination is opposite: from required output to the optimized parameters. Since the model was developed with constant flow rates and the chilled water output temperature almost always has a fixed value in air-conditioning (fan-coils, chilled ceilings), the controlling parameters should be the other two external temperatures (the generator inlet temperature and the absorber/condenser inlet temperature) because they have the greatest influence on the chiller performance. Chilling capacity was chosen as the required output. As will be shown in continuation, the very low percentage of error and short computing time make this methodology suitable for the on-line control of absorption cooling systems.

6.3.1. ANN model

The ANN model of Pink absorption chiller developed in Chapter 5 for $\dot{Q}_{eva}$ as function of three input parameters ($T_{eva}^{out}, T_{ac}^{in}, T_{gen}^{in}$) was used to demonstrate the feasibility of ANNi to be used as control strategy. $\dot{Q}_{eva}$ was defined by equation 6.1:

$$\dot{Q}_{eva} = \sum_{1}^{J}\left[LW_{(1,J)}\left(\frac{2}{1+\exp\left(-2\left(\sum_{1}^{R} IW_{(J,R)} I_R + b_{1_{(J)}}\right)\right)} - 1\right)\right] + b_2 \quad (6.1)$$

where I_R represents the three input temperatures and the values for ANN coefficients can be found in Table 5.8.

6.3.2. Optimal performance using ANNi

A step-by-step procedure for ANNi development is described below in order to avoid any ambiguity. Starting from equation 5.49, the function can be transformed:

$$\dot{Q}_{eva} = b_2 - \sum_{1}^{J} LW_{(1,J)} + \sum_{1}^{J}\left[\frac{2LW_{(1,J)}}{1+e^{\left(-2\left(\sum_{1}^{R} IW_{(J,R)}\cdot I_R + b_{1_{(J)}}\right)\right)}}\right] \quad (6.2)$$

The next step is to select the input(s) $I_{(R=x)}$ to be estimated for the required output (6.3):

$$\dot{Q}_{eva} = b_2 - \sum_{1}^{J} LW_{(1,J)} + \sum_{1}^{J}\left[\frac{2LW_{(1,J)}}{1+e^{\left(-2\left(IW_{(J,x)}\cdot I_x + \sum_{1}^{R} IW_{(J,R\neq x)}\cdot I_{(R\neq x)} + b_{1_{(J)}}\right)\right)}}\right] \quad (6.3)$$

Finally, the objective function which has to be minimized to zero to find the optimal input parameter(s) $I_{(R=x)}$ has the form (6.4):

$$f(I_x) = b_2 - \sum_{1}^{J} LW_{(1,J)} - \dot{Q}_{eva} + \sum_{1}^{J}\left[\frac{2LW_{(1,J)}}{1+e^{\left(-2\left(IW_{(J,x)}\cdot I_x + \sum_{1}^{R} IW_{(J,R\neq x)}\cdot I_{(R\neq x)} + b_{1_{(J)}}\right)\right)}}\right] \quad (6.4)$$

The input parameter(s) can be optimised on-line by using the Nelder-Mead simplex algorithm for unconstrained optimization of non-linear functions [195]. The Nelder-Mead method attempts to minimize a multivariable objective nonlinear function using only function values, without any derivative information ($f:R^n \rightarrow R$). It is, therefore, one of the general classes of direct search methods that do not use numerical or analytic gradients. In addition to that, the term artificial neural network inverse can be misleading sometimes, indicating that required output is back propagated through the network, which is not the case; here the simplex algorithm tries to find the correct input

values of the ANN model based on the required output. However, the term ANNi was adopted since several authors have used this terminology in their works [193, 196, 197].

Table 6.1 Operating ranges

Input parameter	Operating range [°C]
T_{eva}^{out}	[4.98-12.1]
T_{ac}^{in}	[26.95-35.01]
T_{gen}^{in}	[79.9-100.12]

Two different cases were studied to show the applicability of the ANNi method. The desired output or function to be optimised in both cases is the chilling capacity while the number of optimal operating parameters to be calculated differs. It was also necessary to consider the constraints to obtain the input(s) parameter(s): the input values must be within the operation range given by Table 6.1 and they must obey the optimal criterion defined by Equation (6.5). Case I considered the ANNi control with only one manipulable input variable which was calculated in order to obtain the desired chilling capacity (Figure 6.4) while Case II employed ANNi to find two manipulable input variables for the required chilling capacity (Figure 6.5). Simulation outcomes were then compared with experimental data in order to check the accuracy of the ANNi method. The error was calculated according to equation 6.5:

$$\text{error} = 100 \cdot \frac{\left|\dot{Q}_{eva}^{exp} - \dot{Q}_{eva}^{sim}\right|}{\dot{Q}_{eva}^{exp}} \ [\%] \tag{6.5}$$

6.3.2.1. Case I

In this case, the unknown parameter (manipulable variable) was the generator inlet temperature. The control system used ANNi to estimate this parameter in order to obtain required chilling capacity. Figure 6.4 shows a possible strategy for implementing the ANNi method in on-line control of the absorption chiller.

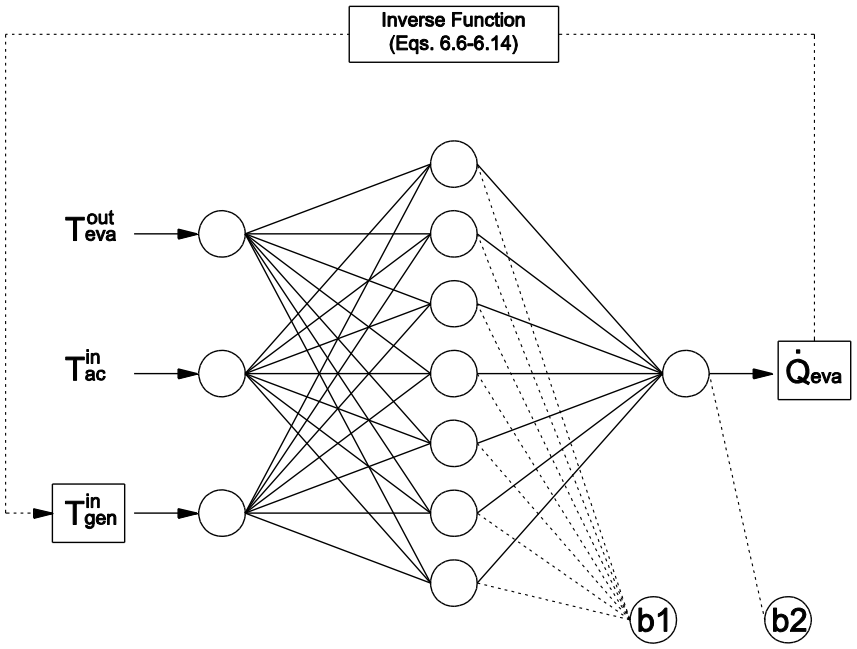

Figure 6.4 ANNi - Case I

Equation 6.4 for Case I with one unknown parameter took the following form (6.6):

$$f\left(T_{gen}^{in}\right) = C_0 + \frac{2LW_{(1,1)}}{1+e^{(C_1+80.45T_{gen}^{in})}} + \frac{2LW_{(1,2)}}{1+e^{(C_2+303.64T_{gen}^{in})}} + \frac{2LW_{(1,3)}}{1+e^{(C_3+2.03T_{gen}^{in})}} + \frac{2LW_{(1,4)}}{1+e^{(C_4-15.8T_{gen}^{in})}} + \frac{2LW_{(1,5)}}{1+e^{(C_5+55.65T_{gen}^{in})}} + \frac{2LW_{(1,6)}}{1+e^{(C_6-6.18T_{gen}^{in})}} + \frac{2LW_{(1,7)}}{1+e^{(C_7+1.84T_{gen}^{in})}} \quad (6.6)$$

where:

$$C_0 = b_2 - LW_{(1,1)} - LW_{(1,2)} - LW_{(1,3)} - LW_{(1,4)} - LW_{(1,5)} - LW_{(1,6)} - LW_{(1,7)} - \dot{Q}_{eva} \quad (6.7)$$

$$C_1 = -2(IW_{(1,1)}T_{eva}^{out} - IW_{(1,2)}T_{ac}^{in} + b_{1_{(1,1)}}) \quad (6.8)$$

$$C_2 = -2(IW_{(2,1)}T_{eva}^{out} - IW_{(2,2)}T_{ac}^{in} + b1_{(2,1)}) \quad (6.9)$$

$$C_3 = -2(IW_{(3,1)}T_{eva}^{out} - IW_{(3,2)}T_{ac}^{in} + b1_{(3,1)}) \quad (6.10)$$

$$C_4 = -2(IW_{(4,1)}T_{eva}^{out} - IW_{(4,2)}T_{ac}^{in} + b1_{(4,1)}) \quad (6.11)$$

$$C_5 = -2(IW_{(5,1)}T_{eva}^{out} - IW_{(5,2)}T_{ac}^{in} + b1_{(5,1)}) \quad (6.12)$$

$$C_6 = -2(IW_{(6,1)}T_{eva}^{out} - IW_{(6,2)}T_{ac}^{in} + b1_{(6,1)}) \quad (6.13)$$

$$C_7 = -2(IW_{(7,1)}T_{eva}^{out} - IW_{(7,2)}T_{ac}^{in} + b1_{(7,1)}) \quad (6.14)$$

In order to test ANNi strategy, the experimental data were used to find the correct values for the generator inlet temperature. Then, with these data, the chilling capacity obtained with neural network inverse method ($\dot{Q}_{eva}^{ANNi}$) was compared with the chilling capacity obtained in the experiments ($\dot{Q}_{eva}^{exp}$). Table 6.2 shows the comparison between the measured parameters and the parameters estimated by ANNi for six randomly chosen data sets.

Table 6.2 Comparison ANNi vs. experimental data - Case I

Sample	T_{eva}^{out} **[ºC]**	T_{ac}^{in} **[ºC]**	T_{gen}^{in} **[ºC]**	$\dot{Q}_{eva}^{exp}$ **[kW]**	$T_{gen}^{in,ANNi}$ **[ºC]**	$\dot{Q}_{eva}^{ANNi}$ **[kW]**	**error [%]**	t_{elap} **[s]**
1	4.98	30.00	79.99	4.07	79.99	4.07	0.04	0.63
2	10.06	33.01	80.00	4.27	80.00	4.22	1.18	0.62
3	9.01	27.04	84.99	10.84	84.99	10.87	0.31	0.64
4	7.00	27.00	90.04	11.17	90.04	11.09	0.75	0.49
5	10.02	27.05	95.02	14.69	95.02	14.67	0.11	0.53
6	7.99	35.00	100.02	8.37	100.02	8.44	0.86	0.61

Mathematical validation showed that the discrepancy between the model-based control and experimental data was lower than 1.2% in the worst case. This very small error in conjunction with a computing time of less than 1 second indicates that ANNi strategy can be used with a high level of confidence for the online control of the absorption system.

6.3.2.2. Case II

In Case II, the difference with respect to Case I was that ANNi was seeking two optimal parameters for required chilling capacity: the inlet temperature to absorber/condenser and the inlet temperature to the generator. In practice, this means that the performance of absorption chiller would be controlled simultaneously from two different external circuits: hot water circuit and cooling water circuit. Figure 6.5 illustrates the ANNi strategy to obtain required chilling capacity with two parameters estimated by Nealder-Mead simplex algorithm.

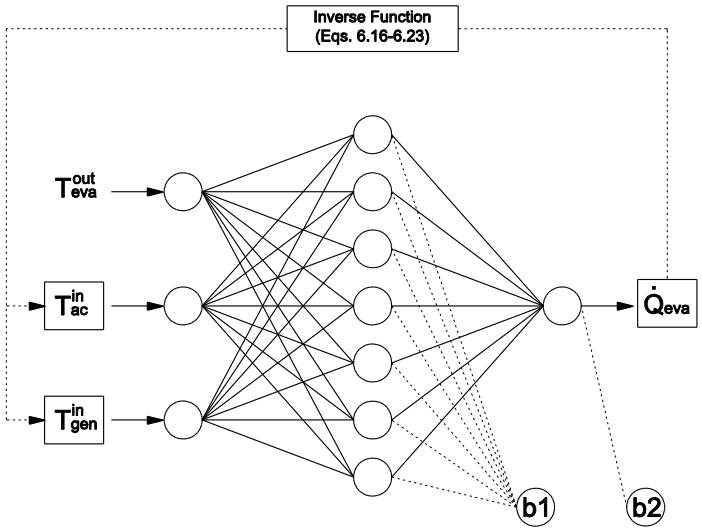

Figure 6.5 ANNi - Case II

Equation 6.4 for Case II with two parameters was slightly modified (6.15):

$$f\left(T_{ac}^{in}, T_{gen}^{in}\right) = C_0 + \frac{2LW_{(1,1)}}{1+e^{(C_1+52.48T_{ac}^{in}+80.45T_{gen}^{in})}} + \frac{2LW_{(1,2)}}{1+e^{(C_2+75.76T_{ac}^{in}+303.64T_{gen}^{in})}} + \frac{2LW_{(1,3)}}{1+e^{(C_3+2.13T_{ac}^{in}+2.03T_{gen}^{in})}} + \frac{2LW_{(1,4)}}{1+e^{(C_4-4.57T_{ac}^{in}-15.8T_{gen}^{in})}} + \frac{2LW_{(1,5)}}{1+e^{(C_5+29.91T_{ac}^{in}+55.65T_{gen}^{in})}} + \frac{2LW_{(1,6)}}{1+e^{(C_6+6.98T_{ac}^{in}-6.18T_{gen}^{in})}} + \frac{2LW_{(1,7)}}{1+e^{(C_7-2.88T_{ac}^{in}+1.84T_{gen}^{in})}} \quad (6.15)$$

Where the coefficients (C_0-C_7) were estimated using the equations (6.16)-(6.23).

$$C_0 = b_2 - LW_{(1,1)} - LW_{(1,2)} - LW_{(1,3)} - LW_{(1,4)} - LW_{(1,5)} - LW_{(1,6)} - LW_{(1,7)} - \dot{Q}_{eva} \quad (6.16)$$

$$C_1 = -2(IW_{(1,1)} T_{eva}^{out} + b1_{(1,1)}) \quad (6.17)$$

$$C_2 = -2(IW_{(2,1)} T_{eva}^{out} + b1_{(2,1)}) \quad (6.18)$$

$$C_3 = -2(IW_{(3,1)} T_{eva}^{out} + b1_{(3,1)}) \quad (6.19)$$

$$C_4 = -2(IW_{(4,1)} T_{eva}^{out} + b1_{(4,1)}) \quad (6.20)$$

$$C_5 = -2(IW_{(5,1)} T_{eva}^{out} + b1_{(5,1)}) \quad (6.21)$$

$$C_6 = -2(IW_{(6,1)} T_{eva}^{out} + b1_{(6,1)}) \quad (6.22)$$

$$C_7 = -2(IW_{(7,1)} T_{eva}^{out} + b1_{(7,1)}) \quad (6.23)$$

The comparison between the experiments and the ANNi simulation for Case II are presented in Table 6.3. Again, the validation of the inverse neural network strategy showed very good agreement with the experimental results. The maximum calculated error was same as in Case I, less than 1.2% and the elapsed time for computation was less than 1.5 second.

Table 6.3 Comparison ANNi vs. experimental data – Case II

Sample	T_{eva}^{out} **[ºC]**	T_{ac}^{in} **[ºC]**	T_{gen}^{in} **[ºC]**	$\dot{Q}_{eva}^{exp}$ **[kW]**	$T_{ac}^{in,ANNi}$ **[ºC]**	$T_{gen}^{in,ANNi}$ **[ºC]**	$\dot{Q}_{eva}^{ANNi}$ **[kW]**	**error [%]**	t_{elap} **[s]**
1	4.98	30.00	79.99	4.07	30.01	80.02	4.07	0.05	0.96
2	10.06	33.01	80.00	4.27	33.01	79.99	4.22	1.16	1.17
3	9.01	27.04	84.99	10.84	27.04	84.99	10.87	0.31	0.78
4	7.00	27.00	90.04	11.17	27.00	90.05	11.09	0.75	1.22
5	10.02	27.05	95.02	14.69	27.07	95.06	14.67	0.11	1.33
6	7.99	35.00	100.02	8.37	35.00	100.03	8.44	0.86	1.25

As can be seen from both cases studied, ANNi seems to be very suitable for implementation in online control of absorption systems. Very close agreement with experimental data and short computation time confirmed that. Also, it is obvious that performance of ANNi is in direct correlation with ANN model of absorption chiller. The more accurate the ANN model is, the better will be the ANNi performance. Therefore, for precise control it is of great importance that ANN model has high statistical indicators. It is also possible to include other input parameters in ANNi control strategy, for instance, external flow rates. In that case, the use of variable speed pumps would be necessary. More information about this can be found in the paper of Labus et al. [198]. With respect to Case II, it is important to mention that sometimes is difficult to control T_{ac}^{in}, especially when absorption chiller is connected to a cooling tower, since it directly depends on ambient temperature and humidity. This problem can be solved by adding more constraints using IF THAN logic (taking care to avoid any confusion within the controller). However, the use of additional constraints depends on requirements of each particular application.

6.4. Genetic Algorithm (GA) coupled with ANN

The genetic algorithm is a method for solving both constrained and unconstrained optimization problems which was inspired by the process of natural evolution. The GA is based on the principles of the evolution via natural selection, employing a population of individuals that undergo selection in the presence of genetic operators such as mutation and crossover. The algorithm mimics the process of the evolution of populations by selecting only fit individuals for reproduction. Therefore, this algorithm belongs to the class of optimum search methods which combine the elements of direct and stochastic search methods. The working principle of GA method is the following: the algorithm continuously modifies a population of individuals and at each step selects individuals randomly from the current population to be parents and uses them to produce offspring for the next generation. Each individual represents a possible solution to a given problem. During the reproduction process, the individuals in the current generation are evaluated by a value of fitness function, which is a measure how close is the individual to the problem solution. Over successive generations, the population of individuals evolves toward an optimal solution. The three most important

aspects of using genetic algorithms are: definition of the fitness function; definition and implementation of the genetic representation; and definition and implementation of the genetic operators.

Coupling GA with ANN can be very interesting in terms of using the advantages which both methods offer, the first in the field of optimization and the latter in the field of forecasting. ANN ability to learn complex nonlinear mapping and the ability of GA to find the global optimum for any multidimensional problem, including problems in which the objective function is discontinuous, non differentiable or highly nonlinear can be used to find the solutions for absorption system control issues. Although the idea of integration GA and ANN into a supervisory control strategy is not new, there are just a few studies which tried to tackle the absorption system control problems with this strategy [171, 199]. With respect to that fact, the following example shows how this integration can be used to develop an optimal control strategy whose result will be minimized energy consumption.

6.4.1. Case study

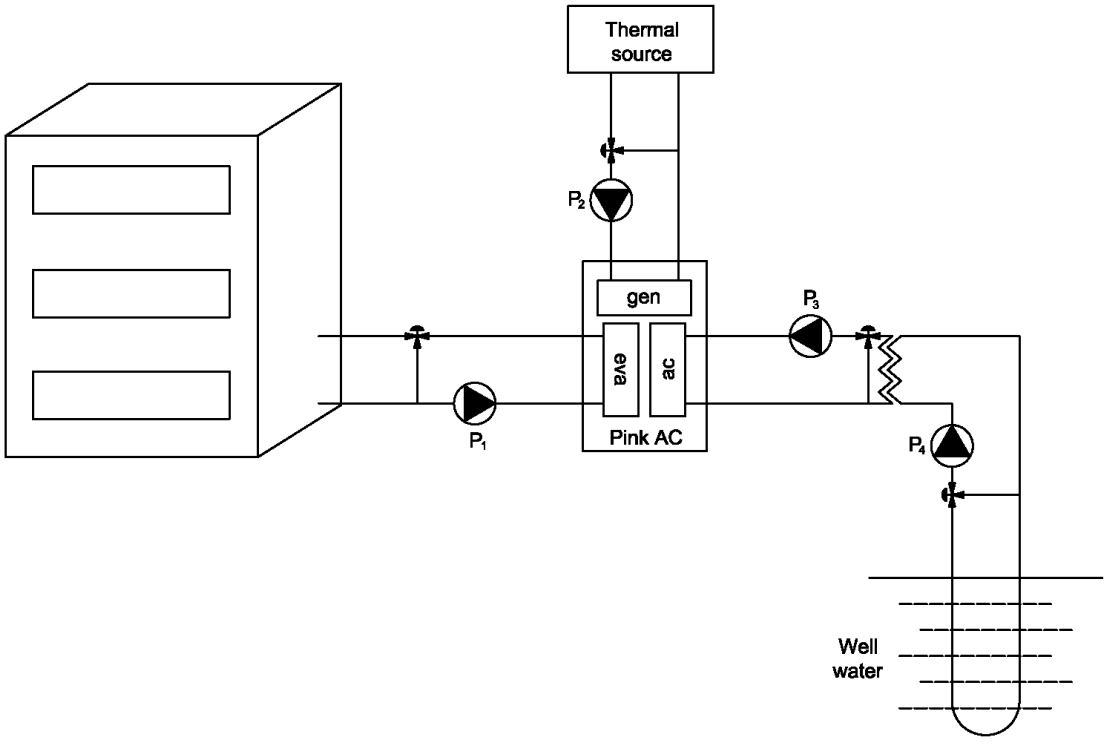

Figure 6.6 Air-conditioning system with absorption chiller

Figure 6.6 shows a simple air-conditioning system designed to test the GA/ANN control strategy. The system consists of a small retail space located in the building basement, absorption chiller, thermal source which provides driving heat for absorption chiller and heat dissipation system with well water. Several assumptions were made about the system for the sake of simplicity: thermal source can always provide necessary heat to drive absorption chiller and the required generator inlet temperature can be achieved using three port valve; the dissipation system with well water is ideal, heat from absorber and condenser is completely dissipated to the water well through heat exchanger and the required inlet temperature to absorber/condenser is controlled with three port valve; and the evaporator outlet temperature is maintained at 7ºC for the purpose of fan-coil application. Also, it was assumed that electrical consumers are only the solution pump of the absorption chiller and the pumps in the external circuits.

6.4.2. Load profile

The one-day cooling load profile was developed for testing the usability of GA/ANN control strategy to absorption chiller. The cooling load profile represents cooling requirements of small retail single-zone space. Retail space is located in the building basement having one external wall which faces west, floor on ground, while other surfaces were assumed to be adiabatic which means that there is no heat exchange through these surfaces. This assumption is reasonable since such retail spaces are quite often surrounded with flats, offices or other retail units. The retail space is 10 meters long and 7 meters depth with 3.5 meters floor-to-ceiling height. External wall has 50% fenestration area. Construction elements are set to comply with the latest Spanish national standards [200]. U-values of the ground floor, external wall and partition walls are 0.85, 1.6 and 1.9 W/m^2K respectively. Glazing is composed of two glass panes with argon-filled cavity between them and benefits from reflective coating which reduces the windows SGHC to 0.2. U-Value of the double glazed unit is 2.3 W/m^2K. Retail spaces belong to building types with clearly defined occupancy pattern. They are in use between 7am and 9pm. During cooling period, the temperature within the retail space is kept at 23°C. Internal heat gains, which can have a significant effect on their thermal behaviour and energy consumption, are relatively high, in particular internal gains from artificial lighting and equipment. Former was set to 30 W/m^2 while latter was set to 25

W/m^2. The occupant density was set to 8 m^2/person with a total heat gain of 125 W/person. In addition to internal gains, fresh air requirements were also defined. A minimum of 10 l/s per person was supplied in order to satisfy fresh air requirements. Fan-coil system was selected to maintain desired indoor conditions. The principle of operation is fairly simplified. Fan coil is composed of fan and cooling coil. Fresh air is supplied directly through fan-coil unit where it is mixed with re-circulated air before passing the cooling coil. Indoor temperature is controlled by local thermostat which varies water flow rate through cooling coil to respond to the zone demand. Chilled water is supplied from the absorption chiller at constant temperature of 7°C. In the case when there is no need for cooling, fan-coil fan is switched off.

In order to test the GA/ANN, the EnergyPlus simulation was run only for the summer design day by using Barcelona Airport weather file. The hourly profile is shown in Figure 6.7.

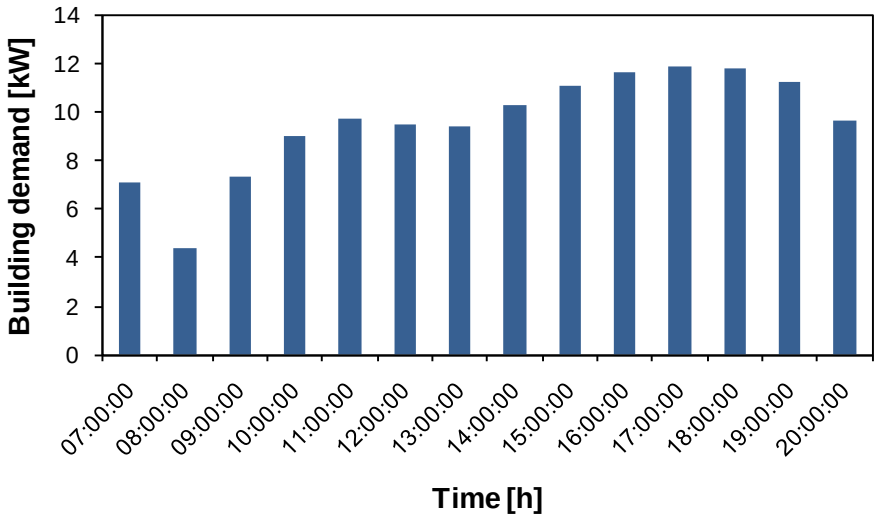

Figure 6.7 Daily profile for July 15

6.4.3. Optimal control settings

The general scheme of the linking of the optimization algorithm with ANN model is given in Figure 6.8. The optimization process starts with identification of the input variables and their constraints. Next step is to initialize the GA population of the input variables for use in optimum search. The prediction of the system outputs based

on ANN model is then evaluated through the fitness function routine. If the stopping criterion is not satisfied new population is created by performing the operations such as selection, crossover and mutation on the individuals whose fitness has measured in the last step. Selection rules select the individuals, called parents, which contribute to the population at the next generation. Crossover rules combine two parents to form children for the next generation. Mutation rules apply random changes to individual parents to form children. The process of creating new populations continues until the optimal solution is found or until the maximum number of generation is reached. The last population is called the winner which gives the optimal solution for the particular optimization problem.

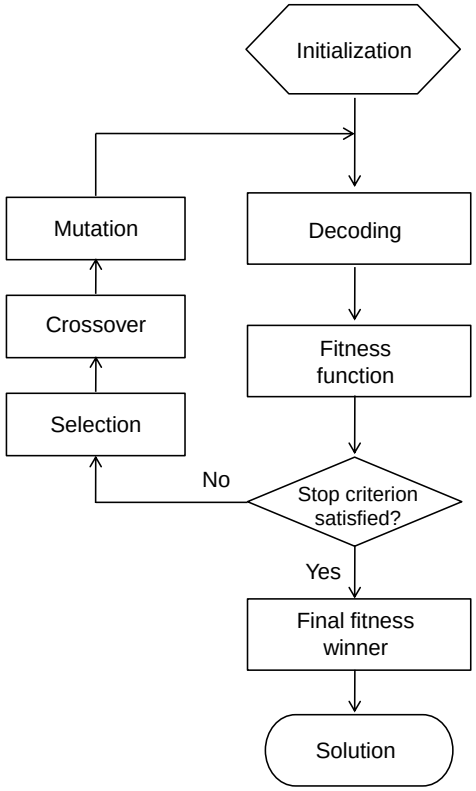

Figure 6.8 Model based optimal control with GA

In a chiller system, the fitness function is usually addressed either to energy consumption or to cost. The objective of the control problem in this test study was to minimize the primary energy consumption using the Primary Energy Ratio (PER). In this particular case, the PER of the system is defined by equation:

$$PER_{sys} = \frac{\dot{Q}_{eva}}{\frac{\dot{Q}_{gen}}{\eta_{hg}} + \frac{P_1 + P_2 + P_3 + P_4 + E}{\eta_{el}}} \tag{6.24}$$

Equation 6.24 represents our fitness function which has to be maximized in order to minimize the primary energy consumption. Since the GA algorithm searches global minimum, to find the global maximum of the fitness function (PER_{sys}) is necessary to put negative sign before. Chilling capacity ($\dot{Q}_{eva}$) and driving heat ($\dot{Q}_{gen}$) are defined by the ANN model functions of Pink absorption chiller developed in Chapter 5. The efficiency of heat generation system (η_{hg}) was supposed to be 0.91 with overall efficiency for electricity production and distribution (η_{el}) equal to 0.33. E is the electrical consumption of absorption chiller necessary for solution pump work and was approximated to 0.62kW from tests conducted in Chapter 4. P_1, P_2, P_3 and P_4 are the shaft powers of external circuit pumps with constant flow rates estimated to be 0.16kW, 0.21kW, 0.4kW and 0.7kW, respectively. These values were approximated using the EnergyPlus software default value for pump head of 300kPa, pump efficiency of 0.87 and corresponding volumetric flow rates.

The constraint values of the control parameters were directly determined by the operating range of ANN chiller model:

$$27℃ \leq T_{ac}^{in} \leq 35℃ \tag{6.25}$$

$$80℃ \leq T_{gen}^{in} \leq 100℃ \tag{6.26}$$

The evaporator outlet temperature was constrained to 7°C due to the requirements of fan coil system. The last constraint was introduced to satisfy cooling requirements of small retail single-zone space at hourly time step by defining nonlinear constraint function:

$$\text{Cooling demand} - \dot{Q}_{eva} = 0 \tag{6.27}$$

where $\dot{Q}_{eva}$ represents nonlinear ANN model function.

The genetic algorithm parameters used during the set up in MatLab GA Toolbox were the following:

- Population size (=60). This value is a trade off between the efficiency of the searching process and computing time, since lower population can terminate the search at false optima while the larger population will increase the execution time.
- Ranking scaling function was selected to convert raw fitness scores returned by the fitness function to values in a range that is suitable for the selection function.
- Roulette-Wheel method was selected as selection operator to choose parents for the next generation based on their scaled values from the fitness scaling function.
- Crossover fraction (=0.8). This parameter specifies the fraction of the crossover products in next generation. The number of individuals that are guaranteed to survive to the next generation was set to 2.
- Adaptive feasible randomly generates directions that are adaptive with respect to the last successful or unsuccessful generation. A step length is chosen along each direction so that linear constraints and bounds are satisfied.
- The selected mutation function was Adaptive feasible function. Mutation function makes small random changes of the individuals in the population and provides genetic diversity. Adaptive feasible function randomly generates directions that are adaptive with respect to the last successful or unsuccessful generation at the same time satisfying the constraints.
- Migration direction of individuals between subpopulations was forward, with migration fraction of 0.2 applied every 20 generations.

6.4.4. Results

Table 6.4 lists the results at each time step after performing GA on observed system. The optimal solutions for the required cooling demand at each time step were found in less than 20 generations. The execution time was approximately 3-4min on 4GHz PC. The obtained control temperatures are all within the constraint limits. It may

look that these temperatures, especially the absorber/condenser inlet temperature, have too much freedom control left. This is the consequence of the idealized system which was chosen for demonstration. But that is not an issue; the same control logic can be applied to more complex systems simply by adding more constraints. Although the observed system was partly idealized, the values of optimal PER_{sys} are in close agreement with the performance of real systems with small capacity absorption chillers. The PER values of around 0.4 is hardly competitive with the PER values for the same systems with compression chillers which is above 1. The main reasons for the low system efficiencies of absorption systems are insufficient system design and high electricity consumptions resulting from a suboptimal control of the parasitic equipment. These problems were already discussed in Chapter 1 and Chapter 2. GA/ANN optimal control strategy can help that absorption system always operates with optimal efficiency, but cannot solve the design problems. An interesting idea might be to combine GA/ANN control strategy with standard ON-OFF strategy in order to reduce the electricity consumption of the pumps and fans and improve the efficiency of these systems. The problem with implementation of GA/ANN control in cooling systems with absorption chillers is common practice of using local controllers for each operating component. These controllers do not allow the implementation of improved control strategies with interactions between the system components. However, this is a matter of technology development and cost.

Table 6.4 Optimal control results

Time	Cooling demand [kW]	$T_{ac}^{in,GA}$ [°C]	$T_{gen}^{in,GA}$ [°C]	PER_{sys}
07:00:00	7.11	32.44	89.88	0.37
08:00:00	4.39	33.29	86.11	0.26
09:00:00	7.37	32.26	89.99	0.38
10:00:00	9.03	30.36	89.19	0.43
11:00:00	9.73	28.53	89.57	0.42
12:00:00	9.48	28.76	89.43	0.41
13:00:00	9.4	28.84	89.37	0.41
14:00:00	10.3	28.04	89.97	0.43
15:00:00	11.08	30.84	100	0.42
16:00:00	11.63	30.19	100	0.43
17:00:00	11.92	29.84	100	0.43
18:00:00	11.85	29.93	100	0.43
19:00:00	11.28	30.61	100	0.42
20:00:00	9.64	28.61	89.52	0.41

6.5. Conclusions

In this Chapter, two different optimal control strategies for small capacity absorption chillers were presented: ANNi and GA coupled with ANN. The both strategies used the ANN model developed with experimental data of Pink absorption machine. Consequently, the performance of both strategies is directly dependent of the ANN model accuracy.

In ANNi, the Nealder-Mead simplex method of optimization was applied to find optimal input parameter(s) for the required chilling capacity. In two cases analysed, ANNi was used to estimate one and two unknown input parameters. The manipulable variables considered to obtain the desired output were the inlet temperatures to the absorber/condenser and to the generator. The results showed that the required output can be achieved with a small error (less than 1.2%). Also, the computing time taken by this methodology was less than 1.5 seconds which is much less than the time needed to achieve steady operating conditions.

GA/ANN control strategy was demonstrated through a case study where the Pink absorption chiller was implemented in a small system particularly designed for this purpose. GA optimization method was applied to find two control input parameters of the system for which the system will satisfy the cooling demand operating with optimal efficiency at the same time. The computation time of the strategy was around 4min. The optimal PER of around 0.4 reflects the reality of the performance of small capacity absorption systems and emphasize again the importance of the system design.

All these facts make the proposed methodologies attractive for implementing in the online control system of absorption chillers.

Chapter 7

Conclusions and Future Work

"As for the future, your task is not to foresee it, but to enable it."

Antoine de Saint-Exupery

7.1. Summary and conclusions

The work carried out in this thesis has met the originally proposed aim, which was the development of the comprehensive methodology of testing, modelling and control strategy development for small capacity absorption machines. The developed methodology covers all the important steps in experimental work with small capacity absorption machines which are the base for simple, yet accurate models of these machines. These models, based only on external circuits' parameters, can be developed by using several approaches. The developed methodology also described how to choose the most appropriate model and how that model can further be implemented in software packages or used for control purposes.

In order to provide better understanding of absorption technologies, comprehensive literature review was presented in Chapter 2. This review provided important information about absorption machines, from operating principles to their usability and applications. Special attention was given to small capacity absorption machines, in accordance with the main aim of this thesis. The latest achievements in the field of small capacity absorption machines were presented as well as the review of actual trends and most promising applications for their use, such as solar cooling and CCHP. The achievements from the last two decades showed a considerable progress; however, there are a lot of barriers which must be overcome in order to make them competitive with vapour compression units. The obstacles such as high first cost, lack of serial production, lower performance, inadequate control and usually poor system design are main reasons which prevent the full use of absorption machines potential, especially in the field of primary energy savings and environmental benefits. Regulations and incentives are some of the measures which are necessary for further

development. However, regulations and incentives are only a part of the solution. The second part of the solution, in order to accelerate the progress and to fill the gap with respect to the conventional systems, is development of appropriate standards, test procedures and best practices guides together with intensified work on simulations, optimization and control strategies improvement.

A state of the art test bench was presented in Chapter 3 as very important tool which facilitates the testing of small capacity absorption machines and helps to evaluate their performance and benefits. In detail description of the test bench was given together with the complete explanation of the different configurations which permit the tests under different modes of operation, depending on machine or application purposes. The multifunctional test bench, built in accordance with existing standards, was a very important element of the developed methodology in order to obtain accurate and reliable data which were further used for modelling and other purposes.

However, the multifunctional test bench itself was not sufficient. To obtain accurate and reliable data, it was necessary to develop a comprehensive procedure which would cover all the important aspects of the experimental work. The procedure which allows obtaining the steady state performance data of any small capacity absorption machine was developed by using and combining the existing knowledge and experience in the fields of absorption and compression machines. The comprehensive tests were performed on two different small capacity absorption machines, Rotarica and Pink, in order to achieve this goal. Off-line steady state detector for absorption chillers was developed based on analogy with steady state detector for vapour compression chillers by using the moving window average. Additional steady state filter was developed to remove all the residual transient samples, if they appear. Two additional checks were added to the steady state detection procedure to confirm steady state operating conditions.

The final result was the test procedure which contains several important steps: test planning, data modelling, how to develop detector for steady-state conditions, the uncertainty estimation and the analysis of the results. Very extensive measurements performed on two absorption machines served to validate the functionality of two operating modes in the novel test bench: chiller and heat pump modes. Around 50

steady state points were obtained for Rotartica operating both as chiller and as heat pump and over 140 steady state points for fan-coil applications of Pink absorption chiller by using water as external heat medium. In addition, the Pink chiller was tested for low temperature application by using the brine in chilled fluid circuit. More than 60 steady state points were obtained in these tests.

The data collected during these tests were used for modelling and analysis of different modelling methods which are able to predict, with high level of accuracy, the performance of small capacity absorption chillers. Five different modelling methods were applied by using both mechanistic and empirical approaches: thermodynamic (TD), adapted Gordon-Ng (GNA), adapted characteristic equation ($\Delta\Delta t'$), multivariate polynomial regression (MPR) and artificial neural networks (ANN) model. The statistical analysis which included all the relevant statistical indicators, showed why the thermodynamic models with constant UA values are not appropriate for software packages and control purposes. Due to their complexity, these models are more appropriate for design stage. The obvious advantage of models developed with empirical methods was that all of them could easily be implemented in simulation tools or control applications due to their simple function form. The adapted Gordon Ng method might be appropriate for the rough estimation of absorption chillers' performance due to its simplicity, however, the statistical indicators showed lower prediction capability in comparison with other methods. Excellent statistical indicators (R^2 values around 0.99, CVs lower than 5% and narrow CL) and close agreement with experimental data showed that any of the three different empirical methods ($\Delta\Delta t'$, MPR and ANN) could be used to obtain high level of prediction. However, the empirical models are reliable only if there are enough data to feed the model. This was demonstrated by using the comparison between the models developed with small data set (Rotartica) and the models with large dataset (Pink). The conclusion was that the models should always be developed with large datasets which fully cover operating range. Small data sets are not reliable and statistically correct, since they are insufficient to form strong relationships within the models. In the case of Pink absorption chiller, the best prediction was obtained with the ANN method. High coefficient of determination (>0.998), low coefficient of variation (<2%) and narrow CL confirmed an excellent overall goodness of fit. Even though the ANN models had the best fit in the

observed case, this method was the most complex with respect to the number of parameters. In such a case, especially when different models have statistical indicators so close and all of them indicate excellent overall goodness of fit, the statistical analysis should be extended in order to select the most appropriate model. The model which will satisfy both criteria: complexity and goodness of fit. Further analysis was carried out by comparing developed models with Akaike Information Criterion (AIC_c) and Bayesian Information Criterion (BIC) statistical tests which confirmed that ANN was the most suitable method to model Pink absorption chiller.

At the end, two types of optimal control strategies for absorption chillers were developed based on ANN models. Both strategies indicated the importance of models' accuracy, since their performance was directly dependent of the ANN model performance. The first strategy, Artificial Neural Network inverse (ANNi), allowed the direct search of the input parameters (inlet temperatures in both hot and cooling water circuits) to control the chilling capacity. Direct search of the input parameters was enabled by performing Nealder-Mead simplex method of optimization over the ANN model in reverse direction. Validation with experimental data showed an error less than 1.2% with very short execution time (<1.5s). The second control strategy used genetic algorithms to estimate the control parameters which provided the optimal primary energy consumption of the air conditioning system with absorption chiller. This strategy was demonstrated by using the small system with Pink absorption chiller, particularly designed for this purpose. The conclusion was that both strategies looked promising to be implemented in on-line control systems of absorption chillers. The main barrier for the implementation of these advanced strategies in control systems is the current practice which uses local controllers which do not allow the implementation of improved control strategies with interactions between the components. However, with the current progress of technology and artificial intelligence, it is only matter of time when these controllers will become popular.

Resumen y conclusiones

El trabajo realizado en esta tesis cumple con el objetivo propuesto inicialmente, el cual fue desarrollar una metodología comprensiva para ensayar, modelar y desarrollar estrategias de control para máquinas de absorción de pequeña potencia. La metodología empleada abarca los pasos necesarios para trabajar experimentalmente con este tipo de máquinas y lograr, con una base sólida, una representación precisa del comportamiento de las máquinas de absorción de pequeña potencia. Los modelos de estas máquinas se basan solamente en parámetros relacionados a los circuitos externos y fueron desarrollados siguiendo varias líneas de tendencia. La metodología utilizada también describe la manera de seleccionar el modelo más adecuado y cómo este modelo puede ser posteriormente implementado en paquetes informáticos o en medidas de control.

El Capítulo 2 presenta una revisión bibliográfica sobre las tecnologías de absorción y así lograr un mejor entendimiento sobre esta temática. Esta temática comprende aspectos relacionados a los principios operativos, usos y aplicaciones de las máquinas de absorción; pero siempre con un enfoque especial en máquinas de pequeña potencia. Un estado del arte de las máquinas de absorción de pequeña potencia presenta los últimos logros en este campo, así como también las tendencias actuales y las aplicaciones más prometedoras como el uso en climatización solar y CCHP. Los logros en las dos últimas décadas muestran un progreso considerable, sin embargo existen obstáculos que deben superarse con el fin de hacerlas competitivas con las unidades de compresión de vapor. Entre algunos de estos obstáculos están: unos elevados costes iniciales, una falta de producción en serie, un bajo rendimiento, un control inadecuado y un diseño pobre del sistema. Estos obstáculos evitan la plena utilización del potencial de las máquinas de absorción, especialmente en el ámbito del ahorro de energía primaria y beneficios ambientales. Para reducir la brecha existente con respecto a los sistemas convencionales, es primordial contar con regulaciones e incentivos por parte del gobierno; de igual manera es importante desarrollar estándares apropiados, procedimientos de ensayos y guías de mejores prácticas que de forma conjunta con un trabajo especializado en simulación, optimización y mejoramiento de estrategias de control lograrían acelerar el desarrollo de este tipo de sistemas.

Como parte del Capítulo 3 se presenta la descripción de un banco de ensayos de punta, el cual ocupa un puesto muy importante al momento de ensayar y evaluar el rendimiento y prestaciones de máquinas de absorción de pequeña potencia. Se realiza una descripción detallada del banco de ensayos y una explicación completa de las distintas configuraciones posibles que dependerán del tipo de máquina y aplicación de la misma. El banco de ensayos multifuncional fue construido bajo estándares existentes y fue un elemento clave al momento de desarrollar la metodología para ensayar máquinas de absorción. Esta metodología permitió obtener datos precisos y fiables para su posterior uso en el modelado de este tipo de máquinas y para otros propósitos.

Es importante señalar que el banco de ensayos multifuncional por sí solo no fue suficiente en este trabajo. Para obtener datos precisos y fiables fue necesario desarrollar un procedimiento comprensivo que permitió abarcar todos los aspectos importantes del trabajo experimental. Al momento de obtener los datos de funcionamiento de cualquier máquina de absorción de pequeña potencia en régimen estacionario fue necesario combinar el conocimiento existente y la experiencia en el manejo de las máquinas de absorción y compresión. Los ensayos con dos máquinas de absorción de pequeña potencia, Rotartica y Pink, fueron realizados para lograr este objetivo. Se desarrolló un proceso de detección de régimen estacionario para analizar los resultados obtenidos en las pruebas. Este detector off-line está basado en una analogía del detector de régimen estacionario para máquinas de compresión de vapor utilizando el método de ventana media móvil. Además este detector cuenta con un filtro adicional para remover todas las muestras residuales transitorias que puedan existir en los datos analizados. Se incluyeron dos revisiones adicionales al procedimiento de detección de régimen estacionario para asegurar condiciones en régimen estacionario.

El resultado final fue el procedimiento que contiene los siguientes pasos importantes: planeación de pruebas, modelado en función de los datos obtenidos, desarrollo del detector de condiciones estacionarias, estimación de la incertidumbre y análisis de resultados. Se realizaron mediciones detalladas en el nuevo banco de pruebas a dos máquinas de absorción en el con el fin de validar la funcionalidad en dos modos de operación: enfriamiento y bomba de calor. Alrededor de 50 puntos en régimen estacionario se obtuvieron de la Rotartica que trabajó tanto como enfriadora y como

bomba de calor, y más de 140 puntos en régimen estacionario con la enfriadora Pink para aplicaciones tipo fan-coil con agua como fluido térmico. Además la enfriadora Pink fue ensayada para aplicaciones de baja temperatura con salmuera como fluido refrigerante y se obtuvieron más de 60 puntos en régimen estacionario.

Los datos recopilados durante estas pruebas fueron utilizados para modelar y analizar los diferentes métodos destinados a predecir, con gran precisión, el comportamiento de las máquinas de absorción de pequeña potencia. Cinco métodos de modelado con enfoques tanto mecanicista como empírico fueron aplicados: método termodinámico (TD), método adaptado de Gordon-Ng (GNA), método de la ecuación característica adaptada ($\Delta\Delta t'$), método de regresión polinomial multivariable (MPR) y modelo de redes neuronales artificiales (ANN). El análisis estadístico que incluye los indicadores estadísticos más relevantes demostró que los modelos termodinámicos con valores UA constantes no son apropiados para paquetes de software y de control. Estos modelos son más apropiados para la etapa de diseño debido a su complejidad. La ventaja de los modelos desarrollados a través de métodos empíricos fue que todos ellos podrían implementarse fácilmente en herramientas de simulación o aplicaciones de control debido a su representación sencilla. El método adaptado Gordon-Ng podría ser apropiado para una estimación aproximada del rendimiento de las enfriadoras de absorción debido a su simplicidad, pero los indicadores estadísticos demostraron una baja capacidad predictiva en comparación con los demás métodos. Cualquiera de los tres métodos empíricos ($\Delta\Delta t'$, MPR y ANN) podría ser utilizados para obtener una predicción de alto nivel ya que todos ellos obtuvieron excelentes indicadores estadísticos (valores de R^2 cercanos a 0.99, valores de CV menores que 5% y un estrecho CL) y sus resultados fueron muy cercanos a los datos obtenidos en los ensayos. Hay que tener presente que los modelos empíricos son confiables solamente cuando se tiene suficiente información para alimentar al modelo. Esta afirmación se demostró al comparar los modelos desarrollados con un pequeño paquete de datos (Rotartica) y los modelos con un paquete de datos grande (Pink). La conclusión fue que los modelos deberían siempre desarrollarse con una gran cantidad de datos para poder cubrir un amplio rango operacional, mientras que una pequeña muestra de datos no es confiable ni estadísticamente correcta. En el caso de la enfriadora de agua Pink el mejor resultado se obtuvo con el método ANN que produjo un alto coeficiente de determinación (>0.998),

un bajo coeficiente de variación (<2%) y un estrecho CL. Estos valores confirmaron un excelente ajuste global. Aunque el modelo ANN obtuvo el mejor ajuste en el caso analizado, este método fue el más complejo con respecto al número de parámetros. En el caso en que los distintos modelos tengan indicadores estadísticos muy similares y que todos indiquen un excelente ajuste global, el análisis estadístico debería ser extendido para seleccionar el modelo más apropiado. Este modelo será el que satisfaga ambos criterios: complejidad y bondad de ajuste. Posteriormente se realizó un análisis comparativo de los modelos desarrollados bajo las pruebas estadísticas del Criterio de Información Akaike (AIC_c) y el Criterio de Información Bayesiano (BIC), y se concluyó que el método más adecuado para modelar la enfriadora de agua por absorción Pink es el método ANN.

Al final se desarrollaron dos estrategias óptimas de control basadas en los modelos de ANN para las máquinas de absorción. Las dos estrategias señalaron la importancia de la precisión del modelo ya que su rendimiento estuvo directamente dependiente del rendimiento del modelo ANN. La primera estrategia fue la inversa de la Red Neuronal Artificial (ANNi) y permitió la búsqueda directa de los parámetros de entrada (temperaturas de entrada tanto en el circuito de activación como en el de enfriamiento) para controlar la capacidad frigorífica. La búsqueda directa de los parámetros de entrada se realizó por medio del método simple de optimización Nealder-Mead sobre el modelo ANN en dirección inversa. La validación del modelo con datos experimentales dio como resultado un error menor al 1.2% con tiempos de ejecución muy cortos (<1.5s). La segunda estrategia de control utilizó algoritmos genéticos para estimar los parámetros de control y así entregar el consumo óptimo de energía primaria para un sistema de aire acondicionado con enfriadoras de agua por absorción. Esta estrategia fue demostrada al utilizar un sistema pequeño de aire acondicionado con la máquina Pink que fue diseñado particularmente para este propósito. La conclusión fue que ambas estrategias podrían ser implementadas en los sistemas de control online de máquinas de absorción con resultados muy prometedores. Es necesario acotar que la barrera principal, al momento de la implementación de estas estrategias en los sistemas de control, es la práctica actual con relación a los controles; ésta no permite la implementación de nuevas y avanzadas estrategias de control que permitan la interacción entre cada uno de los componentes. Es importante indicar que el uso de

estas estrategias de control será cada vez más utilizado con el tiempo debido al progreso actual de la tecnología y al uso de la inteligencia artificial.

7.2. Future work

In addition to the significant contribution this research delivered, some questions have been left for further exploration.

Although the models developed for the purpose of this research are comprehensive, the main constraint is the operation with constant flow rates in external water circuits. Therefore, one of the future tasks will be to improve all the models by including variable flow rates. This will lead to more detailed and accurate models with more manipulable parameters which will permit better adjustment in control systems and simulation tools.

Limited time and resources have prevented me to complete the research in the field of control in terms of testing developed strategies for absorption chillers in real systems. This task, together with the inclusion of economic optimization in GA control strategy, is left for the future.

Another task left for future work is to extend the developed methodology to air-cooled absorption machines and to include economic analysis with comparison to vapour compression machines.

Also, it would be very interesting to use ANN ability of mapping highly non-linear problems to develop dynamic models which would include transient behaviour (start up and shut down periods) and thermal inertia of small capacity absorption machines. The implementation of dynamic models in simulation tools should result in more realistic performance prediction of the HVAC systems.

The step further would be to develop the methodology, or better software tool, which would help in designing and sizing of absorption chiller plants in order to operate with maximum efficiency.

Trabajo futuro

Además de la importante contribución realizada en esta investigación, existen algunos aspectos no incluidos y que podrían ser de mucho interés.

Aunque los modelos desarrollados para el objetivo de esta investigación son exhaustivos, la mayor restricción es la operación con caudales constantes en los circuitos de agua externos. Por lo tanto una de las futuras tareas será incluir caudales variables en cada uno de los modelos presentados. Esta modificación permitirá contar con modelos más detallados y precisos, permitiendo contar con un mayor número de parámetros manipulables y así lograr un mejor ajuste en los sistemas de control y herramientas de simulación.

Tiempo y recursos limitados han impedido que completara la investigación en el campo de control en términos de pruebas de las estrategias desarrolladas para máquinas de absorción en sistemas reales. Esta tarea, junto con la inclusión de optimización económica en la estrategia de control de GA, se deja para el futuro.

Otra tarea dejada para un trabajo posterior es la extensión de la metodología a máquinas de absorción enfriadas por aire y la inclusión de un análisis económico comparativo con máquinas de compresión de vapor.

Además sería muy interesante usar la destreza de las ANN en la resolución de problemas no lineales y en el desarrollo de modelos dinámicos que incluyan comportamiento transitorio (períodos de arranque y paro) e inercia térmica de las máquinas de absorción de pequeña potencia. La implementación de modelos dinámicos en herramientas de simulación permitiría la predicción más realista del comportamiento de los sistemas HVAC.

El siguiente paso sería desarrollar la metodología, o una mejor herramienta informática, que ayudaría a diseñar y dimensionar instalaciones de enfriadoras de agua por absorción y lograr que éstas operen con máxima eficiencia.

References

[1] BP Statistical Review of World Energy, June 2010.

[2] www.epa.gov/climatechange/ [Accessed May 6th 2011].

[3] International Energy Outlook 2010. U.S. Department of Energy, Washington, DC 20585, DOE/EIA-0484(2010); July 2010.

[4] European Commission Climate Action. The EU climate and energy package. http://ec.europa.eu/clima/policies/package/index_en.htm [Accessed May 3rd 2011].

[5] BSRIA, Review of the World Air Conditioning Market 2007.

[6] IEA, Energy Technology Perspectives 2010. Scenarios & Strategies to 2050.

[7] Eurostat, Europe in figures. Eurostat yearbook 2010.

[8] Bertoldi P., Atanasiu B. Electricity Consumption and Efficiency Trends in European Union. *Status Report 2009*. European Commission, Joint Research Centre, Institute for Energy, Renewable Energy Unit EUR 24005 EN; 2009.

[9] 2009 Buildings Energy Data Book. D&R International L., U.S. Department of Energy.

[10] IEA SHC Task 25 - Solar Assisted Air Conditioning of Buildings. http://www.iea-shc.org/task25/ [Accessed March 3rd 2011].

[11] IEA SHC Task 38 - Solar Air-Conditioning and Refrigeration. http://www.iea-shc.org/task38/ [Accessed March 3rd 2011].

[12] Henning H.-M. Solar assisted air conditioning of buildings – an overview. Heat transfer and sustainable energy technologies. 2007; 27(10): 1734-49.

[13] Henning H.M. Solar-Assisted Air-Conditioning in Buildings, A Handbook for Planers: Springer, Wien, New York, 2002.

[14] Pietruschka D. Model Based Control Optimisation of Renewable Energy Based HVAC Systems [PhD thesis]. Leicester: IESD, De Monfort University, 2010.

[15] Ziegler F., Hellmann H.M., Schweigler C. An approximative method for modeling the operating characteristics of advanced absorption chillers. In: 29th International Congress of Refrigeration; 1999 19.-24.09.; Sydney.

[16] Gordon J.M., Ng K.C. Predictive and diagnostic aspects of a universal thermodynamic model for chillers. International Journal of Heat and Mass Transfer. 1995; 38(5): 807-18.

[17] Şencan A. Performance of ammonia–water refrigeration systems using artificial neural networks. Renewable Energy. 2007; 32(2): 314-28.

[18] Kim D.S., Infante Ferreira C.A. Analytic modelling of steady state single-effect absorption cycles. International Journal of Refrigeration. 2008; 31(6): 1012-20.

[19] Lee T.-S., Lu W.-C. An evaluation of empirically-based models for predicting energy performance of vapor-compression water chillers. Applied Energy. 2010; 87(11): 3486-93.

[20] Burgett L.W., Byars M.D., Shultz K. Absorption systems: the future, more than a niche? In: ISHPC '99, Proceedings of the International Sorption Heat Pump Conference; 1999 March, 24-26; Munich, Germany. p. 13-25.

[21] Chen G., He Y. The latest progress of absorption refrigeration in China. In: International Congress of Refrigeration, IIR Conference; 2007; Bejing, China. Paper No. ICR07-174.

[22] 2009 ASHRAE Handbook - Fundamentals (SI Edition) 1791 Tullie Circle, NE, Atlanta, GA 30329: American Society of Heating, Refrigerating and Air-Conditioning Engineers, Inc.

[23] Herold K.E., Radermacher R., Klein S.A. Absorption chillers and heat pumps. Boca Raton, FL: CRC Press, 1996.

[24] Martínez H., Rivera W. Energy and exergy analysis of a double absorption heat transformer operating with water/lithium bromide. International Journal of Energy Research. 2009; 33(7): 662-74.

[25] Dorgan C.B., Leight S.P., Dorgan C.E. Application Guide for Absorption Cooling/Refrigeration Using Recovered Heat: American Society of Heating, Refrigerating and Air-conditioning Engineers (ASHRAE), 1791 Tullie Circle, NE/ Atlanta, GA 30329, 1995.

[26] Macriss R.A., Gutraj J.M., Zawacki T.S. Absorption fluids data survey: final report on worldwide data. Institute of Gas Technology, Chicago; 1988. ORNL/Sub/84-47989/3.

[27] Kurosawa S., Nagaoka Y., Yoshida A., Masato O., Kunugi Y. Working Fluids Survey. In: Working Fluids and Transport Phenomena in Advanced Absorption Heat Pumps (Final Report Annex 14). IEA Heat Pump Center; 1990. HPP-AN14-1.

[28] Gluesenkamp K., Radermacher R., Hwang Y. Trends in absorption machines. In: Lazzarin R.M., Longo G.A., Noro M. editors. International Sorption Heat Pump Conference (ISPHC11); 2011 April 6-8; Padua, Italy. IIR/AICARR.

[29] Salavera D., Esteve X., Patil K.R., Mainar A.M., Coronas A. Solubility, heat capacity, and density of lithium bromide + lithium iodide + lithium nitrate + lithium chloride aqueous solutions at several compositions and temperatures. Journal of Chemical and Engineering Data. 2004; 49(3): 613-9.

[30] Bourouis M., Valles M., Medrano M., Coronas A. Absorption of water vapour in the falling film of water-(LiBr + LiI + $LiNO_3$ + LiCl) in a vertical tube at air-cooling thermal conditions. International Journal of Thermal Sciences. 2005; 44(5): 491-8.

[31] Infante Ferreira C.A. Thermodynamic and physical property data equations for ammonia-lithium nitrate and ammonia-sodium thiocyanate solutions. Solar Energy. 1984; 32(2): 231-6.

[32] Oronel C., Vallès M., Bourouis M., Coronas A. Absorption process with ammonia/lithium nitrate in plate heat exchangers for absorption refrigeration systems. In: The International Sorption Heat Pump Conference 2008 (ISHPC08); 2008 23-26 September; Seoul, Korea.

[33] Zamora M., Bourouis M., Valles M., Coronas A. Development of a small capacity air-cooled ammonia-lithium nitrate absorption chiller - first cooling capacity and COP measurements. In: Lazzarin R.M., Longo G.A., Noro M. editors. International Sorption Heat Pump Conference (ISHPC11); 2011 April 6-8; Padua, Italy. IIR/AICARR, p. 117-24.

[34] World's First Triple-Effect Gas Absorption Chiller Commercialized. http://www.khi.co.jp/english/pressrelease/detail/ba_c3051005-1.html [Accessed April 20th 2011].

[35] Infante Ferreira C.A. Advancement in solar cooling. In: Lazzarin R.M., Longo G.A., Noro M. editors. International Sorption Heat Pump Conference (ISPHC11); 2011 April 6-8; Padua, Italy. IIR/AICARR.

[36] Kalogirou S. The potential of solar industrial process heat applications. Applied Energy. 2003; 76(4): 337-61.

[37] Mokhtar M., Ali M.T., Bräuniger S., Afshari A., Sgouridis S., Armstrong P., et al. Systematic comprehensive techno-economic assessment of solar cooling technologies using location-specific climate data. Applied Energy. 2010; 87(12): 3766-78.

[38] Meunier F. Sorption contribution to climate change control. Clean Technologies and Environmental Policy. 2004; 6(3): 187-95.

[39] Wu D.W., Wang R.Z. Combined cooling, heating and power: A review. Progress in Energy and Combustion Science. 2006; 32(5-6): 459-95.

[40] Heat Pumps in Japan ^Tokyo: Heat Pump Technology Center of Japan; 1995 March 1995.

[41] Alarcón-Padilla D.C., García-Rodríguez L., Blanco-Gálvez J. Design recommendations for a multi-effect distillation plant connected to a double-effect absorption heat pump: A solar desalination case study. Desalination. 2010; 262(1-3): 11-4.

[42] Hwang Y. Potential energy benefits of integrated refrigeration system with microturbine and absorption chiller. International Journal of Refrigeration. 2004; 27(8): 816-29.

[43] Monsberger M., Kim D.S., Malenkovic I., Haslinger G., Claassen D.P., Herunter J. Fuel cell powered hybrid absorption refrigeration system for mobile applications. In: The International Sorption Heat Pump Conference 2008 (ISHPC08); 2008 23-26 September; Seoul, Korea.

[44] Jeong S., Garimella S. Optimal design of compact horizontal tube LiBr/water absorbers. HVAC and R Research. 2005; 11(1): 27-44.

[45] Hu J.S., Chao C.Y.H. Development of an electroosmotic pump-driven micro LiBr absorption heat pump system for controlling microclimate in protective clothing: Feasibility review and role of the pump. HVAC and R Research. 2008; 14(3): 467-87.

[46] Lee J.K., Koo J., Hong H., Kang Y.T. The effects of nanoparticles on absorption heat and mass transfer performance in NH3/H2O binary nanofluids. International Journal of Refrigeration. 2010; 33(2): 269-75.

[47] Ali A.H.H. Design of a compact absorber with a hydrophobic membrane contactor at the liquid-vapor interface for lithium bromide-water absorption chillers. Applied Energy. 2010; 87(4): 1112-21.

[48] Vidal A., Best R., Rivero R., Cervantes J. Analysis of a combined power and refrigeration cycle by the exergy method. Energy. 2006; 31(15): 3401-14.

[49] Ziegler F. Recent developments and future prospects of sorption heat pump systems. International Journal of Thermal Sciences. 1999; 38(3): 191-208.

[50] Grossman G. Solar-powered systems for cooling, dehumidification and air-conditioning. Solar Energy. 2002; 72(1): 53-62.

[51] Ziegler F. Sorption heat pumping technologies: Comparisons and challenges. International Journal of Refrigeration. 2009; 32(4): 566-76.

[52] Wang R.Z., Ge T.S., Chen C.J., Ma Q., Xiong Z.Q. Solar sorption cooling systems for residential applications: Options and guidelines. International Journal of Refrigeration. 2009; 32(4): 638-60.

[53] Onovwiona H.I., Ugursal V.I. Residential cogeneration systems: Review of the current technology. Renewable and Sustainable Energy Reviews. 2006; 10(5): 389-431.

[54] Ge Y.T., Tassou S.A., Chaer I., Suguartha N. Performance evaluation of a tri-generation system with simulation and experiment. Applied Energy. 2009; 86(11): 2317-26.

[55] Aprile M. The market potential of micro-CHCP. Deliverable D2-5 of WP2. PolySMART project .

[56] Jakob U., Kohlenbach P. Recent developments of sorption chillers in Europe. In: 9th IIR Gustav Lorentzen Conference; 2010; Sidney, Australia.

[57] Deng J., Wang R.Z., Han G.Y. A review of thermally activated cooling technologies for combined cooling, heating and power systems. Progress in Energy and Combustion Science. 2011; 37(2): 172-203.

[58] Zogg R.A., Feng M.Y., Westphalen D. Guide to developing air-cooled libr absorption for combined heat and power applications — Report to US Department of Energy and Oak Ridge National Laboratory. Prepared by TIAX LLC. Available at http://www.eere.energy.gov/de/information_resources.html 2005.

[59] Kim D.S., Infante Ferreira C.A. Air-cooled solar absorption air conditioning, Final report. Delft University of Technology 2005. BSE-NEO 0268.02.03.04.0008.

[60] Biermann W., Reimann R. Air Cooled Absorption Chillers for Solar Cooling Applications. DOE Contract No. EG-77-C-03-1587 Report, Carrier Corp. 1978.

[61] Kurosawa S., Nagaoka Y., Kannoh S., Takemoto S., Sugimoto S., Oouchi T., et al. *Double effect air cooled absorption refrigerating machine*. US4841744 (1989)

[62] De Vuono A.C., Hanna W.T., Osborne R.L., Ball D.A. "Development of a Double-effect Air-Conditioner Heater (DEACH). Phase 3 and Final Report, January 1990-December 1991. Phase 3, September 1987-December 1991. Overall Project". Battelle and Gas Research Institute; 1992.

[63] Lowenstein A.I. *Flat-plate absorbers and evaporators for absorption coolers*. US 6176101 (2001)

[64] Tongu S., Makino Y., Ohnishi K., Nakatsugawa S. Practical operating of small-sized air-cooled double-effect absorption chiller-heater by using lithium bromide and aqueous. In: Proceedings of the International Absorption Heat Pump Conference; 1994; New Orleans, LA, USA. Publ by ASME, p. 125-32.

[65] Iizuka H., Nagamatsuya K., Takahashi K., Kuroda J. *Absorbent solution for use with absorption refrigeration apparatus*. US5108638 (1992)

[66] Li Z.F., Sumathy K. Experimental studies on a solar powered air conditioning system with partitioned hot water storage tank. Solar Energy. 2001; 71(5): 285-97.

[67] YAZAKI Environment and Energy Equipment Operations (EEEO) milestones. http://www.yazaki-airconditioning.com/en/airconditioning/history.html [Accessed 14/05 2011].

[68] Sözen A., AltIparmak D., Usta H. Development and testing of a prototype of absorption heat pump system operated by solar energy. Applied Thermal Engineering. 2002; 22(16): 1847-59.

[69] Ezzine N.B., Barhoumi M., Mejbri K., Chemkhi S., Bellagi A. Solar cooling with the absorption principle: First and Second Law analysis of an ammonia - Water double-generator absorption chiller. Desalination. 2004; 168(1-3): 137-44.

[70] Argiriou A.A., Balaras C.A., Kontoyiannidis S., Michel E. Numerical simulation and performance assessment of a low capacity solar assisted absorption heat pump coupled with a sub-floor system. Solar Energy. 2005; 79(3): 290-301.

[71] Jakob U., Eicker U., Schneider D., Taki A.H., Cook M.J. Simulation and experimental investigation into diffusion absorption cooling machines for air-conditioning applications. Applied Thermal Engineering. 2008; 28(10): 1138-50.

[72] Zetzsche M., Koller T., Brendel T., Müller-Steinhagen H. Solar cooling with an ammonia/water absorption chiller. In: The second international conference of solar air-conditioning; 2007; Tarragona, Spain. p. 536–41.

[73] Moser H., Rieberer R. Small-capacity ammonia/water absorption heat pump for heating and cooling–used for solar cooling applications. In: The second international conference of solar air-conditioning; 2007; Tarragona, Spain. p. 56-61.

[74] Castro J., Oliva A., Pérez-Segarra C.D., Cadafalch J. Evaluation of a small capacity, hot water driven, air-cooled H2O-LiBr absorption machine. HVAC and R Research. 2007; 13(1): 59-75.

[75] Eicker U. Low energy cooling for sustainable buildings: John Wiley & Sons 2009.

[76] Kim D.S., Infante Ferreira C.A. Air-cooled LiBr-water absorption chillers for solar air conditioning in extremely hot weathers. Energy Conversion and Management. 2009; 50(4): 1018-25.

[77] Icebook. http://www.solarfrost.com/en/icebook.html [Accessed 16/05 2011].

[78] Bourouis M., Coronas A., Valles M., Zamora M. *Enfriadora de agua por absorción tipo aire-agua o agua-agua de amoniaco y nitratio de litio*. OPEM Madrid P200930758. PCT/ES2010/070608 (2009)

[79] Uppal A.H., Norton B., Probert S.D. A low-cost solar-energy stimulated absorption refrigerator for vaccine storage. Applied Energy. 1986; 25(3): 167-74.

[80] Bansal N.K., Blumenberg J., Kavasch H.J., Roettinger T. Performance testing and evaluation of solid absorption solar cooling unit. Solar Energy. 1997; 61(2): 127-40.

[81] Erickson D.C. Waste-heat-powered icemaker for isolated fishing villages. In: Anon editor 1995; Chicago, IL, USA. ASHRAE, p. 1185-8.

[82] Sierra F.Z., Best R., Holland F.A. Experiments on an absorption refrigeration system powered by a solar pond. Heat Recovery Systems and CHP. 1993; 13(5): 401-8.

[83] Dincer I., Edin M., Ture I.E. Investigation of thermal performance of a solar powered absorption refrigeration system. Energy Conversion and Management. 1996; 37(1): 51-8.

[84] Hammad M., Habali S. Design and performance study of a solar energy powered vaccine cabinet. Applied Thermal Engineering. 2000; 20(18): 1785-98.

[85] De Francisco A., Illanes R., Torres J.L., Castillo M., De Blas M., Prieto E., et al. Development and testing of a prototype of low-power water-ammonia absorption equipment for solar energy applications. Renewable Energy. 2002; 25(4): 537-44.

[86] Pilatowsky I., Rivera W., Romero J.R. Performance evaluation of a monomethylamine-water solar absorption refrigeration system for milk cooling purposes. Applied Thermal Engineering. 2004; 24(7): 1103-15.

[87] Abrahamsson K., Gidner A., Jernqvist Å. Design and experimental performance evaluation of an absorption heat transformer with self-circulation. Heat Recovery Systems and CHP. 1995; 15(3): 257-72.

[88] Bourouis M., Valles M., Medrano M., Coronas A. Performance of air-cooled absorption air-conditioning systems working with water-(LiBr + LiI + $LiNO_3$ + LiCl). Proceedings of the Institution of Mechanical Engineers, Part E: Journal of Process Mechanical Engineering. 2005; 219(2): 205-12.

[89] Lorton R., Gilchrist K., Green R.J. Development and operation of a high performance 10 kw absorption chiller. International Journal of Refrigeration. 2000; 23(8): 572-6.

[90] Srikhirin P., Aphornratana S., Chungpaibulpatana S. A review of absorption refrigeration technologies. Renewable and Sustainable Energy Reviews. 2001; 5(4): 343-72.

[91] Fan Y., Luo L., Souyri B. Review of solar sorption refrigeration technologies: Development and applications. Renewable and Sustainable Energy Reviews. 2007; 11(8): 1758-75.

[92] Wang X., Chua H.T. Absorption cooling: A review of lithium bromide-water chiller technologies. Recent Patents on Mechanical Engineering. 2009; 2(3): 193-213.

[93] Mugnier D. Task 38: Solar Air-Conditioning and Refrigeration Workshop. Solar cooling economics. Aarhus. 28.04.2010.

[94] Sparber W., Napolitano A., Mugnier D., Le Denne A., Preisler A., Motta M. Task 38: Solar Air-Conditioning and Refrigeration. List of existing solar heating and cooling installations. 2009.

[95] PolySMART information brochure: Combined Heating, Cooling and Power Generation in the Small Capacity Range. 2009.

[96] Moya Arevalo M. Sistemas avanzados de microtrigeneracion con microturbinas de gas i enfriadoras por absorcion con disipacion por aire [PhD thesis]. Tarragona: Universitat Rovira i Virgili, 2011.

[97] Khatri K.K., Sharma D., Soni S.L., Tanwar D. Experimental investigation of CI engine operated Micro-Trigeneration system. Applied Thermal Engineering. 2010; 30(11-12): 1505-9.

[98] Yin H., Qu M., Archer D.H. Model based experimental performance analysis of a microscale LiBr-H_2O steam-driven double-effect absorption Chiller. Applied Thermal Engineering. 2010; 30(13): 1741-50.

[99] Rococo project final report: Reduction of costs of Solar Cooling systems. 2008.

[100] Dickinson J.K., Hess R.O., Seaton J., van Lambalgen H., Burnham A.L. Cost and Performance Analysis of a Solar Thermal Cooling Project. ASME Conference Proceedings. 2010; 2010(43956): 217-23.

[101] Moya M., Bruno J.C., Eguia P., Torres E., Zamora I., Coronas A. Performance analysis of a trigeneration system based on a micro gas turbine and an air-cooled, indirect fired, ammonia-water absorption chiller. Applied Energy. Article in press

[102] Sugiartha N., Tassou S.A., Chaer I., Marriott D. Trigeneration in food retail: An energetic, economic and environmental evaluation for a supermarket application. Applied Thermal Engineering. 2009; 29(13): 2624-32.

[103] Directive 2009/28/EC of the European Parliament and of the Council of 23 April 2009 on the promotion of the use of energy from renewable sources and amending and subsequently repealing Directives 2001/77/EC and 2003/30/EC.

[104] Cansino J.M., Pablo-Romero M.D.P., Román R., Yñiguez R. Promoting renewable energy sources for heating and cooling in EU-27 countries. Energy Policy. 2011; 39(6): 3803-12.

[105] BOE-A-2007-10556. Real Decreto 661/2007, de 25 de mayo, por el que se regula la actividad de producción de energía eléctrica en régimen especial.

[106] ASHRAE terminology of heating, ventilation, air conditioning & refrigeration. 1791 Tullie Circle, NE, Atlanta, GA 30329: American Society of Heating, Refrigeration and Air-conditioning Engineers, 1991.

[107] Gordon J.M., Ng K.C. Cool Thermodynamics. First ed. Cambridge: Cambridge International Science Publishing, 2001.

[108] ANSI/AHRI Standard 560-2000, Absorption Water Chilling and Water Heating Packages 4301 North Fairfax Drive, Suite 425, Arlington, VA 22203, USA: Air-Conditioning, Heating, and Refrigeration Institute; 2000.

[109] BS EN Standard 12309-2:2000, Gas-fired absorption and adsorption air-conditioning and/or heat pump appliances with a net heat input not exceeding 70 kW. Rational use of energy. Brussels: European Committee for Standardization (CEN) 2000.

[110] BS EN Standard 12309-1:2000, Gas-fired absorption and adsorption air-conditioning and/or heat pump appliances with a net heat input not exceeding 70 kW. Safety. Brussels: European Committee for Standardization (CEN); 2000.

[111] JIS Standard B 8622:2009 Absorption refrigerating machines. Japanese Standards Association & The Japan Refrigeration and Air Conditioning Industry Association; 2007.

[112] DOE/EIA. Commercial Buildings Characteristics 1992. April 1994.

[113] ASHRAE Standard 41.1-1986 Measurements guide: section on temperature measurement. 1791 Tullie Circle, NE, Atlanta, GA30329, USA: American Society of Heating, Refrigeration, and Air-Conditioning Engineers, Inc.; 1986.

[114] ASME Standard MFC-16M-1995 Measurement of Fluid Flow in Closed Conduit by Means of Electromagnetic Flowmeters. 3 Park Avenue, New York, NY, 10016-5990: American Society of Mechanical Engineers; 1995.

[115] ASME Standard B40.100-2005 Pressure Gaauges and Gauge Attachments. 3 Park Avenue, New York, NY, 10016-5990: American Society of Mechanical Engineers; 2005.

[116] AHRI Standard 550/590-2003, Performance Rating of Water Chilling Packages Using the Vapor Compression. 4301 North Fairfax Drive, Suite 425, Arlington, VA 22203, USA: Air-Conditioning, Heating, and Refrigeration Institute; 2003.

[117] ASHRAE Standard 30-1995, Method of testing liquid Chilling Packages. 1791 Tullie Circle, NE, Atlanta, GA30329, USA: American Society of Heating, Refrigeration, and Air-Conditioning Engineers, Inc.; 1995.

[118] Malenkovic I. Testing and performance evaluation methods for thermally driven heat pumps. *In: IEA Heat Pump Centre Newsletter.* Vol. 29. (No. 1/2011): 23-6.

[119] Pravda M.F. *ROTARY HEAT PUMP*. US3740966 (1973)

[120] Kantor F.W. *Rotary thermodynamic apparatus and method*. US4441337 (1984)

[121] Ramshaw C., Winnington T. *Heat pumps*. US5009085 (1991)

[122] Pravda M.F. *Rotary absorption heat pump of improved performance*. US5303565 (1994)

[123] Winnington T.L., Green R.J., Lorton R., Uselton R.B. *Heat pumps*. US6263682 B1 (2001)

[124] Gorritxategi Retolaza X., Onederra Egaña U., Cano Rodríguez J.M. *Rotary absorption heat pump*. EP 1701115A1 (2006)

[125] Aoune A., Ramshaw C. Process intensification: heat and mass transfer characteristics of liquid films on rotating discs. International Journal of Heat and Mass Transfer. 1999; 42(14): 2543-56.

[126] Gilchrist K., Lorton R., Green R.J. Process intensification applied to an aqueous LiBr rotating absorption chiller with dry heat rejection. Applied Thermal Engineering. 2002; 22(7): 847-54.

[127] Winnington T.L., Lorton R. *Rotary heat and/or mass transfer arrangements*. US6290216 B1 (2001)

[128] Loubet R., Chavarri J.M., Egilegor B., Fernandez R. D 4.2: Rotartica package solution description, Solarcombi+. 2009.

[129] Zaltash A., Petrov A., Linkous R., Vineyard E., Goodnack D., Egilegor B. Performance evaluation of a 4.5 kW (1.3 refrigeration tons) air-cooled lithium bromide/water hot-water-fired absorption unit. In: ASME International Mechanical Engineering Congress and Exposition, Proceedings; 2007; Seattle, WA. vol. 15. p. 197-210.

[130] Izquierdo M., Lizarte R., Marcos J.D., Gutiérrez G. Air conditioning using an air-cooled single effect lithium bromide absorption chiller: Results of a trial conducted in Madrid in August 2005. Applied Thermal Engineering. 2008; 28(8-9): 1074-81.

[131] Monne C., Guallar J., Alonso S., Palacin F. Influencia de la velocidad de giro en las maquinas rotativas de absorcion, Parte II. In: CIES; 2008; Vigo, Spain. p. 363-98.

[132] Agyenim F., Knight I., Rhodes M. Design and experimental testing of the performance of an outdoor LiBr/H_2O solar thermal absorption cooling system with a cold store. Solar Energy. 2010; 84(5): 735-44.

[133] Labus J., Marimon M.A., Coronas A. Experimental evaluation of a small capacity H_20-LiBr absorption heat pump in cooling and heating modes. International Journal of Air-Conditioning and Refrigeration. 2010; 18(4): 317-25.

[134] M3003. The Expression of Uncertainty and Confidence in Measurement. United Kingdom Acreditation Service 2007.

[135] Methods for Minitab 16 Assistant (White papers for Assistant Menu): Regression. 2010.

[136] Lauer M., Padinger R. Environmentally Friendly Energy Supply in Wineries. In: Varbanov P., Klemeš J., Bulatov I. editors. ENERGY FOR SUSTAINABLE FUTURE; 5-6 May, 2008; University of Pannonia,Veszprém, Hungary.

[137] Jakob U., Spiegel K., Pink W. Development and experimental investigation of a novel 10kW ammonia/water absorption chiller chilli PSC - for air-conditioning and

refrigeration systems. In: International IEA Heat Pump conference; 20-22 May, 2008; Zurich, Switzerland.

[138] Kim M., Yoon S.H., Domanski P.A., Vance Payne W. Design of a steady-state detector for fault detection and diagnosis of a residential air conditioner. International Journal of Refrigeration. 2008; 31(5): 790-9.

[139] Sjöberg J., Zhang Q., Ljung L., Benveniste A., Delyon B., Glorennec P.Y., et al. Nonlinear black-box modeling in system identification: A unified overview. Automatica. 1995; 31(12): 1691-724.

[140] Joudi K.A., Lafta A.H. Simulation of a simple absorption refrigeration system. Energy Conversion and Management. 2001; 42(13): 1575-605.

[141] Kaynakli O., Kilic M. Theoretical study on the effect of operating conditions on performance of absorption refrigeration system. Energy Conversion and Management. 2007; 48(2): 599-607.

[142] Silverio R.J.R., Figueiredo J.R. Steady state simulation of the operation of an evaporative cooled water-ammonia absorption scale ice maker with experimental basis. Journal of the Brazilian Society of Mechanical Sciences and Engineering. 2006; 28: 413-21.

[143] Grossman G., Zaltash A. ABSIM - modular simulation of advanced absorption systems. International Journal of Refrigeration. 2001; 24(6): 531-43.

[144] Garimella S., Christensen R.N., Lacy D. Performance evaluation of a generator-absorber heat-exchange heat pump. Applied Thermal Engineering. 1996; 16(7): 591-604.

[145] Florides G.A., Kalogirou S.A., Tassou S.A., Wrobel L.C. Design and construction of a LiBr-water absorption machine. Energy Conversion and Management. 2003; 44(15): 2483-508.

[146] Gordon J.M., Ng K.C. A general thermodynamic model for absorption chillers: Theory and experiment. Heat Recovery Systems and CHP. 1995; 15(1): 73-83.

[147] Hellmann H.-M., Ziegler F.F. Simple absorption heat pump modules for system simulation programs. ASHRAE Transactions. 1999; 105.

[148] Labus J., Korolija I., Marjanovic-Halburd L., Coronas A. The Influence of Weather Conditions on Energy Performance of HVAC System and Absorption Cooling System Coupling. In: IAQVEC 2010: The 7th International Conference on Indoor Air Quality, Ventilation and Energy Conservation in Buildings; 2010 August 15-17; Syracuse, New York, USA.

[149] Sözen A., Akçayol M.A. Modelling (using artificial neural-networks) the performance parameters of a solar-driven ejector-absorption cycle. Applied Energy. 2004; 79(3): 309-25.

[150] Manohar H.J., Saravanan R., Renganarayanan S. Modelling of steam fired double effect vapour absorption chiller using neural network. Energy Conversion and Management. 2006; 47(15-16): 2202-10.

[151] Kühn A., Ziegler F. Operational results of a 10 kW absorption chiller and adaptation of the characteristic equation. In: Proceedings of First International Conference on Solar Air Conditioning; 2005; Bad-Staffelstein, Germany.

[152] Puig-Arnavat M., Lopez-Villada J., Bruno J.C., Coronas A. Analysis and parameter identification for characteristic equations of single- and double-effect absorption chillers by means of multivariable regression. International Journal of Refrigeration. 2010; 33(1): 70-8.

[153] Reddy T.A., Niebur D., Andersen K.K., Pericolo P.P., Cabrera G. Evaluation of the Suitability of Different Chiller Performance Models for On-Line Training Applied to Automated Fault Detection and Diagnosis (RP-1139). HVAC&R Research. 2003; 9(4): 385-414.

[154] Kim M., Yoon S.H., Payne W.V., Domanski P.A. Development of the reference model for a residential heat pump system for cooling mode fault detection and diagnosis. Journal of Mechanical Science and Technology. 2010; 24(7): 1481-9.

[155] McCulloch W.S., Pitts W. A logical calculus of the ideas immanent in nervous activity. Bulletin of Mathematical Biophysics. 1943; 5(Journal Article): 115-3.

[156] Narendra K.S., Parthasarathy K. Identification and control of dynamical systems using neural networks. IEEE transactions on neural networks / a publication of the IEEE Neural Networks Council. 1990; 1(1): 4-27.

[157] Bishop C.M. Neural networks and their applications. Review of Scientific Instruments. 1994; 65(6): 1803-31.

[158] Kalogirou S.A. Artificial neural networks in renewable energy systems applications: a review. Renewable and Sustainable Energy Reviews. 2001; 5(4): 373-401.

[159] Sözen A., Arcaklioglu E., Özalp M. A new approach to thermodynamic analysis of ejector–absorption cycle: artificial neural networks. Applied Thermal Engineering. 2003; 23(8): 937-52.

[160] Şencan A., Yakut K.A., Kalogirou S.A. Thermodynamic analysis of absorption systems using artificial neural network. Renewable Energy. 2006; 31(1): 29-43.

[161] Rosiek S., Batlles F.J. Modelling a solar-assisted air-conditioning system installed in CIESOL building using an artificial neural network. Renewable Energy. 2010; 35(12): 2894-901.

[162] Hagan M., Menhaj M. Training Feedforward Networks with the Marquardt Algorithm. IEEE Transactions on Neural Networks. 1994; 5(Journal Article): 989-93.

[163] Kim D.S., Infante Ferreira C.A., Tanda G.T., Pronk P. Optimization of a solar ammonia-water absorption chiller. In: Proceedings of the IIR Conference on Thermophysical Properties and Transfer Processes of Refrigerants; 2005; Vicenza, Italy.

[164] Evola G., Le Pierres N., Boudehenn F., Papillon P. Simulation and Experimental Results of a Small-size Solar-assisted Absorption Cooling System. In: Proceedings of ECOS 2010, 23rd International Conference on Efficiency, Cost, Optimization, Simulation, and Environmental Impact of Energy Systems; 2010 June 14-17; Lausanne, Switzerland.

[165] Mann L.J., Stewart, David O. *Refrigerating apparatus*. (1963)

[166] Anderson C.M. *Control systems*. (1966)

[167] Ogawa A., Hitomi K., Maekawa M., Yoshii K., Arima H., Enomoto E. *Control system for absorption refrigerator*. (1992)

[168] Yeung M.R., Yuen P.K., Dunn A., Cornish L.S. Performance of a solar-powered air conditioning system in Hong Kong. Solar Energy. 1992; 48(5): 309-19.

[169] Jenkins N. *Absorption chiller control logic*. (2003)

[170] Koeppel E.A., Mitchell J.W., Klein S.A., Flake B.A. Optimal supervisory control of an absorption chiller system. HVAC and R Research. 1995; 1(4): 325-42.

[171] Chow T.T., Zhang G.Q., Lin Z., Song C.L. Global optimization of absorption chiller system by genetic algorithm and neural network. Energy and Buildings. 2002; 34(1): 103-9.

[172] Wang S., Ma Z. Supervisory and optimal control of building HVAC systems: A review. HVAC and R Research. 2008; 14(1): 3-32.

[173] TRANE. Absorption Water Chillers - A Trane Air Conditioning Clinic. USA: The Trane Company, Worldwide Applied Systems Group, 3600 Pammel Creek Road, La Crosse, WI 54601-7599; 2000.

[174] YORK. YIA Single-Effect Absorption Chillers Steam and Hot Water Chillers. USA: Johnson Controls, Inc. P.O. Box 423, Milwaukee, WI 53201; 2010.

[175] CENTION. HWAR-L Hot Water Driven Absorption Chiller Product Data. CHP Solution Inc; 2007.

[176] TRANE. Thermachill Two-Stage Direct Fired Absorption Chillers 100-1100 Tons. USA: The Trane Company, Worldwide Applied Systems Group, 3600 Pammel Creek Road, La Crosse, WI 54601-7599; 2004.

[177] Pérez De Viñaspre M., Bourouis M., Coronas A., García A., Soto V., Pinazo J.M. Monitoring and analysis of an absorption air-conditioning system. Energy and Buildings. 2004; 36(9): 933-43.

[178] Lazzarin R. Steady and transient behaviour of LiBr absorption chillers of low capacity. International Journal of Refrigeration. 1980; 3(4): 213-8.

[179] Lazzarin R.M. Solar cooling plants: How to arrange solar collectors, absorption chillers and the load. International Journal of Low Carbon Technologies. 2007; 2(4): 376-90.

[180] YAZAKI 10, 20 and 30 RT S-series water fired single-effect absorption chiller / chiller-heater. Yazaki Energy Systems, Inc., 701 E. Plano Parkway, Suite 305, Plano, TX 75073-6700.

[181] Rotartica Solar 045, Installation and Maintenance Manual. Rotartica, S.A.

[182] Chilli PSC12 12kW absorption chiller, *Operating instructions / Installation manual*. SolarNext AG, Nordstrase 10, 83253 Rimsting, DE; 2008.

[183] Meléndez-González L.V., González-Cruz J.E., Beauchamp-Báez G. *Automation and control of solar air conditioning systems*. (2003)

[184] Storkenmaier F., Harm M., Schweigler C., Ziegler F., Albers J., Kohlenbach P., et al. Small-capacity water/LiBr absorption chiller for solar cooling and waste-heat driven cooling In: International Congress of Refrigeration 2003; Washington, D.C.

[185] Ziegler F., Hellmann H.M., Schweigler C. An approximative method for modeling the operating characteristics of advanced absorption chillers. In: 29th International Congress of Refrigeration; 1999 19.-24.09.; Sydney, Australia

[186] Lazzarin R.M. Solar cooling plants: Some characteristic system arrangements. International Journal of Low Carbon Technologies. 2007; 2(4): 391-404.

[187] Kohlenbach P. Solar Cooling Systems with Absorption Chillers: Control Strategies and Transient Chiller Performance [PhD thesis]. Erding, Germany: Technical University of Berlin, Forschungsberichte des Deutschen Kälte und Klimatechnischen Vereins, Nr. 74, 2006.

[188] Clauß V., Kühn A., Ziegler F. A new control strategy for solar driven absorption chillers. In: 2nd International Conference Solar Air Conditioning 2007; Tarragona, Spain. p. 44-50.

[189] Kühn A., Corrales Ciganda J.L., Ziegler F. Comparison of control strategies of solar absorption chillers. In: 1st International Conference on Heating, Cooling and Buildings, EUROSUN 2008; 2008; Lisbon, Portugal.

[190] Albers J., Kuhn A., Petersen S., Ziegler F. Control of absorption chillers by insight: the characteristic equation. In; 2008; Krakow, Poland.

[191] Pietruschka D., Jakob U., Hanby V., Eicker U. Simulation based optimisation and experimental investigation of a solar cooling and heating system. In: Solar air conditioning, 2nd international conference; 2006; Tarragona, Spain.

[192] Zetzsche M., Koller T., Müller-Steinhagen H. Solar cooling with an ammonia/water absorption chiller. In: EUROSUN 2008: Proceedings of the 1st International Conference on Heating, Cooling and Buildings; 2008; Lisboa, Portugal.

[193] Hernández J.A. Use of neural networks and neural network inverse in optimizing food processes. CAB Reviews: Perspectives in Agriculture, Veterinary Science, Nutrition and Natural Resources. 2009; 4(10).

[194] Hernández J.A. Optimum operating conditions for heat and mass transfer in foodstuffs drying by means of neural network inverse. Food Control. 2009; 20(4): 435-8.

[195] Lagarias J.C., Reeds J.A., Wright M.H., Wright P.E. Convergence properties of the Nelder—Mead simplex method in low dimensions. SIAM Journal of Optimization. 1998; No 1 vol 9(Journal Article): 112-47.

[196] Cortés O., Urquiza G., Hernández J.A. Optimization of operating conditions for compressor performance by means of neural network inverse. Applied Energy. 2009; 86(11): 2487-93.

[197] Colorado D., Hernández J.A., Rivera W., Martínez H., Juárez D. Optimal operation conditions for a single-stage heat transformer by means of an artificial neural network inverse. Applied Energy. 2011; 88(4): 1281-90.

[198] Labus J., Hernández J.A., Bruno J.C., Coronas A. Inverse neural network based control strategy for absorption chillers. Renewable Energy. 2012; 39(1): 471-82.

[199] Li H., Nalim R., Haldi P.A. Thermal-economic optimization of a distributed multi-generation energy system - A case study of Beijing. Applied Thermal Engineering. 2006; 26(7): 709-19.

[200] Documento Básico 2009. HE1: Limitación de demanda energética, Código Técnico de la Edificación aprobados por Real Decreto 314-2006 y el Real Decreto 1371-2007, (BOE 23-abril-2009), Ministerio de vivienda, España.

[201] prEN 14825: Air conditioners, liquid chilling packages and heat pumps, with electrically compressors, for space heating and cooling - Testing and rating at part load conditions and calculation of seasonal performance. European Committee for Standardization (CEN) 2009.

[202] Narasimhan S., Mah R.S.H., Tamhane A.C., Woodward J.W., Hale J.C. COMPOSITE STATISTICAL TEST FOR DETECTING CHANGES OF STEADY STATES. AIChE Journal. 1986; 32(9): 1409-18.

[203] Narasimhan S., Kao C.S., Mah R.S.H. DETECTING CHANGES OF STEADY STATES USING THE MATHEMATICAL THEORY OF EVIDENCE. AIChE Journal. 1987; 33(11): 1930-2.

[204] Loar J. Control for the Process Industries. Putman Publications: Chicago, IL. 1994; VII, No.11: 62.

[205] Alekman S.L. Control for the Process Industries. Putman Publications: Chicago, IL. 1994; VII, No.11: 62.

[206] Jubien G., Bihary G. Control for the Process Industries. Putman Publications: Chicago, IL. 1994; VII, No.11: 64.

[207] Glass A.S., Gruber P., Roos M., Todtli J. Qualitative model-based fault detection in air-handling units. IEEE Control Systems Magazine. 1995; 15(4): 11-22.

[208] Cao S., Rhinehart R.R. An efficient method for on-line identification of steady state. Journal of Process Control. 1995; 5(6): 363-74.

[209] Cao S., Rhinehart R.R. A self-tuning filter. Journal of Process Control. 1997; 7(2): 139-48.

[210] Cao S., Rhinehart R.R. Critical values for a steady-state identifier. Journal of Process Control. 1997; 7(2): 149-52.

[211] Önöz B., Bayazit M. The power of statistical tests for trend detection. Turkish Journal of Engineering and Environmental Sciences. 2003; 27(4): 247-51.

[212] Bhat S., Chatterjee T., Saraf D.N. On-line Data Processing and Product Properties Prediction for Crude Distillation Units

In: AIChE 2003 Spring National meeting 2003 March 30 - April 3; New Orleans, Louisiana. p. Paper No.115c.

[213] Bhat S.A., Saraf D.N. Steady-state identification, gross error detection, and data reconciliation for industrial process units. Industrial and Engineering Chemistry Research. 2004; 43(15): 4323-36.

[214] Jiang T., Chen B., He X., Stuart P. Application of steady-state detection method based on wavelet transform. Computers and Chemical Engineering. 2003; 27(4): 569-78.

[215] Schladt M., Hu B. Soft sensors based on nonlinear steady-state data reconciliation in the process industry. Chemical Engineering and Processing: Process Intensification. 2007; 46(11): 1107-15.

[216] Pilar Moreno R. Steady State Detection, Data Reconciliation, and Gross Error Detection: Development for Industrial Processes [MsC thesis]. New Brunswick: University of New Brunswick, 2010.

[217] Le Roux G.A.C., Santoro B.F., Sotelo F.F., Teissier M., Joulia X. Improving steady-state identification. In: Bertrand B., Xavier J., editors. Computer Aided Chemical Engineering: Elsevier; 2008. p. 459-64.

[218] Savitzky A., Golay M.J.E. Smoothing and Differentiation of Data by Simplified Least Squares Procedures. Analytical Chemistry. 1964; 36(8): 1627-39.

[219] Crowe C.M. Data reconciliation - Progress and challenges. Journal of Process Control. 1996; 6(2-3 SPEC. ISS.): 89-98.

[220] Melograno P.N., Fedrizzi R., Sparber W., Franchini G. Test Procedures for Sorption Chillers Based on the Working Mode. In: EUROSUN: International Conference on Solar Heating, Cooling and Buildings; October 2010; Graz.

Papers by the Author

Journal papers:

Labus J., Hernández J.A., Bruno J.C., Coronas A. Inverse neural network based control strategy for absorption chillers. Renewable Energy. 2012; 39(1): 471-82.

Labus J., Marimon M.A., Coronas A. Experimental evaluation of a small capacity H20-LiBr absorption heat pump in cooling and heating modes. International Journal of Air-Conditioning and Refrigeration. 2010; 18(4): 317-25.

Labus J., Bruno J.C., Coronas A. Performance analysis of small capacity absorption systems by means of different modelling approaches. Applied Thermal Engineering. (paper submitted)

Conference papers – refereed:

Labus J., Korolija I., Marjanovic-Halburd L., Coronas A. The Influence of Weather Conditions on Energy Performance of HVAC System and Absorption Cooling System Coupling. In: IAQVEC 2010: The 7th International Conference on Indoor Air Quality, Ventilation and Energy Conservation in Buildings; 2010 August 15-17; Syracuse, New York, USA.

Labus J., Marimon M.A., Coronas A. Experimental evaluation of small capacity H2O-LiBr absorption heat pump in cooling and heating modes. In: 9th IIR Gustav Lorentzen Conference; 2010; Sidney, Australia. p. 94.

Marimon M.A., **Labus J.**, Coronas A. Análisis experimental del funcionamiento de una enfriadora de agua por absorción de LiBr de pequeña potencia en un banco de ensayos. In: VI Jornadas Nacionales de Ingeniería Termodinámica; 2009 Jun 3-5; Córdoba, Spain.

Appendix A. Performance indicators

A.1 Seasonal Energy Efficiency Ratio (SEER)

SEER is a measure of equipment energy efficiency over the cooling season. It represents the total heat removed from the conditioned space during the normal cooling season as compared to the total electric energy input consumed during the same period. SEER is the similar to EER, but instead of being evaluated at a single operating condition, it represents the expected overall performance for a typical year's weather in a given location. According to CEN Standard prEN 14825 [201] it can be calculated:

$$\mathrm{SEER} = \frac{\sum_{j=1}^{n} h_j Q_c(T_j)}{\sum_{j=1}^{n} h_j \left(\frac{Q_c(T_j)}{\mathrm{EER}(T_j)}\right)}$$

T_j - the bin temperature

j - the bin number

n - the amount of bins

$Q_c(T_j)$ - the cooling demand of the building for the corresponding temperature T_j

h_j - the number of bin hours occurring at the corresponding temperature T_j

$\mathrm{EER}(T_j)$ - the EER values of the unit for the corresponding temperature T_j

A.2 Primary Energy Ratio (PER)

The primary energy ratio, also called the energy utilization coefficient, evaluates the energy-saving efficiency of air-conditioning systems, which is the ratio of the seasonal (annual) cooling capacity (or heating capacity) to the primary energy consumption of air-conditioning system, that is:

$$PER = \frac{Q_{c/h}}{Q_{driving,CHP} \cdot f_{P,CHP} + Q_{driving,solar} \cdot f_{P,solar} + Q_{driving,boiler} \cdot f_{P,boiler} + E_{tot,sys} \cdot f_{P,el}}$$

PER - primary energy ratio, $\left[\frac{kWh_{cold/heat}}{kWh_{PE}}\right]$

$Q_{c/h}$ – seasonal cooling/heating capacity, [kWh]

$Q_{driving}$ - driving heat for the system from different thermal sources (CHP, solar, natural gas boiler), [kWh]

$E_{tot,sys}$ - total electricity consumption of the system, [kWh]

f_P - primary energy factors

A.3 Primary Energy Savings (PES)

The amount of primary energy saved by some observed system (micro CCHP, solar thermal) is calculated as the difference between the primary energy of the reference (conventional) system necessary to meet the cooling (heating) demand, and the primary energy required by the observed system, given by:

$$PES = PE_{reference\ sys} - PE_{observed\ sys}$$

In the case of micro CCHP system, the primary energy savings associated to useful cool, for example, can be calculated using the vapour compression chiller as the reference. The micro-CHCP generates cooling in two steps: fuel is converted into heat and electricity first, and then heat is converted into cool by the thermally driven chiller at the additional expense of some electricity. In contrast, vapour compression chiller converts electricity directly into useful cool. The electricity is converted into primary energy.

$$PE_{cool,conv} = \frac{1}{EER} PRF_{el} \qquad \left[\frac{kWh_{cool}}{kWh_{LHV}}\right]$$

$$PE_{cool,mCCHP} = \frac{1}{COP \cdot \eta_{th}} PRF_{fuel} - \left(\frac{\eta_{el}}{COP \cdot \eta_{el}} - \varepsilon\right) PRF_{el} \qquad \left[\frac{kWh_{cool}}{kWh_{LHV}}\right]$$

$$PES_{cool} = PE_{cool,conv} - PE_{cool,mCCHP} \qquad \left[\frac{kWh_{cool}}{kWh_{LHV}}\right]$$

COP - chiller thermal coefficient of performance

EER - energy efficiency ratio of the vapour compression chiller

PRF_{fuel} - primary resource factor of fuel

η_{th} - thermal heat efficiency of the CHP

η_{el} - thermal electrical efficiency of the CHP

ε - parasitic consumption of the thermally driven chiller

PRF_{el} - primary resource factor of electricity

In the case of solar thermal systems PES can be calculated:

$$PES = \frac{Q_{fossil,ref} - Q_{aux,tot}}{\eta_{boiler} C_{fossil}} + \frac{E_{ref,tot} - E_{solar,tot}}{C_{el}} \qquad [kWh_{PE}]$$

$Q_{fossil,ref}$ - cooling (heating) demand in the reference system, [kWh]

$Q_{aux,tot}$ - total auxiliary heat of the observed solar system, [kWh]

$E_{ref,tot}$ - total electricity consumption of the reference system, [kWh]

$E_{solar,tot}$ - total electricity consumption of the observed solar system, [kWh]

C_{fossil} - conversion factor fossil heat, [$kWh_{heat,fossil}/kWh_{PE}$]

C_{el} - conversion factor electricity, [$kWh_{el,fossil}/kWh_{PE}$]

A.4 Annual savings CO_2

The amount of CO_2 saved can be calculated as a sum of CO_2 saved from heat of fossil fuels and CO_2 saved from electricity consumption when observed system is compared to reference (conventional) system:

$$\mathrm{CO_2}_{\mathrm{save}} = \frac{\mathrm{PES_{fossil}}}{\mathrm{CO_2}_{\mathrm{fossil}}} + \frac{\mathrm{PES_{el}}}{\mathrm{CO_2}_{\mathrm{el}}} \qquad [\mathrm{kgCO_2}]$$

PES_{fossil} - primary energy savings from fossil fuels when observed system is compared to reference system, [kWh_{PE}]

PES_{el} - primary energy savings from electricity consumption when observed system is compared to reference system, [kWh_{PE}]

$CO_{2_{fossil}}$- conversion factor fossil heat, [$kgCO_2/kWh_{heat,useful}$]

$CO_{2_{el}}$- conversion factor conventional electricity, [$kgCO_2/kWh_{el,useful}$]

A.5 General cost indicator

One of the cost indicators is the one which simply shows the cost of whole installation per kW of installed cooling (heating) capacity. This indicator takes into account the price of all the elements of the system (chiller, collectors, cooling tower, pumps,..) and the price for control and regulation.

$$\mathrm{Cost} = \frac{\mathrm{Investment}}{\mathrm{Installed\ cooling\ capacity}} \qquad \left[\frac{€}{\mathrm{kW}}\right]$$

Appendix B. Uncertainty estimation

The evaluation of uncertainty was done by constructing the uncertainty budgets for each of the derived variables. Two examples of uncertainty budgets constructed for Q_{eva} and $COP_{chiller,all}$ are shown in Table B.1 and Table B.2 with all the corresponding contributors.

Table B.1 Uncertainty budget for Q_{eva}

Quantity X_i	**Estimate x_i**	**Repeatability $u_1(x_i)$**	**Probability distribution divisor p_1**	**Accuracy $u_2(x_i)$**	**Probability distribution divisor p_2**	**Resolution $u_3(x_i)$**	**Probability distribution divisor p_3**	**Reference data $u_4(x_i)$**	**Probability distribution divisor p_4**	**Sensitivity coefficient c_i**	**Uncertainty contribution $u_i(y)$**
$T_{cw,in}$	Value	St.dev	1	0.1	$\frac{1}{\sqrt{3}}$	0.01	$\frac{1}{2\sqrt{3}}$			$\frac{\delta \dot{Q}_{eva}}{\delta T_{cw,in}}$	$\sqrt{\sum_{i=1}^{n} p_i^2 u_i^2 (x_i)}$
$T_{cw,out}$	Value	St.dev	1	0.1	$\frac{1}{\sqrt{3}}$	0.01	$\frac{1}{2\sqrt{3}}$			$\frac{\delta \dot{Q}_{eva}}{\delta T_{cw,out}}$	$\sqrt{\sum_{i=1}^{n} p_i^2 u_i^2 (x_i)}$
$\dot{V}_{cw}$	Value	St.dev	1	0.5% $\dot{V}_{cw}$	$\frac{1}{\sqrt{3}}$	0.01	$\frac{1}{2\sqrt{3}}$			$\frac{\delta \dot{Q}_{eva}}{\delta \dot{V}_{cw}}$	$\sqrt{\sum_{i=1}^{n} p_i^2 u_i^2 (x_i)}$
ρ_{cw}	Value							0.001 % ρ_{cw}	$\frac{1}{\sqrt{3}}$	$\frac{\delta \dot{Q}_{eva}}{\delta \rho_{cw}}$	$\sqrt{\sum_{i=1}^{n} p_i^2 u_i^2 (x_i)}$
Cp_{cw}	Value							0.1% Cp_{cw}	$\frac{1}{\sqrt{3}}$	$\frac{\delta \dot{Q}_{eva}}{\delta Cp_{cw}}$	$\sqrt{\sum_{i=1}^{n} p_i^2 u_i^2 (x_i)}$
Combined Uncertainty											$\boldsymbol{u(y) = \sqrt{\sum_{i=1}^{n} c_i^2 u_i^2 (y_i)}}$
Expanded Uncertainty											$\boldsymbol{U = k \cdot u(y)}$

Table B.2 Uncertainty budget for $COP_{chiller,all}$

Quantity X_i	Estimate x_i	Repeatability $u_1(x_i)$	Probability distribution divisor p_1	Accuracy $u_2(x_i)$	Probability distribution divisor p_2	Resolution $u_3(x_i)$	Probability distribution divisor p_3	Reference data $u_4(x_i)$	Probability distribution divisor p_4	Sensitivity coefficient c_i	Uncertainty contribution $u_i(y)$
$T_{cw,in}$	Value	St.dev	1	0.1	$\frac{1}{\sqrt{3}}$	0.01	$\frac{1}{2\sqrt{3}}$			$\frac{\delta COP_{chiller,all}}{\delta T_{cw,in}}$	$\sqrt{\sum_{i=1}^{n} p_i^2 u_i^2 (x_i)}$
$T_{cw,out}$	Value	St.dev	1	0.1	$\frac{1}{\sqrt{3}}$	0.01	$\frac{1}{2\sqrt{3}}$			$\frac{\delta COP_{chiller,all}}{\delta T_{cw,out}}$	$\sqrt{\sum_{i=1}^{n} p_i^2 u_i^2 (x_i)}$
$\dot{V}_{cw}$	Value	St.dev	1	0.5% $\dot{V}_{cw}$	$\frac{1}{\sqrt{3}}$	0.01	$\frac{1}{2\sqrt{3}}$			$\frac{\delta COP_{chiller,all}}{\delta \dot{V}_{cw}}$	$\sqrt{\sum_{i=1}^{n} p_i^2 u_i^2 (x_i)}$
ρ_{cw}	Value							0.001% ρ_{cw}	$\frac{1}{\sqrt{3}}$	$\frac{\delta COP_{chiller,all}}{\delta \rho_{cw}}$	$\sqrt{\sum_{i=1}^{n} p_i^2 u_i^2 (x_i)}$
Cp_{cw}	Value							0.1% Cp_{cw}	$\frac{1}{\sqrt{3}}$	$\frac{\delta COP_{chiller,all}}{\delta Cp_{cw}}$	$\sqrt{\sum_{i=1}^{n} p_i^2 u_i^2 (x_i)}$
$T_{hw,in}$	Value	St.dev	1	0.1	$\frac{1}{\sqrt{3}}$	0.01	$\frac{1}{2\sqrt{3}}$			$\frac{\delta COP_{chiller,all}}{\delta T_{hw,in}}$	$\sqrt{\sum_{i=1}^{n} p_i^2 u_i^2 (x_i)}$
$T_{hw,out}$	Value	St.dev	1	0.1	$\frac{1}{\sqrt{3}}$	0.01	$\frac{1}{2\sqrt{3}}$			$\frac{\delta COP_{chiller,all}}{\delta T_{hw,out}}$	$\sqrt{\sum_{i=1}^{n} p_i^2 u_i^2 (x_i)}$
$\dot{V}_{hw}$	Value	St.dev	1	0.5% $\dot{V}_{hw}$	$\frac{1}{\sqrt{3}}$	0.01	$\frac{1}{2\sqrt{3}}$			$\frac{\delta COP_{chiller,all}}{\delta \dot{V}_{hw}}$	$\sqrt{\sum_{i=1}^{n} p_i^2 u_i^2 (x_i)}$
ρ_{hw}	Value							0.001% ρ_{hw}	$\frac{1}{\sqrt{3}}$	$\frac{\delta COP_{chiller,all}}{\delta \rho_{hw}}$	$\sqrt{\sum_{i=1}^{n} p_i^2 u_i^2 (x_i)}$
Cp_{hw}	Value							0.1% Cp_{hw}	$\frac{1}{\sqrt{3}}$	$\frac{\delta COP_{chiller,all}}{\delta Cp_{hw}}$	$\sqrt{\sum_{i=1}^{n} p_i^2 u_i^2 (x_i)}$
E	Value	St.dev	1	1% E	$\frac{1}{\sqrt{3}}$	0.001	$\frac{1}{2\sqrt{3}}$			$\frac{\delta COP_{chiller,all}}{\delta E}$	$\sqrt{\sum_{i=1}^{n} p_i^2 u_i^2 (x_i)}$
Combined Uncertainty											$\boldsymbol{u(y) = \sqrt{\sum_{i=1}^{n} c_i^2 u_i^2 (y_i)}}$
Expanded Uncertainty											$\boldsymbol{U = ku(y)}$

Appendix C. Steady state identification

C.1 Literature review

Optimization, control and process performance assessment are strongly dependant on steady-state detection. The use of steady-state identification and simulation techniques is fundamental in several fields such as: process optimization, fault detection, performance assessment, gross error detection, sensor analysis, data reconciliation and empirical models built with regression or ANN. The data for such models should be collected in steady-state conditions, otherwise entire modelling can lead to failure. Usually, the information about steady-state identification when post-processing the experimental or whatever process measurements in order to develop accurate steady-state models is very scarce or even omitted in open literature. The adaptation of models to data obtained exclusively in steady-state operation leads to better solutions. Before proceeding, we should define what steady-state is, because this term can mislead. It is not "stationary" like in statistics, because there is no process parameter which is ever steady, but a process with parameters maintaining within some previously established thresholds. The steady-state identification can be on-line or off-line, depending on purpose of application. The analysis of real data is complex because they include stochastic component and, therefore, the use of statistical methods is necessary to perform the task.

The most common methods for steady-state identification are based on calculating either the mean, variance or regression slope over a data window and performing the statistical test such as t-test. Generally, all the statistical methods tend to reduce type I and II errors. Type I error is the error of rejecting the null hypothesis (not at steady-state) when it is actually true. Type II error is the error of failing to reject the null hypothesis when it should be rejected. Despite the existence of different steady-state detection procedures, one cannot say with assurance which provides the best results. The following section provides a literature review on different steady-state detection techniques, trying to highlight the advantages and disadvantages in order to find the optimal and the simplest to apply it for absorption equipment.

Narasimhan et al. [202] proposed a composite statistical test to detect when process variables change steady-states. It is well-known fact in multivariate statistics that the distribution arises with the differences between the means of different populations. Thus, the authors suggested comparing the covariance matrices in two consecutive time periods. Hotelling T^2 method (which is the multivariate counterpart of Student's t-distribution) would be performed to check whether the periods have equal means in case when the covariance matrices are the same. Conversely, in case when the covariance matrices are unequal, non central T^2 test is performed. This method assumes that only random errors exist with zero means, and successive periods of time are assumed to be steady. A change of steady-state may occur from one period to the next, but within each period the process is in steady-state. Narasimhan and co-workers [203] also suggested a test for detecting changes in steady state by using the mathematical theory of evidence. A key element of this method is the assignment of beliefs to the different propositions of interest. Since this usually involves subjective judgement, the authors used the probabilities from the T^2 distribution to assign beliefs that process is at steady state, non-steady state, and uncertain. Hotelling T^2-statistic is used again, defined by comparing the difference of means between periods to the variability within the periods. In addition, the results of simulation analysis in the same study showed that both methods (composite statistical test and method with mathematical theory of evidence) have the same performance. However, in practice is not so easy to find successive time periods within which process variables are in steady state. Hence, it is very difficult to satisfy this specific assumption for both methods. The Type I error of the composite test is theoretically independent of the number of variables and period size. However, in practice it was found to be strongly dependent on both the number of variables and period size when applied to plant data.

In 1994 three papers were addressed to the topic how to detect steady-state conditions automatically. Loar [204] suggested a moving average chart with thresholds of $\pm 3\sigma$. When the moving average breaks the thresholds value, the alarm indicates that some irregularity has occurred. However, this method cannot indicate steady-state; it is used to trigger control. Another method [205] compares the average from a recent history to a "standard" based on an earlier history and then use t-statistic test to check if the average changed. A problem of this approach is that the steady-state hypothesis and

equal mean are quite different. If the process is oscillating and the data window happens to bracket the "standard" mean, then the t-test could accept the equal mean hypothesis when, in fact, the process steady-state hypothesis should be rejected. On the other hand, data storage and data processing are computational burden. The third method reported by Jubien and Bihary [206] is based on calculating the standard deviation of selected process variables over a moving window of recent data period. The measured standard deviation must be within some established limits; otherwise, not at steady-state condition is triggered. The success of the method depends on the process variables time period, selection of process variables and the "threshold" standard deviation. Same as previous, this method is computational burden.

Glass et al. [207] in their study on fault detection in air-handling units control the steady-state behaviour of the system by mixing the outside air with return air to ensure that the temperature of the mixed air is closed to the supply air set-point temperature. It is considered that the system operates in steady-state conditions if the fraction of outside air in the mix is within constrained bounds. The geometrically weighted variance is used to identify steady state, where the older data are removed by multiplication with forgetting factor based on time constant. In other words, the steady state identification is based on very simple approach, defining the upper and down limits using user's expertise.

Cao and Rhinehart [208, 209] developed a new method for the on-line identification of steady-state. Their method uses critical values of an F-like test applied to the ratio of two different estimates of variances of data time series. When the ratio (evaluated at each time step) is close to one, the process can be considered as steady-state. The first estimate of variance is based on the filtered squared deviation from previous filtered value while the second estimate is based on filtered square differences of successive data. Each of the estimates of variances is calculated using a conventional exponentially weighted moving average or conventional first-order filter in order to replace the sample mean. In this way, moving data windows are avoided and consequently storage and computational requirements are reduced. The filter factors λ_1, λ_2 and λ_3, varying from 0 to 1, must be tuned empirically in order to allow the minimization of type I and type II errors. The authors presented a short note about the

critical values [210]. The filter factors values are set based on the relevance of the actual values in comparison to the past ones, and could be interpreted as forgetting factors expressing something analogue to a window size. Although Cao and Rhinehart method can perform at any point of time, time delay is still present as well as the insensitivity to changes due to use of filtering techniques. Also, the adequate selection of the filter factors (which is empirical) requires a certain amount of experience.

Önöz and Bayazit [211] compared the t-test for trend detection with Mann-Kendall's test. The results of a simulations showed that the t-test is slightly more powerful when the probability distribution is normal, while for moderately skewed distribution Mann-Kendall test gives slightly better results. The authors' conclusion is that these two tests can be used interchangeably in practical applications.

A development of steady-state identifier for industrial process units was also addressed in two papers of Bhat and co-authors [212, 213]. Actually, the authors applied the method of Cao and Rhinehart with some modifications. These modifications are related to optimization of the exponential filter constants. This optimization is based on minimizing the delay to identify steady-state or unsteady-state, minimizing at the same time type I and II errors. However, this optimization is empirical (trial and error) since there are not analytical relationship between the exponential filter constant and the delay time and type I and II errors.

Jiang et al. [214] proposed a method for steady-state detection in continuous processes based on wavelet transform. Multi-scale wavelet processing technique was used to remove random noise and non-random errors extracting the process trends from raw measurements. The process status is measured using an index ranging from 0 to 1 according to the wavelet transform modulus indicating steady-state if its value is close to zero. Although authors demonstrated this method can be implemented on-line in crude oil unit, there are several problems which must be addressed. Real-time data have to be truncated to fit the window size, the determination of characteristic scale for steady state detection, boundary effects are introduced since the wavelet transform is carried out with finite dimension data set and there is a time delay. The solution, according to the authors, is to use a symmetric extent technique. However, the method seems to be mathematically very complex and the same authors emphasize the

importance of the experience with the process being considered. The experience and the data treatment method to determine key parameters such as the threshold values and the degree of the contribution from the second-order wavelet transform.

Regression is a useful technique in data analysis when one or more variables influence or affect a second or multiple variables. This method belongs to a group of so-called direct approaches. Normally, it consists in performing linear regression over a data window and then to use a t-test on the regression slope. For a given sample size and confidence interval, the calculated t values are compared with critical values of t in a standard table. If the hypothesis that there is no correlation between the x and y variables is not rejected at the chosen level of significance, the slope of the line cannot be shown to differ statistically from zero. This can be statistically considered as a steady-state in the y-variable. The examples of this approach can be found in the paper of Schladt and Hu [215] and in thesis of Pilar Moreno [216]. Schladt and Hu used t-test-type steady-state check by comparing the mean values of two subsequent time intervals. Pilar Moreno in her thesis performed the least square linear regression over a moving data window in order to find the equation of the best-fitting line for a set of data, and to analyze the rate-of-change of the line reflected in the slope. Steady-state can be identified if the slope is smaller than the threshold for several samples. The threshold in this case is not a constant but a function which depends on set point change and standard deviation of the noise. Another parameter, the size of the moving window depends upon the time constant of the variable and not on sampling time, which is usual practice.

Kim et al. [138] developed a steady-state detector for fault detection and diagnosis of vapour compression system based on moving window and using standard deviation of seven selected variables. The threshold value of three standard deviations ($\pm 3\sigma$) was selected as boundary within which the variable is considered to be in steady-state. The standard deviations of each variable were calculated based on three repeated measurements of the start-up transient tests. Again, the problem which usually follows moving window methods is time delay which can cause that some of the transient periods escape filtering. Another disadvantage is the optimum size of the moving

window which has to be determined empirically and which depends upon the system controller and instrumentation.

Le Roux et al. [217] in their study compared four different steady-state identification methods: modified F-test (Cao and Rhinehart), Reverse Arrangements Test, Rank von Newman Test and Polynomial Interpolation Test (based on Sawitzky and Golay algorithm [218]). Using a Monte-Carlo simulation and data from crude oil distillation unit the authors drove a conclusion that for simulated data Polynomial Interpolation Test performs better than the other tests considered.

Some other statistical methods like Wald-Wolowitz Runs test, the Mann-Kendall or Principal Component Analysis were also mentioned in a literature [215, 219] as a possibility for steady-state identification, but the practical application was not found.

As can be seen from this review, there are different methods which can be applied for steady-state identification. All of them have their cons and pros which depend on type of application and purpose. For off-line identification the moving window charts are usually the most suitable solution while for on-line identification in process plant more suitable are methods such as Cao and Rhinehart modified F-test or Polynomial Interpolation Test which are not computational burden. On the other hand, these tests can be mathematically very complex requiring some additional filter factors and very often some user expertise. Very often there is a problem with time-delay when detecting changes from steady-state to transient conditions. Therefore, when choosing a method for steady-state identification, one should make a balance between the purpose of the application and the complexity of the detector. Usually, in different system applications or experimental set ups such as URV multifunctional test bench, absorption equipment is already controlled through the external circuit temperatures and flow rates. The use of steady-state detectors is hence off-line, when post-processing the data which will further be used in model development. The steady-state detector developed in this thesis is based on moving window methodology, the modified methodology for absorption equipment of the one proposed by Kim et al. [138]. The problem with additional remaining transients periods caused by time delays when changing from one

steady-state to another is solved by applying a simple additional filter developed to reduce this noise.

C.2 Moving window

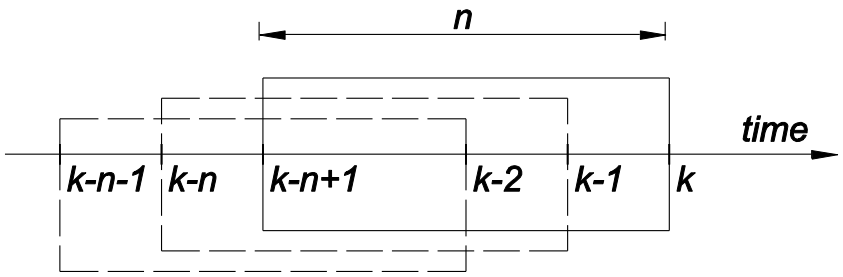

Figure C.1 Moving window

In statistics, the simple moving average algorithm is an equally weighted sum of the previous n historical samples where each weight equals 1/n for each historical sample. The algorithm resembles to a rectangular window which slides over the data points as the moving average moves, and therefore, the parameter n is often called the window size. The window size is a predefined time interval over which important parameters are sampled at regular intervals. This is equal to a low pass filter, where a moving window replaces each historical sample within the timespan. This is illustrated in Figure C.1.

In this way, the moving window can be used as steady-state detector which identifies steady operation of the selected parameters if they fall below the defined threshold. Following the work of Kim et al., we selected the value of the $\pm 3\sigma$ as a threshold. In other words, if the selected parameter falls within plus or minus three standard deviation of its average value, the parameter is considered to be in steady-state.

By using a recursive formulation of the moving window algorithm, the average of the latest n samples of a data sequence x_i at any instant k was calculated by using equation C.1:

$$\bar{x}_k = \frac{1}{n}\sum_{i=k-n+1}^{k} x_i \tag{C.1}$$

A difference between averages of two consecutive samples, at the time k, and the previous time interval k-1 was given by (C.2):

$$\bar{x}_k - \bar{x}_{k-1} = \frac{1}{n}\left[\sum_{i=k-n+1}^{k} x_i - \sum_{i=k-n}^{k-1} x_i\right] = \frac{1}{n}[x_k - x_{k-n}] \tag{C.2}$$

Or rearranged in other form:

$$\bar{x}_k = \bar{x}_{k-1} + \frac{1}{n}(x_k - x_{k-n}) \tag{C.3}$$

A moving window variance was defined similarly (equations C.4 and C.5):

$$var_k - var_{k-1} = \frac{1}{n}\sum_{i=k-n+1}^{k}(x_k - \bar{x}_{k-n})^2 = \frac{1}{n}\sum_{i=k-n+1}^{k} x_i^2 - \bar{x}_k^2 \tag{C.4}$$

$$var_k = var_{k-1} + \frac{1}{n}\left(x_k^2 - x_{k-n}^2\right) - \left(\bar{x}_k^2 - \bar{x}_{k-1}^2\right) \tag{C.5}$$

The standard deviation of the moving window was calculated as a square root of moving window variance (C.6):

$$\sigma_k = \sqrt{var_k} \tag{C.6}$$

The monitored parameters which have to pass the moving window filter were: all the directly measurable parameters of external flow circuits (inlet and outlet temperatures and flow rates). The standard deviations of all nine selected parameters had to stay within their respective threshold values as the window moved to indicate steady-state. If any of these parameters passed the threshold limits, the operation of the absorption machine would not be considered as steady-state. Start up transient test was

included for defining steady-state detection parameters. The start up repeatability was verified by repeating the start up test three times under the same operating conditions.

The most delicate part of moving window method is determining the appropriate window size and the standard deviation threshold value. Special care has to be taken when determining window size since too small thresholds can cause that detector never detects steady-state while large thresholds carry the risk of including some transient data. In our case, the standard deviation threshold values for each parameter were calculated as average values of standard deviations for five different steady-state tests. The moving window size was established by using start up transient tests. According to Kim et al., time interval should include at least 30 samples in transient region and also has to be extended with steady-state samples in order to size the window properly. The steady-state region begins, as mentioned above, when all the selected parameters fluctuate within $\pm 3\sigma$ of their steady-state mean values.

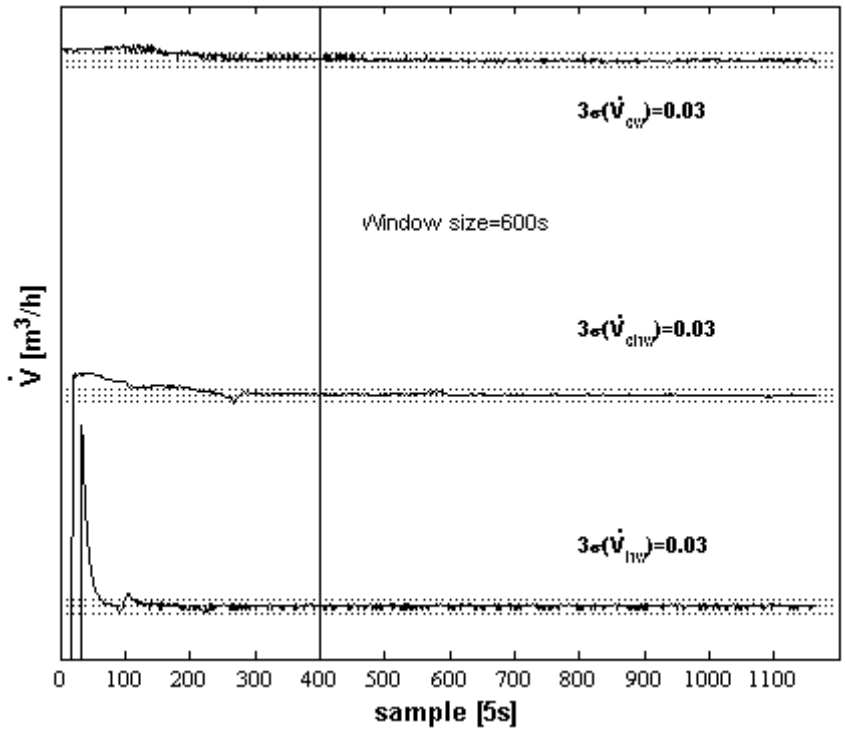

Figure C.2 Variation of flow rates during a start up test

Figure C.2 and Figure C.3 show the variation of the monitored parameters during one of the start up transient tests. The flow rates reached steady-state conditions

approximately after 220 samples as can be seen from Figure C.2. Some of the temperatures also reached steady-state conditions soon after the flow rates. The last parameters to reach steady-state conditions were cooling water inlet temperature and hot water outlet temperature. As indicated in Figure C.3, the moment when all the parameters reached steady-state was 2245 seconds after the start up.

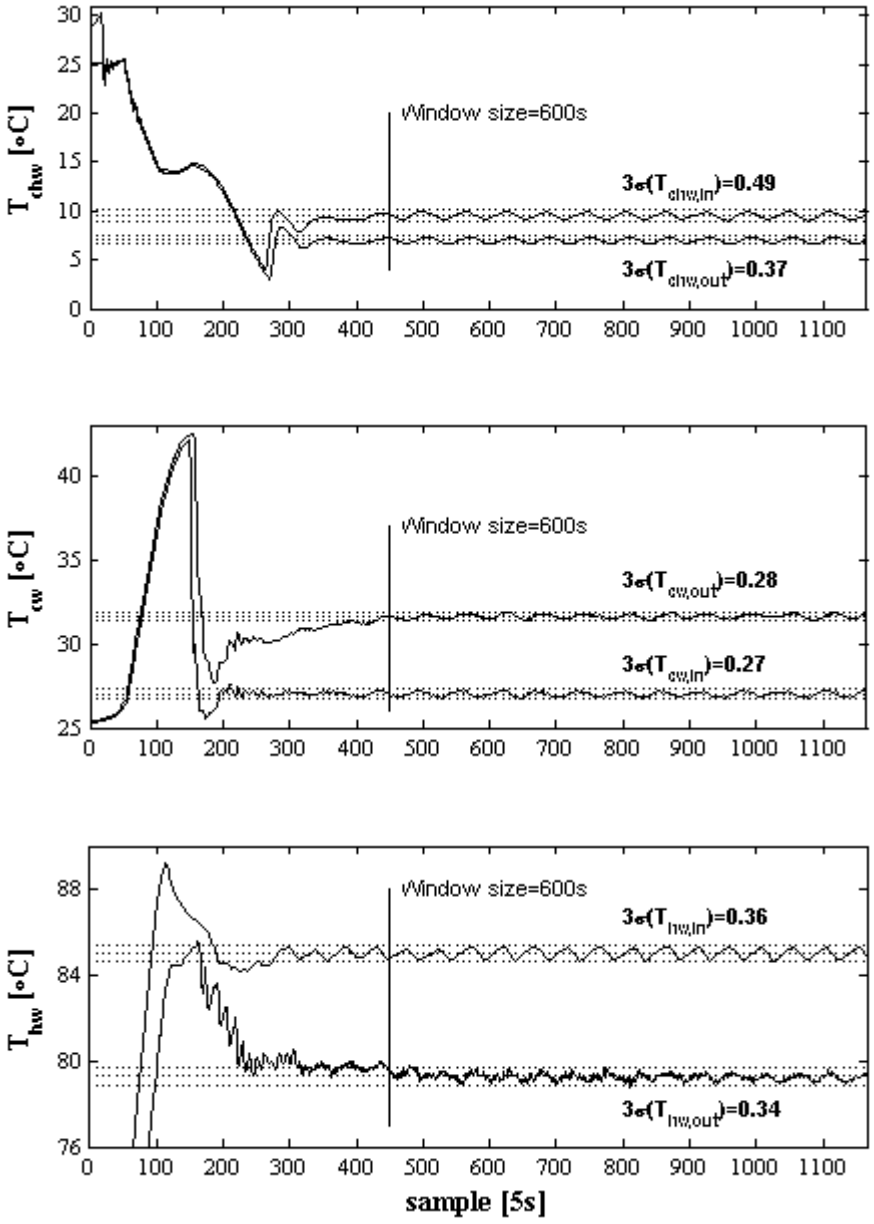

Figure C.3 Variation of temperatures during a start up test

However, the main problem is how to find the minimum window size which will detect steady-state at the point where it really begins. Too small window size can cause

that detector detects steady-state when it is still in transient region. On the other hand, larger window sizes could be acceptable, but they would indicate the onset of steady-state after it really occurred. That would not be the minimum window size which satisfies the criteria that all monitored parameters remain within their $\pm 3\sigma$ thresholds.

As can be seen, the procedure of finding the minimum window size is based on trial and error. For all parameters, the moving window standard deviation versus time was calculated for a range of moving window selected. In the case of the tested absorption chiller, several window sizes were tried in the range from 100s to 700s. Finally, the window size of 600s was chosen since it showed the best detection performance. This window size was confirmed by applying it on several transient start up tests.

The disadvantage of every moving average window is that it may introduce a lag in the computed curve, which in our case might cause that some transient samples are detected as steady-state. This was prevented by applying a simple additional filter developed to reduce this noise.

C.3 Additional steady state filter

The simple additional filter was developed based on requirements of absorption chiller Standards [108, 109] for tests of water-cooled chillers in steady-state conditions. The steady-state condition is considered to be obtained and maintained when all the measured quantities caused by technical operation of the control and regulation devices remain within the permissible deviation listed in Table C.1. These conditions can be easily implemented by writing few lines of program code in Excel (using Macros) or any suitable software. By using this filter, the steady-state regions detected by moving window detector will be cleaned from residual transient samples if they appear.

Table C.1 Permissible deviation from set values in steady- state conditions

Measured quantity	**Permissible deviation of the arithmetic mean values from set values ±**	**Permissible deviation of the individual measured values from set values ±**
Inlet temperature	0.2ºC	0.5ºC
Outlet temperature	0.3ºC	0.6ºC
Flow	2%	5%

C.4 Check

The check of filtered steady-state intervals can be performed by using the work of Melograno et al. [220] According to the authors, the ratio of the average of the real temperatures divided by the difference between the set inlet temperature and outlet average temperature should be equal or higher to 0.95 to be considered as steady-state as presented by equation C.7. Also the static pressure difference in the external circuits should not vary more than ±10%.

$$R = \frac{\overline{T_{in,real} - T_{out,real}}}{T_{in,set} - \overline{T_{out,real}}} \geq 0.95 \quad (C.7)$$

Appendix D. Test Results

Table D.1 shows the summary of the operation for absorption chiller Pink chilli 12 under different temperature conditions.

Table D.1 ***Summary of the tests with Pink chilli 12 for fan-coil applications***

No	$T_{chw,in}$ [ºC]	$T_{chw,out}$ [ºC]	$\dot{V}_{chw}$ [$\frac{m^3}{h}$]	$T_{cw,in}$ [ºC]	$T_{cw,out}$ [ºC]	$\dot{V}_{cw}$ [$\frac{m^3}{h}$]	$T_{hw,in}$ [ºC]	$T_{hw,out}$ [ºC]	$\dot{V}_{hw}$ [$\frac{m^3}{h}$]	$\dot{Q}_{eva}$ [kW]	$\dot{Q}_{ac}$ [kW]	$\dot{Q}_{gen}$ [kW]	$COP_{chiller,th}$
1	8.66	5.04	1.72	27.00	30.84	4.75	80.01	75.00	2.24	7.26	21.11	12.72	0.57
2	9.94	5.99	1.72	27.00	31.06	4.76	79.97	74.77	2.24	7.92	22.34	13.20	0.60
3	11.26	7.01	1.72	27.02	31.18	4.78	79.99	74.68	2.24	8.50	23.04	13.49	0.63
4	12.50	7.86	1.72	27.00	31.48	4.78	80.00	74.38	2.24	9.27	24.81	14.26	0.65
5	14.12	8.97	1.72	27.02	31.75	4.78	79.98	74.19	2.24	10.29	26.11	14.70	0.70
6	15.41	9.99	1.72	27.03	31.93	4.77	79.97	74.05	2.24	10.83	27.04	15.05	0.72
7	16.59	10.95	1.72	27.02	32.11	4.77	79.98	73.89	2.24	11.28	28.08	15.46	0.73
8	7.01	4.98	1.72	30.00	32.46	4.75	79.99	76.73	2.24	4.07	13.53	8.28	0.49
9	8.36	6.02	1.72	29.99	32.65	4.76	80.00	76.59	2.24	4.70	14.60	8.65	0.54
10	9.66	7.04	1.72	29.99	32.79	4.76	80.00	76.44	2.24	5.23	15.42	9.03	0.58
11	10.95	8.02	1.72	30.00	32.95	4.76	80.00	76.33	2.24	5.88	16.23	9.33	0.63
12	12.25	9.03	1.72	30.00	33.10	4.76	79.99	76.18	2.24	6.43	17.11	9.65	0.67
13	13.88	10.03	1.72	30.00	33.52	4.76	80.01	75.82	2.24	7.69	19.37	10.65	0.72
14	15.16	11.01	1.72	30.01	33.67	4.76	80.00	75.70	2.24	8.29	20.15	10.92	0.76
15	16.37	12.07	1.72	29.99	33.80	4.77	80.00	75.58	2.24	8.59	20.97	11.24	0.76
16	5.52	5.00	1.72	33.00	34.23	4.80	80.00	77.99	2.24	1.05	6.82	5.11	0.21
17	6.82	6.01	1.72	32.98	34.48	4.80	80.02	77.80	2.24	1.63	8.27	5.65	0.29
18	8.09	6.99	1.72	33.00	34.66	4.80	79.99	77.59	2.24	2.22	9.18	6.07	0.36
19	9.27	7.98	1.72	33.00	34.70	4.79	79.90	77.59	2.24	2.59	9.39	5.87	0.44
20	10.92	9.07	1.72	33.02	34.97	4.78	79.94	77.41	2.24	3.70	10.76	6.43	0.58
21	12.20	10.06	1.72	33.01	35.09	4.79	80.00	77.35	2.24	4.27	11.55	6.73	0.63
22	6.29	6.04	1.72	35.00	36.08	4.79	80.00	78.17	2.24	0.49	5.99	4.64	0.11
23	7.39	6.98	1.72	35.00	36.17	4.79	80.01	78.10	2.24	0.83	6.50	4.83	0.17
24	8.50	8.01	1.72	34.99	36.20	4.79	80.02	78.07	2.24	0.99	6.69	4.95	0.20
25	9.65	8.99	1.72	35.00	36.31	4.79	80.00	77.95	2.24	1.33	7.23	5.20	0.26
26	10.80	9.89	1.72	34.99	36.49	4.79	79.94	77.82	2.24	1.83	8.29	5.38	0.34
27	9.15	5.00	1.71	27.00	31.38	4.78	84.99	79.09	2.23	8.28	24.19	14.85	0.56
28	10.45	5.98	1.72	27.00	31.55	4.78	85.00	79.01	2.23	8.95	25.15	15.09	0.59
29	12.03	7.02	1.72	27.00	31.82	4.78	84.99	78.84	2.24	10.03	26.62	15.60	0.64
30	13.23	8.00	1.72	26.98	31.91	4.78	84.98	78.81	2.24	10.46	27.21	15.64	0.67
31	14.44	9.01	1.72	27.04	32.24	4.78	84.99	78.62	2.24	10.84	28.79	16.16	0.67
32	15.75	10.00	1.72	27.07	32.29	4.78	85.03	78.39	2.24	11.49	28.87	16.83	0.68
33	17.04	11.01	1.72	27.05	32.45	4.77	85.02	78.27	2.24	12.03	29.77	17.11	0.70

34	8.00	5.04	1.73	30.00	33.38	4.76	85.01	80.38	2.24	5.96	18.66	11.73	0.51
35	9.22	6.04	1.71	30.00	33.50	4.77	84.99	80.29	2.23	6.34	19.30	11.87	0.53
36	10.65	6.99	1.72	30.00	33.79	4.77	84.98	79.94	2.24	7.33	20.94	12.76	0.57
37	11.97	7.98	1.73	30.00	34.05	4.77	85.01	79.65	2.24	8.03	22.29	13.54	0.59
38	13.10	8.99	1.74	30.00	34.10	4.77	84.98	79.62	2.24	8.31	22.58	13.59	0.61
39	14.39	10.01	1.74	30.00	34.22	4.77	85.03	79.67	2.24	8.85	23.28	13.58	0.65
40	15.71	10.98	1.72	29.99	34.41	4.77	85.00	79.41	2.24	9.45	24.36	14.13	0.67
41	17.00	12.00	1.72	29.98	34.59	4.77	84.97	79.23	2.23	9.99	25.41	14.50	0.69
42	6.47	5.03	1.72	33.00	35.04	4.79	85.01	81.88	2.24	2.89	11.31	7.92	0.36
43	7.68	6.01	1.71	33.00	35.18	4.80	85.01	81.70	2.23	3.33	12.09	8.37	0.40
44	8.87	6.99	1.71	33.01	35.37	4.81	85.04	81.51	2.23	3.75	13.12	8.91	0.42
45	10.51	7.99	1.71	33.01	35.85	4.78	85.01	81.06	2.24	5.00	15.68	10.00	0.50
46	11.83	8.98	1.71	33.00	36.07	4.78	85.00	80.76	2.24	5.67	16.95	10.71	0.53
47	13.10	10.02	1.71	33.00	36.24	4.79	85.01	80.57	2.24	6.14	17.92	11.24	0.55
48	14.45	11.10	1.72	32.99	36.42	4.78	85.00	80.36	2.24	6.68	18.92	11.73	0.57
49	15.62	12.05	1.72	33.00	36.56	4.78	85.00	80.22	2.24	7.15	19.62	12.07	0.59
50	5.52	5.01	1.73	35.00	36.36	4.79	85.01	82.62	2.25	1.03	7.50	6.07	0.17
51	6.83	5.99	1.73	34.99	36.59	4.79	85.01	82.43	2.24	1.70	8.83	6.56	0.26
52	8.18	7.01	1.73	35.00	36.81	4.77	85.00	82.18	2.24	2.36	9.97	7.13	0.33
53	9.50	8.01	1.73	35.00	37.03	4.77	85.00	81.94	2.23	3.00	11.19	7.73	0.39
54	10.77	9.02	1.73	35.00	37.23	4.77	85.00	81.73	2.23	3.53	12.28	8.27	0.43
55	12.12	10.02	1.73	35.00	37.43	4.77	85.00	81.53	2.23	4.25	13.36	8.75	0.49
56	13.40	11.04	1.73	35.00	37.61	4.76	84.99	81.36	2.23	4.76	14.35	9.18	0.52
57	14.60	12.03	1.73	35.00	37.80	4.75	85.00	81.16	2.23	5.15	15.38	9.70	0.53
58	9.96	5.01	1.72	27.02	32.04	4.76	90.04	83.39	2.24	9.92	27.67	16.82	0.59
59	11.17	6.04	1.72	26.99	32.20	4.75	90.04	83.23	2.24	10.26	28.63	17.22	0.60
60	12.58	7.00	1.72	27.00	32.42	4.75	90.04	83.05	2.24	11.17	29.75	17.66	0.63
61	13.89	7.93	1.72	27.05	32.61	4.75	90.04	82.92	2.24	11.91	30.52	18.02	0.66
62	15.28	8.99	1.72	27.00	32.88	4.75	89.99	82.68	2.24	12.56	32.27	18.48	0.68
63	16.51	9.96	1.72	26.95	32.98	4.75	90.04	82.67	2.24	13.09	33.13	18.66	0.70
64	17.78	11.02	1.72	27.02	33.10	4.75	90.07	82.54	2.24	13.52	33.41	19.03	0.71
65	8.73	5.00	1.72	30.00	33.92	4.76	90.01	84.81	2.24	7.47	21.53	13.12	0.57
66	10.08	6.02	1.72	30.00	34.13	4.76	90.00	84.60	2.24	8.13	22.75	13.64	0.60
67	11.41	7.01	1.72	30.01	34.31	4.76	90.01	84.46	2.24	8.81	23.72	14.03	0.63
68	13.06	7.99	1.72	30.01	34.79	4.77	90.00	83.95	2.24	10.13	26.38	15.30	0.66
69	14.40	9.00	1.72	30.02	34.95	4.77	90.01	83.88	2.24	10.80	27.17	15.51	0.70
70	15.67	10.01	1.72	30.01	35.09	4.78	90.02	83.72	2.24	11.30	28.06	15.93	0.71
71	16.83	10.93	1.72	30.00	35.19	4.79	90.02	83.66	2.24	11.79	28.75	16.09	0.73
72	7.62	5.03	1.72	33.00	35.99	4.78	90.00	85.82	2.24	5.18	16.53	10.56	0.49
73	8.92	6.02	1.72	33.00	36.18	4.78	90.00	85.65	2.24	5.82	17.56	10.98	0.53
74	10.32	7.01	1.72	33.00	36.39	4.78	90.00	85.50	2.24	6.62	18.74	11.39	0.58
75	11.71	8.01	1.72	32.99	36.66	4.78	90.00	85.22	2.24	7.40	20.26	12.09	0.61
76	13.01	9.02	1.72	33.01	36.77	4.79	90.00	85.16	2.24	7.97	20.81	12.26	0.65
77	14.14	10.04	1.72	32.99	37.03	4.76	90.00	84.82	2.24	8.21	22.17	13.11	0.63

78	15.45	11.05	1.72	33.00	37.21	4.76	89.99	84.65	2.24	8.78	23.12	13.50	0.65
79	16.62	12.05	1.72	33.00	37.25	4.79	90.00	84.61	2.24	9.13	23.51	13.64	0.67
80	6.40	4.98	1.72	35.00	37.21	4.78	90.00	86.57	2.24	2.84	12.19	8.67	0.33
81	7.77	6.05	1.72	35.00	37.43	4.78	89.99	86.36	2.24	3.46	13.41	9.18	0.38
82	9.07	7.00	1.72	35.00	37.66	4.79	90.01	86.11	2.24	4.14	14.66	9.86	0.42
83	10.42	8.02	1.72	35.00	37.86	4.78	89.99	85.91	2.24	4.81	15.80	10.33	0.47
84	11.72	9.04	1.72	35.00	38.09	4.78	89.99	85.64	2.24	5.37	17.08	11.00	0.49
85	13.04	10.04	1.72	35.00	38.32	4.78	89.98	85.39	2.24	6.00	18.30	11.60	0.52
86	14.32	10.99	1.72	35.00	38.52	4.78	90.00	85.20	2.24	6.65	19.39	12.11	0.55
87	15.66	12.10	1.72	34.99	38.72	4.77	89.99	85.03	2.24	7.12	20.51	12.53	0.57
88	10.80	5.05	1.72	27.01	33.01	4.75	95.03	87.31	2.24	11.52	32.97	19.48	0.59
89	11.94	6.01	1.72	27.01	33.20	4.77	95.07	87.06	2.24	11.86	34.14	20.24	0.59
90	13.37	6.98	1.72	27.05	33.32	4.78	95.06	86.94	2.24	12.79	34.68	20.52	0.62
91	14.74	8.03	1.72	27.03	33.55	4.78	95.05	86.75	2.24	13.42	36.03	20.94	0.64
92	16.02	8.99	1.72	26.99	33.73	4.78	95.04	86.57	2.24	14.04	37.24	21.38	0.66
93	17.38	10.02	1.72	27.05	33.99	4.78	95.02	86.51	2.24	14.69	38.41	21.48	0.68
94	9.22	5.00	1.72	30.00	34.83	4.76	95.05	88.33	2.24	8.46	26.56	16.96	0.50
95	10.66	5.99	1.72	30.01	35.10	4.76	95.03	88.16	2.24	9.35	28.00	17.34	0.54
96	12.08	7.01	1.72	30.01	35.42	4.76	95.05	87.81	2.24	10.13	29.71	18.27	0.55
97	13.78	7.99	1.72	30.00	35.48	4.76	95.04	88.21	2.24	11.57	30.11	17.24	0.67
98	14.69	9.01	1.72	30.00	35.68	4.76	95.07	87.71	2.24	11.36	31.23	18.56	0.61
99	16.05	9.98	1.72	30.03	35.92	4.76	95.03	87.43	2.24	12.12	32.39	19.19	0.63
100	17.27	11.01	1.72	30.03	36.10	4.75	95.07	87.27	2.24	12.52	33.40	19.71	0.64
101	7.81	5.00	1.72	33.00	36.71	4.77	95.00	89.53	2.24	5.63	20.41	13.80	0.41
102	9.41	6.00	1.72	33.00	37.01	4.77	95.01	89.38	2.24	6.82	22.08	14.21	0.48
103	10.80	7.00	1.72	33.00	37.25	4.77	95.00	89.14	2.24	7.59	23.41	14.77	0.51
104	12.08	8.00	1.72	33.00	37.48	4.76	95.01	88.87	2.24	8.16	24.63	15.50	0.53
105	13.49	9.00	1.72	33.01	37.72	4.77	95.01	88.63	2.24	8.97	25.94	16.12	0.56
106	14.72	10.00	1.72	33.00	37.91	4.77	95.02	88.42	2.24	9.43	27.01	16.66	0.57
107	16.12	11.00	1.72	33.00	38.14	4.76	95.04	88.26	2.24	10.23	28.26	17.12	0.60
108	17.21	11.92	1.72	32.99	38.31	4.76	95.04	88.11	2.24	10.58	29.29	17.50	0.60
109	7.42	5.01	1.72	35.00	38.04	4.80	95.00	90.61	2.24	4.83	16.81	11.09	0.44
110	8.74	6.02	1.72	35.00	38.23	4.79	95.01	90.40	2.24	5.45	17.90	11.63	0.47
111	10.04	7.01	1.72	35.00	38.43	4.79	95.00	90.20	2.24	6.06	18.99	12.11	0.50
112	11.23	7.99	1.72	35.00	38.59	4.79	95.00	90.04	2.24	6.50	19.81	12.49	0.52
113	12.63	9.00	1.72	35.01	38.73	4.79	94.99	89.99	2.24	7.26	20.56	12.61	0.58
114	13.81	10.03	1.72	35.00	39.17	4.77	95.01	89.35	2.24	7.55	22.94	14.29	0.53
115	15.08	11.04	1.72	35.00	39.35	4.77	95.00	89.14	2.24	8.08	23.95	14.79	0.55
116	16.35	12.03	1.72	35.00	39.49	4.77	94.99	88.99	2.24	8.64	24.75	15.14	0.57
117	11.22	5.03	1.72	27.01	33.68	4.77	100.01	91.19	2.24	12.39	36.80	22.20	0.56
118	12.50	6.01	1.72	27.01	33.92	4.77	99.99	90.92	2.24	13.00	38.04	22.85	0.57
119	13.84	6.96	1.72	26.99	34.03	4.77	100.03	90.84	2.24	13.77	38.79	23.16	0.59
120	15.40	8.03	1.72	27.06	34.26	4.77	99.94	90.71	2.24	14.73	39.70	23.24	0.63
121	16.46	8.96	1.72	27.03	34.41	4.77	99.99	90.58	2.24	14.99	40.67	23.71	0.63

122	17.19	9.57	1.72	26.95	34.57	4.77	99.93	90.39	2.24	15.23	41.98	24.04	0.63
123	10.20	5.00	1.72	30.00	35.43	4.76	100.05	93.01	2.24	10.42	29.88	17.74	0.59
124	11.25	6.00	1.72	30.00	35.51	4.76	100.06	92.86	2.24	10.50	30.27	18.13	0.58
125	12.70	6.99	1.72	30.00	35.85	4.76	100.07	92.51	2.24	11.42	32.21	19.05	0.60
126	14.10	7.96	1.72	29.99	36.13	4.76	100.12	92.25	2.24	12.26	33.76	19.84	0.62
127	15.75	9.03	1.72	30.04	36.47	4.77	100.07	92.01	2.24	13.44	35.43	20.31	0.66
128	16.67	9.83	1.72	29.93	36.58	4.76	100.11	91.98	2.24	13.67	36.58	20.48	0.67
129	8.71	5.01	1.72	32.99	37.40	4.76	100.03	93.81	2.24	7.42	24.23	15.65	0.47
130	10.11	6.00	1.72	33.00	37.74	4.76	100.05	93.44	2.24	8.23	26.08	16.63	0.49
131	11.64	7.03	1.72	33.00	38.00	4.77	100.06	93.27	2.24	9.23	27.49	17.09	0.54
132	12.94	8.01	1.72	33.00	38.17	4.76	100.04	93.15	2.24	9.87	28.39	17.36	0.57
133	14.23	8.99	1.72	33.00	38.41	4.76	100.09	92.90	2.24	10.46	29.73	18.12	0.58
134	15.63	9.99	1.72	33.00	38.55	4.77	100.01	92.85	2.24	11.26	30.53	18.04	0.62
135	8.10	5.00	1.72	35.00	38.77	4.77	100.01	94.60	2.24	6.20	20.73	13.63	0.46
136	9.62	6.03	1.72	35.00	39.05	4.77	100.01	94.43	2.24	7.18	22.29	14.05	0.51
137	10.96	7.04	1.72	35.00	39.28	4.76	100.00	94.19	2.24	7.84	23.50	14.62	0.54
138	12.18	7.99	1.72	35.00	39.47	4.76	100.02	93.97	2.24	8.37	24.55	15.23	0.55

Table D.2 ***Summary of the tests with Pink chilli 12 for fan-coil applications-continuation***

No	**W [kW]**	**$COP_{chiller,all}$**	**EER**	**P_{high} [bar]**	**P_{low} [bar]**	**ΔP_{hw} [bar]**	**ΔP_{chw} [bar]**	**ΔP_{cw} [bar]**	**U ($\dot{Q}_{eva}$) ±**	**U ($\dot{Q}_{ac}$) ±**	**U ($\dot{Q}_{gen}$) ±**	**U (COP) ±**	**U (loss) ±**
1	0.57	0.50	4.20	12.00	3.80	0.54	0.05	1.40	0.54	1.87	1.27	0.09	3.68
2	0.57	0.53	4.59	12.00	3.90	0.54	0.05	1.40	0.55	1.86	1.27	0.10	3.69
3	0.57	0.56	4.92	12.00	3.90	0.05	0.05	1.40	0.56	1.87	1.27	0.10	3.71
4	0.58	0.58	5.27	11.50	4.00	0.53	0.05	1.40	0.58	1.88	1.28	0.10	3.74
5	0.58	0.63	5.85	11.25	4.00	0.53	0.05	1.40	0.58	1.87	1.27	0.10	3.73
6	0.59	0.64	6.06	11.50	4.00	0.53	0.05	1.40	0.59	1.88	1.27	0.10	3.74
7	0.60	0.65	6.21	11.50	4.40	0.54	0.05	1.40	0.60	1.88	1.27	0.09	3.75
8	0.57	0.41	2.35	11.50	3.70	0.05	0.05	1.40	0.53	1.91	1.27	0.10	3.72
9	0.58	0.45	2.67	11.60	3.80	0.54	0.05	1.40	0.54	1.91	1.27	0.10	3.73
10	0.59	0.48	2.93	11.75	4.00	0.54	0.05	1.40	0.55	1.92	1.27	0.10	3.74
11	0.59	0.53	3.29	11.80	4.20	0.54	0.05	1.40	0.56	1.92	1.27	0.10	3.75
12	0.59	0.56	3.60	11.90	4.30	0.54	0.05	1.40	0.56	1.92	1.27	0.11	3.76
13	0.60	0.62	4.23	12.00	4.50	0.54	0.05	1.40	0.57	1.91	1.27	0.10	3.75
14	0.60	0.65	4.56	12.00	4.60	0.54	0.05	1.40	0.58	1.91	1.27	0.10	3.77
15	0.60	0.66	4.72	12.25	4.70	0.53	0.05	1.40	0.59	1.91	1.27	0.10	3.77
16	0.64	0.15	0.54	14.10	4.80	0.52	0.04	1.40	0.53	1.97	1.28	0.12	3.78
17	0.59	0.22	0.91	12.25	3.80	0.54	0.05	1.40	0.54	1.97	1.28	0.12	3.79
18	0.59	0.28	1.24	12.25	4.00	0.54	0.05	1.40	0.54	1.97	1.28	0.12	3.79
19	0.60	0.34	1.42	12.50	4.10	0.54	0.05	1.40	0.56	1.98	1.28	0.14	3.81
20	0.60	0.45	2.04	13.00	4.20	0.54	0.05	1.40	0.57	1.98	1.28	0.15	3.81
21	0.60	0.50	2.35	13.00	4.20	0.54	0.05	1.40	0.58	1.97	1.28	0.15	3.82

22	0.60	0.08	0.27	13.00	4.00	0.54	0.05	1.40	0.53	2.00	1.28	0.12	3.81
23	0.60	0.12	0.45	13.00	4.00	0.54	0.04	1.40	0.54	2.00	1.28	0.12	3.82
24	0.60	0.15	0.54	13.00	4.00	0.54	0.04	1.40	0.55	2.00	1.28	0.12	3.82
25	0.60	0.19	0.73	13.00	4.20	0.55	0.04	1.40	0.56	2.00	1.28	0.12	3.83
26	0.61	0.25	0.99	13.00	4.40	0.54	0.04	1.40	0.57	2.01	1.28	0.13	3.85
27	0.56	0.50	4.88	11.50	3.80	0.51	0.05	1.40	0.54	1.85	1.30	0.06	3.68
28	0.57	0.64	5.18	11.40	3.60	0.51	0.05	1.40	0.56	1.85	1.30	0.06	3.71
29	0.60	0.65	5.52	11.50	4.00	0.55	0.05	1.40	0.56	1.87	1.31	0.06	3.74
30	0.67	0.64	5.15	12.20	4.20	0.52	0.04	1.40	0.58	1.88	1.31	0.07	3.77
31	0.67	0.64	5.34	11.75	4.20	0.51	0.05	1.40	0.62	1.90	1.31	0.07	3.83
32	0.68	0.64	5.58	12.00	4.40	0.51	0.04	1.40	0.69	1.91	1.33	0.07	3.93
33	0.70	0.64	5.67	12.00	4.60	0.51	0.04	1.40	0.71	1.89	1.31	0.07	3.91
34	0.60	0.44	3.28	12.00	3.70	0.51	0.05	1.40	0.54	1.92	1.31	0.07	3.77
35	0.60	0.64	3.49	12.00	3.90	0.51	0.05	1.40	0.54	1.90	1.30	0.07	3.74
36	0.61	0.50	3.97	12.25	4.00	0.51	0.05	1.40	0.56	1.93	1.31	0.07	3.79
37	0.62	0.52	4.27	12.25	4.00	0.51	0.05	1.40	0.56	1.93	1.30	0.07	3.80
38	0.62	0.64	4.42	12.50	4.20	0.51	0.05	1.40	0.57	1.92	1.31	0.07	3.80
39	0.61	0.64	4.79	12.25	4.00	0.51	0.05	1.40	0.61	1.93	1.31	0.08	3.85
40	0.61	0.64	5.11	12.25	4.40	0.51	0.05	1.40	0.60	1.92	1.31	0.07	3.82
41	0.62	0.64	5.32	12.50	4.20	0.51	0.05	1.40	0.61	1.92	1.31	0.08	3.84
42	0.61	0.30	1.56	12.50	3.60	0.51	0.05	1.40	0.54	1.97	1.31	0.09	3.82
43	0.60	0.33	1.83	12.50	3.80	0.51	0.05	1.40	0.54	1.98	1.31	0.09	3.82
44	0.60	0.35	2.06	12.25	4.00	0.51	0.05	1.40	0.55	1.99	1.31	0.09	3.85
45	0.61	0.64	2.71	13.00	4.20	0.51	0.05	1.40	0.56	1.95	1.31	0.09	3.82
46	0.62	0.64	3.02	12.50	4.20	0.51	0.05	1.40	0.56	1.95	1.31	0.08	3.81
47	0.63	0.64	3.22	13.05	4.40	0.51	0.05	1.40	0.57	1.95	1.31	0.08	3.82
48	0.63	0.64	3.50	13.18	4.60	0.51	0.05	1.40	0.58	1.95	1.31	0.08	3.84
49	0.63	0.64	3.74	13.13	4.80	0.51	0.05	1.40	0.59	1.96	1.31	0.08	3.85
50	0.60	0.13	0.56	13.00	3.60	0.51	0.05	1.40	0.54	2.00	1.32	0.10	3.85
51	0.61	0.20	0.92	13.00	3.80	0.51	0.05	1.40	0.54	2.00	1.32	0.10	3.86
52	0.61	0.26	1.27	13.00	3.90	0.51	0.05	1.40	0.55	2.00	1.31	0.10	3.86
53	0.62	0.31	1.59	13.25	4.00	0.50	0.05	1.40	0.55	2.00	1.31	0.10	3.86
54	0.63	0.35	1.85	13.25	4.20	0.51	0.05	1.40	0.56	2.00	1.31	0.10	3.87
55	0.63	0.40	2.22	13.50	4.40	0.52	0.05	1.40	0.57	2.00	1.31	0.10	3.88
56	0.63	0.43	2.49	13.50	4.60	0.51	0.05	1.40	0.58	2.00	1.31	0.10	3.88
57	0.64	0.44	2.68	13.60	4.80	0.52	0.05	1.40	0.58	2.00	1.31	0.09	3.89
58	0.62	0.53	5.28	12.00	3.60	0.52	0.05	1.40	0.57	1.89	1.34	0.06	3.80
59	0.61	0.54	5.55	11.80	3.80	0.52	0.04	1.40	0.56	1.89	1.34	0.06	3.80
60	0.60	0.57	6.14	12.00	3.90	0.52	0.04	1.40	0.59	1.89	1.34	0.06	3.82
61	0.61	0.60	6.45	12.20	4.20	0.52	0.04	1.40	0.58	1.87	1.35	0.06	3.79
62	0.62	0.62	6.69	12.40	4.30	0.52	0.04	1.40	0.60	1.87	1.35	0.06	3.82
63	0.62	0.64	6.97	12.40	4.30	0.52	0.04	1.40	0.59	1.87	1.34	0.06	3.80
64	0.62	0.65	7.19	12.50	4.40	0.52	0.04	1.40	0.71	1.91	1.35	0.06	3.97
65	0.59	0.50	4.18	12.25	3.70	0.52	0.05	1.40	0.55	1.93	1.35	0.07	3.82

66	0.59	0.53	4.55	12.25	3.70	0.52	0.05	1.40	0.55	1.93	1.35	0.07	3.83
67	0.60	0.56	4.85	12.50	4.00	0.52	0.05	1.40	0.56	1.93	1.34	0.07	3.84
68	0.62	0.59	5.39	12.70	4.20	0.52	0.05	1.40	0.57	1.94	1.34	0.07	3.85
69	0.62	0.62	5.75	12.90	4.40	0.52	0.05	1.40	0.58	1.95	1.35	0.07	3.87
70	0.62	0.63	6.01	12.80	4.40	0.52	0.05	1.40	0.59	1.95	1.34	0.07	3.88
71	0.64	0.65	6.08	13.00	4.70	0.52	0.05	1.35	0.59	1.96	1.35	0.07	3.90
72	0.61	0.42	2.80	13.00	3.70	0.52	0.05	1.40	0.54	1.98	1.35	0.08	3.86
73	0.62	0.45	3.10	13.00	3.80	0.52	0.05	1.40	0.54	1.98	1.35	0.08	3.87
74	0.62	0.50	3.52	13.20	4.00	0.52	0.05	1.40	0.55	1.98	1.35	0.08	3.88
75	0.63	0.53	3.87	13.25	4.20	0.52	0.05	1.40	0.56	1.99	1.35	0.08	3.89
76	0.62	0.56	4.24	13.25	4.20	0.52	0.05	1.40	0.57	1.99	1.35	0.09	3.90
77	0.63	0.64	4.30	13.50	4.50	0.52	0.05	1.40	0.58	1.96	1.35	0.08	3.88
78	0.64	0.64	4.53	13.70	4.70	0.52	0.05	1.40	0.59	1.96	1.34	0.08	3.89
79	0.64	0.64	4.71	13.60	4.80	0.52	0.05	1.40	0.60	1.97	1.35	0.08	3.91
80	0.62	0.27	1.51	13.25	3.60	0.52	0.05	1.40	0.53	2.01	1.35	0.08	3.89
81	0.62	0.31	1.84	13.50	3.80	0.52	0.05	1.40	0.54	2.01	1.35	0.08	3.90
82	0.63	0.35	2.17	13.50	4.00	0.52	0.05	1.40	0.55	2.01	1.35	0.08	3.91
83	0.63	0.39	2.52	13.70	4.20	0.53	0.05	1.40	0.55	2.01	1.35	0.08	3.91
84	0.63	0.42	2.81	13.75	4.20	0.52	0.04	1.40	0.56	2.01	1.35	0.08	3.92
85	0.63	0.44	3.15	13.80	4.40	0.53	0.04	1.40	0.57	2.02	1.35	0.08	3.93
86	0.65	0.47	3.38	14.00	4.60	0.52	0.04	1.40	0.58	2.02	1.35	0.08	3.94
87	0.64	0.49	3.67	14.10	4.80	0.52	0.04	1.40	0.59	2.02	1.35	0.08	3.95
88	0.60	0.54	6.34	12.00	3.40	0.54	0.04	1.40	0.57	1.90	1.38	0.05	3.84
89	0.62	0.64	6.31	12.50	3.90	0.54	0.04	1.40	0.60	1.90	1.38	0.05	3.89
90	0.61	0.64	6.92	12.50	3.80	0.54	0.04	1.40	0.58	1.90	1.38	0.05	3.87
91	0.63	0.64	7.03	13.75	3.60	0.54	0.04	1.40	0.58	1.90	1.38	0.05	3.86
92	0.61	0.64	7.60	12.50	4.00	0.54	0.04	1.40	0.60	1.91	1.38	0.05	3.88
93	0.64	0.64	7.57	13.00	4.20	0.54	0.04	1.40	0.61	1.94	1.38	0.05	3.93
94	0.61	0.45	4.58	12.75	4.80	0.54	0.04	1.40	0.55	1.94	1.38	0.05	3.87
95	0.61	0.49	5.06	13.00	3.90	0.54	0.04	1.40	0.55	1.94	1.38	0.05	3.87
96	0.62	0.50	5.39	13.00	4.00	0.54	0.04	1.40	0.58	1.95	1.38	0.05	3.90
97	0.62	0.60	6.16	13.10	4.20	0.54	0.04	1.40	0.58	1.95	1.38	0.06	3.92
98	0.64	0.55	5.86	13.25	4.40	0.53	0.04	1.40	0.59	1.96	1.38	0.06	3.93
99	0.64	0.57	6.30	13.25	4.60	0.53	0.04	1.40	0.59	1.96	1.38	0.05	3.93
100	0.64	0.58	6.45	14.00	4.60	0.53	0.04	1.40	0.63	1.96	1.38	0.05	3.97
101	0.60	0.36	3.10	13.30	3.80	0.53	0.04	1.40	0.54	1.98	1.38	0.06	3.90
102	0.63	0.42	3.57	13.50	3.80	0.54	0.44	1.40	0.54	1.98	1.38	0.06	3.91
103	0.64	0.45	3.91	13.50	4.00	0.54	0.04	1.40	0.55	1.99	1.38	0.06	3.92
104	0.63	0.47	4.27	13.50	4.00	0.53	0.04	1.40	0.56	1.99	1.38	0.06	3.93
105	0.64	0.50	4.63	13.75	4.20	0.53	0.04	1.40	0.57	1.99	1.38	0.06	3.94
106	0.65	0.51	4.79	14.00	4.40	0.54	0.05	1.40	0.58	1.99	1.38	0.06	3.95
107	0.65	0.54	5.19	14.00	4.60	0.53	0.04	1.40	0.59	2.00	1.38	0.06	3.97
108	0.65	0.54	5.37	14.10	4.80	0.53	0.04	1.40	0.59	2.00	1.38	0.06	3.97
109	0.64	0.37	2.49	13.75	3.60	0.54	0.04	1.40	0.53	2.02	1.38	0.07	3.94

110	0.63	0.40	2.85	13.50	3.80	0.54	0.04	1.40	0.54	2.02	1.38	0.07	3.95
111	0.64	0.43	3.12	14.00	4.00	0.54	0.05	1.40	0.55	2.02	1.38	0.07	3.96
112	0.65	0.45	3.30	14.00	4.00	0.54	0.05	1.40	0.56	2.02	1.38	0.07	3.97
113	0.65	0.50	3.68	14.00	4.25	0.53	0.05	1.40	0.57	2.03	1.38	0.08	3.98
114	0.65	0.46	3.83	14.40	4.50	0.54	0.04	1.40	0.58	2.02	1.38	0.07	3.98
115	0.66	0.48	4.04	14.50	4.70	0.54	0.04	1.40	0.58	2.02	1.38	0.06	3.99
116	0.67	0.50	4.25	14.60	4.90	0.54	0.04	1.40	0.59	2.02	1.38	0.07	4.00
117	0.64	0.64	6.39	12.90	3.90	0.55	0.04	1.40	0.58	1.90	1.41	0.04	3.89
118	0.62	0.64	6.92	12.60	3.70	0.55	0.05	1.40	0.59	1.90	1.42	0.04	3.91
119	0.63	0.64	7.21	12.80	3.80	0.55	0.05	1.40	0.60	1.91	1.41	0.04	3.92
120	0.64	0.64	7.60	12.90	3.90	0.55	0.04	1.40	0.66	1.92	1.41	0.05	3.99
121	0.64	0.64	7.73	12.90	4.00	0.54	0.05	1.40	0.67	1.93	1.42	0.05	4.01
122	0.63	0.64	7.98	13.00	4.00	0.54	0.04	1.40	0.60	1.94	1.42	0.04	3.96
123	0.62	0.64	5.54	13.00	3.70	0.55	0.05	1.40	0.56	1.89	1.42	0.06	3.87
124	0.61	0.64	5.68	13.00	3.80	0.55	0.05	1.40	0.57	1.89	1.42	0.05	3.88
125	0.63	0.64	5.98	13.50	4.00	0.55	0.05	1.40	0.57	1.90	1.42	0.05	3.89
126	0.63	0.64	6.42	13.50	4.20	0.55	0.05	1.40	0.58	1.91	1.42	0.05	3.91
127	0.64	0.64	6.93	13.60	4.20	0.55	0.05	1.40	0.60	1.91	1.42	0.05	3.93
128	0.64	0.64	7.05	13.80	4.40	0.55	0.05	1.40	0.60	1.91	1.42	0.05	3.93
129	0.64	0.65	3.83	13.50	3.60	0.55	0.05	1.40	0.54	1.93	1.42	0.06	3.89
130	0.64	0.65	4.24	14.00	3.80	0.55	0.05	1.40	0.55	1.93	1.42	0.05	3.90
131	0.65	0.65	4.69	14.50	4.00	0.55	0.04	1.40	0.56	1.93	1.42	0.06	3.91
132	0.64	0.65	5.09	14.00	4.20	0.55	0.05	1.40	0.57	1.93	1.42	0.06	3.92
133	0.65	0.65	5.31	14.20	4.40	0.55	0.05	1.40	0.58	1.94	1.42	0.06	3.94
134	0.65	0.65	5.72	14.40	4.50	0.55	0.05	1.40	0.58	1.94	1.42	0.06	3.94
135	0.63	0.65	3.25	14.00	3.60	0.55	0.05	1.40	0.54	1.96	1.42	0.06	3.92
136	0.62	0.65	3.82	14.00	3.80	0.55	0.05	1.40	0.55	1.96	1.42	0.06	3.93
137	0.65	0.65	3.98	14.50	4.00	0.55	0.04	1.40	0.56	1.96	1.42	0.06	3.94
138	0.66	0.65	4.19	14.60	4.00	0.55	0.04	1.40	0.56	1.96	1.42	0.06	3.95